Development of a Non-Linear Multi-body Dynamics Model for Active Suspension Control Design and Evaluation of a Formula Student Racecar

Daniel Alexander Wageman

A thesis submitted in partial fulfillment of the requirements for the degree of

Master of Science in Mechanical Engineering

University of Washington

2015

Committee:

Ashley Emery (Chair)

Joseph Garbini

Brian Fabien

Program Authorized to Offer Degree:

Mechanical Engineering

University of Washington

Abstract

Development of a Non-Linear Multi-body Dynamics Model of a Formula Student Racecar for Active Suspension Control Design and Evaluation

Daniel Alexander Wageman

Chair of the Supervisory Committee:

Professor Ashley Emery

Mechanical Engineering

A seven degree of freedom non-linear multi-body dynamics model was built as a tool to help design and analyze the effects and requirements of an active suspension system on a Formula Student Racecar. The model offers several improvements over a 'typical' linear model by accepting nonlinear damping characteristics (as are commonly found in racing applications by design), suspension travel limits, and most notably 'ballistic' effects where the wheel loses contact with the ground. Developed using a combination of MATLAB and Simulink[1] (The Mathworks, Inc.), the model is both functional and flexible.

[1] MATLAB, short for matrix laboratory software platform specifically tailored for numerical computing problems including, but not limited to, data processing, plotting, symbolic manipulation, matrix processing, differential equations, and many additional functions extended by the use of various toolboxes. Simulink is primarily a graphical programing environment for use with MATLAB.

ACKNOWLEDGEMENTS

My thesis project has been a final culmination of many years of school. First of all, I would like to thank my thesis committee, Dr. Emery, Dr. Garbini, and Dr. Fabien for their help, support, and guidance through this long and at times wandering process.

I would like to thank the University of Washington Formula SAE team for providing me an auxiliary education experience and opportunities far beyond what can be achieved solely in a classroom. It has taught me not only sound engineering principles, but teamwork, project management, sleep management, budgeting, public relations, corporate interaction, conflict management, and of course the "oh, this doesn't fit together… but it worked in CAD!?" lessons.

Along those lines, I would also like to thank everyone involved in organizing and running the SAE events, around the world. Having run one small team, I can appreciate the immeasurable work that goes into organizing these events. I would like to thank the design judges that painfully pry at the concepts they feel you don't understand – knowing you will spend the time to understand it later.

Next, I would like to thank Lund Engineering Inc. for putting up with my *very* irregular work hours over the course of this project.

Finally, I would of course like to thank my family and friends. They have all supported me throughout my education, and also put up with the long periods of infrequent contact.

Table of Contents

Development of a Non-Linear Multi-body Dynamics Model for Active Suspension Control Design and Evaluation of a Formula Student Racecar i

ACKNOWLEDGEMENTS iii

Table of Contents iv

List of Figures ix

List of Tables xiii

List of Equations xiv

Executive Summary xv

NOTATION xvii

Terms xvii

Diagrams and Coordinate Systems xviii

Single Mass Model xviii

Quarter Car Model xx

Bicycle Model xxi

Full Car Model xxii

Abbreviations and Annotations xxiii

Conventions xxiii

1. Introduction 1

2. Purpose 3

2.1. Safety 3

2.2. Performance 3

2.3. Attitude Control 3

3. Background 5

3.1. Formula SAE 5

3.2. Project History 5
3.3. Model History 6
3.4. Other Models and Software 7
3.5. Types of Active Suspension 8
3.6. Active Suspension Actuation Methods 9
3.7. Controller Types 10
3.8. Existing Systems 13
3.9. Notes on Improvements and Marginal Gains 14
3.10. Disclaimers 14
4. Model Limitations 16
4.1. Simplifications 16
4.2. Mathematical Limitations 16
4.3. Physical System vs Model Limitations 16
4.4. Model Assumptions 17
4.5. Setup Assumptions 17
5. Performance Evaluation 18
5.1. Concepts and Definitions 18
5.1.1. Wheel Contact Time 23
5.1.2. Tire Load Variation 24
5.1.3. Power Usage 24
5.2. Quantification Methods 25
5.2.1. Average Disturbance Magnitude Reduction 25
5.2.2. Load Fluctuation Rate 25
5.2.3. Contact Patch Force Standard Deviation 26
5.2.4. Ballistic Time of Flight Reduction 26

6. Model Development 27
6.1. Linear Models 27
6.1.1. Single Mass Test Case 27
6.1.2. Linear Quarter Car 28
6.1.3. Linear Bicycle Model 29
6.1.4. Linear Full Car 30
6.2. Non-Linear, Non Ballistic Models 31
6.2.1. Comparisons 34
6.3. Non-Linear Ballistic Models 37
6.3.1. Non-Linear Quarter Car 38
6.3.2. Non-Linear Bicycle Model 43
6.3.3. Non-Linear Full Car 44
7. Controller Development 51
7.1. Controller Selection 51
7.2. Feedback Control Response 55
7.2.1. Quarter Car 55
7.2.2. Bicycle Model 65
7.2.3. Full Car 66
8. Results 78
8.1. Average Disturbance Magnitude Reduction 78
8.2. Load Fluctuation Rate 79
8.3. Contact Patch Force Standard Deviation 79
8.4. Time of Flight Reduction 80
9. Conclusions 82
10. Future Work 84

10.1. Optimal Controller Design 84
10.1.1. Controller Selection 84
10.1.2. Parameters 85
10.1.3. Coefficients 85
10.2. Actuator Design 85
10.3. Physical Implementation 86
10.4. Other Considerations 86
APPENDICIES 89
Appendix A – Dynamic Equation Derivations 89
Appendix B – Linear State Space Modeling 90
Resultant Equations: 90
Full Car Linear Response to basic input: 94
Appendix C – Simulink Models 101
Models 101
Blocks 106
Appendix D – MATLAB Code 110
Appendix E – Complete Bicycle Model Simulation Set 111
Ballistic vs Non Ballistic Comparison 111
Feedback Control Response 116
Appendix F – Comparison of Ballistic and Non-Ballistic Model 124
Appendix G – Bump Profile Development 126
StepUp 126
StepDown 126
Sawtooth 127
Pothole 128

Sinusoid 129
Chirp 130
Appendix H – Additional Model Functions and Capabilities 132
BIBLIOGRAPHY 133

List of Figures

Figure 1 - Passive Single Spring - Mass - Damper System xix
Figure 2 - Active Spring - Mass - Damper System with Variable Force Actuator xix
Figure 3 – Passive Quarter Car Model xx
Figure 4 – Active Quarter Car Model with Variable Force Actuator xx
Figure 5 - Passive Bicycle Model xxi
Figure 6 - Active Bicycle Model with Variable Force Actuators xxi
Figure 7 - Passive Full Car Model xxii
Figure 8 - Active Full Car Model with Variable Force Actuators xxii
Figure 9 - Feedback Control Block Diagram 11
Figure 10 - Tire Deformation and Slip Angle 20
Figure 11 - Tire Slip Ratio, Zero, Positive, and Negative 21
Figure 12 - Example Empirical fit of Lateral Force [Fy] vs Slip Angle [SA] at different Normal Loads [Fz] at a Fixed Inclination Angle [IA] for an FSAE Tire 22
Figure 13 - Example of Longitudinal Force [Fx] vs Slip Ratio [SR] and Normal Load 23
Figure 14 - Linear Single Mass Test Case Model – StepUp 28
Figure 15 - Linear Quarter Car Test Case Model – StepUp 29
Figure 16 - Linear Bicycle Test Case Model – StepUp 30
Figure 17 - Linear Full Car Test Case Model - StepUp 31
Figure 18 - Linear vs Non Linear Damping Force 33
Figure 19 - Quarter Car StepUp Damper Velocity Histogram 34
Figure 20 - Quarter Car StepUp Fully Linear vs Non-Ballistic Response 35
Figure 21 - Quarter Car Pothole Fully Linear vs Non-Ballistic Response 36
Figure 22 - Quarter Car 10 Hz Sinusoid Fully Linear vs Non-Ballistic Response 37
Figure 23 - Non-Linear Quarter Car StepUp Response 38
Figure 24 - Non-Linear Quarter Car StepDown Response 39
Figure 25 - Non-Linear Quarter Car Impulse Response 40
Figure 26 - Non-Linear Quarter Car Pothole Response 41
Figure 27 - Non-Linear Quarter Car 2 Hz Sinusoid Response 42
Figure 28 - Non-Linear Quarter Car 10 Hz Sinusoid Response 43
Figure 29 - Non-Linear Bicycle Model StepUp Response 44

Figure 30 - Non-Linear Full Car StepUp Response 45
Figure 31 - Non-Linear Full Car StepDown Response 46
Figure 32 - Non-Linear Full Car Sawtooth Response 47
Figure 33 - Non-Linear Full Car Pothole Response 48
Figure 34 - Non-Linear Full Car 2 Hz Sinusoid Response 49
Figure 35 - Non-Linear Full Car 10 Hz Sinusoid Response 50
Figure 36 - Quarter Car Model LQR Gain K Graphical Representation 53
Figure 37 - Bicycle Model LQR Controller Gain K Graphical Representation 54
Figure 38 - Full Car Model LQR Controller Gain K Graphical Representation 55
Figure 39 - Quarter Car StepUp Response with LQR 56
Figure 40 - Quarter Car StepDown Response with LQR 57
Figure 41 - Quarter Car Sawtooth Response with LQR 58
Figure 42 - Quarter Car Pothole Response with LQR 59
Figure 43 - Quarter Car 2 Hz Sinusoid Response with LQR 60
Figure 44 - Quarter Car 10 Hz Sinusoid Response with LQR 61
Figure 45 - Chassis Displacement Response to Chirp Input 62
Figure 46 - Normalized Chassis Displacement Amplitude to Chirp Input 63
Figure 47 - Contact Patch Force Amplitude to Chirp Input 64
Figure 48 - Actuator Response Amplitude to Chirp Input 65
Figure 49 – Bicycle Model StepUp Response with LQR 66
Figure 50 - Full Car StepUp Response with LQR 67
Figure 51 - Full Car StepDown Response with LQR 68
Figure 52 - Full Car Sawtooth Response with LQR 69
Figure 53 - Full Car Pothole Response with LQR 70
Figure 54 - Full Car 2 Hz Sinusoid Response with LQR 71
Figure 55 - Full Car 10 Hz Sinusoid Response with LQR 72
Figure 56 - Full Car Zc Response Envelope to Chirp Input 73
Figure 57 - Full Car Zc Response Amplitude to Chirp Input 74
Figure 58 - Full Car Chassis Pitch Amplitude to Chirp Input 75
Figure 59 - Full Car Contact Patch Force Magnitude Variation to Chirp Input 76
Figure 60 - Full Car Actuator Amplitude to Chirp Input 77

Figure 61 - Sudo Random Noise Input 88
Figure 62 - Linear State Space Full Car Step Input Response 95
Figure 63 - Linear State Space Full Car Step Input Phase Plot 96
Figure 64 - Linear State Space Full Car Impulse Input Response 97
Figure 65 - Linear State Space Full Car Impulse Input Phase Plot 98
Figure 66 - Linear State Space Full Car Profile Input Response 99
Figure 67 - Linear State Space Full Car Profile Input Phase Plot 100
Figure 68 - Simulink Single Mass Linear and Non-Linear Models 102
Figure 69 – Simulink Quarter Car Linear, Ballistic, and Ballistic with LQR Feedback Models 103
Figure 70 – Simulink Bicycle Linear, Ballistic, and Ballistic with LQR Feedback Models 104
Figure 71 - Simulink Full Car Linear, Ballistic, and Ballistic with LQR Feedback Models 105
Figure 72 – Simulink Non-Linear Damper Subsystem Block 106
Figure 73 – Simulink Vertical Chassis Translation Subsystem 107
Figure 74 – Simulink Chassis Pitch Subsystem 107
Figure 75 – Simulink Chassis Roll Subsystem 108
Figure 76 – Simulink Wheel Subsystem 109
Figure 77 - Non-Linear Bicycle Model StepDown Response 111
Figure 78 - Non-Linear Bicycle Model Sawtooth Response 112
Figure 79 - Non-Linear Bicycle Model Pothole Response 113
Figure 80 - Non-Linear Bicycle Model 2 Hz Sinusoid Response 114
Figure 81 - Non-Linear Bicycle Model 10 Hz Sinusoid Response 115
Figure 82 – Bicycle Model StepDown Response with LQR 116
Figure 83 – Bicycle Model Sawtooth Response with LQR 117
Figure 84 – Bicycle Model Pothole Response with LQR 118
Figure 85 – Bicycle Model 2 Hz Sinusoid Response with LQR 119
Figure 86 – Bicycle Model 10 Hz Sinusoid Response with LQR 120
Figure 87 - Bicycle Model Zc Response Amplitude to Chirp Input 121
Figure 88 - Bicycle Model Zt Response to Chirp Input 122
Figure 89 - Bicycle Model Contact Patch Force Response to Chirp Input 123
Figure 90 - RMS Difference Between Ballistic and Non-Ballistic Quarter Car Models 125
Figure 91 - StepUp Input 126

Figure 92 - StepDown Input 127
Figure 93 - Sawtooth Input 128
Figure 94 - Pothole Input 129
Figure 95 - Sinusoid Input 130
Figure 96 - Chip Input Frequency and Waveform 131

List of Tables

Table 0.1 - Terms and Definitions xvii
Table 0.2 - Common Abbreviations xxiii
Table 3.1 - Active Suspension Types 8
Table 3.2 - Active Suspension Actuation Methods 9
Table 3.3 - Controller Types 11
Table 8.1 - Average Disturbance Magnitude Reduction 78
Table 8.2 – Load Fluctuation Rate 79
Table 8.3 – Contact Patch RMS Force 80
Table 8.4 – Time of Flight Reduction (seconds) 80

List of Equations

Equation 1 – Single Mass Lagrange T – Kinetic Energy Relations 90
Equation 2 – Single Mass Lagrange V – Potential Energy Relations..... 90
Equation 3 - Single Mass Vertical Chassis Translation – Equation of Motion 90
Equation 4 - Single Mass A Matrix – State or System Matrix 90
Equation 5 – Single Mass B Matrix – Input Matrix..... 90
Equation 6 – Quarter Car Lagrange T – Kinetic Energy Relations 90
Equation 7 – Quarter Car Lagrange V – Potential Energy Relations 90
Equation 8 - Quarter Car Vertical Chassis Translation – Equation of Motion..... 91
Equation 9 - Quarter Car Vertical Tire Translation – Equation of Motion 91
Equation 10 - Quarter Car A Matrix – State or System Matrix..... 91
Equation 11 – Quarter Car B Matrix – Input Matrix 91
Equation 12 – Bicycle Model Lagrange T – Kinetic Energy Relations 91
Equation 13 – Bicycle Model Lagrange V – Potential Energy Relations..... 91
Equation 14 - Bicycle Model Vertical Chassis Translation – Equation of Motion 91
Equation 15 - Bicycle Model Vertical Front Tire Translation – Equation of Motion 92
Equation 16 - Bicycle Model Vertical Rear Tire Translation – Equation of Motion 92
Equation 17 - Bicycle Model Chassis Pitch – Equation of Motion 92
Equation 18 - Bicycle Model A Matrix – State or System Matrix 92
Equation 19 – Bicycle Model B Matrix – Input Matrix..... 92
Equation 20 – Full Car Lagrange T – Kinetic Energy Relations..... 92
Equation 21 – Full Car Lagrange V – Potential Energy Relations 92
Equation 22 - Full Car Vertical Chassis Translation – Equation of Motion..... 93
Equation 23 - Full Car Chassis Pitch – Equation of Motion 93
Equation 24 - Full Car Chassis Roll – Equation of Motion..... 93
Equation 25 - Full Car FL Tire Vertical Translation – Equation of Motion..... 93
Equation 26 - Full Car FR Tire Vertical Translation – Equation of Motion 93
Equation 27 - Full Car RL Tire Vertical Translation – Equation of Motion 93
Equation 28 - Full Car RR Tire Vertical Translation – Equation of Motion..... 93
Equation 29 - Full Car A Matrix – State or System Matrix..... 93
Equation 30 – Full Car B Matrix – Input Matrix 94

Executive Summary

Active suspension made its first real public appearance in the late 1990's in Formula One racing. The systems represented the pinnacle of automotive technology at the time, and were quickly banned in an attempt to level the playing field for teams that could not afford to develop such systems.

Since then, various forms of active suspension have found their way into numerous racecars, passenger cars, and even motorcycles. These systems range from very low frequency adaptive damping systems to high frequency setups with only active elements (passive spring and damper removed entirely). Such systems have generally proven themselves to be capable of several modes of operation – increasing performance, increasing comfort, and increasing safety, sometimes simultaneously.

However, due to the complex nature of the required control system, an accurate model of the system must exist to be able to develop an optimal controller and simulate its response. In this thesis, several models are developed and tested with mock actuators, allowing the accuracy of the model (to be determined by comparison to drive data), and effectiveness of the controller to be qualitatively and quantitatively evaluated. Because the vehicle's suspension system is nonlinear, and many controllers rely on localized system linearization, any attempt at control must demonstrate reasonable stability and effectiveness within the system's expected range of operation. In other words, if the system characteristics vary greatly away from the point of linearization, it should be shown that either the system will not reach such states, or that the controller is still capable of stable response. The developed suite of models range from the most basic, linear, spring-mass-damper system, to the nonlinear, full vehicle system. The linear controller effectiveness can thus be evaluated and compared on a range of system models.

In order to explore the resultant models and to characterize controller performance, a rudimentary LQR controller is developed. Because the primary focus of this thesis is to develop the dynamics model and not to create a fully optimized controller, the controller is developed only enough to show net improvements in the response of the vehicle as a proof of concept.

The system proposed for the UWashington FSAE team consists of active force elements installed in parallel with the passive spring and damper. Such a system allows the passive elements to

support the weight of the vehicle and to damp large inputs, while the actuator is left to adjust the response by either augmenting or diminishing the combined force of the passive elements. This approach greatly reduces the power required when compared to a system which relies solely on active elements to both support *and* control the vehicle.

The evaluation of the controller required the development of a ‘reasonable’ set of system inputs. Such a set is based on isolated elements of ground inputs frequently seen in driving surfaces.

Finally, the development and evaluation of the model, controller, and inputs show that the nonlinear system can be sufficiently controlled with a linear control system. In addition, the parallel augmentation approach is an effective actuation method. Finally, the combination of model and virtual controller allow for simple sizing of the required actuators, where the predicted response improvement can be compared to weight and cost drawbacks. In this project, it was found that *any* active input improves the response of the system, while larger inputs (and thus actuators) are increasingly effective.

NOTATION

Terms

Table 0.1 provides definitions for terms used throughout this thesis. Some otherwise generic terms are defined specifically in the context of this document.

Table 0.1 - Terms and Definitions

Term	**Definition**
Dynamic Model	A system model which describes the *time variant* response of a system
Ballistic	The motion taken by tire or other object subject primarily to gravity, not influenced by any rigid support from below
Controller	Specifically an *optimal controller* that is designed to achieve some balance of effectiveness vs 'cost' of exerted effort
Bump	Any physical disturbance, that imparts a vertical displacement, velocity, or acceleration to the wheel and thus to the suspension system
Quarter Car Model	A simplified dynamic model representing ¼ of a car, or more specifically, one wheel, spring(s), damper(s) and ¼ of the chassis
Bicycle Model	A simplified dynamic model that represents ½ (lateral split) of the car
Full Car Model	A complete dynamic model representing all 4 wheels, springs, dampers, chassis and other interlinked elements
Quasi Steady State	A model that accounts for the final, static weight distribution and resultant displacement of the vehicle due to external inputs, but does *not* solve for the model's arrival at that condition. The final condition may be changing, but the model does not account for the time variant spring and damper forces
Sprung Mass	The mass of the car that is supported by the suspension system

Unsprung Mass	The mass of the car that is *not* supported by the suspension – this usually includes, but is not limited to, wheels, tires, hubs, uprights, brakes (if outboard), and ½ of the articulating suspension members.
RMSD	Root Mean Square Deviation – a way to quantify the difference between values predicted by a model and what is observed, or between two models. It is defined by the following relationship $RMSD = \sqrt{\frac{\sum_{t=1}^{n}(x_{1,t}-x_{2,t})^2}{n}}$ i.e. the square root of the average of the sum of the squared differences.
Wheel	Specifically in this case, wheel will refer to the complete wheel and tire assembly. Wheel displacements are the displacement of the center of the wheel, or hub, from the static loaded position relative to the ground.

Diagrams and Coordinate Systems

The following diagrams are referenced throughout this project. Masses are designated with "M", spring constants with "K", and damping coefficients as "C". Subscripts of "c" and "t" refer to chassis and tire, respectively. Combination of "f", "r", and "l" may be used to designate front, right or rear, and left locations, respectively. In two letter locations, the first letter will always represent front or rear (to avoid right and rear confusion). The circle between the ground and tire represents a point contact.

Single Mass Model

Note, in this project, the single mass, spring, and damper were chosen to represent the chassis mass, spring, and damper since the mass is typically an order of magnitude larger, and the spring rate is several times smaller than that of the tire. In addition, a standalone model of the tire without the chassis elements would be very misleading.

Without Actuator

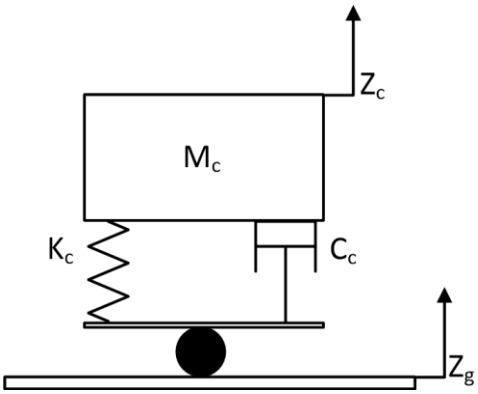

Figure 1 - Passive Single Spring - Mass - Damper System

With Actuator

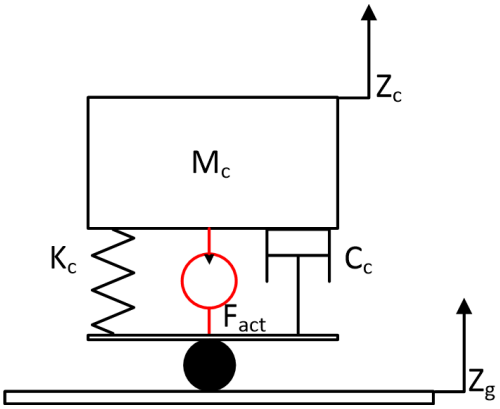

Figure 2 - Active Spring - Mass - Damper System with Variable Force Actuator

Quarter Car Model

Without Actuator

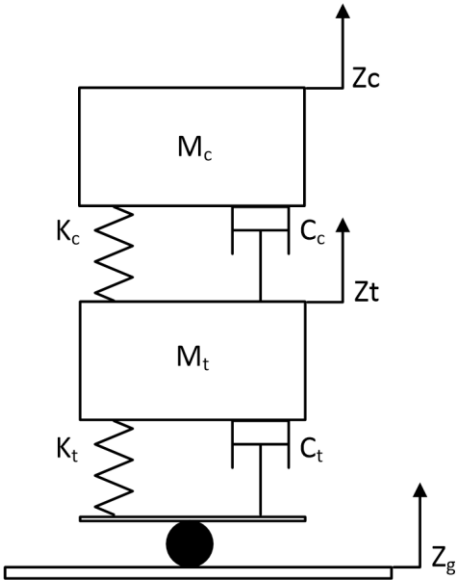

Figure 3 – Passive Quarter Car Model

With Actuator

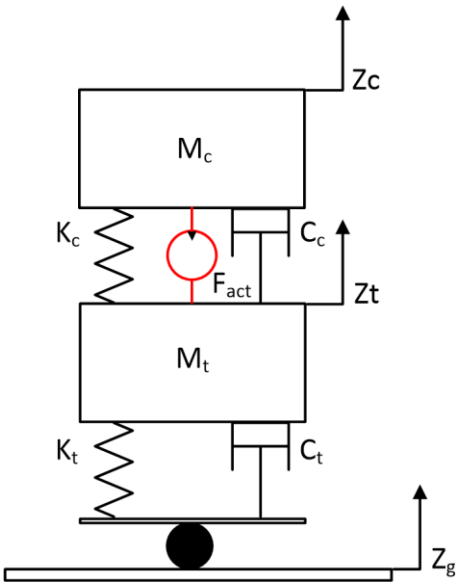

Figure 4 – Active Quarter Car Model with Variable Force Actuator

Bicycle Model

Without Actuators

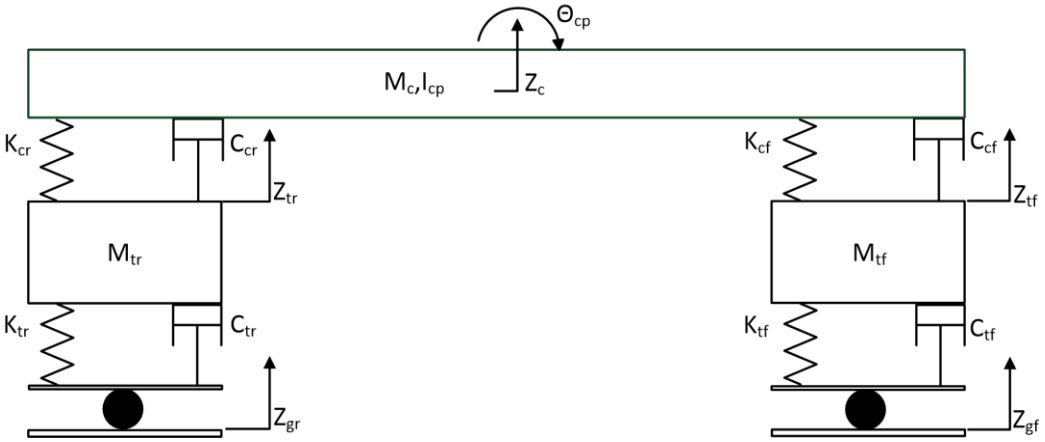

Figure 5 - Passive Bicycle Model

With Actuators

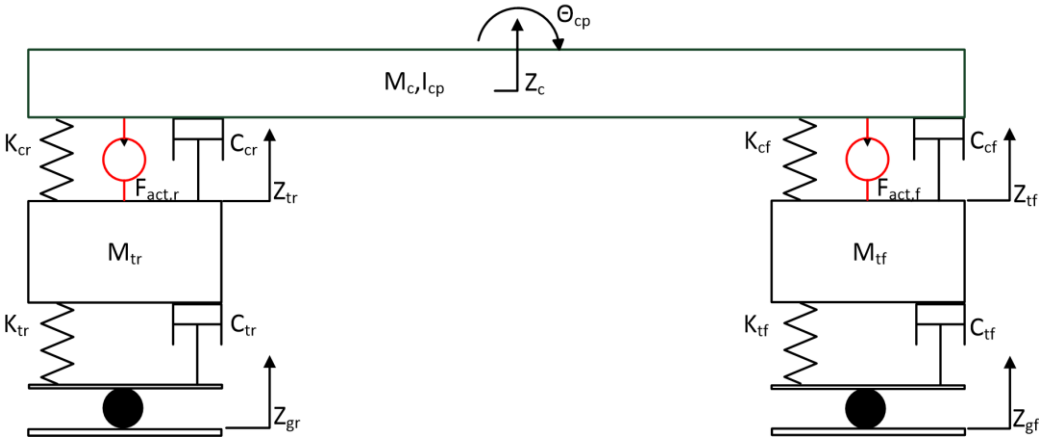

Figure 6 - Active Bicycle Model with Variable Force Actuators

Full Car Model

Without Actuators

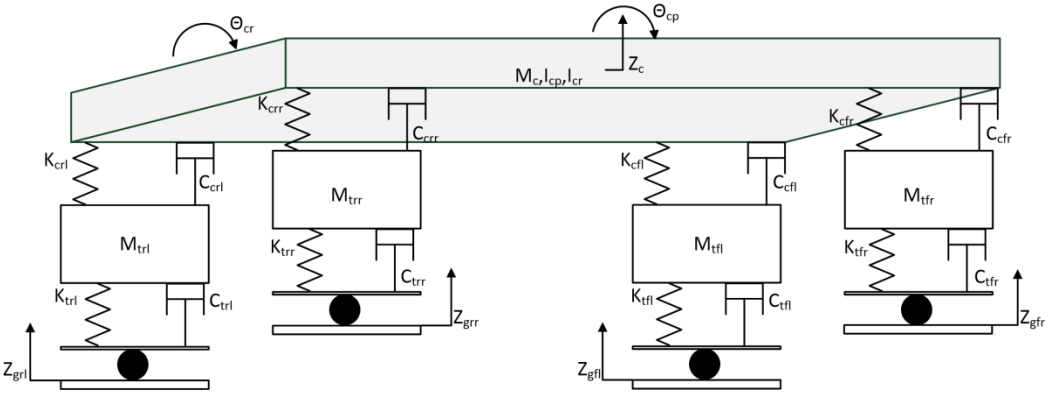

Figure 7 - Passive Full Car Model

With Actuators

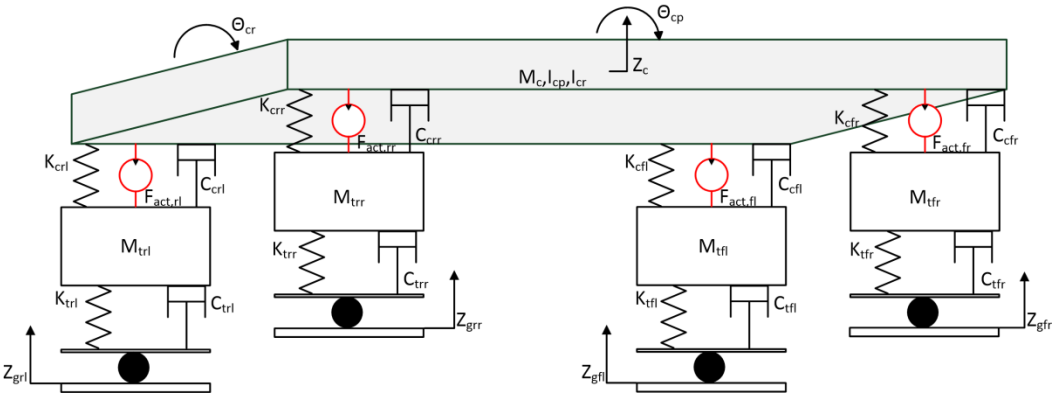

Figure 8 - Active Full Car Model with Variable Force Actuators

Abbreviations and Annotations

Because of the relatively long setup descriptions, many parameters and values are abbreviated as follows:

Table 0.2 - Common Abbreviations

B (suffix)	Ballistic Model
BL (suffix)	Ballistic LQR Enabled Model
FL (suffix)	Fully Linear Model
D (suffix)	Derivative (Velocity)
DD (suffix)	2nd Derivative (Acceleration)
fl, fr, rl, rr (suffix)	Front left, front right, rear left, rear right of any parameter
NB (suffix)	Non-Ballistic Model
TCP	Tire Contact Patch Force
Thcp	Chassis Pitch (theta)
Thcr	Chassis Roll (theta)
Zc	Chassis Z Displacement
Zcp	Tire Contact Position
Zg	Ground Displacement
Zt	Tire Z Displacement

Conventions

There are a number of conventions used throughout the system model and this thesis. First, all coordinate systems follow the aviation standard roll, pitch, yaw coordinate system. +z has been defined as vertical body motion away from and perpendicular to the ground plane.

1. Introduction

“Sometimes I think that I would have enjoyed racing more in the days of the friction shock. Since you couldn’t do anything much to them or with them, I would have spent a lot less time being confused” (Smith). As vehicle suspensions have become more and more complex, it has become increasingly important as well as difficult to accurately predict their behavior. In return for this effort, however, it is possible to design a vehicle with an acceptable compromise between stability, ride comfort, and performance.

When a vehicle tire loses contact with the ground, it cannot produce a lateral cornering force or a longitudinal braking (or accelerating) force. Thus, one specific goal of any effective active suspension system is to maximize the amount of time the tire spends in contact with the ground and to distribute the tire’s normal loads as evenly as possible – to allow for more grip to be generated and higher performance to be achieved. In order to design and simulate a functional optimal controller and actuation system, a vehicle model must account for tires temporarily leaving the road surface and any consequent dynamic load variations.

In addition, a mathematical model is only as useful as its ability to reflect the real world characteristics. In the case of many existing dynamic vehicle models, the possibility for the wheel to leave the ground (presumably following a sufficiently large bump or disturbance) or for the ground to retract from under the wheel (as it would while traveling over a pothole), is left unaccounted for. In addition, most spring and damper elements are modeled as ideal linear devices, which is very rarely the case in the actual physical system.

The reason for this exclusion and simplification is an issue of complexity. However, the impact of the nonlinear elements on the accuracy of the model can be significant in several specific situations that are likely to occur in real driving conditions, especially in the context of an active control system. These differences are highlighted in Chapter 6.

In the following thesis, a set of flexible, linear and non-linear models that account for ballistic (airborne) tire motion and non-linear elements (chassis dampers) is developed to be used for the design of an optimal LQR controller for a Formula Student Racecar active suspension. The first section contains an analysis of the potential performance impacts of such a system as well as relevant background and supporting information required to fully understand concepts and ideas

presented later on. Then, the limitations of the developed model will be examined. Following that, the development of the models and initial controller will be discussed in detail leading into the comparative results and suggestions for future development.

2. Purpose

2.1. Safety

Because a tire can only generate a heading changing force on the vehicle while in contact with the ground, it is critical for both braking and obstacle avoidance that the contact time be maximized. The more quickly a vehicle can stop and steer, the greater the chance the driver has of avoiding potential accidents and hazards. In the context of passenger vehicles especially, safety is that the primary concern of every automotive engineer.

2.2. Performance

In the context of the performance of racing vehicles, an active suspension system has significant merit, as measured in stability and lap time reduction. The focus of this thesis is specifically on a dynamic model and active suspension controller for a Formula Student racecar, but is equally applicable, albeit scaled, to any size, multi-wheeled vehicle intended to extract maximum performance from its tires.

It should be noted that while this multi-body model could be adapted to optimal car *comfort*, the primary purpose is for vehicle *performance* maximization, *not* driver comfort. This distinction affects the entire design target of the LQR controller, since the vehicle setup that turns the quickest lap times is not necessarily the most comfortable setup. Some compromise must be made however. There are a number of reported cases in which a race driver has pulled into the pit with a car setup that was ‘fastest’ during testing, but to physically demanding to drive for extended periods.

2.3. Attitude Control

An auxiliary benefit of the system is the ability to limit and control the attitude of the vehicle in pitch and roll situations. In aerodynamically assisted cars, proper and consistent location of the aerodynamic devices is critical to their performance and stability. Since the effectiveness of some aerodynamic devices is dependent on, and highly sensitive to their proximity to the ground, it is common in motorsport to run a significantly less compliant suspension than would otherwise be deemed ideal in order to preserve aerodynamic downforce. The UWashington FSAE team has encountered this compromise on various occasions, working to find an acceptable balance of

mechanical grip (grip generated due to specific suspension setup, which generally *increases* as the suspension is softened), and aerodynamic grip due to downforce. While this effect will not be quantitatively developed in this thesis, it is worthy of remark, and future investigation. It has been rumored that this mode of operation was the primary purpose for using active suspension on the Formula One cars of the late 1980's and early 1990s.

3. Background

3.1. Formula SAE

Formula SAE is a student design competition that was started 1981 by SAE International as a way to help prepare students for "real life engineering" situations. Through the years, the event has evolved from a 6 team competition held in Austin Texas to an international series with over 500 teams worldwide from 6 continents and 11 competitions annually at the time of this writing. Each team builds a new car each year they wish to compete. The premise of the competition is that a fictional company has hired the team to design and develop a prototype, open wheel racecar. Each competition is based on a points system with a maximum of 1000 points available. There are 5 dynamic (driving) events and 3 static events. The dynamic events include a 75 meter Acceleration (drag strip), Figure 8 Skidpad, Autocross, 22 km Endurance, and Fuel Economy (measured during the endurance event). The static events include Engineering Design, Cost and Manufacturability, and Business. Each team is scored according to their performance relative to the other teams. The team with the most total points wins overall. A team must be well rounded in all disciplines to do well. They must have a sound understanding of the functioning of the car as well as the ability to *build* a fast car, manage its development, fundraise, publicize, and even drive the car. Internationally, Formula SAE has gained a reputation for helping create well rounded engineers who are able to transition to post educational jobs quickly.

The University of Washington Formula SAE team was started in 1989. Over the years the team has won numerous individual awards including first places in every sub discipline except for cost. The team began competing internationally in 2012, placing 14th at the premier competition in Hockenheim Germany. In 2013 the team won its first overall victory at Formula SAE Lincoln by winning endurance and engineering design and earning 3rd place in business, skidpad, and fuel economy. 2013 also marked the first electric car entry in the new electric class. The University of Washington is one of only a handful of teams that build both a combustion and an electric car.

3.2. Project History

The University of Washington Formula SAE team began in house performance and vehicle simulation when team alumnus Gilbert Gede wrote LapSim, a quasi-steady state lap time

simulation in 2009. Written as a set of MATLAB script files It accepted several vehicle parameters such as mass, wheelbase, engine torque vs rpm, a tire model, and a course 'map' and returned various performance indicators such as lap time and speeds around the specified course. In this quasi-steady state simulation, the car advances around the track in discrete time steps according to the maximum potential of the car in acceleration, braking, and cornering situations. The maximum potential was determined by the tire characteristics and tire loadings accounting for static weight distribution and weight transfer.

Over the following years, LapSim became CompSim as the code was packaged into functions and the interface was simplified. Lap times were correlated to points at competition, and numerous analysis tools were added, such as the impact of aerodynamic downforce and drag, active drag reduction systems, mechatronic shift systems, energy usage, and brake system heating. While not as powerful as some commercial vehicle simulation packages, it's in house development has made it easy to integrate new features. As a quasi-steady state simulation, however, it is unable to predict the effect of any dynamic response changes, either due to passive transients through the springs and dampers or active control inputs. The model described in this thesis aims to bridge the gap to a functional dynamic simulation.

3.3. Model History

Because of the complex nature of full vehicle models, the process of model generation was split into manageable sub steps. This made 'sanity checks' and response verification much simpler.

First, a series of linear systems was developed using Lagrangian mechanics to derive all of the equations of motion for each system and linearized about the static equilibrium point (where the car sits in its suspension travel when not moving). Each system was expressed in terms of state space for compactness and ease of use within MATLAB. The simplest system – a single spring, mass, and damper (Figure 1) – was built and subject to several of MATLAB's built in system response evaluation tools to make sure that responses of reasonable magnitude and direction were achieved. Next, a quarter car model – two masses, springs, and dampers, representing one tire and one quarter of the chassis (Figure 3) – was developed. This system was again linearized about the same point and physical properties matching the car were assigned. Following that, a "Bicycle" model – front and rear tires, in line, from one side of the car (Figure 5) was produced. This model allowed for the inclusion of pitch of the chassis due to driver input (accelerating or

braking), wheel disturbances, or external actuators. Again, this model was linearized and its fundamental response set validated. The final step of the initial phase was the creation of a full car model. With all four tires, anti-roll bars, springs, dampers, and chassis (Figure 7) this model took into account all of the primary dynamic influences. The equations of motion, as well as fundamental response plots for these four linear models can be found in Appendix A – Dynamic Equation Derivations and Appendix B – Linear State Space Modeling.

For ease of development and expansion, a full migration to Simulink was performed. Simulink not only allowed for quick model development, and a reduction of lines of code, but also made comparisons to the analogous physical systems much more apparent. While the nonlinear systems could have been coded in script based functions evaluated with a standard solver such as ODE45, this approach would have taken significantly more time, been more difficult to debug, difficult to expand, and more abstracted from the physical system. The quarter car, bicycle model, and full car systems were completely remodeled in Simulink and a series of standard inputs was developed. Each Simulink model file solves multiple setups of the system at once, allowing for easy comparison of the ballistic, non-ballistic, and actively controlled responses to identical input.

3.4. Other Models and Software

A number of other models and modeling software exist in the commercial and proprietary market. While (assumedly) well validated and ‘pretty’ from a user standpoint, these models tend to be closed source and do not tend to lend themselves to modification and functional understanding. A brief description of some of the more common models and software is as follows.

- Adams/Car (MSC Software) is written and sold by MSC Software Corporation and is arguably one of the most popular solvers for automotive dynamics as well as general multibody dynamics. It is able to simulate full vehicle maneuvers, linear and nonlinear elements, and control systems. Some work on earlier projects for the UW Formula Team was dedicated to developing a functional Adams/Car model (to varying degrees of success). However, it requires a large set of inputs due to its comprehensive output set and does not lend itself well to model manipulations and parameter variations as does a purpose built model. For instance, the vehicle’s kinematics are not required at this stage

for top level active suspension system evaluation. For the course of this thesis, it will be assumed that this active control system will be applied to a car with at least acceptable passive kinematic performance.

- Optimum Dynamics (Optimum G) is written and distributed by Optimum G and was released toward the end of the development of this thesis and there is not much information on it available. The UW Formula SAE team has been using several of Optimum G's other software packages for several years.
- CarSim (Mechanical Simulation Corporation) is written and distributed by Mechanical Simulation Corporation and is also capable of simulation nonlinear dynamics of a vehicle around a course. It is one of the more flexible of the prebuilt vehicle modeling packages.
- veDYNA (Tesis DYNAware) is written and distributed by Tesis Dynaware. It is another fairly flexible modeling platform that is based on MATLAB. Its specialty is closed loop driver simulation and obstacle avoidance maneuvers.
- Modelica (The Modelica Association) is not actually a dynamics model, but rather a modeling language targeted at dynamic multiphysics systems.
- Dymola (Dassault Systemes AB) is the commercial implementation of Modelica.

While Adams/Car is arguably the most complex and complete model already, it is very expensive for non-student use, and requires a large (and complete) set of inputs to yield any meaningful output. While MATLAB is also expensive, there are similar, free alternatives that could be used if the Simulink models were reduced into their constituent differential equation forms. In this state, the model would be less flexible, but also more accessible.

3.5. Types of Active Suspension

There are three main types of active suspension systems, summarized in Table 3.1 below.

Table 3.1 - Active Suspension Types

Type	**Description**
Adaptive	Usually refers to very low frequency systems, capable of changing spring or damper rates over the course of several seconds.
Semi Active	Systems that provide modest frequency control, on the order of 1Hz+ but may not have control over all elements in the system at all times

	(i.e. magnetorheological damping can vary but cannot generate a force while not moving).
Fully Active	Systems capable of high frequency response (10Hz+) capable of generating an additive or subtractive force at any time.

3.6. Active Suspension Actuation Methods

There are also several different methods for exerting a controlling force upon the system, the most common of which are summarized in Table 3.2 below.

Table 3.2 - Active Suspension Actuation Methods

Method	**Description**
MR Damper	MR (Magnetorheological) Damping is a creative way to help control wheel motion. It requires far less power than the other actuation methods since its primary force generation model is passive, but its primary disadvantage is that it is only able to exert a force on bodies moving relative to one another. It is unable to make any system states changes once the system has settled.
Linear Electric Motor	Linear electric actuators are like rotary motors that have been cut down the side and unrolled. They act directly, creating a force in a linear direction without the need for ball screws or other motion conversion. Linear motors are fast and can exert a force in either direction at any time, but can be very expensive, heavy, and complex to actuate.
Hydraulic Cylinder	Hydraulic cylinders were used early on in race active suspension development (FW-14b and other Formula One cars in the early 90s) because they have the potential to exert very high forces, very quickly, with little weight. However, they also require a complex high pressure hydraulic system and expensive servo control valves.
Voice Coil	Voice coil actuation is similar in concept to a single pole linear electric motor, or can be thought of as the driver in a typical

	loudspeaker. While simple, they tend to have large variation in force output as they travel to their extents, and generally have very short working travel limits.

3.7. Controller Types

In a control system, there are several components that are typically grouped together and referred to generically as "the controller". However, in the practical sense, this refers to a minimum of two components. First, there is the mathematical controller which receives state (sensor) data, implements the chosen control scheme as series of multiplications (scalar, array, or matrix), and finally outputs the control signal(s). The second part of the controller consists of any physical hardware required to convert the controller's output signal(s) into a measureable effect on the system. This hardware may generate a force or pressure that is fed back into the system, or use some other method that is able to change the position, velocity, or acceleration of elements in the system. In this project, "controller" will almost always be used to refer the first, mathematical component exclusively.

There are many different types of control schemes, and most likely more than one of them *could* be developed and tuned to provide improvements in the system response of the vehicle. Each system has advantages and disadvantages, and there is rarely, if ever, a perfect solution. In choosing a controller, several considerations must be taken into account, including the desired effectiveness, ease of implementation, and robustness of the controller.

While the physical vehicle, and the model used in this project is non-linear, most control systems are linear. This means that most controllers are implemented as a linear combination of a set of constant coefficients that multiply the state of system before being fed back via some form of actuation. This approach generally works very well with linear systems and can be made to work with non-linear systems by 'linearizing' the model about some chosen point of operation. It should also be noted that there is no fundamental limit to the number of linearization points, and in fact, some more advanced controllers take advantage of this, shifting between the corresponding system state models. The selection of this linearization point, as well as careful consideration as to the degree of nonlinearity is important to ensure predictable, stable behavior of the system. Fortunately in the case of this project, the initial system is inherently stable. The

vehicle rests upon the ground, with more than three points of contact (in contrast to a flying vehicle or balanced two wheel vehicle). Thus, the primary concern is ensuring that no oscillations or vibrations that excite some resonant mode of the system are induced. Since a fully active system is capable of adding energy to the system at any point, it is theoretically possible to create resonant instabilities.

The two primary categories of controllers are feed forward and feedback controls. Feed forward controls are well suited to repetitive systems such as industrial automation, but because the racecar must react to unknown inputs, a feed forward scheme is not appropriate. Feedback controllers are well suited to varied and unpredictable states. The generic feedback mechanism is shown in Figure 9. There are then a number of feedback controllers that must be considered. These are briefly described in Table 3.3.

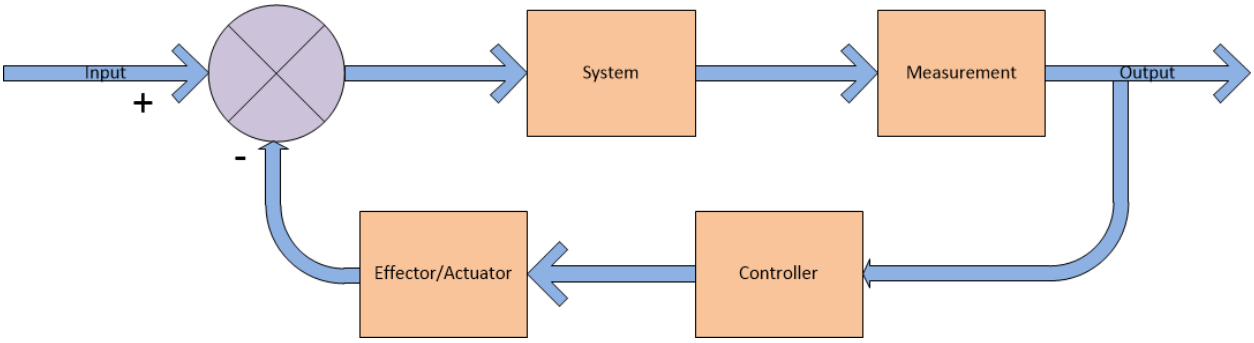

Figure 9 - Feedback Control Block Diagram

Table 3.3 - Controller Types

Type	**Description**
PID	Proportional Integral Differential controller. Feeds back a signal proportional to the difference (error) between the measured signal and desired state or set point, the time integral of the error (how long the error has remained), and the derivative of the error. A single PID controller is capable of controlling a single input, single output (SISO) system. Variations of this controller exist as P, PI, and PD. The vehicle

	could be controlled by using multiple PID controllers acting on each wheel. Simple and effective, but limited to SISO systems.
LQR	Linear Quadratic Regulator. An optimal, state feedback controller that is designed to optimize the control effort vs cost (usually power). It is capable of controlling Multi Input, Multi Output (MIMO) systems. The LQR may be setup to control multiple vehicle aspects (i.e. pitch, roll, and wheel motion). For certain systems meeting certain constraints, stability is guaranteed. Very flexible but requires complete system model.
LQG	Linear Quadratic Gaussian control. Closely related to the LQR controller, the LQG includes a state estimator for systems with missing state variables, and/or process and measurement noise. This controller is a good next step for this project when it is physically implemented on a real vehicle. Same requirements as LQR, but also needs information about measurement and process noise.
H-Infinity	A fairly complex and difficult controller targeting MIMO systems and stability with guaranteed performance. A very good mathematical system model is needed, but does not handle some non-linearities such as saturation well.
Gain Scheduling	A broader class of controller, that changes between multiple controllers or even types of controllers depending on the current system state. A properly setup gain scheduling scheme is capable of controlling very nonlinear systems over broad operating ranges.

Because of its ability to control MIMO systems, relative simplicity, and readily available design tools (such as those included with MATLAB), an LQR control scheme has been selected for initial evaluation in this project.

An LQR controller is considered one of the fundamental problems in control theory. It is an "optimal" controller in that its purpose is to control a dynamic system with minimum cost. "Cost" is defined by the engineer developing the controller but is always a combination of the

system state inputs. Some inputs may be bound by physical limitations of maximum force, or inaccessibility (the controller cannot move the ground in the context of this project, and attempts to move the ground are assigned very high cost). In addition, depending on problem setup, not all of the states are measureable (observability). As a quadratic cost minimization problem, the solution to the LQR problem uses the error of each state relative to zero to produce a strategy that minimizes those weighted errors with the least possible cost.

For this project, the state variables were chosen to be the position and the velocity of each mass (including rotational pitch and roll). These states can all be measured either directly or indirectly by integration of accelerometer data and/or position between masses (via linear potentiometer). The system inputs are the ground position and velocity at each corner, actuator force at each corner, and external torque applied to the chassis about the pitch and roll axis that model weight transfer due to lateral or longitudinal acceleration.

3.8. Existing Systems

Even though active suspension technology has been around for several decades, its use and implementation is still rare. However, there are a number of consumer vehicles that employ it. Mercedes Benz has used systems of varying complexity as have Toyota, Audi, Range Rover, Volkswagen, BMW, Citroën, and several smaller makes. The systems have seen varying degrees of success, but have been limited to top line models and in most cases focus on ride comfort rather than performance. Adaptive damping systems are generally the cheapest and are by far the most common type. Following that, are low frequency (3-4Hz) systems, and finally the scarce high frequency (>10Hz) fully active system.

There are two particularly well known active suspension control methods that have been around for a many years but are still used frequently today. The most common method is called skyhook in which the force actuator tries to match the force that would be generated by a hypothetical damper connected between the damper and the “sky” (effectively chassis velocity control). While this simple and tried and effective way of providing some control over the response, *it does not* allow for weighting of multiple system states simultaneously, nor does it allow for control of effects that are coupled across the car. Skyhook control is most frequently implemented as a comfort improving system. The second method is called groundhook. Like skyhook, this method involves a virtual damper, but between the wheel and the road. In theory

this approach should help keep the tire in contact with the ground, but in practice seems to yield high forces and exaggerated chassis motion.

3.9. Notes on Improvements and Marginal Gains

A concept that should be understood throughout the course of this thesis is that in the world of racing and racecars in the modern era, performance gains are very rarely more than a couple percent. Professional teams have been known to spend millions of dollars to go a few tenths of a second faster over a minute and a half lap. Thus, it should be understood from the onset that this project is in no way trying to achieve 'perfect' system response and control. While not even mathematically possible (since it would require the use of an infinite force), such a system would be extremely impractical due to the magnitude of the required forces. The goal is to provide a noticeable improvement in any part of the system response that either directly or indirectly allows the car to navigate its course more quickly. Because of this, the project should be considered worthwhile and a success if it finds control strategies by which system responses could be improved by as little as 5%.

3.10. Disclaimers

There are several important disclaimers to consider when evaluating this project.

First and foremost, the goal of this project is to develop a full vehicle, dynamic model for the design of an active suspension controller, it is not the goal to *fully* design the controller itself. Granted, some controller design was required in order to exercise the model and as proof of concept, but in no way should the controller design be considered as complete or optimal.

In addition, this project is *not* a study of pure, theoretical controls. Few mentions of analytical stability, or any proofs of control theory are provided. The core principles of the project are tied to applied dynamics, then using established control methods. If I were to repeat my undergraduate and graduate educations, I would probably have taken the opportunity to study control theory more rigorously. However, after completing this project, I feel that despite not having much if any formal controls education, an interesting, exciting, and functional system was designed.

An interesting aspect of this project is an impression of nearly endless scope. While many projects would have picked one specific detail of *either* the dynamic development *or* the controls

aspect, this project looks at several aspects of each. Part of this is due to the long duration of this project, and also to the relatively undocumented, complexity of the system. There were many points during this project when the scope had to be decreased to an appropriate magnitude. Thus, there are several conceptual branches that have been left for future development, and many more that were briefly considered but not developed in depth either due to relative unimportance or misalignment with project targets.

4. Model Limitations

4.1. Simplifications

A typical approach to model simplification is to reduce the scope of the model – to look at relatively small subsets of the system. There are additional simplifications that can be made, such as neglecting the effect of the damping of the tire since it is generally accepted to be several orders of magnitude smaller than that of the 'chassis' dampers. Many models are run with relatively simplistic inputs such as pure step and impulse. However, in these cases, if tire damping is *not* neglected, then neither of these inputs yield valid results since the derivative (velocity) of the input is infinite, and thus the force developed in the tire damper is also infinite. Neither of these cases are acceptable, so several 'well-conditioned' inputs were contrived as described in Appendix G – Bump Profile Development.

4.2. Mathematical Limitations

While the model proposed in this thesis is not constrained by many mathematical limitations, there are a few restrictions. The primary restriction is solution time. The more accurate and complete the system model becomes, and as more non-linearities and discontinuities are introduced (such as the inclusion of friction and hysteresis in particular), the more difficult it is for the iterative numerical solver, ODE45 in this case, to converge. Since damping is included in both the chassis and tire masses, numerical derivatives can be problematic as they approach infinity for certain input conditions such as the classical step input. These conditions can sometimes be avoided by taking into account an increasing number of physical factors such as the semi-cycloidal profile taken by the wheel as it encounters an input such as a sharp step. However, at some point, the complexity incurred by the inclusion of increasingly trivial effects is more detrimental to the final usefulness of the model than their explicit exclusion due to the law of diminishing returns.

4.3. Physical System vs Model Limitations

There are a number of increasingly minor effects that are not included in the model. As previously mentioned, the 'true' path of the wheel center is not necessarily represented perfectly for all input cases, however, if a true profile is required, it is possible to modify the input to effectively map the desired motion profile to the singular contact point of the tire as modeled. In

addition, many of the minor frictional and hysteresis effects (small suspension member rotations about bearings and bushings) have been left out because their overall impact is thought to be several orders of magnitude smaller than that of the primary elements. Finally, the model is limited by the accuracy of the input parameters. In some cases, particularly for the tire damping coefficient, empirical data is very difficult to acquire, and is left out of many other, simpler models.

4.4. Model Assumptions

The model proposed in this thesis has a number of assumptions. First of all, it is assumed that the chassis behaves as a rigid body. This is justified by the fact that, for the UW Formula SAE car, the chassis torsional stiffness projected to the tire contact patch is approximately an order of magnitude greater than the chassis spring rate. The model also assumes that all physical properties are known – masses, dimensions, spring rates, and damping coefficients.

4.5. Setup Assumptions

The full system model contains 7 degrees of freedom – Chassis Pitch, Roll, and Vertical Displacement, and the Vertical displacement of each wheel. For the purposes of this model, neither the lateral or longitudinal velocities, nor the vehicle yaw are calculated. The purpose of this model is not to look at the response of the vehicle to any external input, but rather to provide a mechanism for predicting and tuning the required parameters for an active suspension system that acts by exerting a variable force between the chassis and wheel. It is assume that the motion between the chassis and wheel is constrained to be in the vertical ±z direction. Joint compliance and member flex (in the x and y directions) are assumed to be small relative to wheel motion and are outside the scope of this model. In addition, all ground displacement inputs to the tires are modeled as fixed profiles over which the car travels over *at constant speed.* Since the model does not have a longitudinal degree of freedom, this approach allows the ‘travel’ of the car to be abstracted to vertical ground displacements in the time domain.

5. Performance Evaluation

5.1. Concepts and Definitions

When evaluating an active suspension system, careful consideration must be placed on what exactly the controller should be trying to do. As previously mentioned, the two main, general targets are handling performance and comfort. While not necessarily mutually exclusive, the basis of each system is very different. In the case of handling optimization, the interaction of the tire with the road surface is the most important phenomena. On the other hand, comfort driven systems generally focus on minimizing the acceleration or jerk transmitted to the driver. Since the target vehicle in this project is a Racecar, all effort is placed in improving handling.

While the scope of this project does not include a comprehensive study into tire theory, it is important to understand several key properties and phenomena. Tires and their characterization are an extremely complex affair. Despite having been around for well over 100 years, there are still numerous researches and engineers spending millions of dollars annually to develop faster, longer wearing, lighter, and more predictable tires. In addition, tire strategy can make or break a racer's weekend, and there is still no "unified tire theory". Thus, most aspects of tire evaluation rely on a battery of empirical tests. The saving grace of this complexity is that a single tire, once characterized on a testing machine, tends to behave predictable and repeatable, and most tires follow similar behavioral trends. These trends can be encapsulated in one of a few available empirical models. These models fit the trends well, but have no explicit tie to any physics or chemistry principles. It should also be noted that tire performance is dependent upon *many* different effects, including but not limited to type (radial, bias ply), rubber compound, shape, tread pattern, normal load, camber angle, inflation pressure, speed, and temperature. To further complicate the situation, many of these parameters are interdependent, such as inflation pressure and temperature. One of the foremost experts in tire testing, Calspan (Calspan Corporation) generously donates a full set of raw data for each of the tires available to Formula SAE teams. All tire data and or plots not otherwise cited come from the raw data they provide and analyzed by the UWashington team.

To begin with, tires are *highly* non-linear. The elementary physics view of frictional force being directly proportional to normal force should be all but thrown out. While the force generated by a

tire usually increase with an increased application of load, this effect diminishes and sometimes inverts at very high loads. This is usually referred to as tire progressiveness. This effect can be seen in Figure 12. In addition, certain aspects of a tire behave like a spring. In order for a tire to generate force, there must be deformation of at least part of the tire (usually the contact patch and/or sidewalls). Because of this, a tire must be rotated about the vertical Z axis *beyond* the tangent of its direction of travel to generate a lateral force. This is referred to as Slip Angle (SA), typically measured in degrees. In addition a tire must be spun about the hub axis *faster or slower* than the ground speed to generate a longitudinal force. This is referred to as Slip Ratio (SR), typically measured in percent over or under ground speed. These two principles are shown graphically in Figure 10 and Figure 11. The dependence of lateral grip vs normal load and slip angle or slip ratio can be seen in Figure 12 and Figure 13. In summary, tires are extraordinarily complex. Their nuances are well beyond the scope of this project and several very knowledgeable folk including Paul Haney (Haney) and Hans Pacejka (Pacejka) have written volumes about them. Further explanation is relegated to those resources.

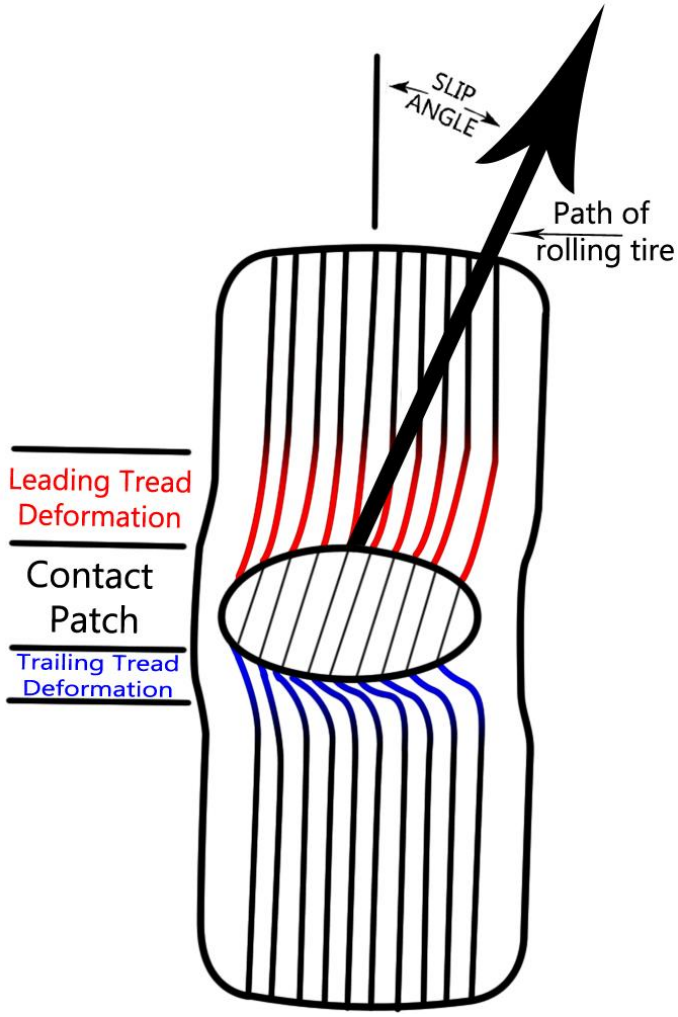

(Mouzouris)

Figure 10 - Tire Deformation and Slip Angle

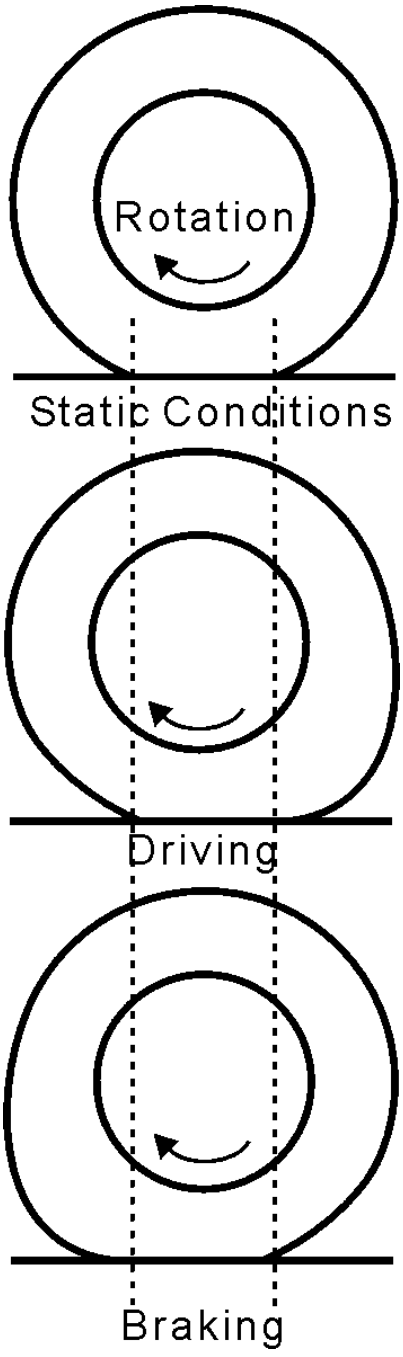

(Haney)

Figure 11 - Tire Slip Ratio, Zero, Positive, and Negative

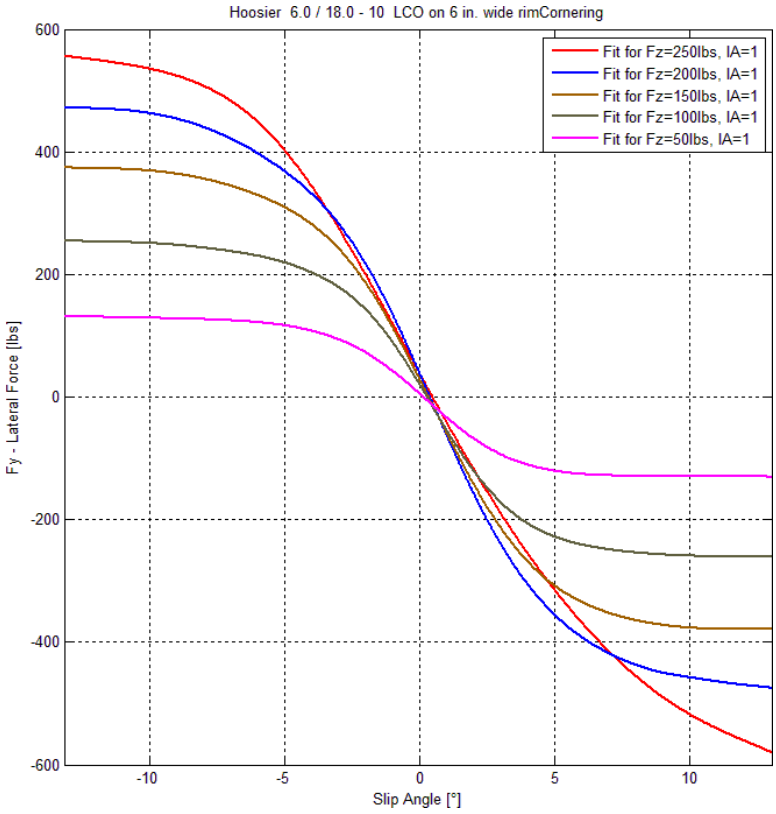

Figure 12 - Example Empirical fit of Lateral Force [Fy] vs Slip Angle [SA] at different Normal Loads [Fz] at a Fixed Inclination Angle [IA] for an FSAE Tire

Note the Fy fit lines do not increase linearly with Fz normal load.

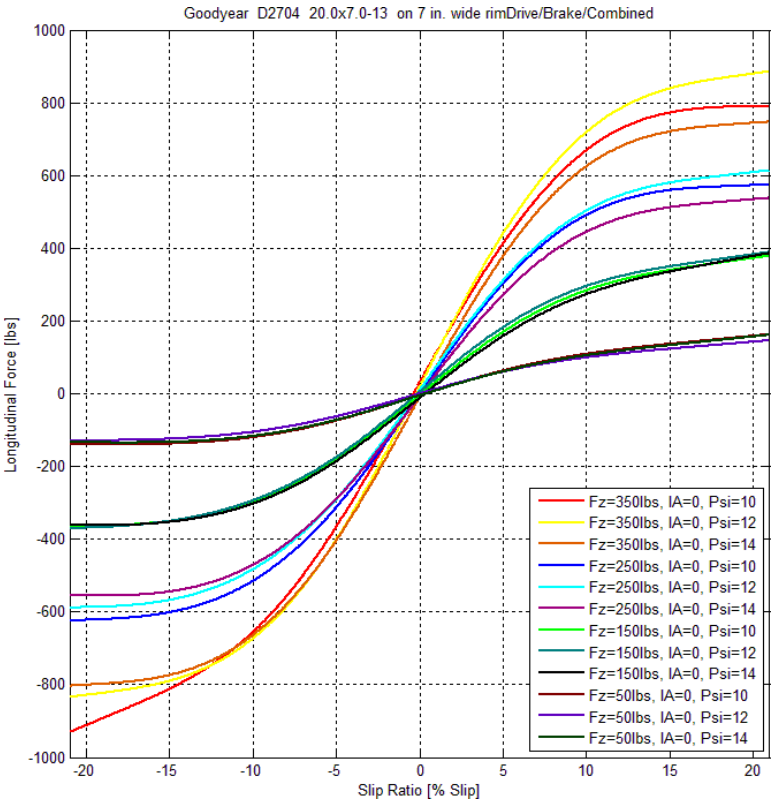

Figure 13 - Example of Longitudinal Force [Fx] vs Slip Ratio [SR] and Normal Load

Fundamentally, *any* directional change (cornering, braking, and accelerating) must be induced by forces generated by the tires. In four wheeled vehicle, and specifically the UWashington FSAE car, there is nothing more than four small contact patches (the area between the tire and the ground) not much larger than the area of an outstretched adult hand (15x15 cm) responsible for generation all direction changing force. Thus, it is critical than any system aiming to improve handling focus first on utilizing as much of the available tire performance possible. For the remainder of this project, all references to "force generated by the tires" specifically represents *direction changing* force – in other words, forces acting in parallel to the ground, in the (x, y) plane.

For the purpose of this project, three major performance affecting effects will be considered.

5.1.1. Wheel Contact Time

Though it might seem obvious, it should be explicitly stated that any time a tire loses contact with the ground *for any reason*, it then becomes incapable of generating force. There are a

number of instances in which such a separation may occur such as the ground receding from under the car very quickly (drop off or pothole), an upward bump sufficiently large to launch the vehicle into the air, or suspension setups that are prone to lift one or more wheels during lateral cornering.

5.1.2. Tire Load Variation

Another property of the pneumatic tire is that it inherently experiences hysteresis. Again, the specific details of how and why are far beyond the scope of this project, but it is asserted that because of this hysteresis, any rapid change in normal load, slip angle, or slip ratio causes a loss of force *greater* than would otherwise be predicted by the figures presented earlier in this chapter. In other words, a tire with a constant load is cable of generating more work (force over a distance, i.e. a force over time) than a tire with a periodic variation of normal load *even at the same average load*.

5.1.3. Power Usage

While not a parameter that will be explicitly presented within this thesis, an important consideration for future development is the power usage of any control scheme. It is also important to note that power cannot be calculated *only* by the classical approach of $Power = \frac{Work}{Time}$, where $Work = Force \times Distance$ (or $Power = Force \times Velocity$). While these relationships are of course true, they do not suffice to fully describe the system. In order to calculate the power consumed by the system, the force generated by the actuator and the specific design of the actuator are required. In motor design, output force is proportional to current flow consumed by the actuator. Thus an actuator 'force constant' can be calculated in terms of force per unit power (Newtons / Watt in this case). Again, this parameter depends on the design of the specific actuator, but can be used to calculate the power draw of each actuator, even when providing a constant force (where the classical power calculations would indicate zero power used). The provisions for power calculations have been included in the MATLAB code, but since the design of the actuator is beyond the scope of this project, will not be used. Lacking this information, it must suffice to say that the system should use the least power possible to achieve acceptable performance. This could be thought of effectively as controller efficiency and could be part of the future controller optimization described in Future Work.

5.2. Quantification Methods

During the course of model development and various qualitative 'improvement' evaluations, a more explicit set of methods needed to be developed. Some approaches, such as the Load Fluctuation Rate, were developed by other researchers, while others have been created specifically to the needs of this project.

5.2.1. Average Disturbance Magnitude Reduction

The primary quantification method was developed through careful consideration of what effect the 'ideal' controller would have on the system. Thus, depending on which state is chosen for error minimization when constructing the controller, a corresponding decrease should be seen in the system response between that state and the chosen reference. This may be quantified by taking the average of the difference of the absolute value of the passive and the active response over the time duration of interest. This average value is then normalized by the maximum magnitude of the input disturbance. An RMS deviation was not used in order to preserve the sign of the difference.

$$ADMR = \frac{mean(|Response, Passive| - |Response, Active|)}{\max(|input|)}$$

For the purposes of this project, the time duration was considered to begin at the start of the input disturbance and end when the chassis position (Zc) was within 5% of its equilibrium position. A larger (positive) number indicated increased performance, negative numbers indicate decreased performance.

5.2.2. Load Fluctuation Rate

Another method used for the quantification of the effectiveness of the control scheme is the load fluctuation rate as proposed by (Sugasawa) which is effectively a scaled RMSD between the ground and wheel displacements.

$$R = \frac{k_1}{(m_1 + m_2)g} \times \bar{\sigma}$$

Where

k_1 = vertical tire spring rate

m_1 = unsprung mass

m_2 = sprung mass

g = gravitational constant

$\bar{\sigma}$ = root mean square of $X_g - X_t$

In this situation, a *smaller* value of R is preferred, indicating a smaller load fluctuation rate.

5.2.3. Contact Patch Force Standard Deviation

A final method for evaluating the effectiveness of the controller is simply the RMS deviation of the tire contact point for each model.

$$RMS(Force_{Contact\ Patch})$$

This method allows for a direct quantification of the tire load variation, which is known to decrease overall vehicle grip potential (Pacejka). In this case, a *smaller* RMS deviation indicates an increased performance potential.

5.2.4. Ballistic Time of Flight Reduction

Finally, a quick comparison between the passive and active systems can be accomplished by comparing any change in the amount of time the wheel(s) are not in contact with the ground. Any increase in contact time increases the amount of time the tire is capable of generating force, and thus increased the maximum performance potential of the tire.

6. Model Development

The models and results in the following chapter are all for passive systems, with no actuator or controller input. This chapter covers the development and results Linear Models, Non-Linear Non-Ballistic Models, and finally the Non-Linear Ballistic Models.

6.1. Linear Models

In order to split the development into manageable chunks, the model was progressively expanded and checked to ensure agreement with previous models. The linear models were created by beginning with the simplest dynamic system of a single spring mass and damper, then extending to quarter car model, then to the bicycle model, and finally to the full vehicle. The resultant equations of motion can be found in Appendix B – Linear State Space Modeling.

In the context of this project "linear" specifically refers to the characteristics of the springs and dampers throughout the system. A linear spring is one which follows Hooke's Law of $F = -K \times X$, where X is the displacement from equilibrium of the spring and K is constant. A linear damper follows $F = -C \times \frac{dX}{dt}$, where C is constant and dx/dt is the velocity of the damper shaft relative to the body.

6.1.1. Single Mass Test Case

To test the setup of Lagrangian derivation, inputs, and plotting, the classical dynamics case was developed. The response to step and impulse inputs mirrored the typical single spring-mass-damper system that would be encountered in any elementary system dynamics class. In this example, relatively arbitrary spring and damper coefficients were chosen to loosely model an under damped system since the single mass model has no analogous system on the physical car.

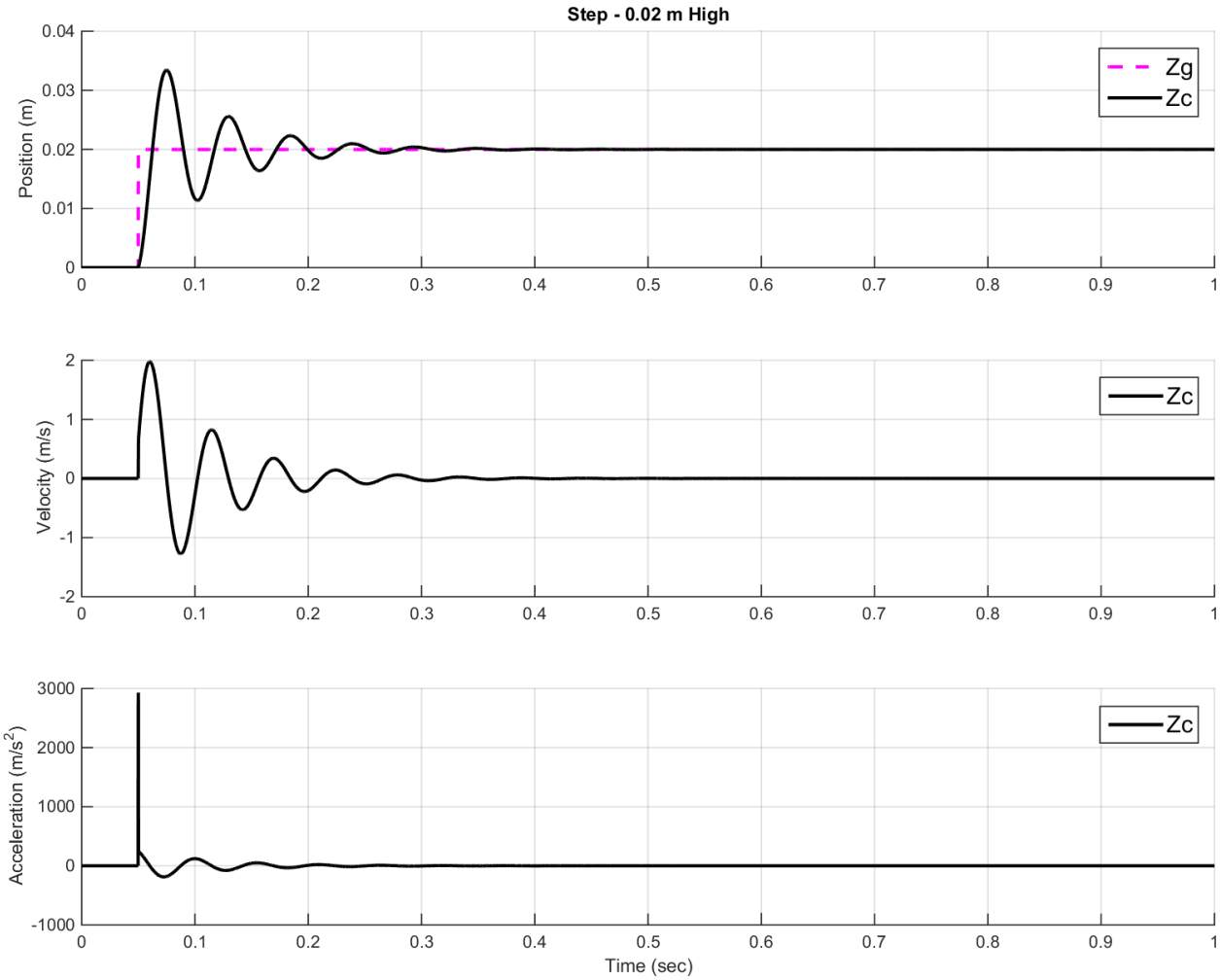

Figure 14 - Linear Single Mass Test Case Model – StepUp

6.1.2. Linear Quarter Car

Next, the double spring-mass-damper system (also commonly referred to as a quarter car model) was implemented taking into account one wheel and ¼ the vehicle sprung mass. This is generally considered the simplest model that can be used to approximate the dynamics of an actual vehicle.

The response of the quarter car model to step and impulse inputs also imitated a 'typical' elementary system dynamics course example with both masses oscillating then settling about equilibrium at the same frequency with a measurable phase lag.

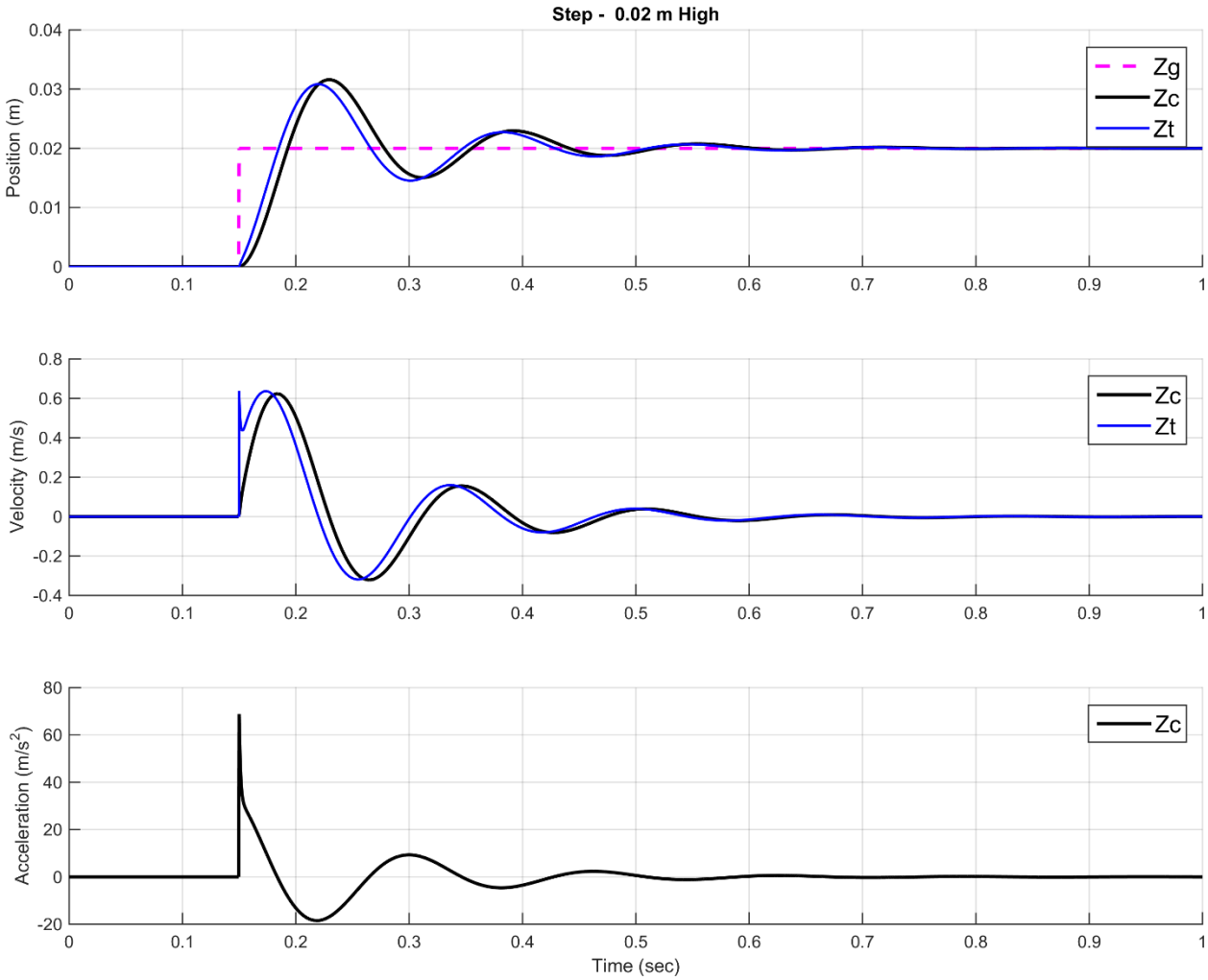

Figure 15 - Linear Quarter Car Test Case Model – StepUp

6.1.3. Linear Bicycle Model

Next, the 'bicycle model' was implemented taking into account one front and one rear wheel and ½ of the vehicle sprung mass.

This model response falls outside of the scope of most entry level system dynamics courses. However, it should expected that if both wheels are excited by exactly the same input, and if all of the masses, spring rates, and damping coefficients are the same, the system should behave roughly like a larger double spring-mass-damper system as seen in Figure 16.

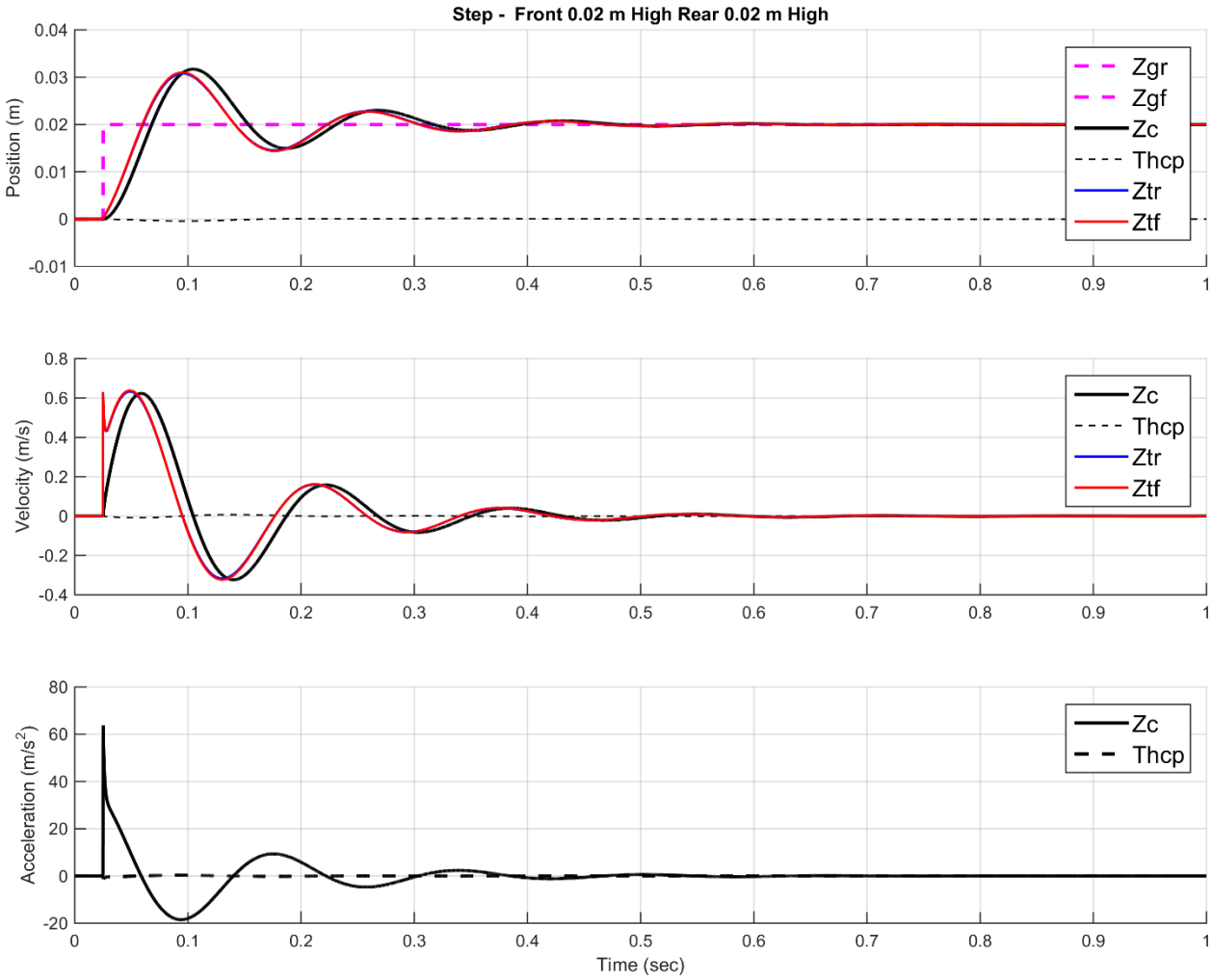

Figure 16 - Linear Bicycle Test Case Model – StepUp

6.1.4. Linear Full Car

Finally, the full car model was created taking into account all four wheels and the entire vehicle sprung mass.

The setup and response of this system is certainly beyond the scope of entry level dynamics classes, but in certain states and excitations, like the bicycle model, should behave in relatively intuitive and predictable ways.

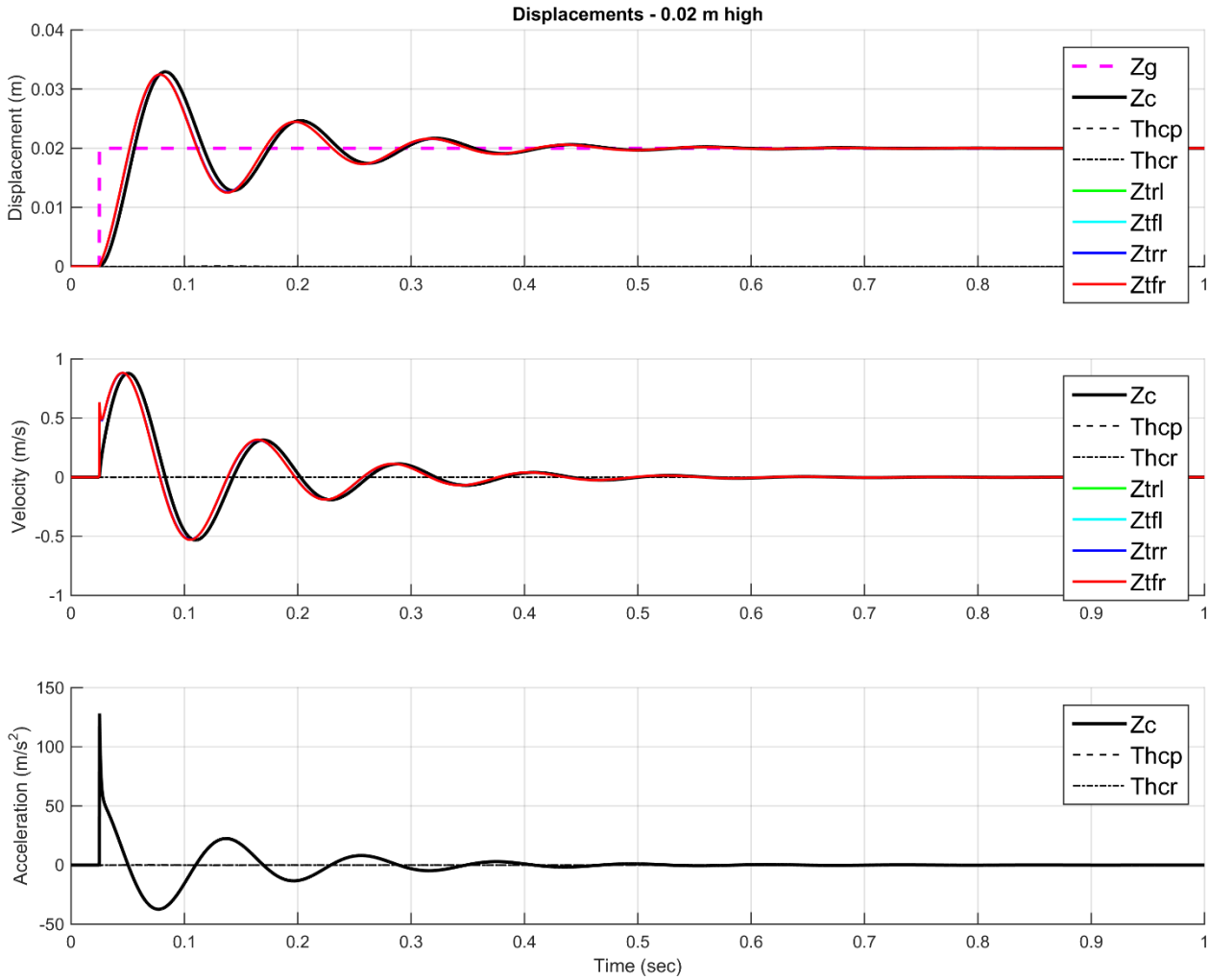

Figure 17 - Linear Full Car Test Case Model - StepUp

6.2. Non-Linear, Non Ballistic Models

After the linear models were created, the relevant non-linearities were included. In the context of this project, "Non-Linear" specifically refers to the characteristics of the springs and dampers, in addition to any discontinuities in either motion or forces. These discontinuities can be caused by many things, but particularly by the physical travel limits of the suspension or by tires leaving contact with the ground temporarily. In some cases, such as the chassis dampers, this inclusion was as simple as replacing a constant coefficient with a lookup table in Simulink. In other cases, such as the ballistic wheel trajectory, entire new subsystems were created. Non Ballistic models

do not permit the tire to lose contact with the ground, thus implying the ability for the ground to pull down on the tire.

It is important to note that, by design, the non-ballistic Simulink mode *is still nonlinear* – with nonlinear damping characteristics, It is simply constrained to prevent the tire from losing contact with the ground (i.e., the ground may 'pull' the tire down). While the non-ballistic case is thus not particularly representative in some cases, it is theoretically a simpler model and thus easier to solve.

The difference in damping force between the linear and nonlinear damping is shown in Figure 18. Values to the right of 0 m/s represent compression damping, while values to the left represent rebound damping. The 'knee' in both the compression and rebound curves represents the internal transaction between 'high' and 'low' speed damping settings as determined by the manufacture of the particular shock currently in use by the UWashington Formula Motorsports team (Öhlins TTX25 Mark II). The damping curves specific to that shock may be found on the Öhlins website (Öhlins USA).

The linear damping coefficient was chosen to approximate the slope of the low speed region of the Öhlins dampers while still passing through the origin by necessity. Presumably this is where the model will spend most of its time after initial impact as seen in Figure 19.

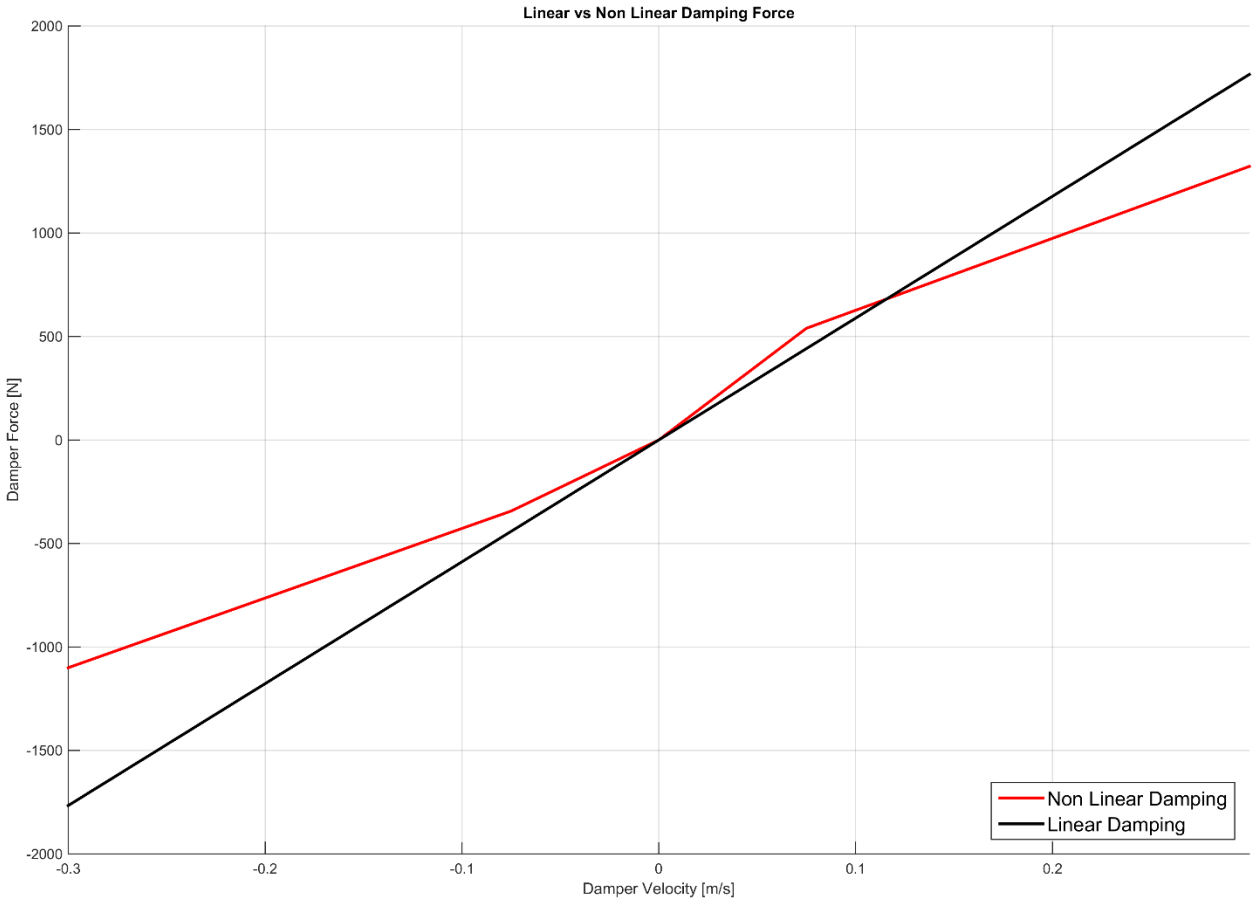

Figure 18 - Linear vs Non Linear Damping Force

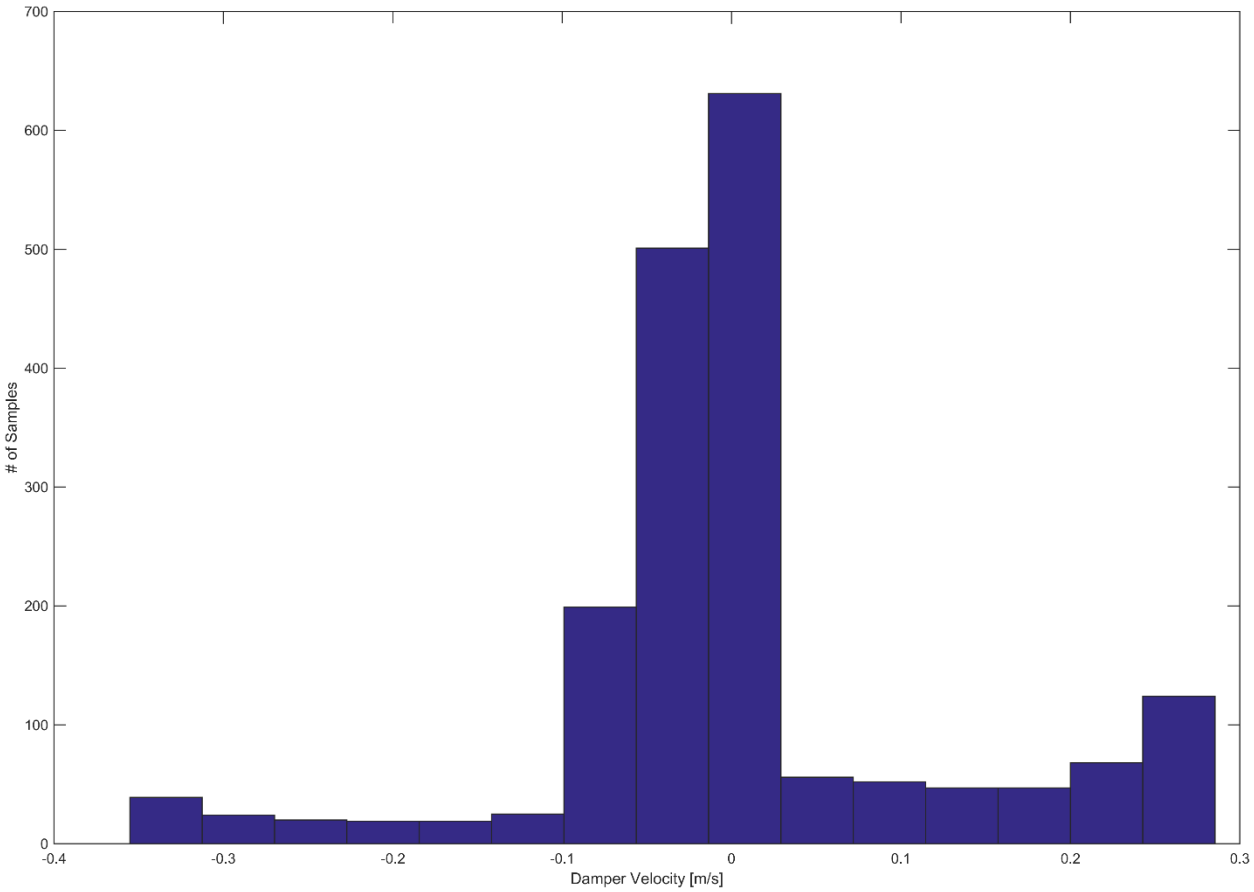

Figure 19 - Quarter Car StepUp Damper Velocity Histogram

6.2.1. Comparisons

Figure 20 through Figure 22 show the impact of the nonlinear damper on the quarter car model. The notable trajectory difference in all three cases is explained by the damping force characteristics of the nonlinear damper. Since the damping force of the nonlinear damper drops off at higher velocities (digressive damping), less energy is dissipated during the initial high velocity 'impact' resulting in a greater total displacement and settling time. While this effect seems like the opposite of what is typically desired when designing damped systems, it should be noted that in the relatively uncommon *but possible* extremely high velocity impact, correspondingly extremely high forces would be generated by a damper that did not have digressive force characteristics. This allows for significantly smaller and lighter suspension components to be specified. Like most engineering decisions, the tradeoff between damping performance and loads (vehicle weight) is one that must be made by the vehicle designer.

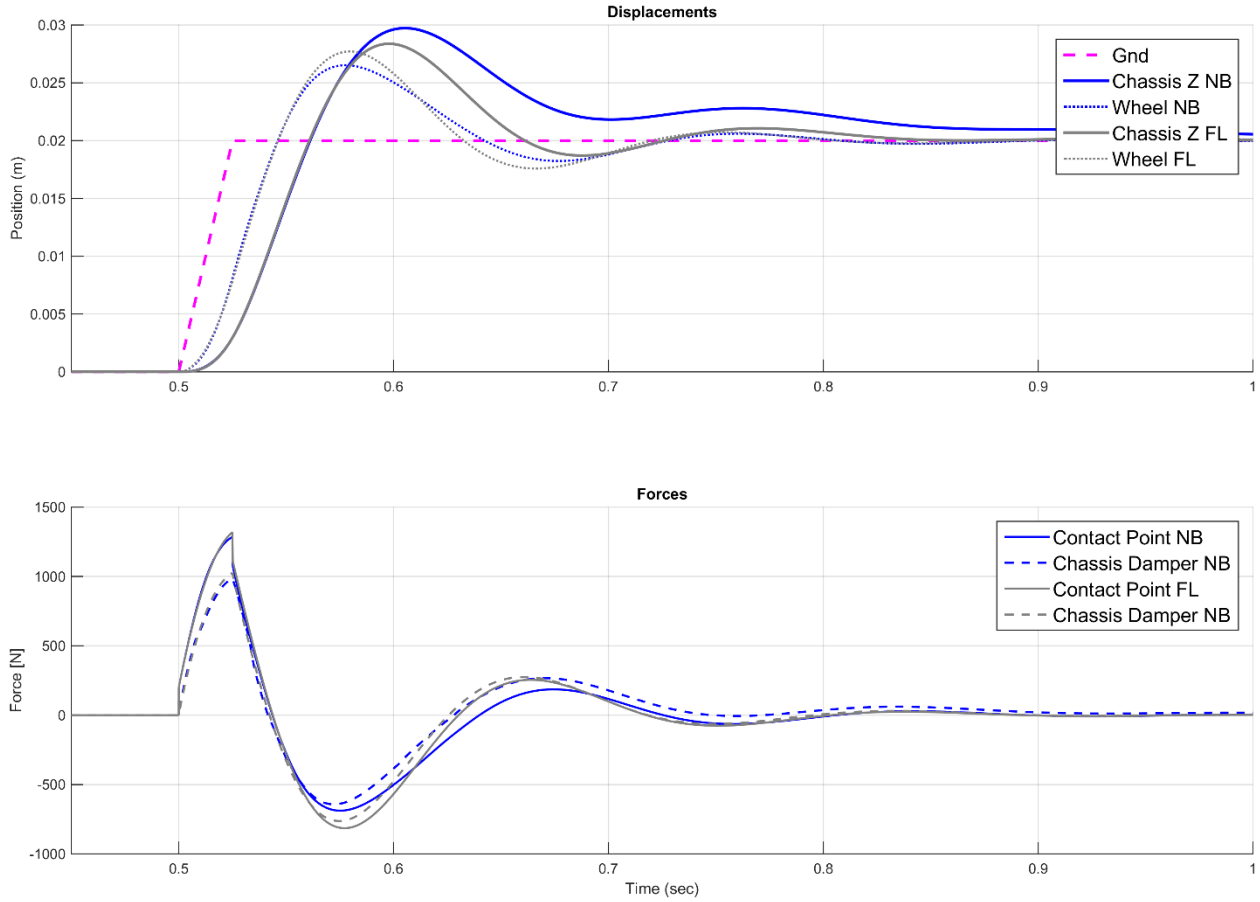

Figure 20 - Quarter Car StepUp Fully Linear vs Non-Ballistic Response

(NB = Non Ballistic Model, FL = Fully Linear Model)

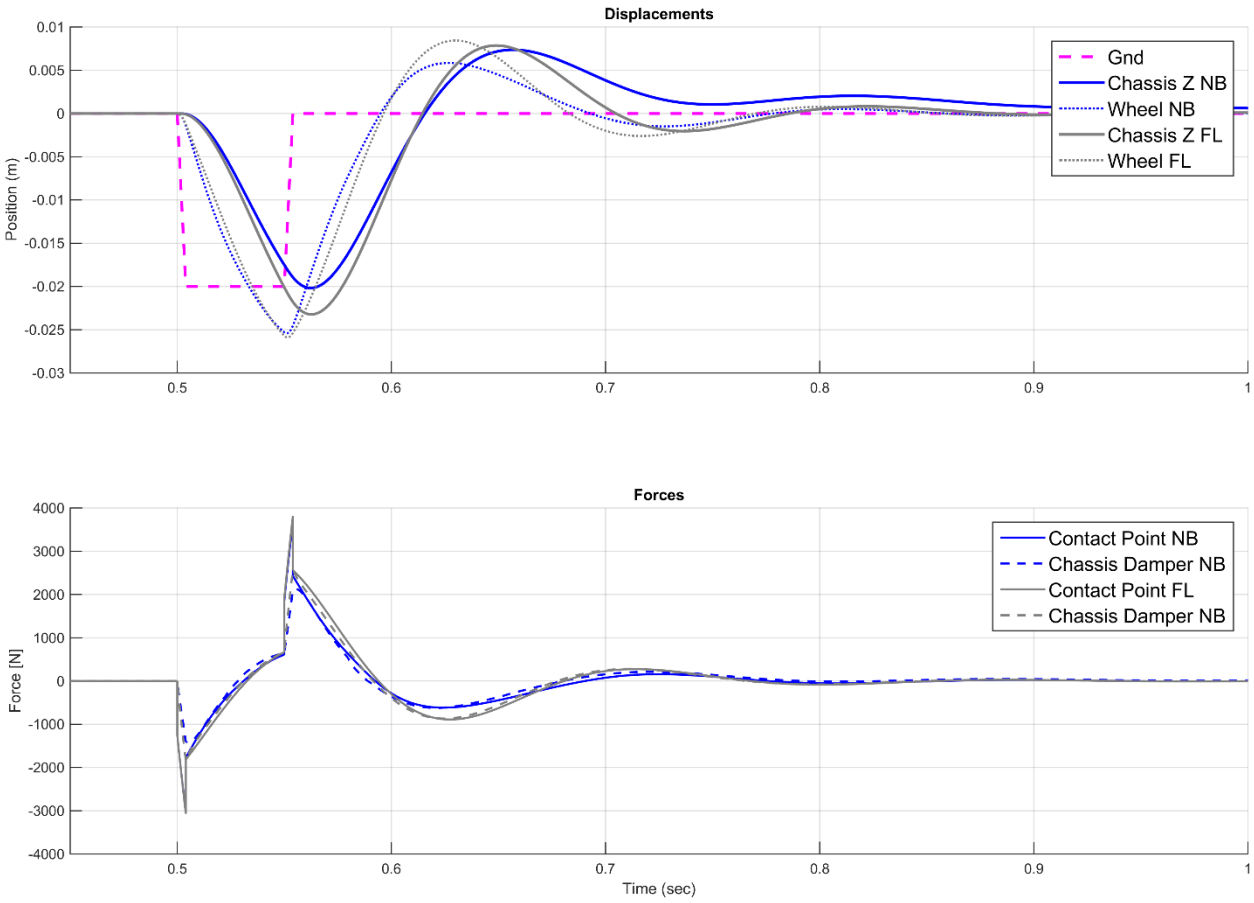

Figure 21 - Quarter Car Pothole Fully Linear vs Non-Ballistic Response

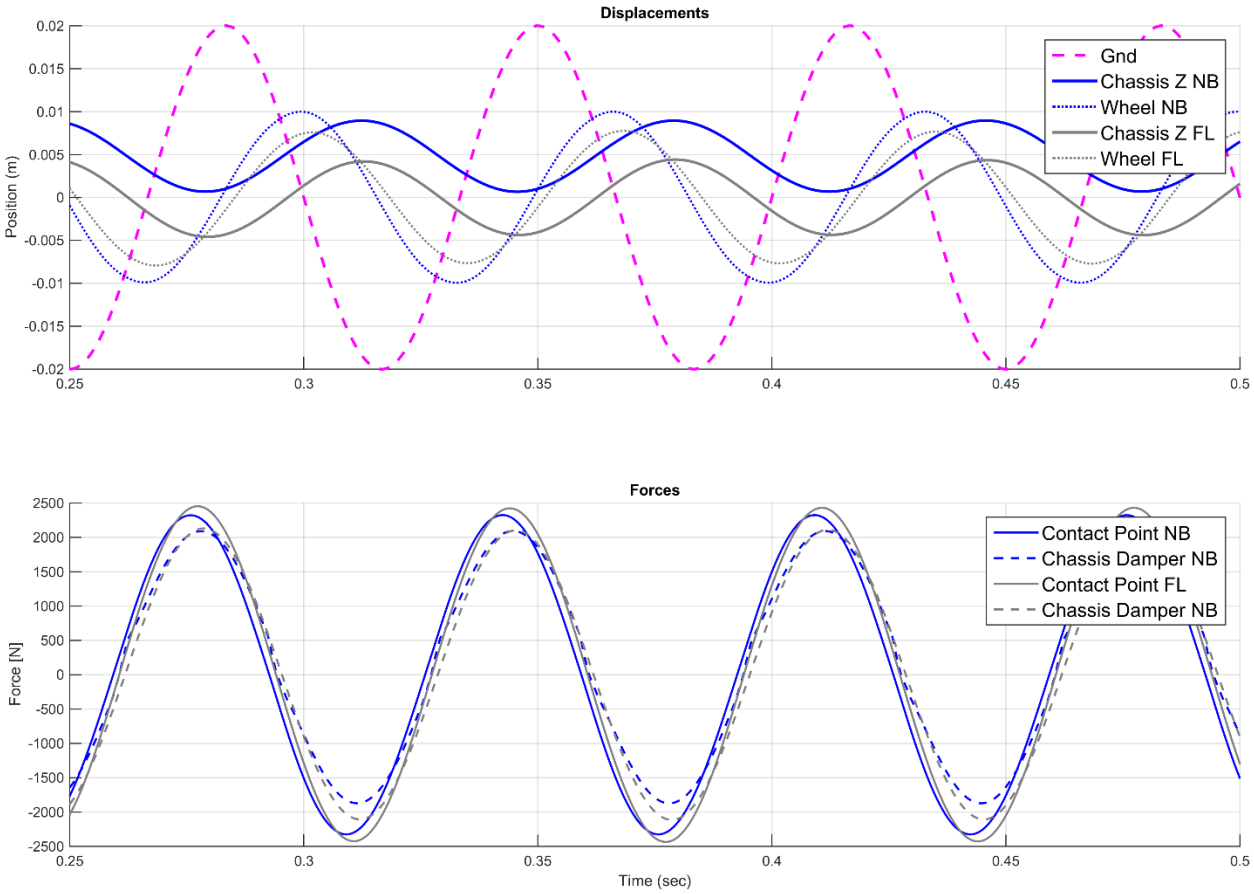

Figure 22 - Quarter Car 10 Hz Sinusoid Fully Linear vs Non-Ballistic Response

6.3. Non-Linear Ballistic Models

The nonlinear system models were developed in Simulink using the equations of motion that were generated by the Lagrangian approach for the linear models as a starting point.

In order to do a first order validation of the models, relatively simple input cases were tested which corresponded to well ‘known’ responses of simpler models. These cases include StepUp, StepDown, and Sawtooth (impulse). In addition to the classical inputs, a series of inputs emulating common physical world conditions was developed including a ‘pothole’, two sinusoidal frequency inputs (one above and one below the system resonant frequency), and a frequency sweep (chirp).

6.3.1. Non-Linear Quarter Car

The quarter car model responded predictably to the three input types based on system responses that would typically be seen in an introductory system dynamics class. The non-ballistic model closely follows the linear model, but the ballistic model starts to show a significant response difference as the tire mass is 'launched' into the air following the initial step.

In Figure 23, it can be seen that the ballistic and non-ballistic cases nearly identically overlay each other except for one brief period at about 0.57 seconds when the tire leaves the ground momentarily. While this event has little impact on the final trajectory of the tire *or* chassis, there is a notable deviation in the force seen at the tire contact point.

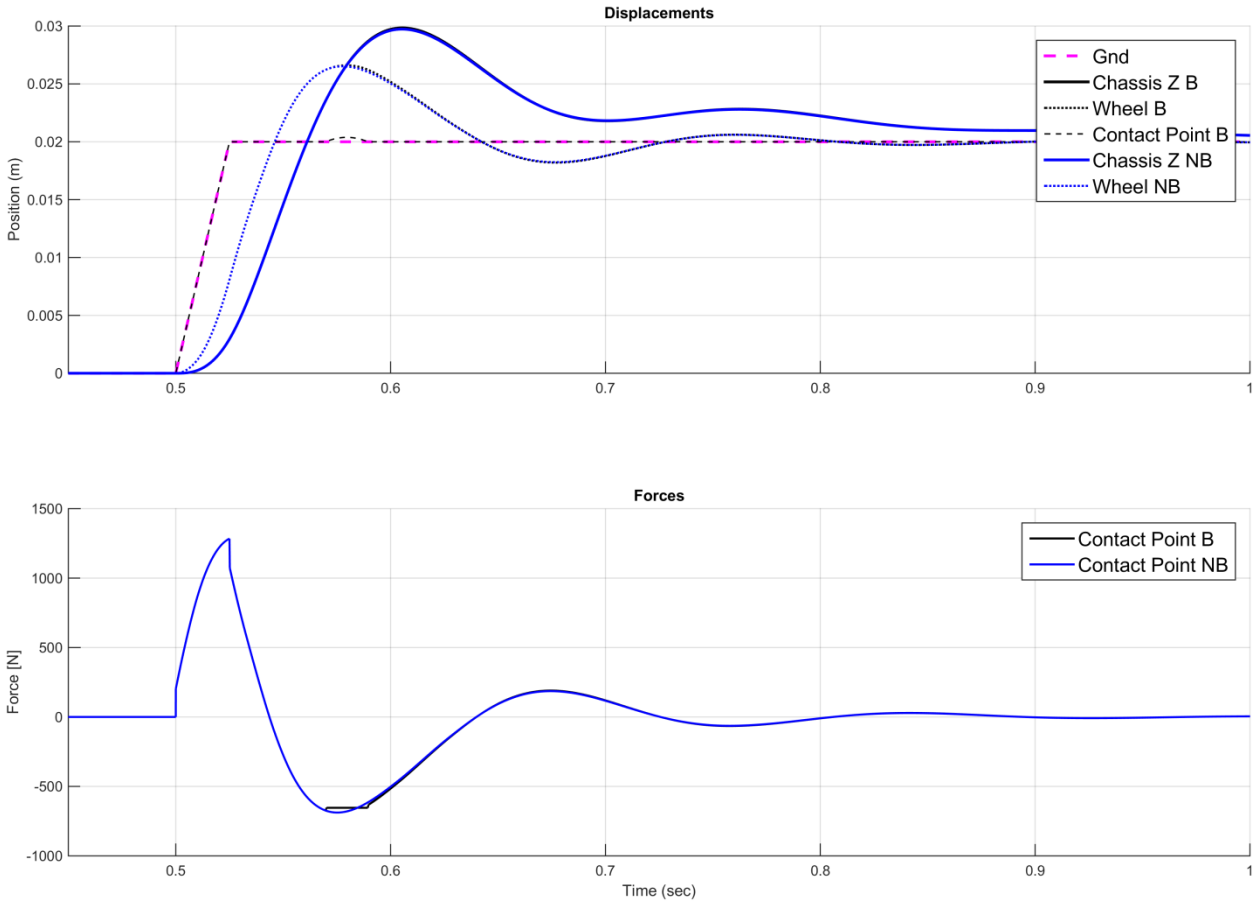

Figure 23 - Non-Linear Quarter Car StepUp Response

(B = Ballistic Model, NB = Non Ballistic Model) Note: Some curves overlay each other identically.

In Figure 24, the nature of ballistic case becomes significantly more noticeable as the tire ‘falls’ off the edge of the step. The resultant wheel and chassis trajectories are significantly impacted by this ballistic event as is the contact point force.

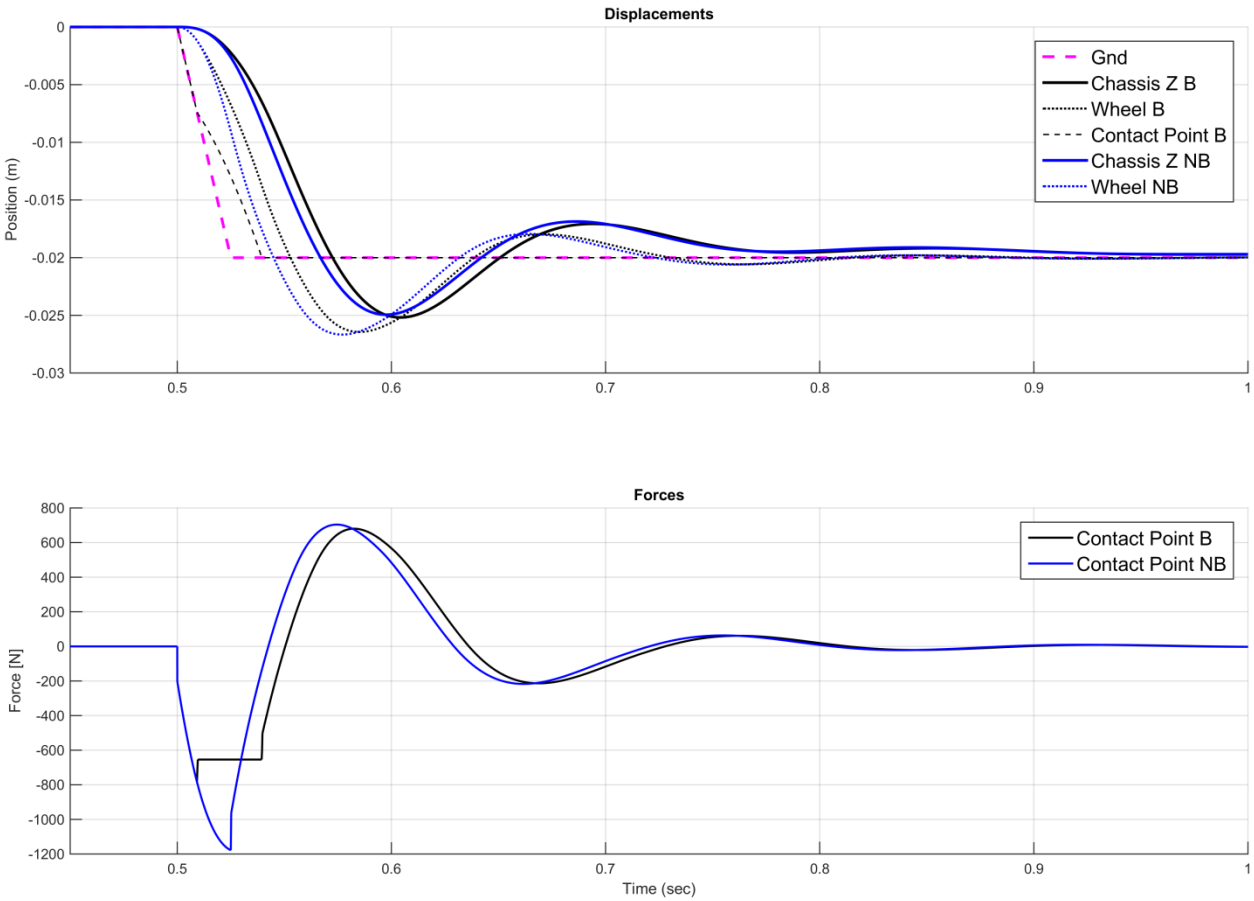

Figure 24 - Non-Linear Quarter Car StepDown Response

It is interesting to note that in the Sawtooth bump case shown in Figure 25, there is little difference between models, presumably because the majority of the bump is absorbed by the tire spring, preventing the wheel from moving significantly. If the magnitude of the bump were increased significantly (proposed to be loosely dependent on tire spring rate and bump duration), the tire would be unable to keep up with the bump profile and be forced to ‘fall’ back to the ground afterward.

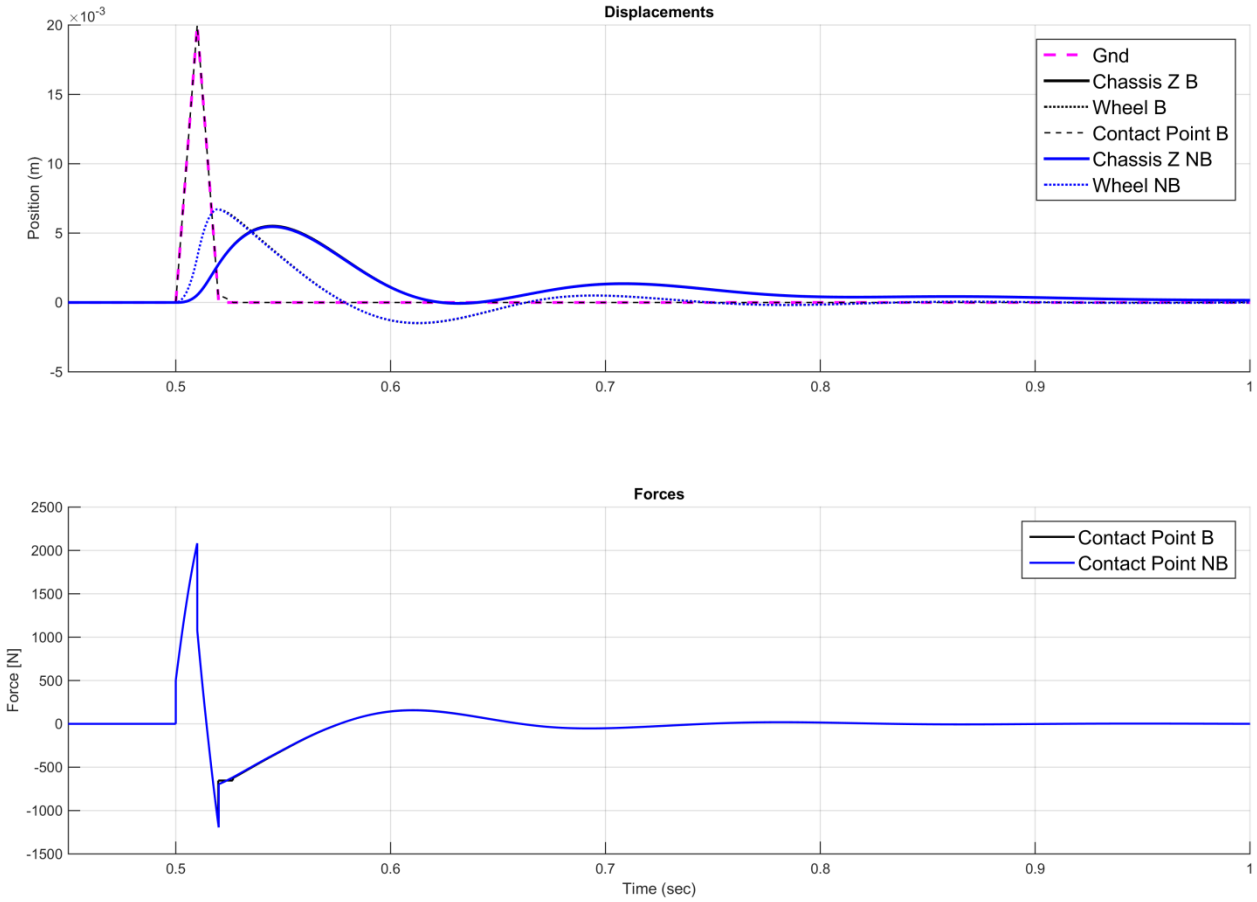

Figure 25 - Non-Linear Quarter Car Impulse Response

In a similar manner as the StepDown response, the pothole model shown in Figure 26 exhibits significant ballistic behavior as the tire falls into the hole, but is not launched into the air again afterward. Again, this response is assumed to be dependent on the depth and width of the hole.

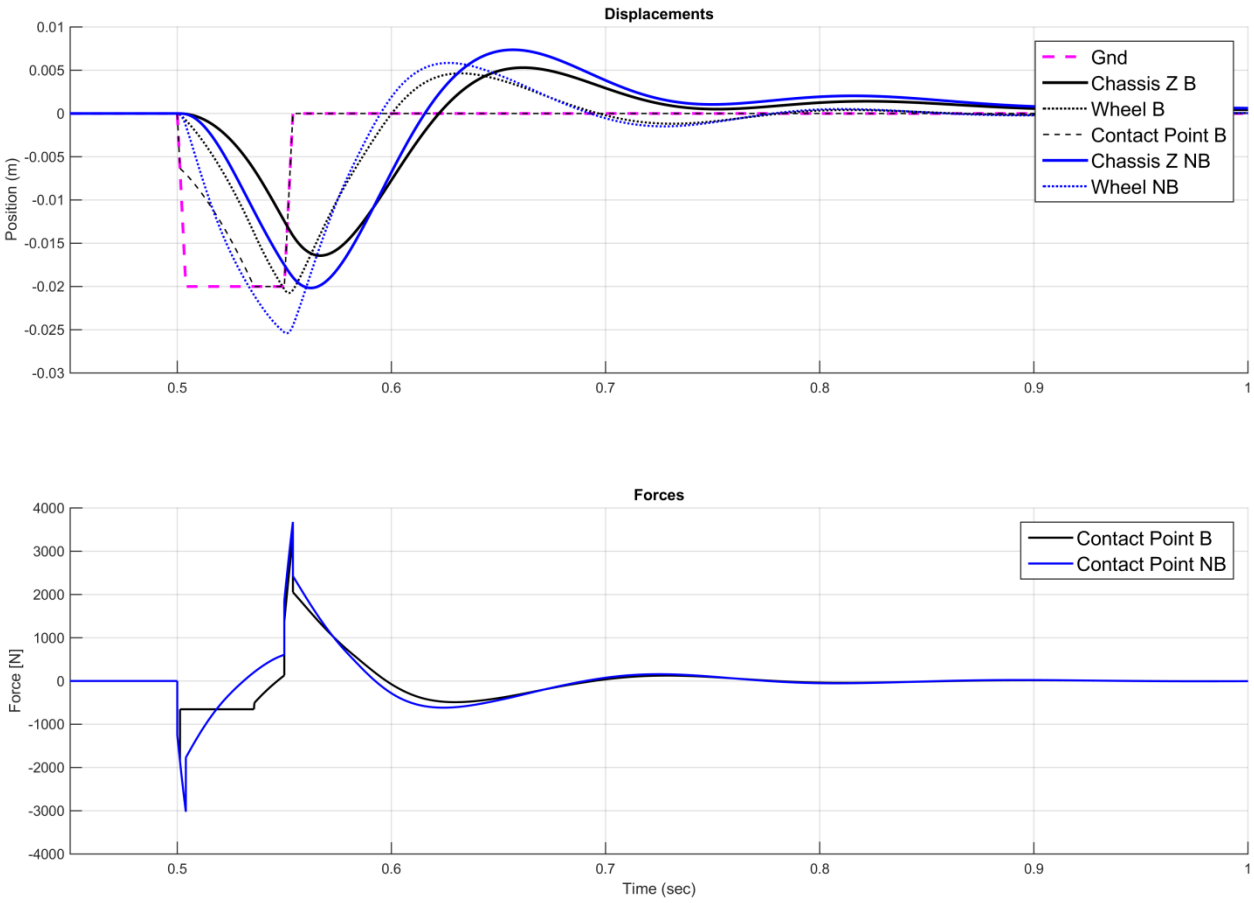

Figure 26 - Non-Linear Quarter Car Pothole Response

Figure 27 shows that in low frequency situations (less than the system natural frequency), the tire remains in contact with the ground and the non-ballistic model is sufficient to describe its response.

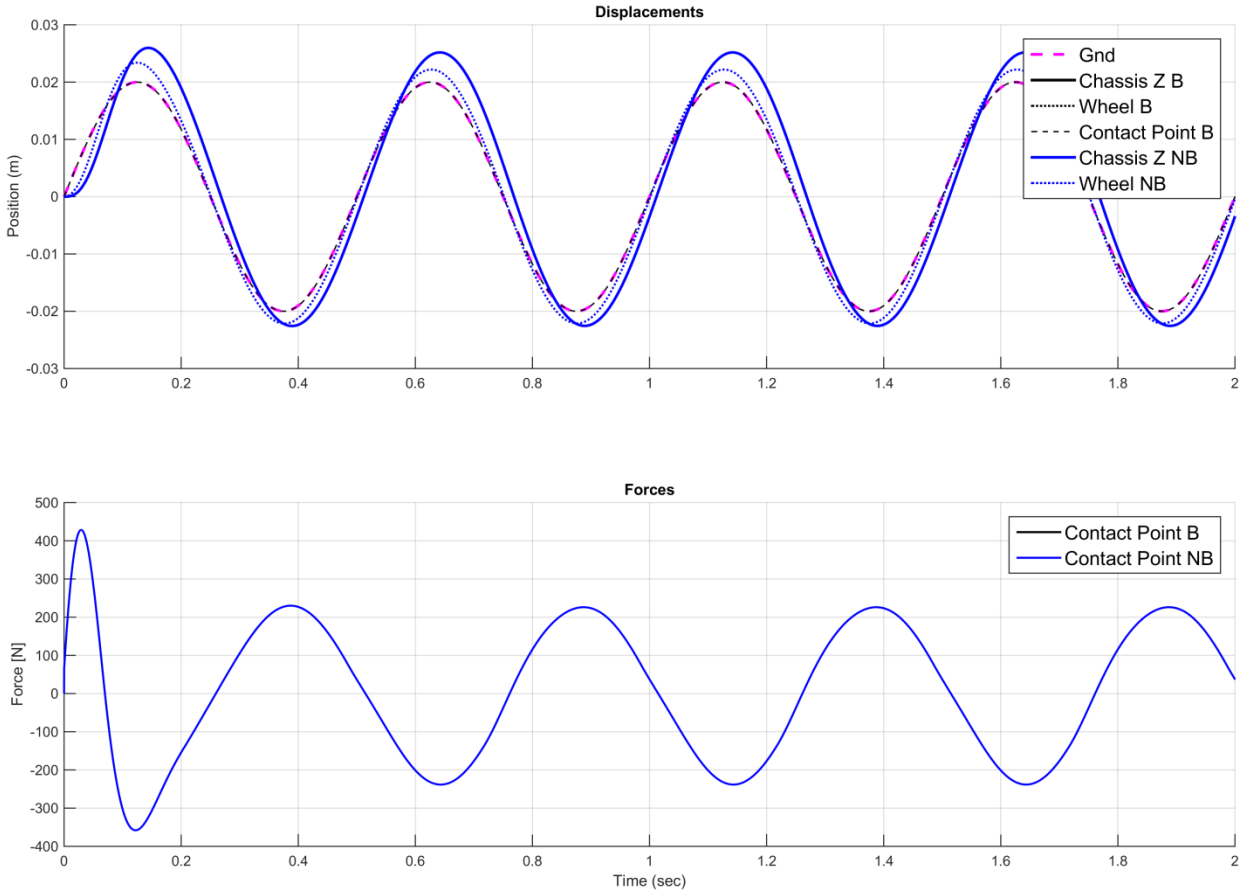

Figure 27 - Non-Linear Quarter Car 2 Hz Sinusoid Response

Once the input frequency is increased above the natural frequency of the system, a very significant ballistic motion can be seen. This corresponds very well to the physical world situation of driving over a washboard surface. Most people who have driven for any length of time have probably noticed that many times driving *faster* over such surfaces allows the wheels to 'skim' over the surface, greatly decreasing the motion (in the form of chassis acceleration) experienced by the driver.

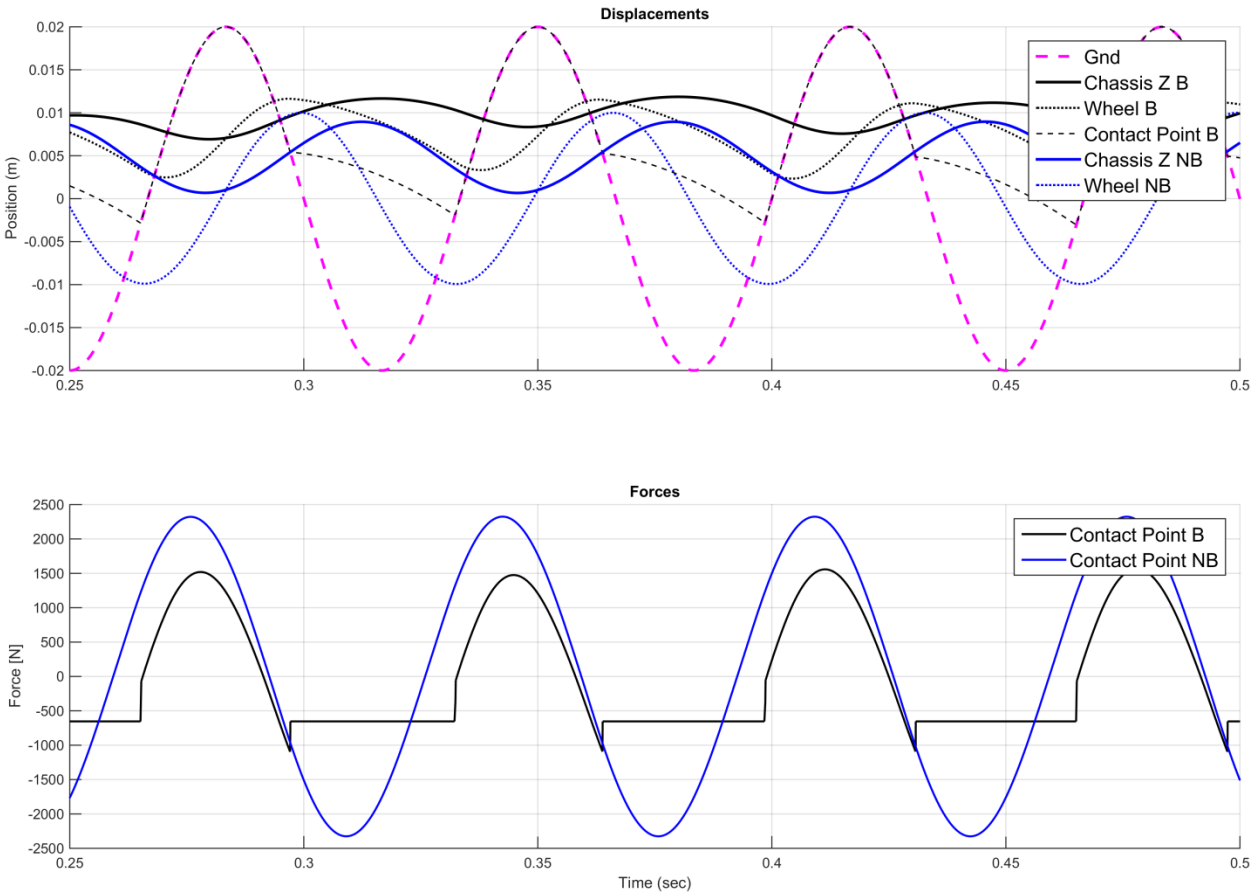

Figure 28 - Non-Linear Quarter Car 10 Hz Sinusoid Response

6.3.2. Non-Linear Bicycle Model

For analysis of the bicycle model, the input was setup such that the rear input lagged the front by an amount of time defined by the vehicle wheelbase and its velocity (set relatively arbitrarily to 50 kph in this case). This provides a more realistic view than exciting both ends of the car at once and allows for the pitch mode to be observed. Since, in the scope of this project, bumps are evaluated across each axle (both front wheels and both rear wheels together), the response of the full car model is very similar to the bicycle model. Because of this similarity and for the sake of brevity, all but one of the bicycle model responses are relegated to Appendix F.

Like the quarter car StepUp response, the bicycle model response in Figure 29 does not experience any notable ballistic motion.

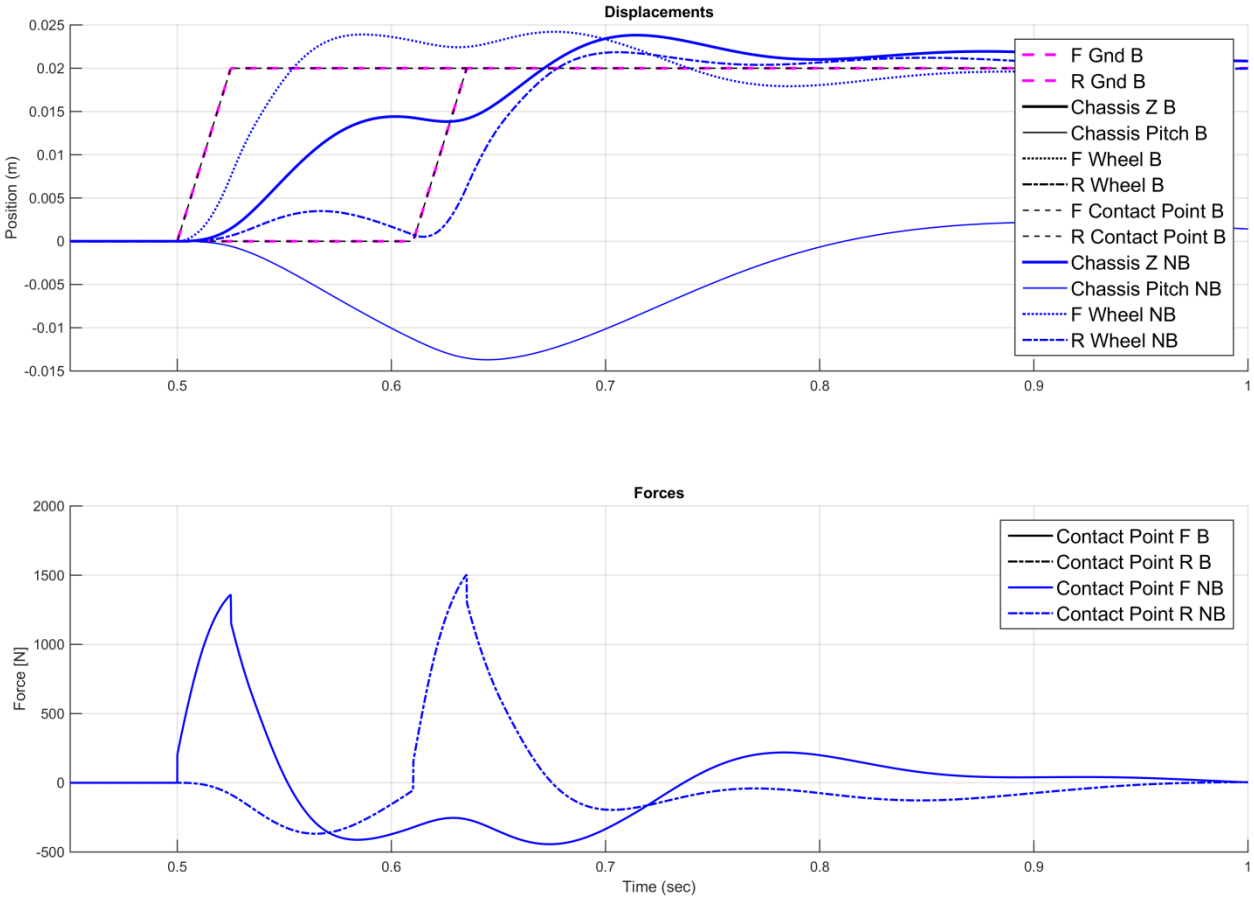

Figure 29 - Non-Linear Bicycle Model StepUp Response

6.3.3. Non-Linear Full Car

Like the bicycle model, the full car is evaluated with a time delay between front and rear inputs that is defined by wheelbase and velocity. In the case of the sinusoidal frequency inputs shown in Figure 34 and Figure 35, it is critical to note that the 'frequency' of the input is defined *independently* of speed. Depending on the exact surface desired, the speed *and* frequency must be defined. This requirement is intentional and allows for the concept of X displacement and velocity (longitudinal) to be abstracted out of the model and to be defined solely in terms of time.

Figure 30 shows similar response characteristics to both the quarter car and bicycle models.

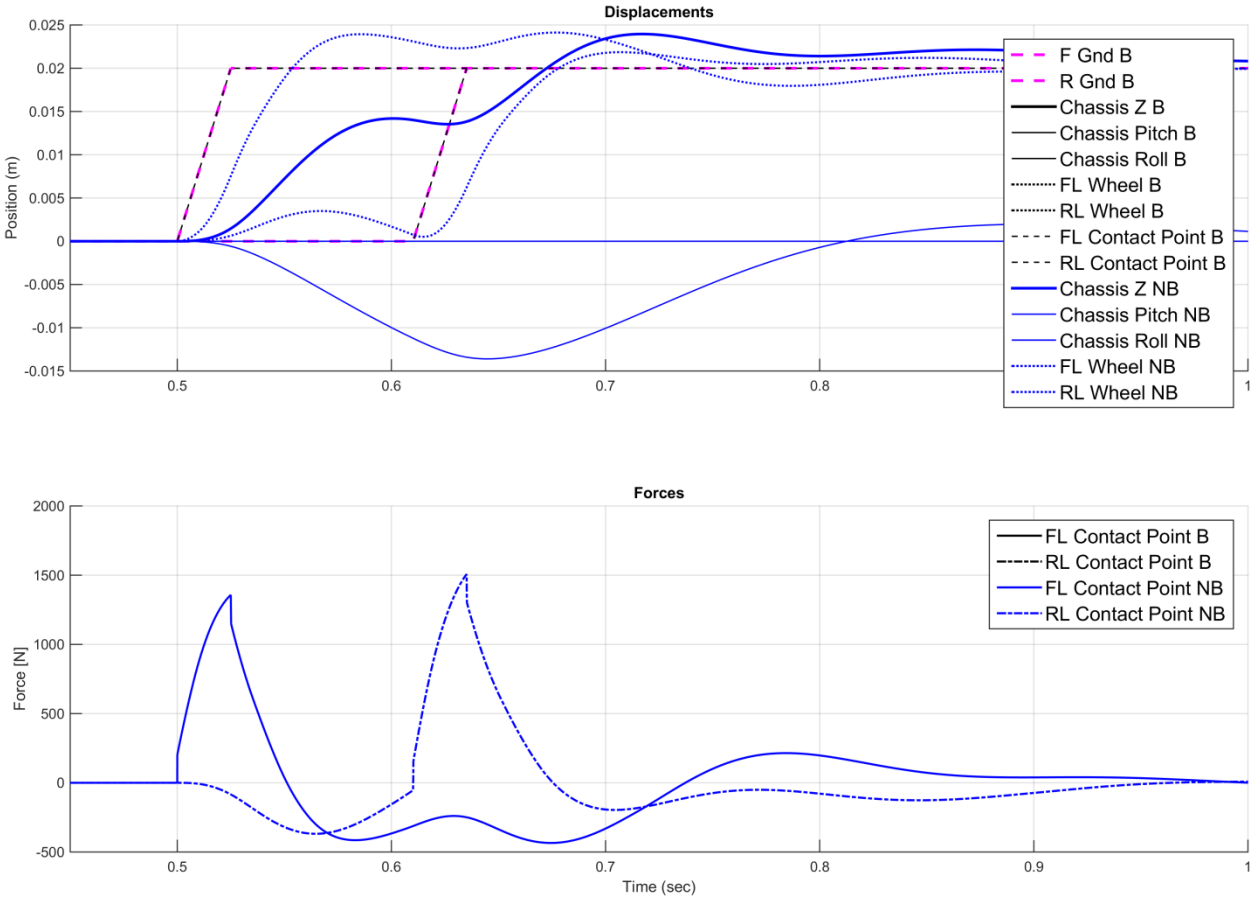

Figure 30 - Non-Linear Full Car StepUp Response

The StepDown response shown in Figure 31 again shows that the ballistic model becomes important particularly in cases when the ground is receding away from the wheel. The chassis and wheel trajectories are significantly different as are the forces at the tire contact points.

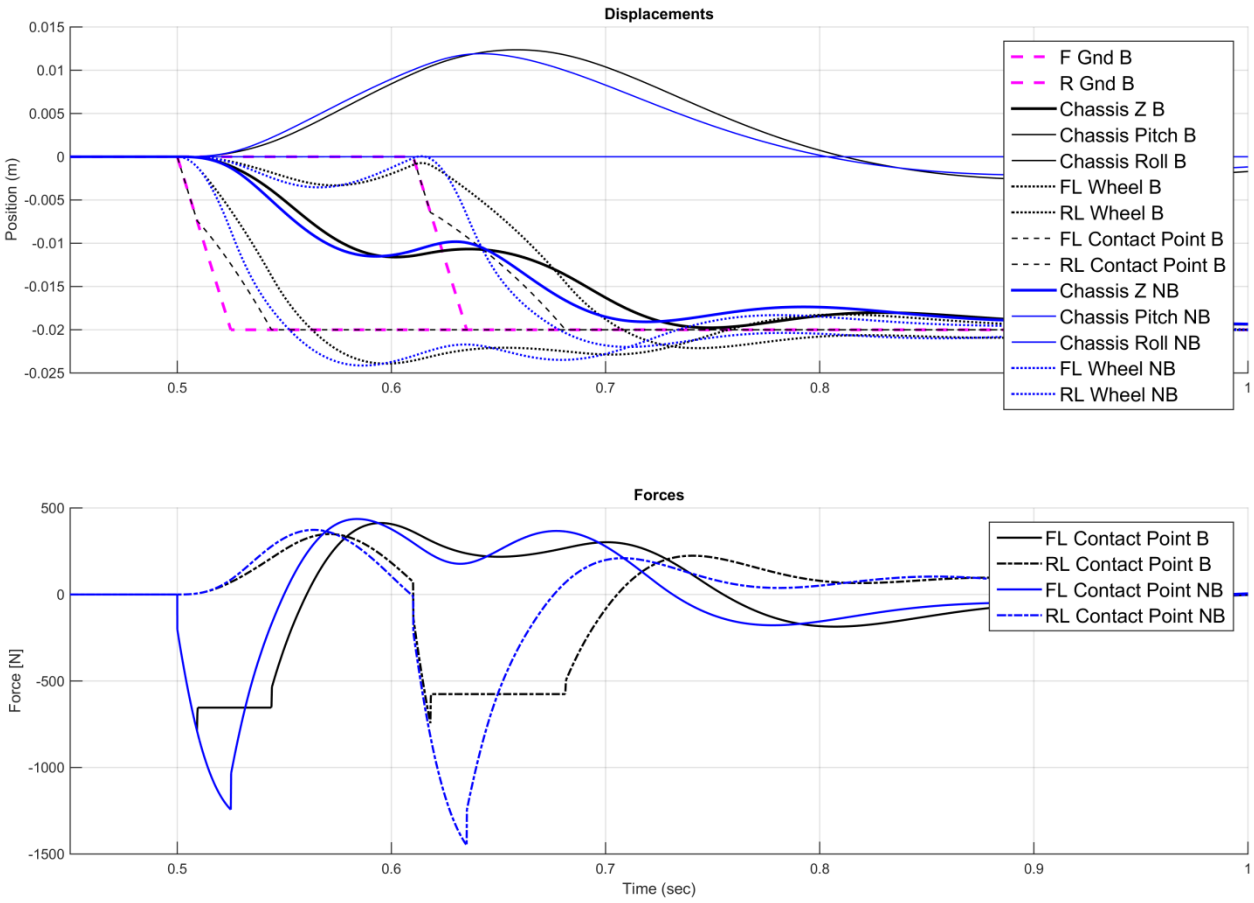

Figure 31 - Non-Linear Full Car StepDown Response

As seen in previous models, sharp inputs such as those in Figure 32 do not tend to cause ballistic motion.

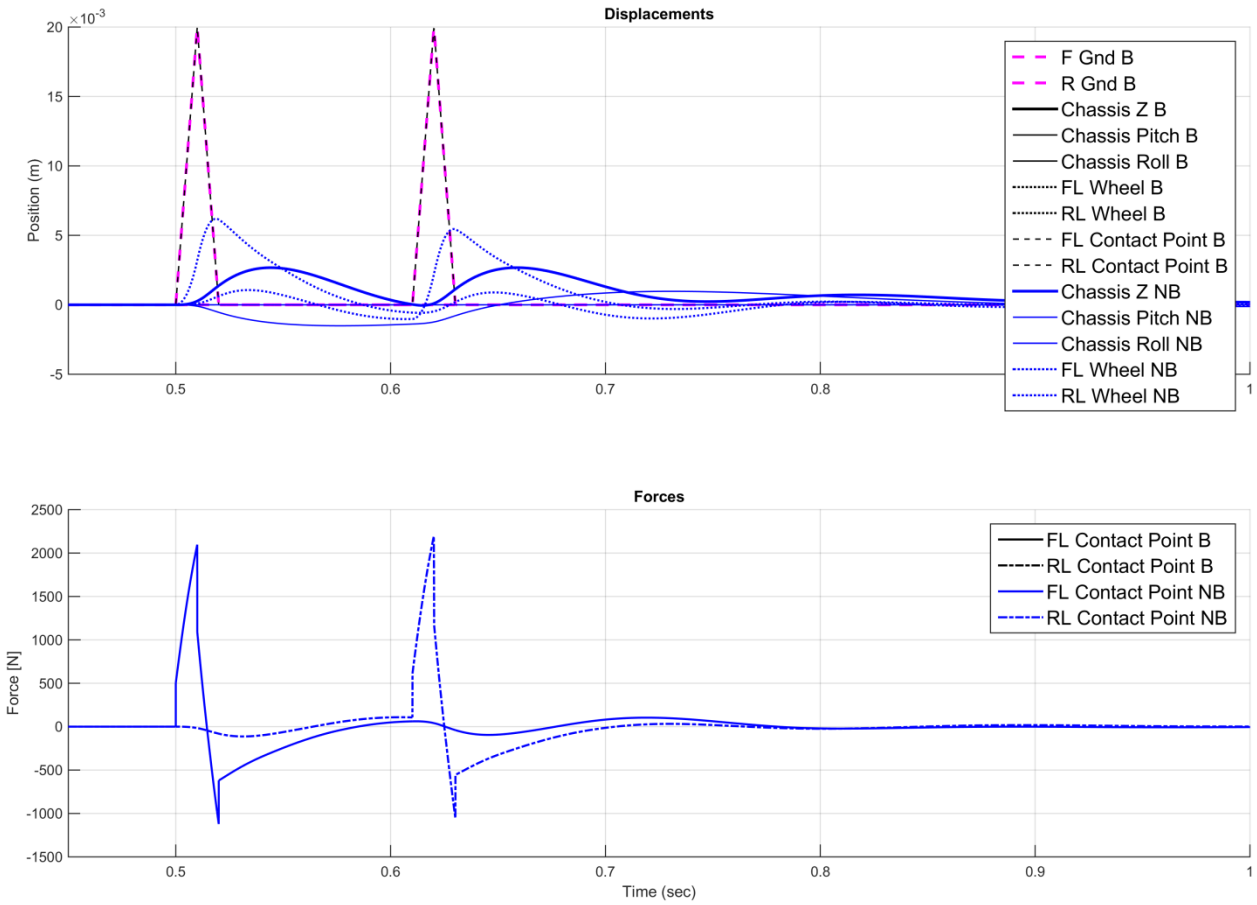

Figure 32 - Non-Linear Full Car Sawtooth Response

While the response to a pothole shown in Figure 33 is not dissimilar to that of the quarter car model, there are some significant differences to note.

First of all, the effect of chassis pitch becomes important since in this specific front to rear delay, the chassis pitch angle does not have a chance to recover fully before the second set of wheels contacts the pothole. This means that the rear wheels will take a very different trajectory through the pothole. While the overall impact of this effect on damper and spring selections is not clear and outside the scope of this project, it is important to note that there may be something worth further evaluation here.

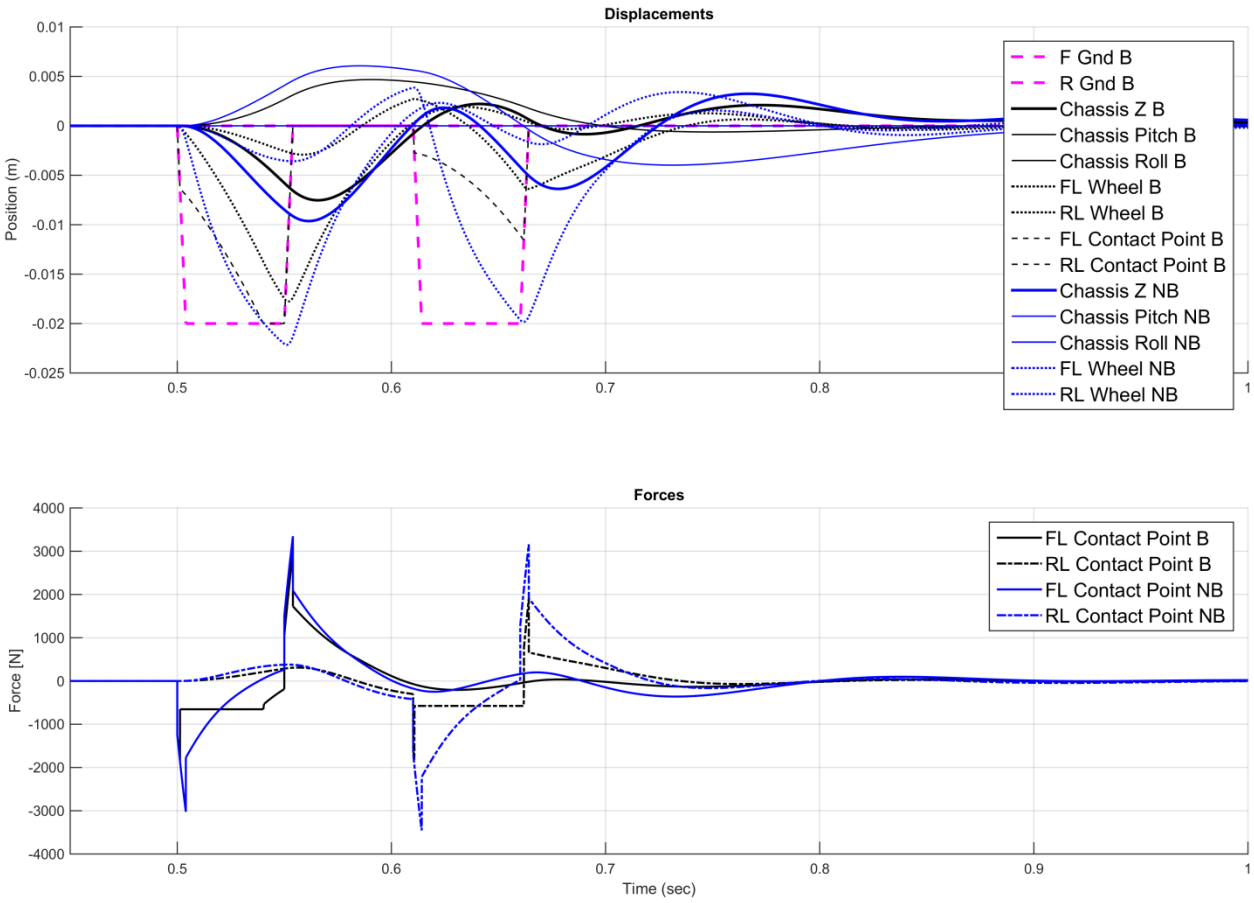

Figure 33 - Non-Linear Full Car Pothole Response

The low frequency response of Figure 34 shows an interesting difference compared to the quarter car model in that the model *does* go ballistic. Like the pothole response, it is proposed that this deviation from the quarter car model is due to the effect of chassis pitch. When the front and rear axles are excited symmetrically, this effect disappears and the response is analogous to that of the quarter car.

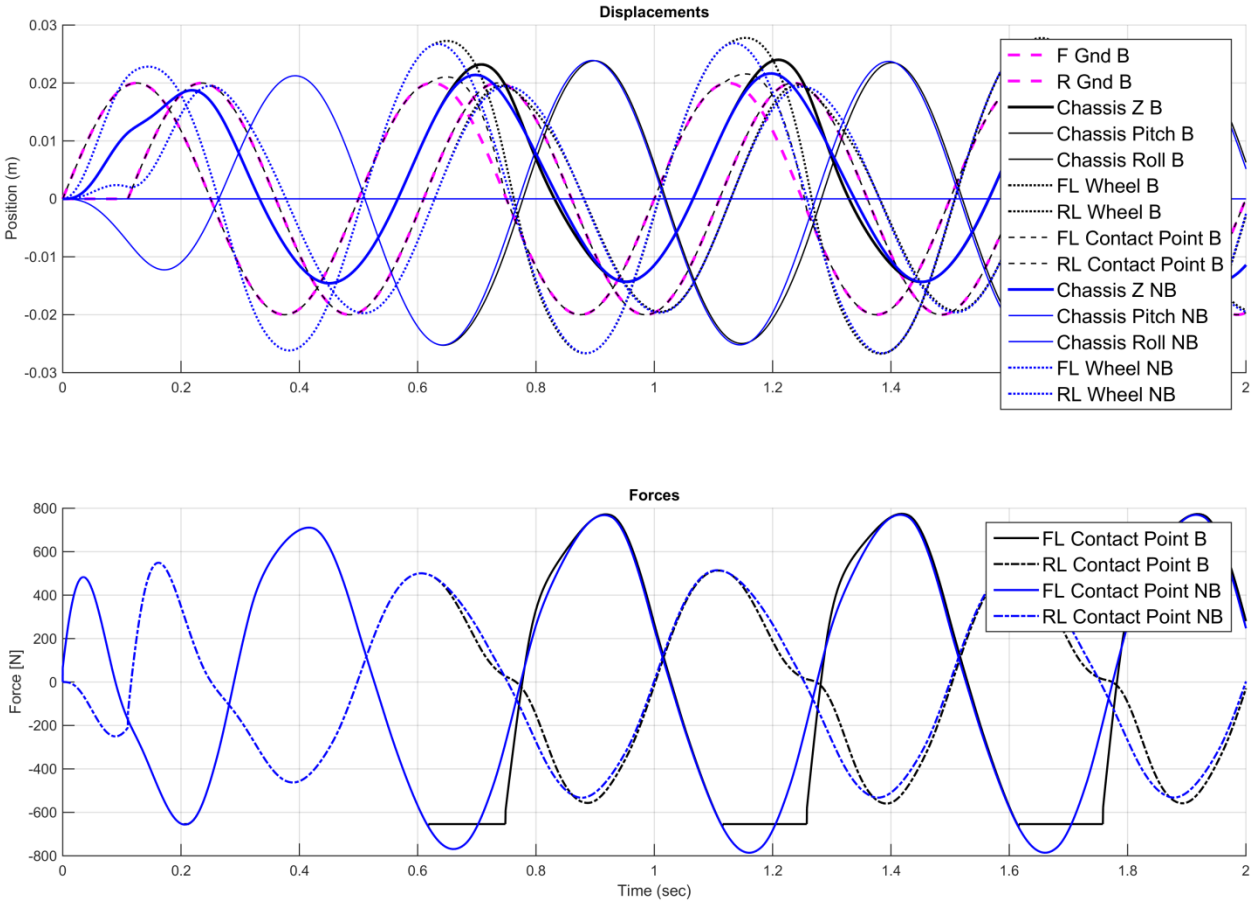

Figure 34 - Non-Linear Full Car 2 Hz Sinusoid Response

Like the quarter car model, the full car model in Figure 35 exhibits a large response difference between ballistic and non-ballistic modes. The chassis is significantly more stable in both the Z direction and in pitch. Interestingly, the tires only spend *approximately half* of the time in contact with the ground.

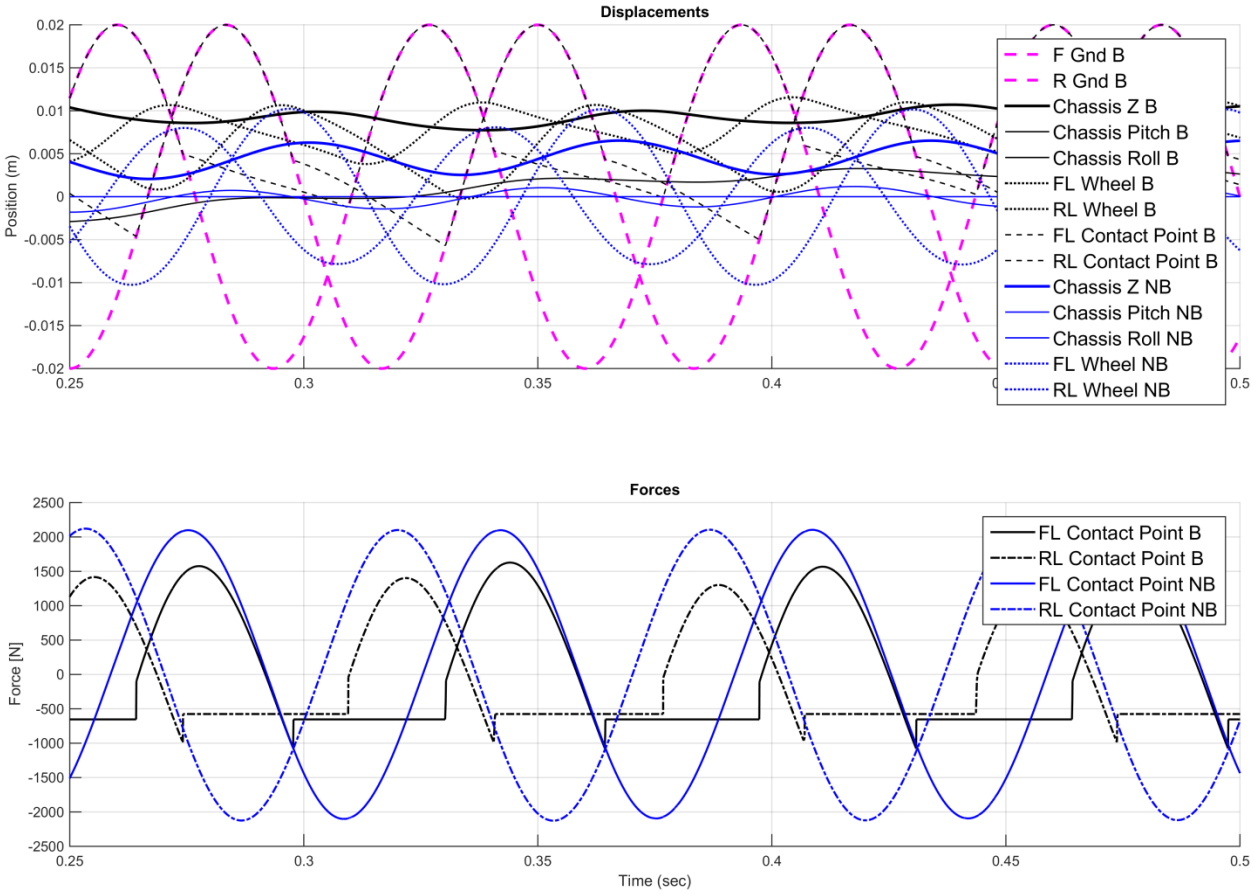

Figure 35 - Non-Linear Full Car 10 Hz Sinusoid Response

7. Controller Development

The results presented in this chapter are for the active, controlled systems. Their purpose is to investigate how an optimal controller will affect the trajectories shown in Chapter 6.

7.1. Controller Selection

As mentioned in section 3.7, this project makes use of an LQR state feedback model. There are several properties of the pure LQR solution (such as guaranteed performance and stability) that do not necessarily apply to this project. Certain requirements cannot be explicitly fulfilled such as the existence of a linear state space, observability (the ability to directly observe ALL states), or controllability (a theorem of controls that relates the rank of the state matrices to the ability of the controller to exert full control over every state). One ultimate goal of this project is to discover if an LQR controller based upon a linearized state space model of the system is able to control the system and produce trajectories that are more desirable than those shown in Chapter 6.

MATLAB has a host of tools available to generate the solution of the LQR problem, which condenses into an M x N state multiplication matrix where M is the number of inputs and N is the number of system states. In order to generate this output matrix, K, there must be a state space model of the target system and weighting matrices Q and R which assign state error weights and controller cost penalties. There are several rules of thumb to be used when assigning these weights, but frequently LQR design is an iterative process of trying initial values and adjusting from there. In addition, the Q and R matrices are relative. The magnitude of each value within is meaningless other than in relation to its surrounding values.

Several assumptions allowed the process to be simplified for this problem. Critically, the controller will only be able to command the actuator at each corner of the car. It is unable to impart a displacement or velocity to the ground, or to apply external gravitational forces to the chassis. Thus, the actuators are assigned a cost of 1, while the ground and external inputs are assigned values many orders of magnitude higher (which was decided upon by picking larger and larger values until the *attempted* control of the ground was sufficiently small). The state error weights were significantly more difficult to assign, but the rule of thumb is to assign $weight = \frac{1}{MaxDesiredError^2}$. While this provides a reasonable starting place, it is a little nebulous in the

context of this problem. The controller should be minimizing tire load variation and keeping the tire on the ground. Because these are not explicit states, some experimentation is required to find what states *do* effect these parameters, and what magnitude the MaxDesiredError should have. After significant experimentation and many iterations, it was found that the controller should not be concerned with controlling position of the chassis or tires. The car should be allowed to reach a new positional equilibrium if it is driven over a StepUp or StepDown. The controller also should not be concerned with the absolute position *or* velocity of the *wheels* as the contact point force is not dependent on these parameters. The primary purpose of suspension is to allow the wheels to follow the ground while the chassis remains relatively stable. One of the setups that were found to be effective in minimizing tire load variation was assigning high weight to the velocity of the chassis and roll and pitch angles (the car should remain relatively level in all cases). Interestingly, this approach also reduced the magnitude of the chassis displacement as well as decreasing the system settling time, providing a more comfortable ride although this was not an explicit goal. In this way, it might be possible to increase the performance of the tire while *also* improving comfort in some cases.

This approach does make intuitive sense upon inspection. If the controller wants to keep the chassis from acquiring a velocity (accelerating), the most direct way of doing so is to minimize force disturbances from below. Since the only dynamic forces under the chassis are caused by the tires acting through the chassis spring, damper, and actuators, the actuator will try to reduce this force transmission by contracting in order to balance out the force generated in the spring and damper as the wheel is force upward rather than transmit the force into the chassis.

Taking all of this into account, the initial Q weighting were set via a rule of thumb, then progressively decreased until the controller was *trying* to use most of the available control force, 500 Newtons each in this case. Once installed on a real car, these values would no doubt need to be tuned in order to both maximize effectiveness and power usage.

In order to create similar controller characteristics between models, similar Q and R matrices were constructed, using similar error weightings and actuator penalties. Identical Q, R, and K matrices could not be used due to differing numbers of states and inputs between models.

The resultant controller K matrices are shown graphically in Figure 36 to Figure 38. It is worth noting that in this case, the gain matrices are relatively sparse, as would be expected of a controller that is only allowed to feed back selected states and inputs.

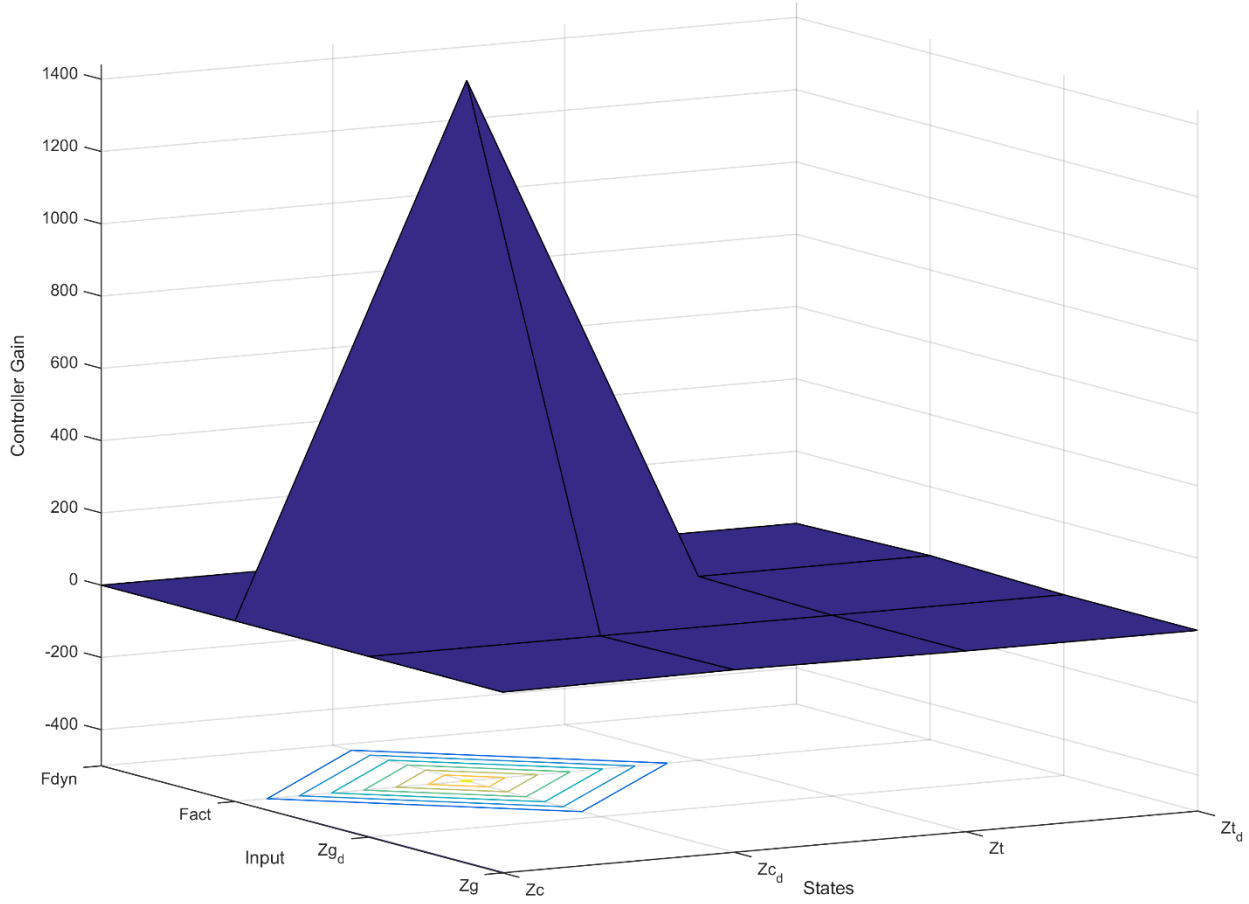

Figure 36 - Quarter Car Model LQR Gain K Graphical Representation

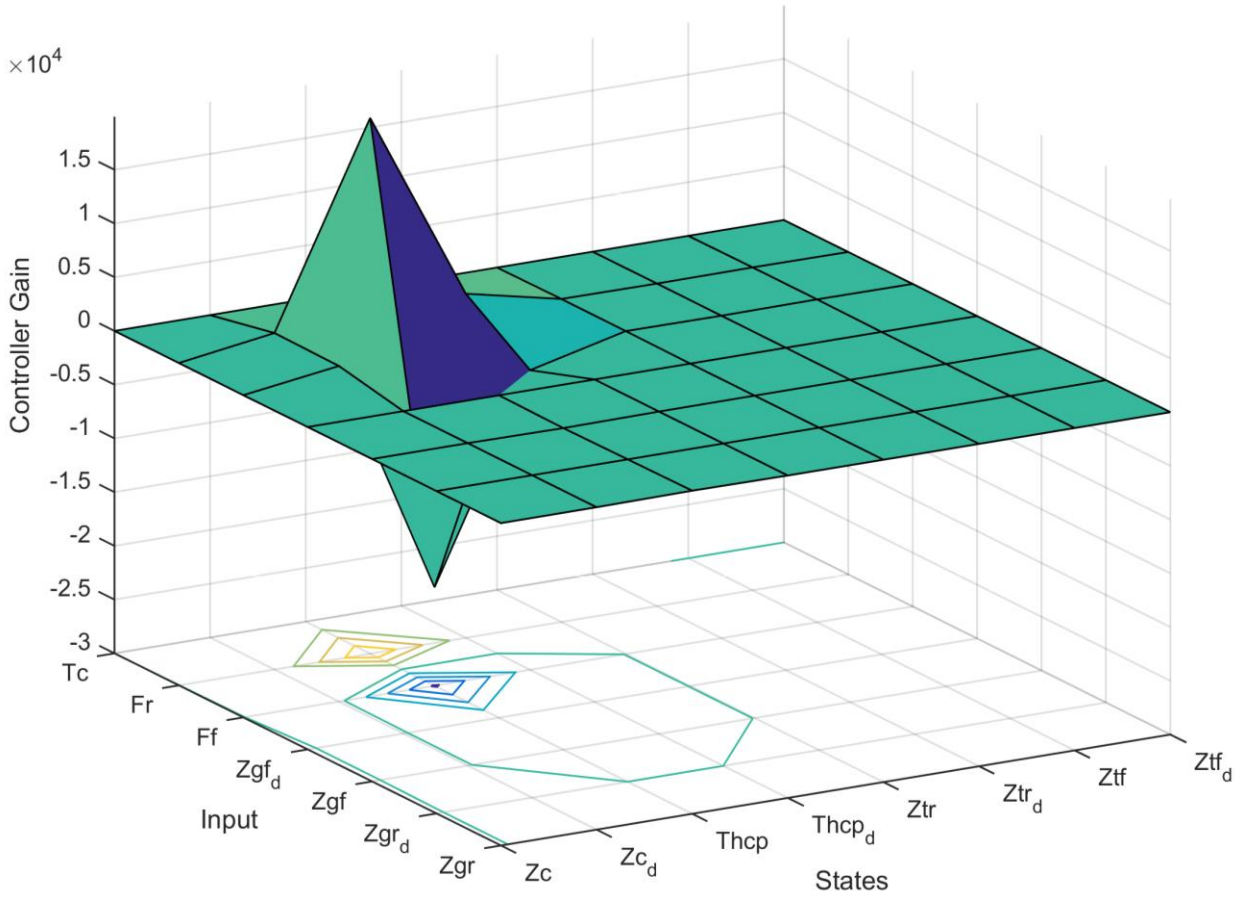

Figure 37 - Bicycle Model LQR Controller Gain K Graphical Representation

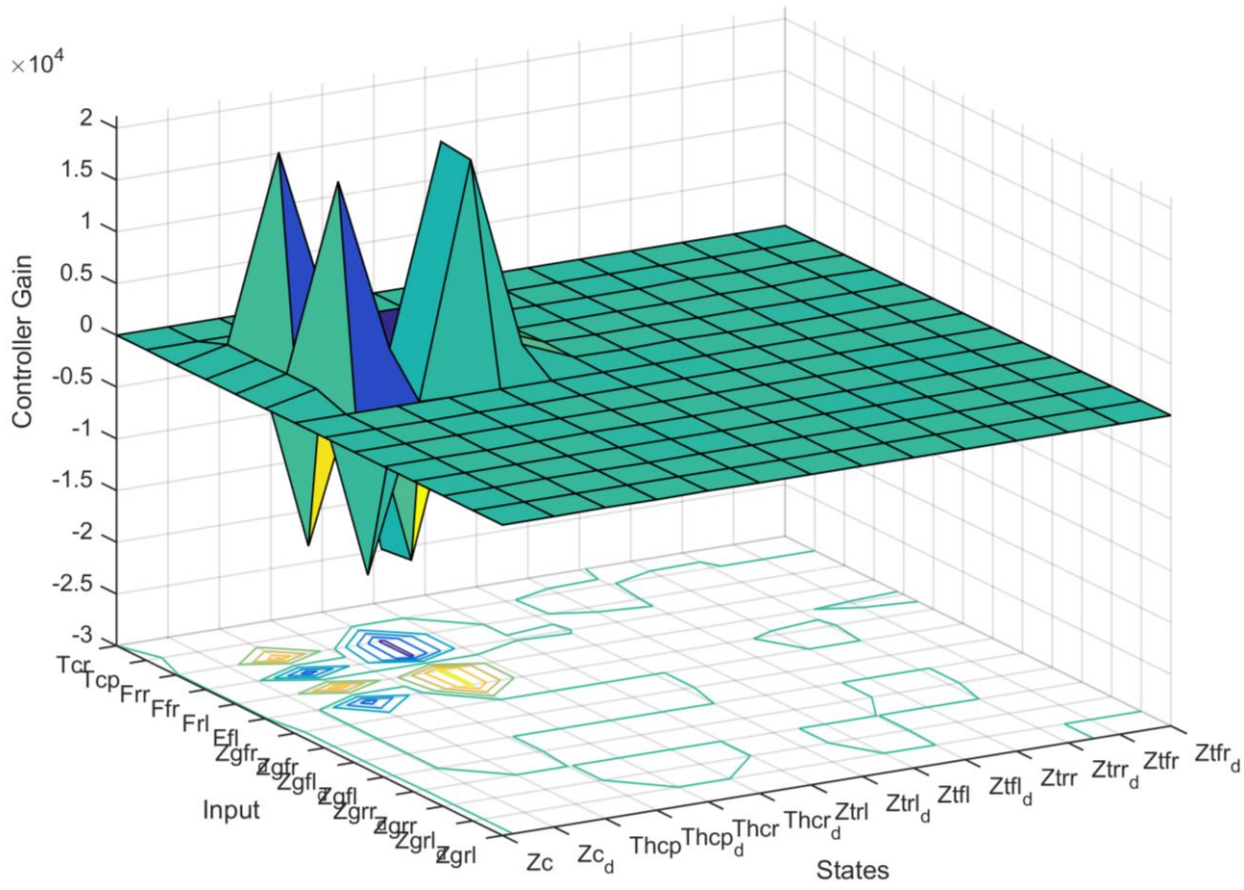

Figure 38 - Full Car Model LQR Controller Gain K Graphical Representation

7.2. Feedback Control Response

In this section, the effect of the initial LQR control algorithm will be demonstrated. It should be noted that the design of the controller itself should not be considered fully tuned or ideal, but it is developed sufficiently to demonstrate its effectiveness on such a nonlinear system, and to allow for approximate actuator sizing, etc. Further work is required to develop the final controller for the car (in terms of Q and R weightings), and significant effort will also be required once the system is installed on the car.

7.2.1. Quarter Car

Figure 39 shows the StepUp response when subject to the controller. As seen in the figure, the LRQ chassis displacement response is significantly improved, both in reduction of overshoot, but

also in settling time. In addition, the magnitude of the contact point force disturbance is reduced as well as its oscillation. The dashed red line in the force plot represents the generated actuator force.

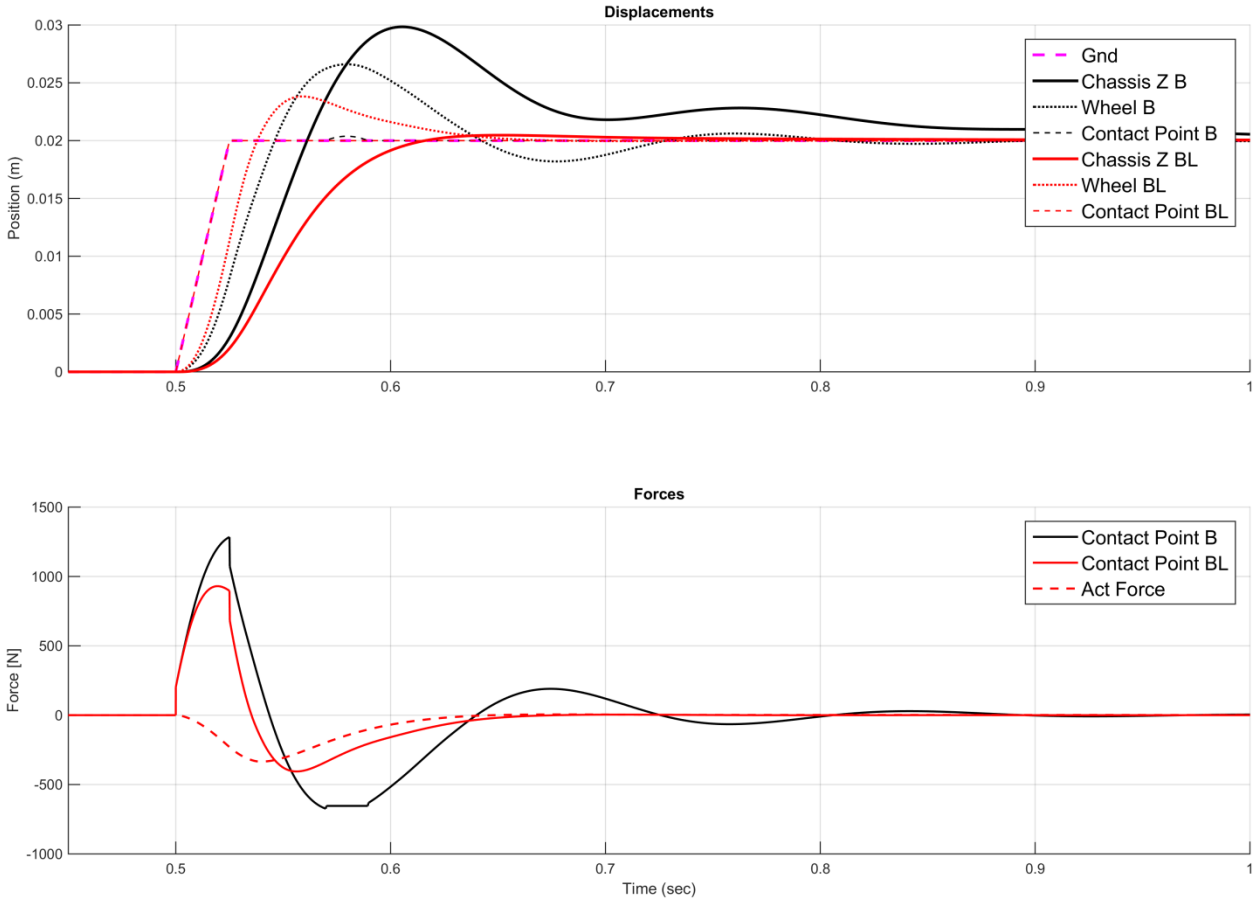

Figure 39 - Quarter Car StepUp Response with LQR

(B = Ballistic Model, BL = Ballistic Model with LQR Control, Act = Actuator)

Like the StepUp model, the StepDown model shown in Figure 40 responds favorably well to the controller input with reductions in chassis velocity as well as force variation.

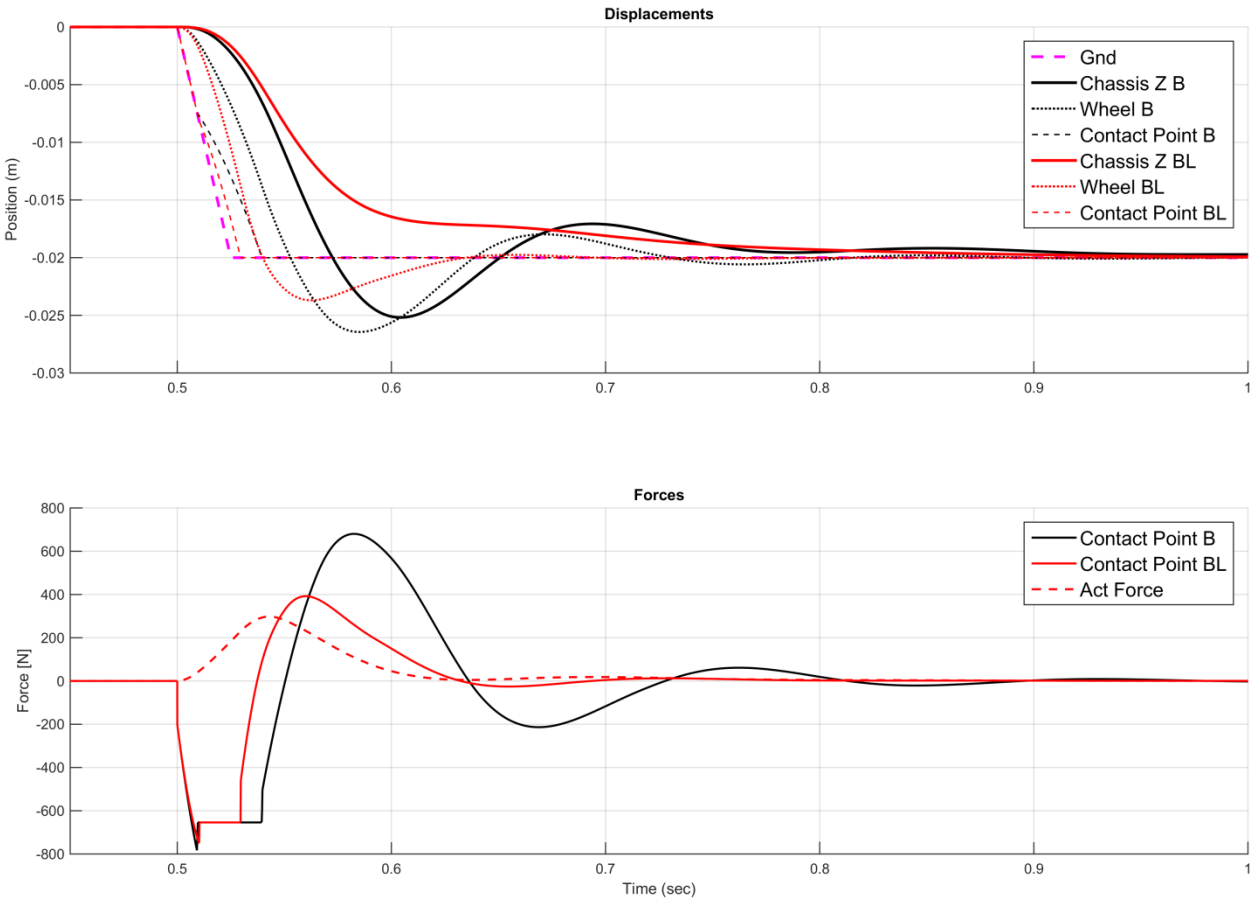

Figure 40 - Quarter Car StepDown Response with LQR

Impulses like that shown in Figure 41 demonstrate a less clear improvement, but do seem to decrease the maximum displacement amplitudes. It also seems to slightly increase the load variation of the tire contact point, which is generally considered to decrease grip. It is hypothesized that a different Q matrix weighting may improve this situation for this bump profile.

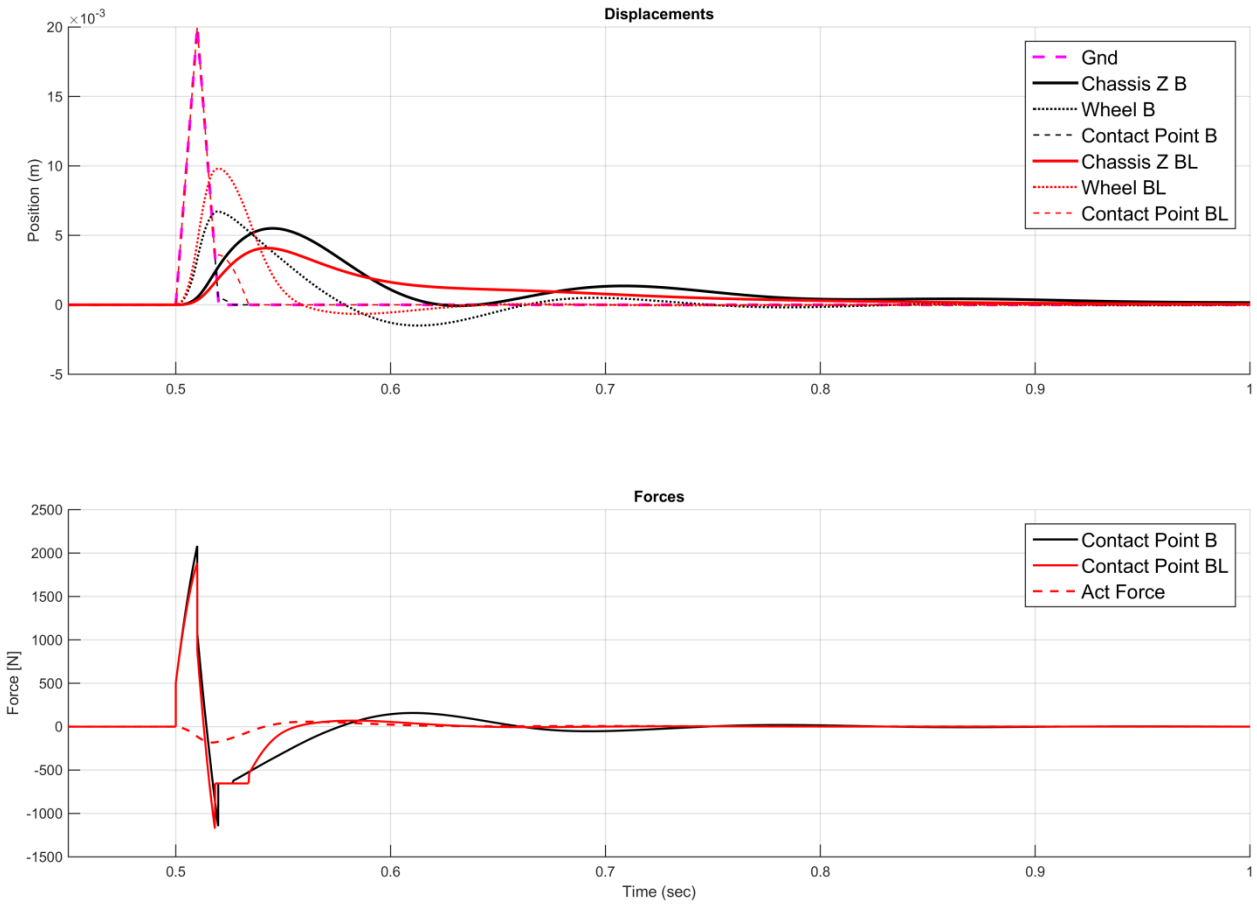

Figure 41 - Quarter Car Sawtooth Response with LQR

The pothole, effectively a combination of the StepUp and StepDown inputs also shows marked response improvement under LQR control as seen in Figure 42.

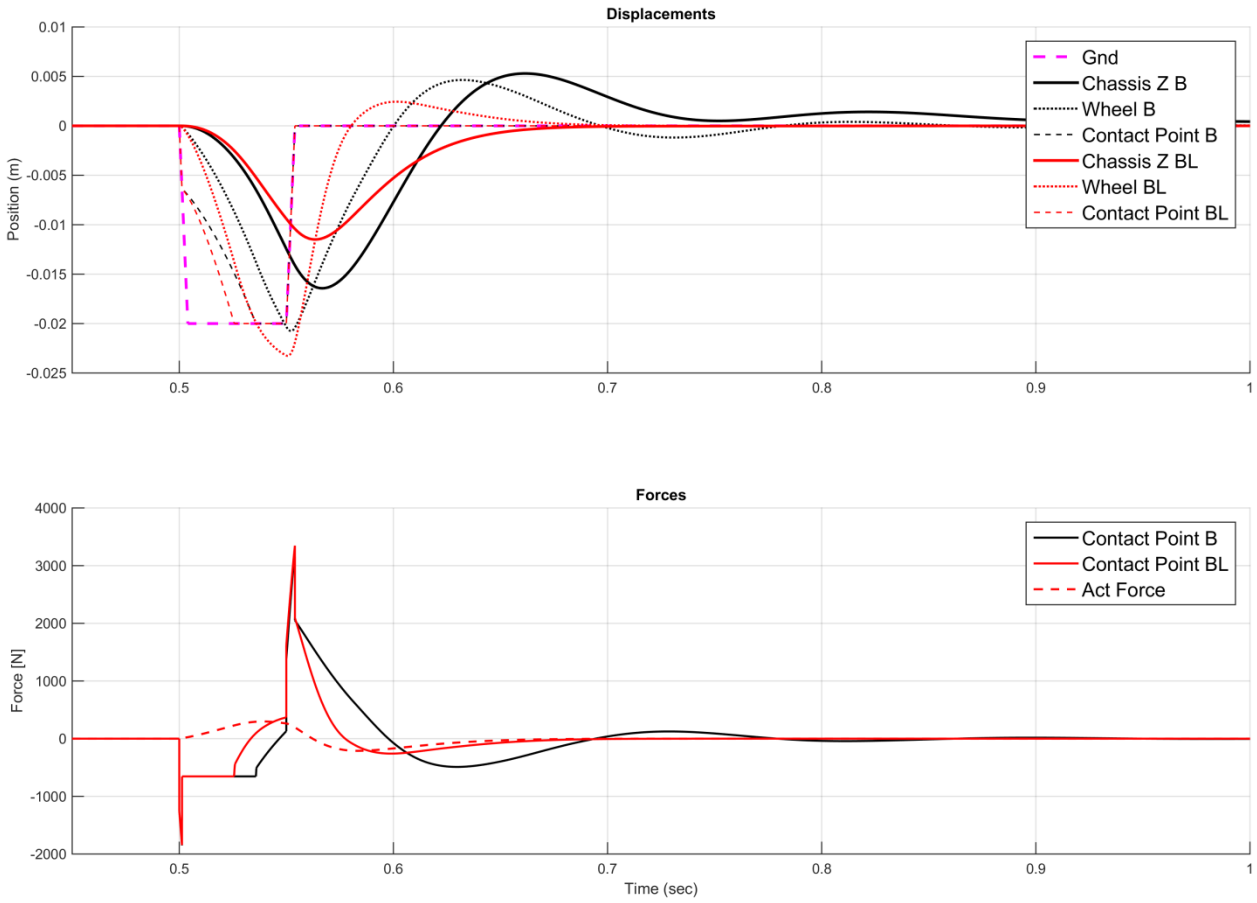

Figure 42 - Quarter Car Pothole Response with LQR

The controller had a relatively large contribution to the system response as shown in Figure 43. While the peak amplitudes were reduced on the order of 30%, the tire load variation decreased as well.

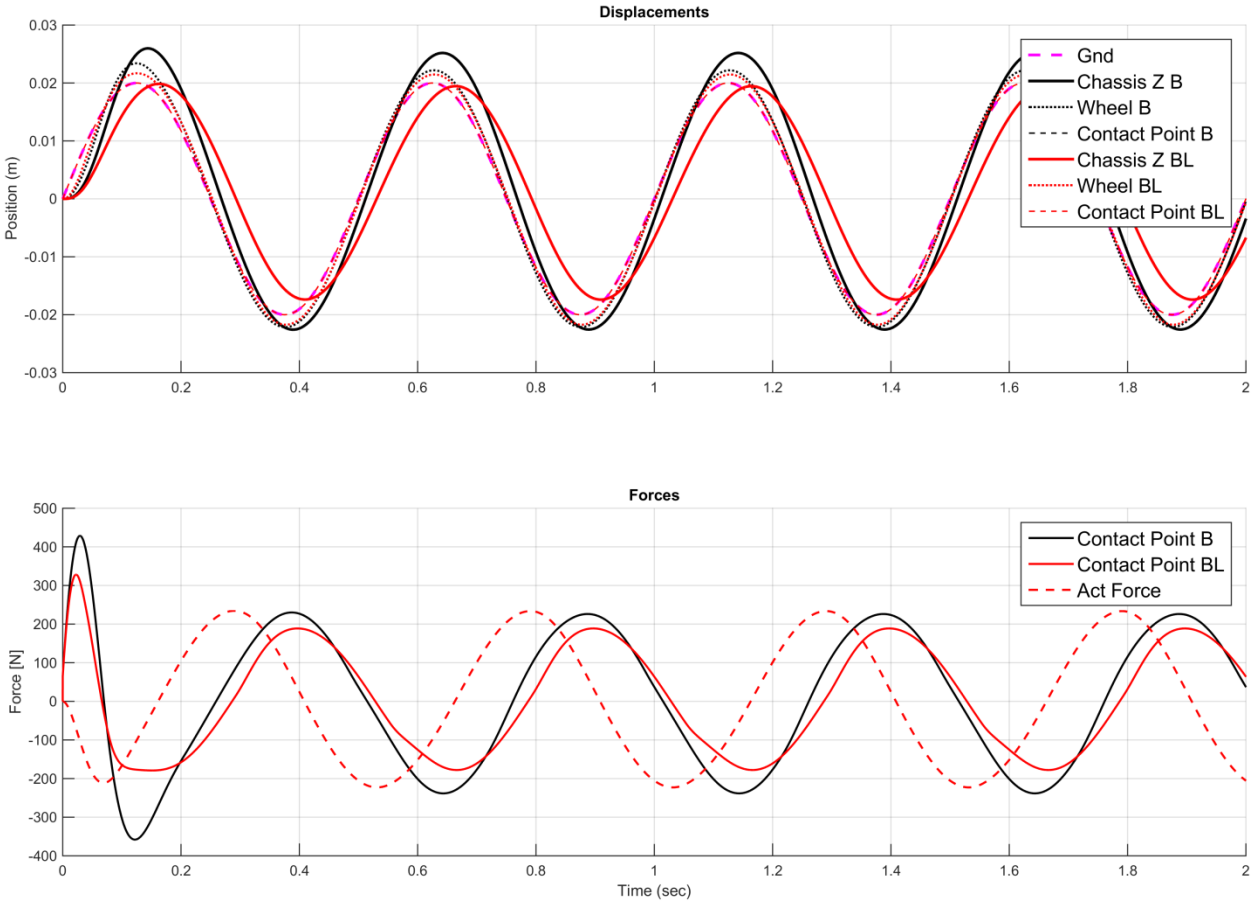

Figure 43 - Quarter Car 2 Hz Sinusoid Response with LQR

The full car response to a 10 Hz input is very similar to the passive response. While there does not seem to be any obvious qualitative performance improvement, the actuator is still exerting significant forces and thus using a significant amount of power.

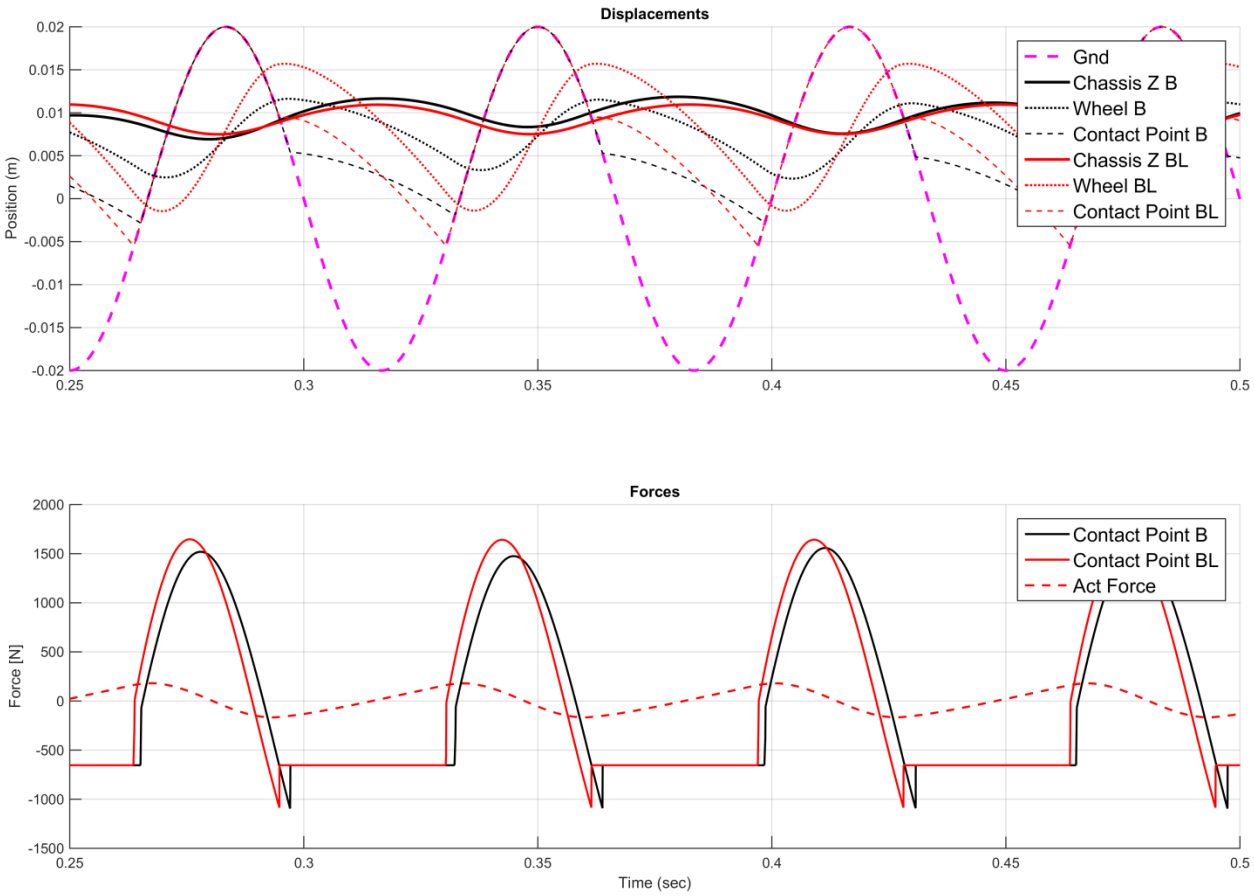

Figure 44 - Quarter Car 10 Hz Sinusoid Response with LQR

While the 2Hz and 10Hz inputs were chosen relatively arbitrarily (as one frequency above and one below the vehicle natural frequency), the response over a range of frequencies exhibits some interesting patterns. These are presented in several ways. Figure 45 shows the envelope (minima and maxima) of the chassis response from 0.5 to 10 Hz. The black lines (fully linear model) show symmetric response about the equilibrium position, and peak response around the natural frequency of the system (6 Hz). This trace further supports the previous assertion that the differences between the linear and ballistic systems can be large in some situations. The blue lines (ballistic, passive model) show a response that shifts toward positive Z at higher frequencies, and multiple peaks that correspond to transitions of ballistic behavior. Finally, the red lines (ballistic, active model) show an overall decrease in the amplitude, peak, and resonant points of the system.

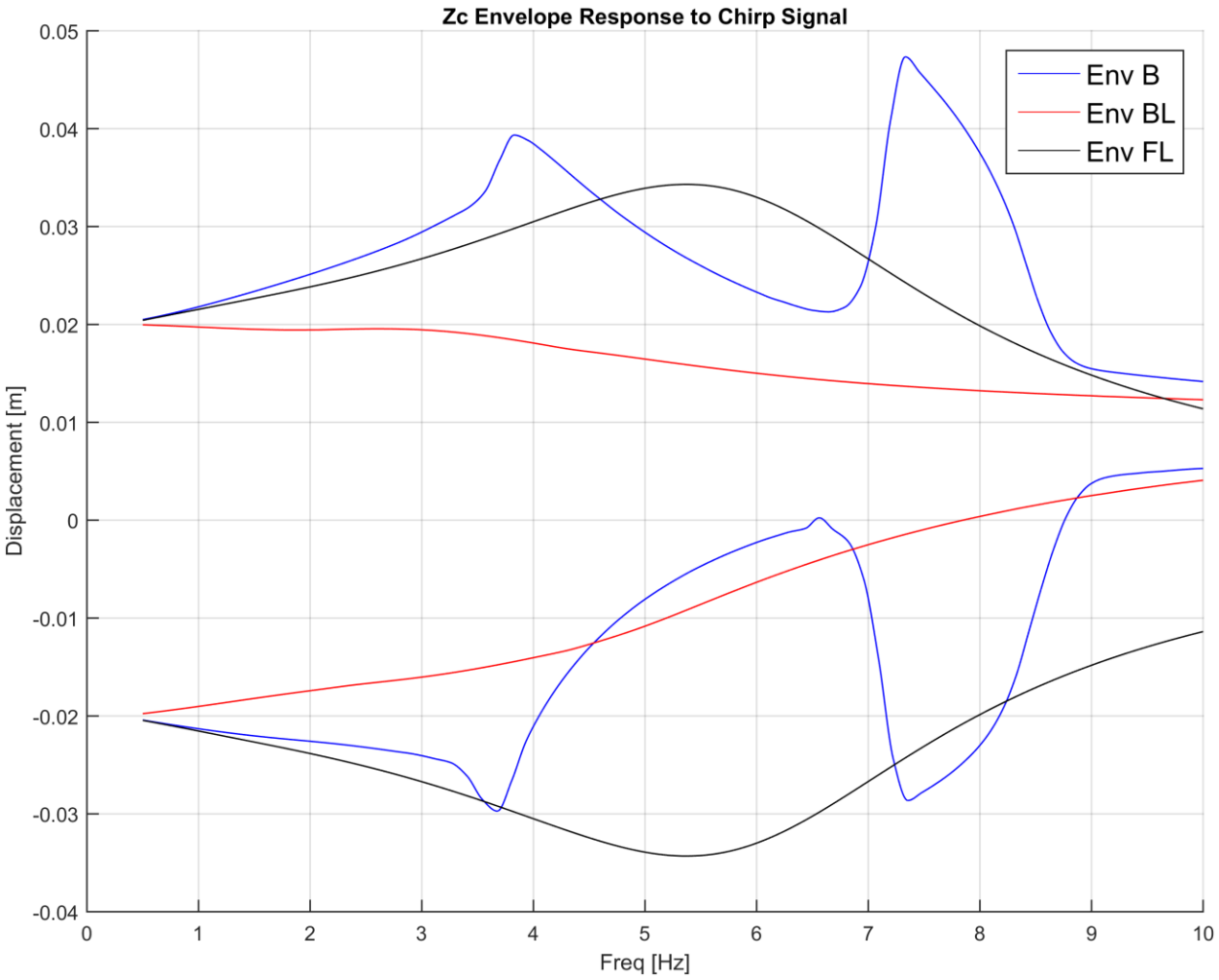

Figure 45 - Chassis Displacement Response to Chirp Input

(B = Ballistic Model, BL = Ballistic Model with LQR Control, FL = Fully Linear Model)

Figure 46 is an explicit representation of normalized response amplitude. Because of the small frequency range shown, the frequency scale is not logarithmic. These amplitudes are computed as one half of the difference between the minima and the maxima of each response, normalized. Interestingly, the amplitudes of the ballistic and fully linear systems are very similar until approximately 3.5 Hz. This is the frequency at which the system first exhibits ballistic behavior. Between 4 and 7Hz, the system demonstrates ballistic “skimming” behavior, and large response peak near 7.5 Hz is the frequency at which the ballistic wheel reconnects with the ground such that peak tire forces are generated. Again, the active response is decreased at all frequencies.

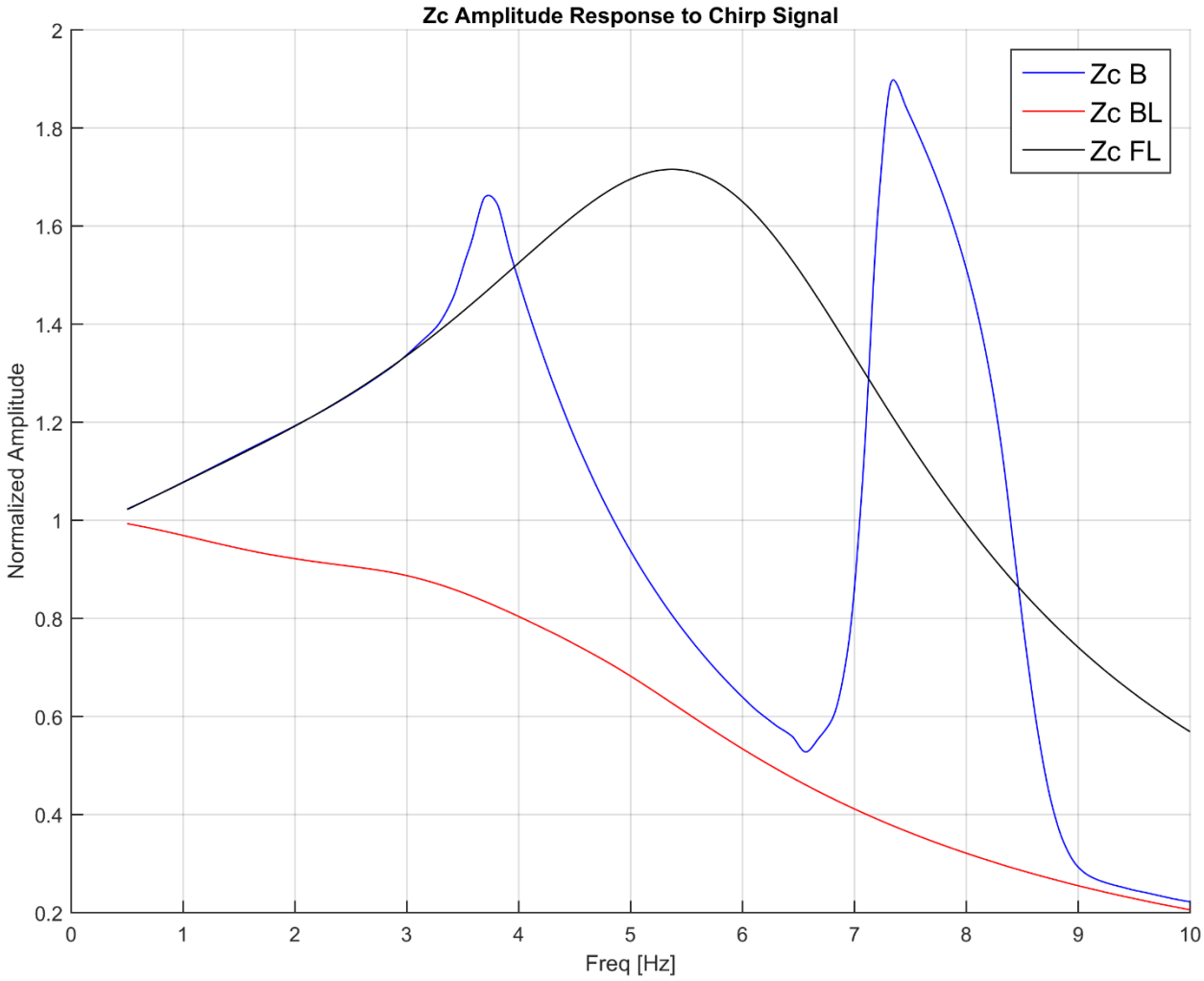

Figure 46 - Normalized Chassis Displacement Amplitude to Chirp Input

More importantly, Figure 47 shows the amplitude of the contact patch forces generated. The linear amplitude is up to twice as high once the wheel begins ballistic motion since the ground cannot pull down on the tire. Critically, a decrease in the amplitude of the force variation across all frequencies is seen for the active system. This decrease implies the ability of the tire to generate higher forces, thereby increasing vehicle handling, as described in Chapter 5.

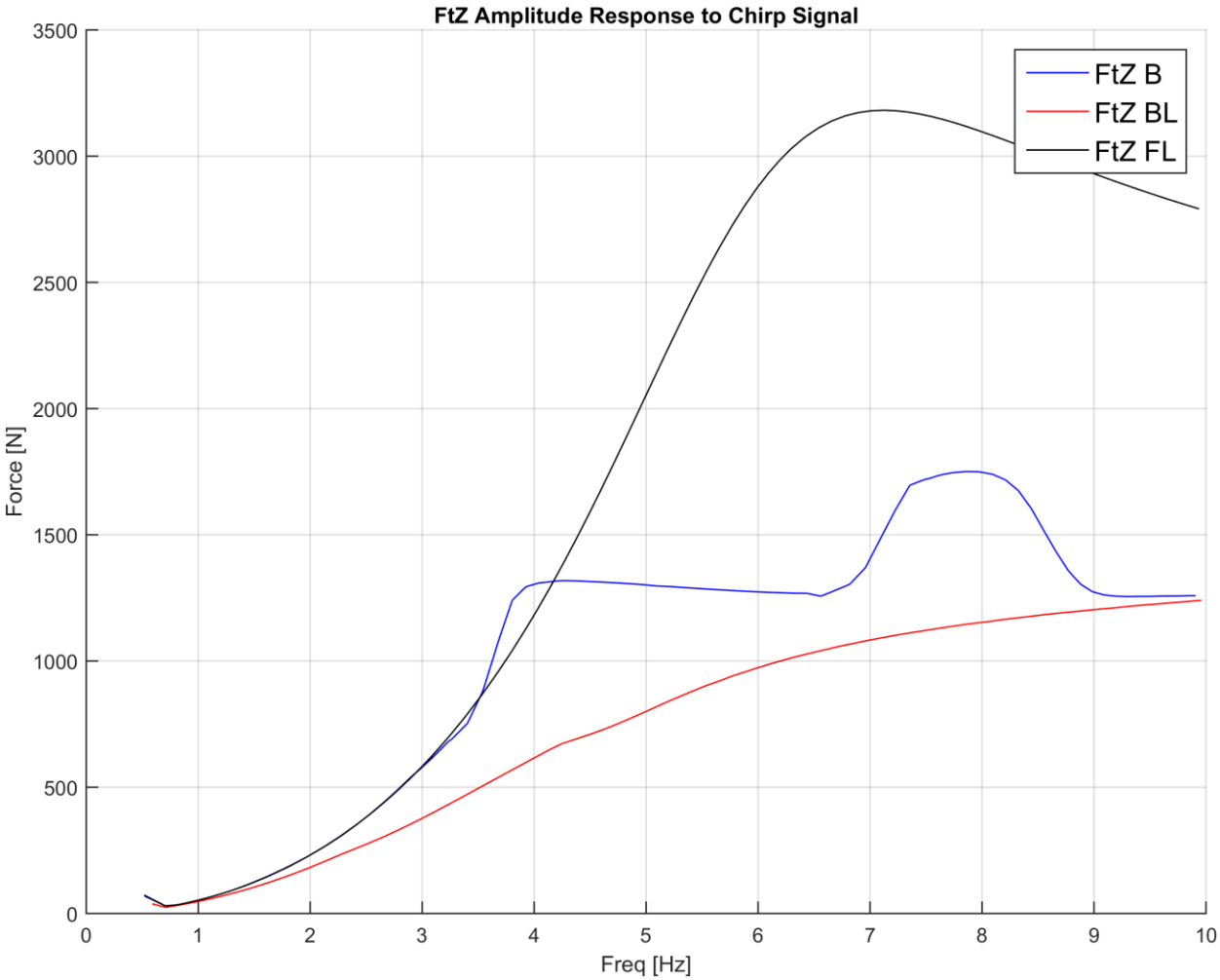

Figure 47 - Contact Patch Force Amplitude to Chirp Input

A final performance metric is shown in Figure 48, actuator force amplitude generated at each frequency. Interestingly, peak force generation occurs around 5Hz. The reason for this is unknown and could be explored in future research.

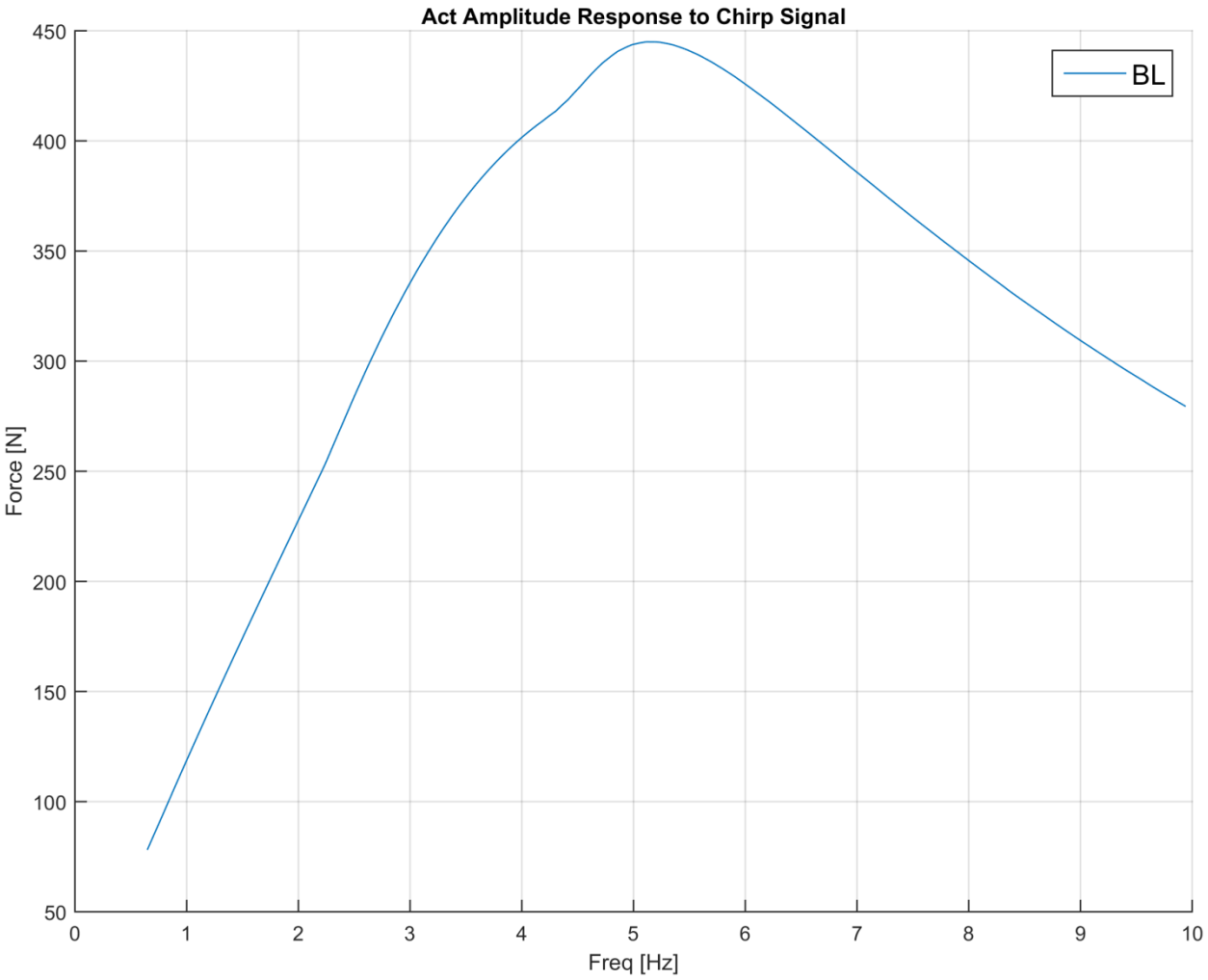

Figure 48 - Actuator Response Amplitude to Chirp Input

7.2.2. Bicycle Model

Like the previous comparison between the ballistic and non-ballistic bicycle model response, the full set of feedback control response for the bicycle will be deferred to Appendix F.

Figure 49 shows the simple StepUp case for the bicycle model. While the results are a little more difficult to determine qualitatively, it is apparent that the overshoot and settling time are reduced for both the chassis and the tires slightly and that the chassis pitch is reduced significantly. More importantly, the force spike seen by both tires is greatly reduced as are subsequent force oscillations.

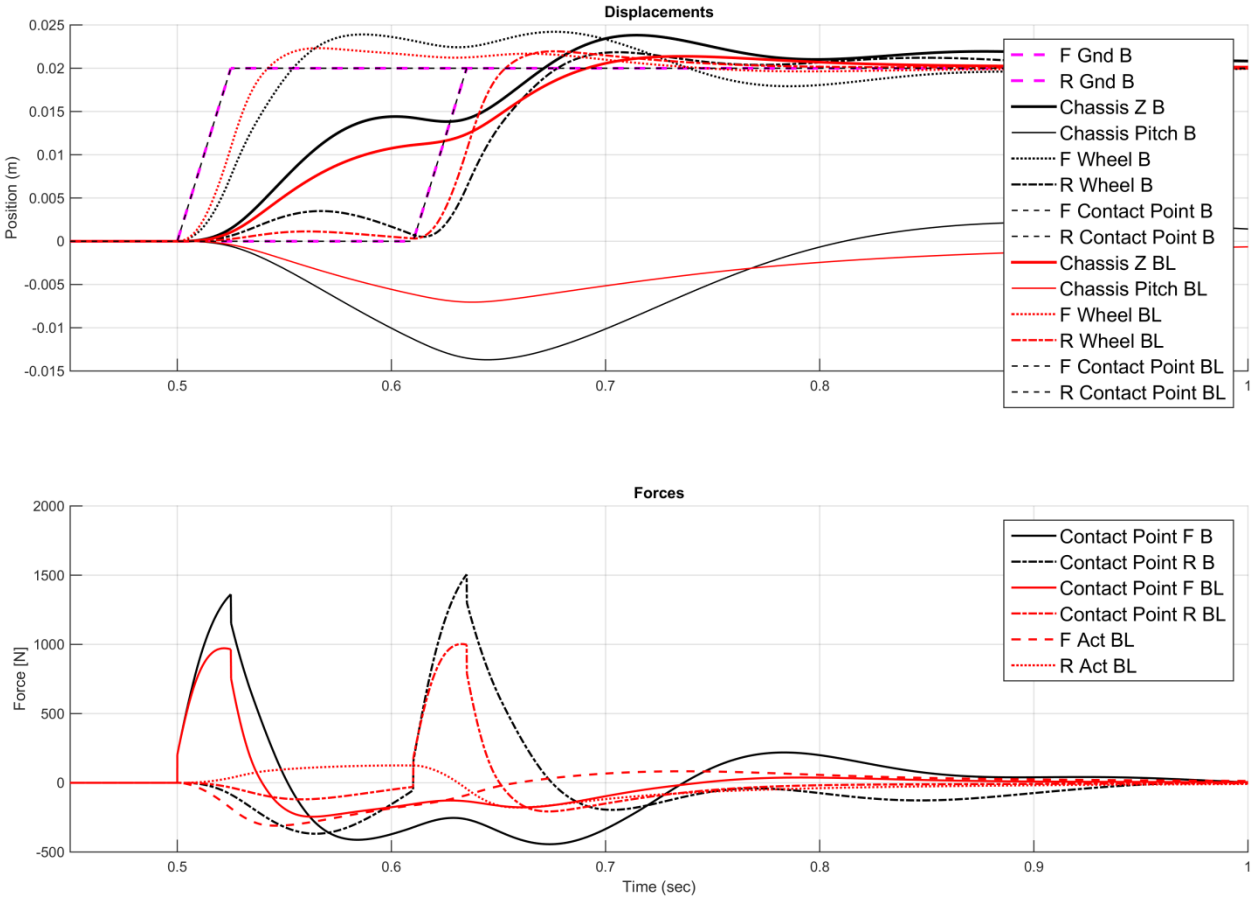

Figure 49 – Bicycle Model StepUp Response with LQR

7.2.3. Full Car

Figure 50 through Figure 55 show markedly similar controller effects for the quarter car and bicycle models. In most circumstances, either response magnitude, overshoot, settling time, or some combination of these were improved.

Like the quarter car and bicycle models, the full vehicle StepUp response in Figure 50 shows a reduction in both chassis velocity, and chassis pitch. In addition, the peak contact patch forces are reduced as well as their oscillation.

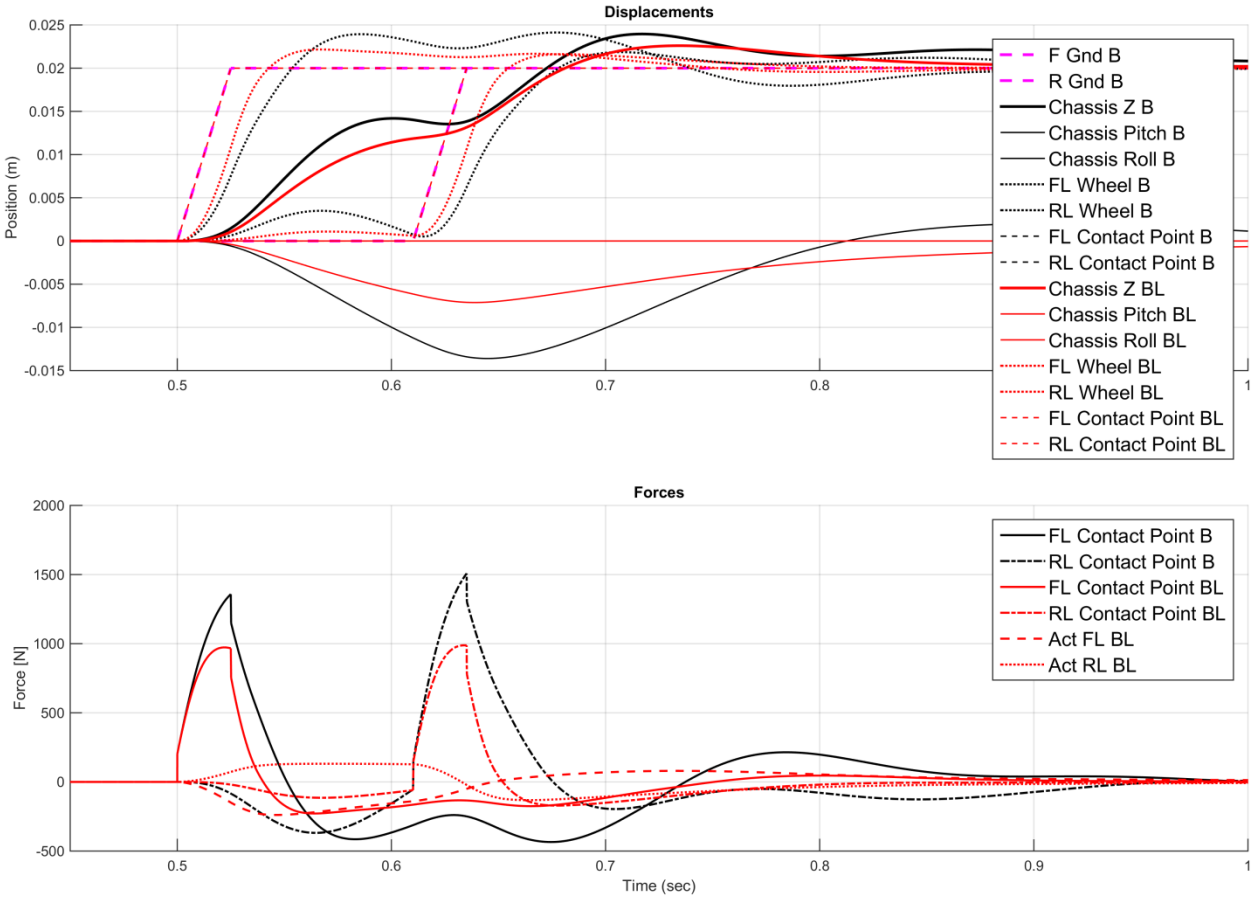

Figure 50 - Full Car StepUp Response with LQR

The full car StepDown response in Figure 51 demonstrates the desired reduction in chassis velocity and settling time, as well as significant reduction of peak contact patch forces as well as a time of flight reduction by nearly one half.

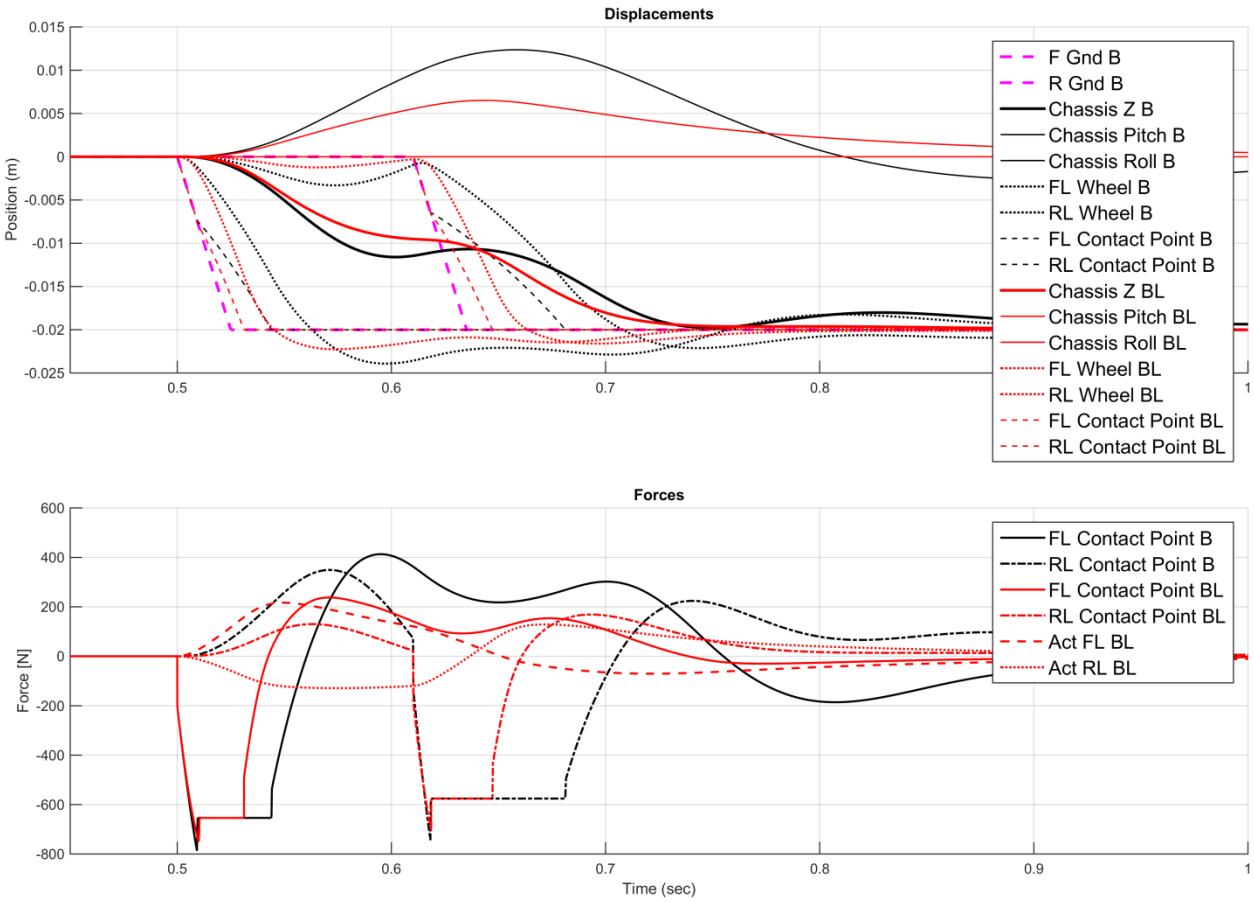

Figure 51 - Full Car StepDown Response with LQR

Reminiscent of the quarter and bicycle models, the full car Sawtooth response shows a slight reduction of chassis velocity and an increase of tire displacement and velocity. However, the changes in contact patch force are not as clearly beneficial. The peak forces remain nearly identical, while time of flight is increased slightly. However, the settling time of the forces are reduced.

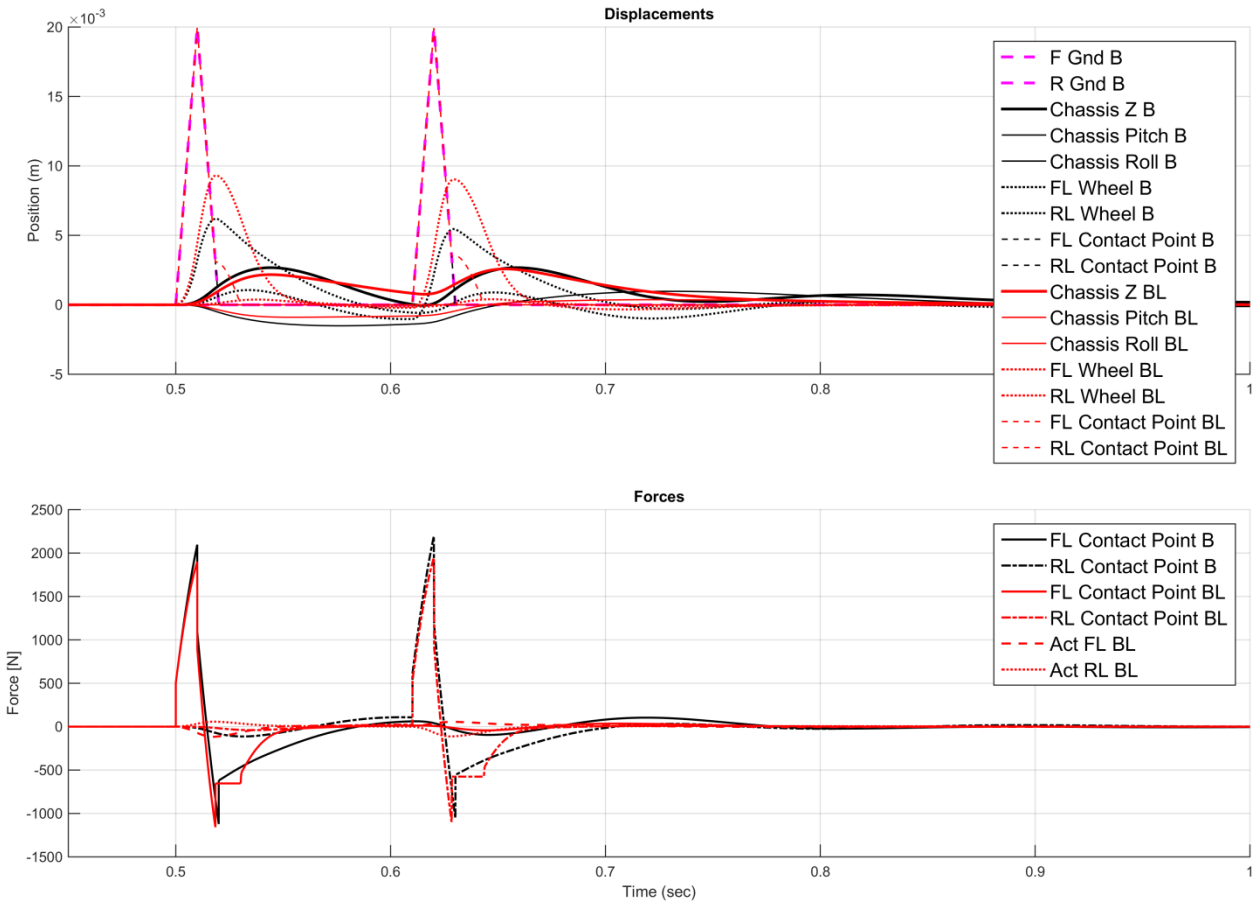

Figure 52 - Full Car Sawtooth Response with LQR

The full car pothole response seen in Figure 53 has an interesting characteristic in that the active and passive response difference of the chassis is more pronounced when the rear tires cross over the pothole. This is due in part to the fact that chassis has residual pitch displacement caused by the first bump. While the peak contact patch forces are similar, there is a settling time improvement as well as a time of flight reduction.

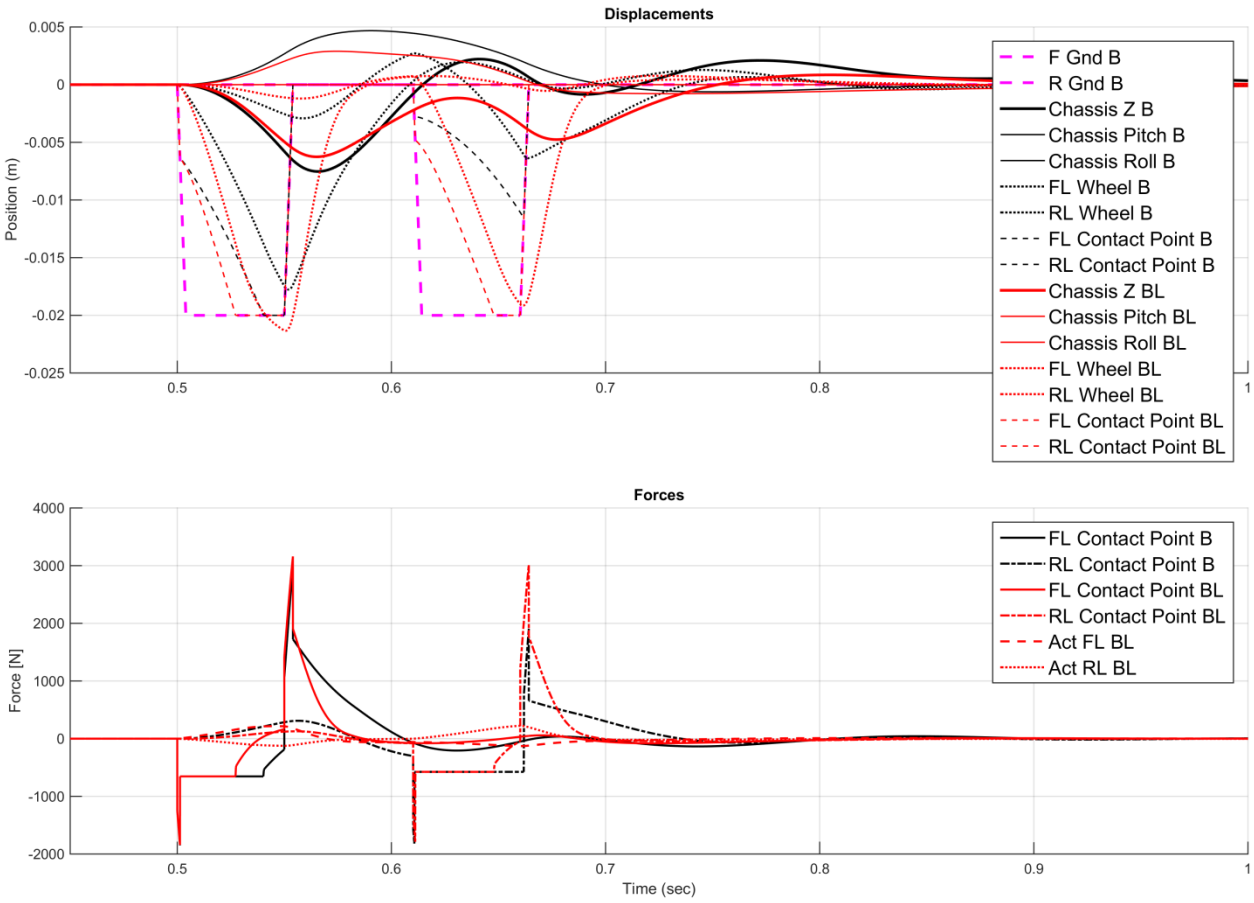

Figure 53 - Full Car Pothole Response with LQR

For relatively low frequency sinusoidal inputs as shown in Figure 54, the active chassis response is reduced by a factor of almost two. Ballistic motion is eliminated, and peak contact patch forces reduced by a factor of nearly two as well.

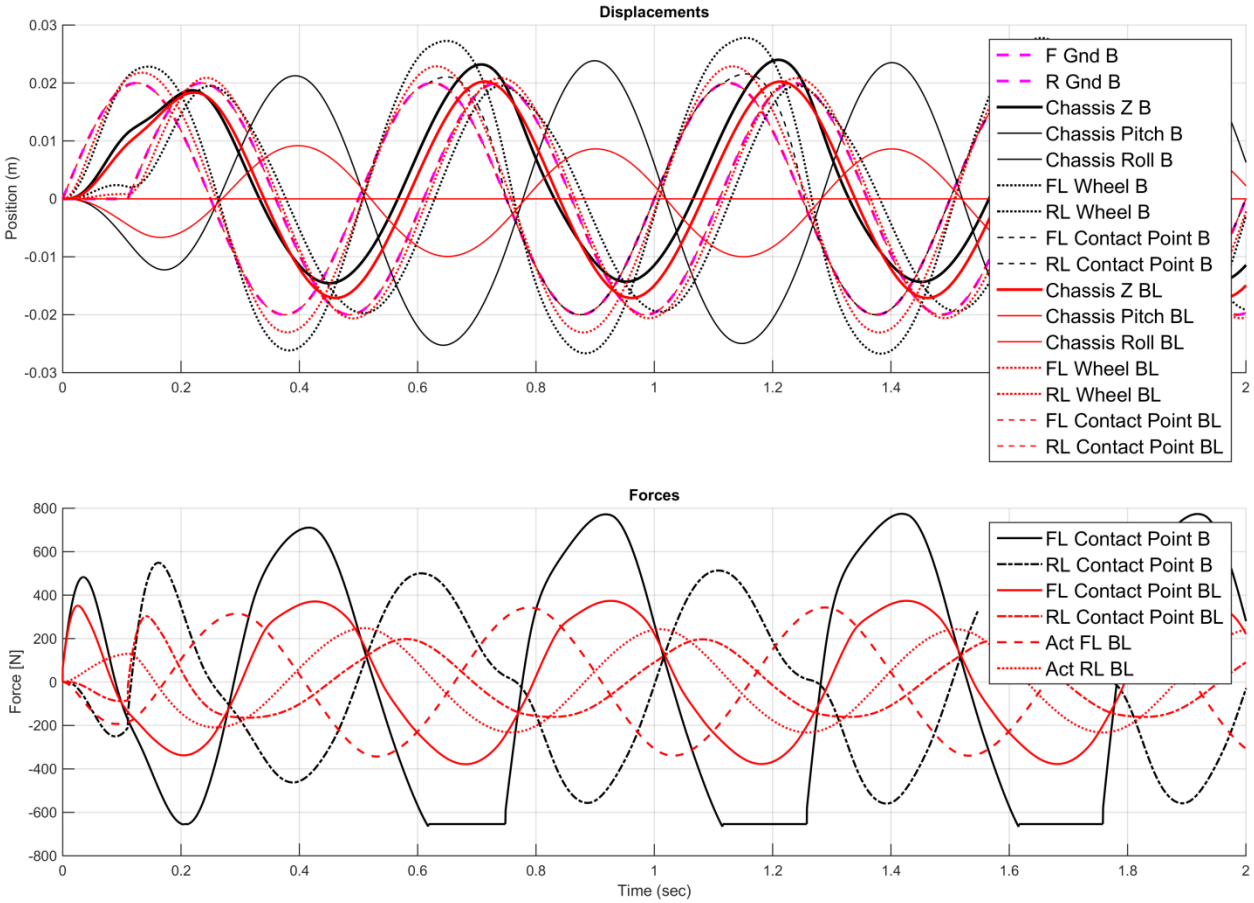

Figure 54 - Full Car 2 Hz Sinusoid Response with LQR

In the case of the high frequency sinusoid (10Hz) in Figure 55, the active system responses are less noticeably different. Peak displacements and forces are nearly the same. There are differences in the tire displacement and velocity.

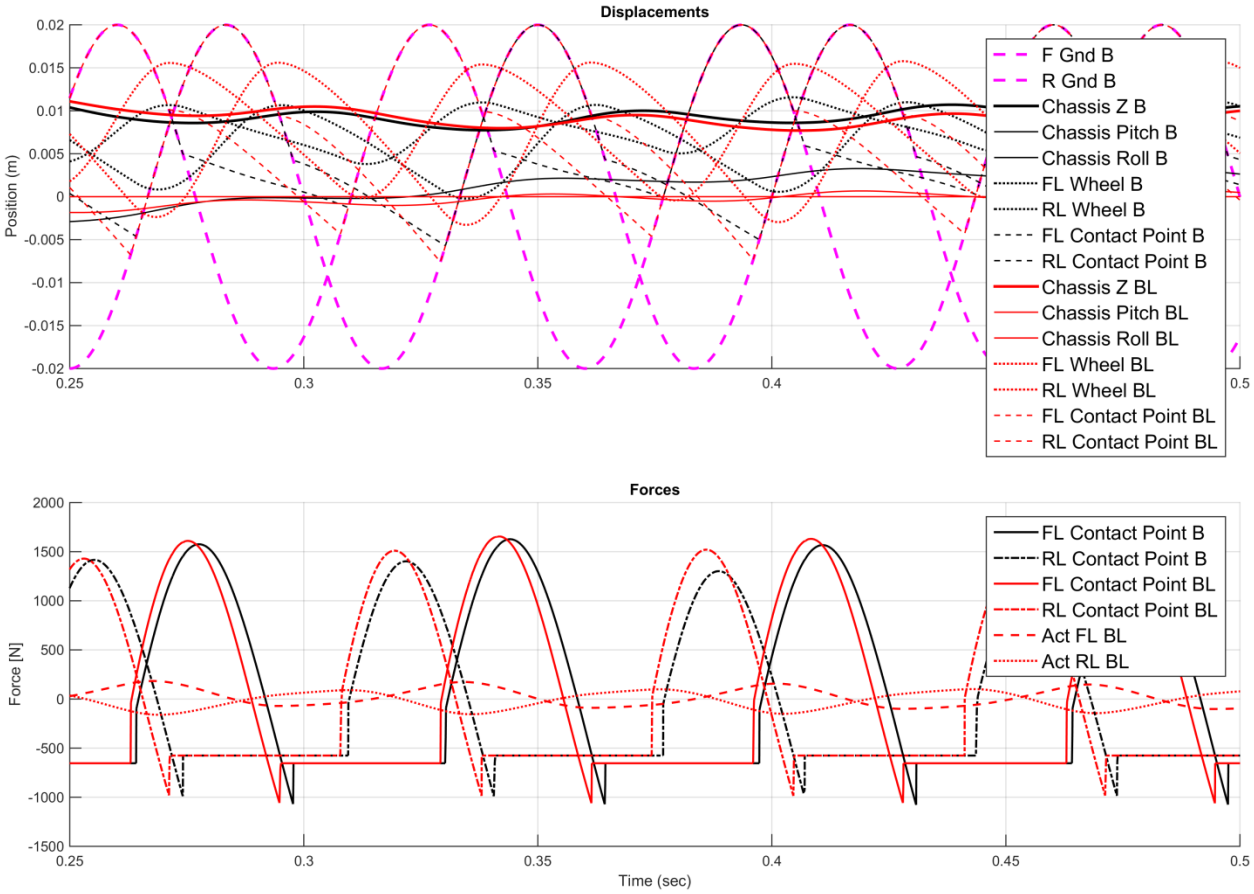

Figure 55 - Full Car 10 Hz Sinusoid Response with LQR

Like the previous two models, the frequency response of the chassis in Figure 56 shows that the linear model is responds very differently to inputs over 2Hz, and that the active system decreases chassis displacement and velocity at all tested frequencies.

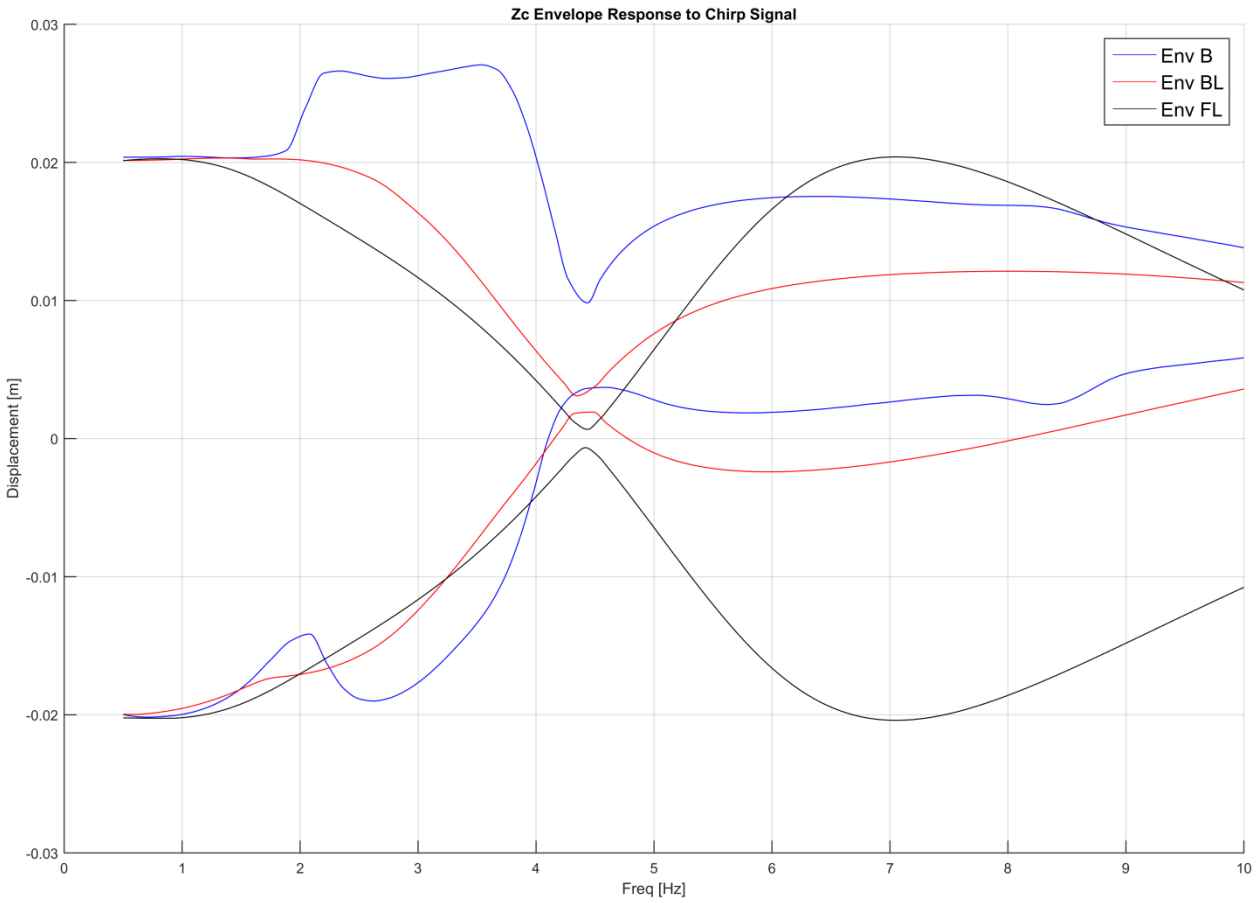

Figure 56 - Full Car Zc Response Envelope to Chirp Input

Chassis motion presented as normalized amplitude is seen in Figure 57. A local amplitude minima exists near 4.4Hz, and the deviation of the linear model is particularly noticeable in the upper half of the test frequencies.

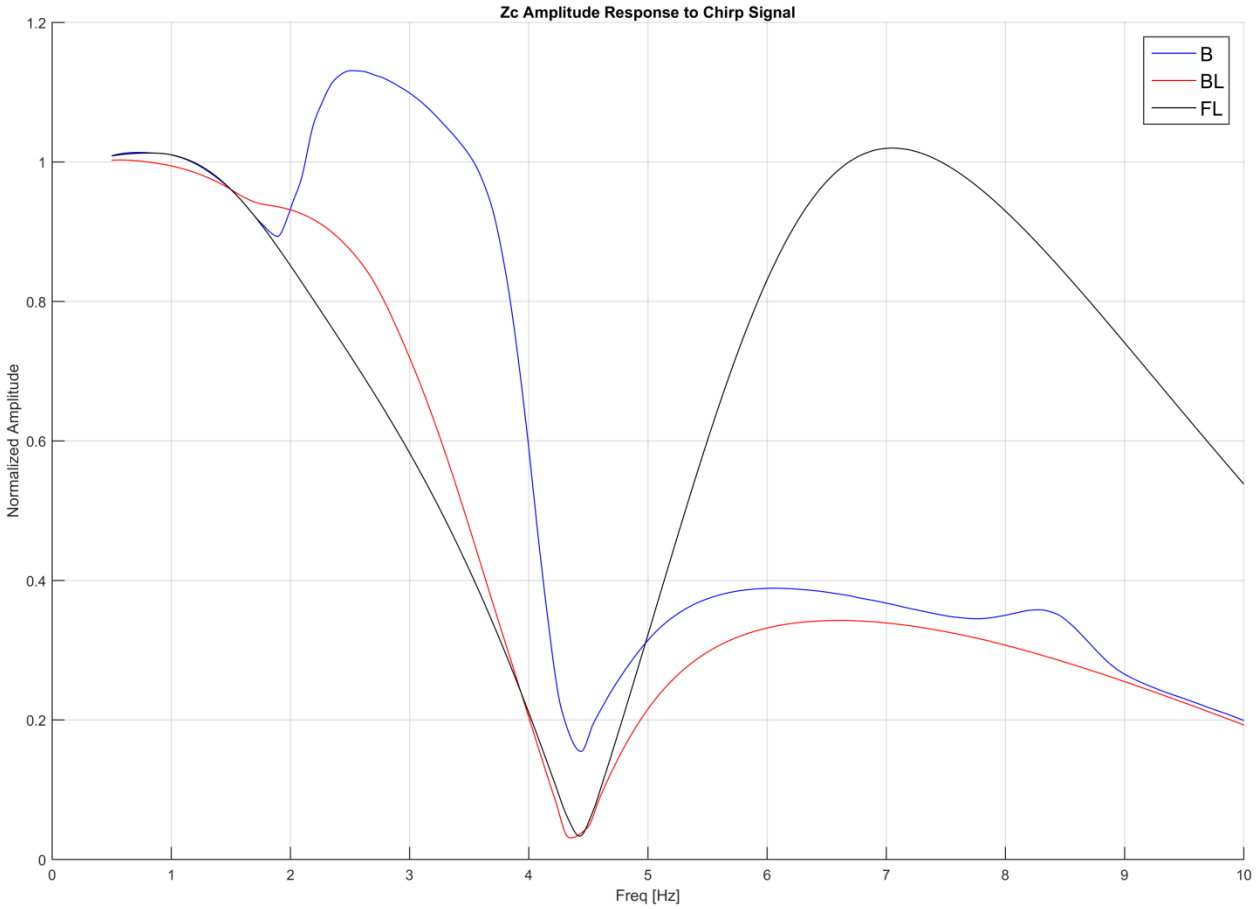

Figure 57 - Full Car Zc Response Amplitude to Chirp Input

Since pitch velocity control was included in these test controller cases, a reduction in pitch magnitude and velocity was observed in Figure 58 as expected.

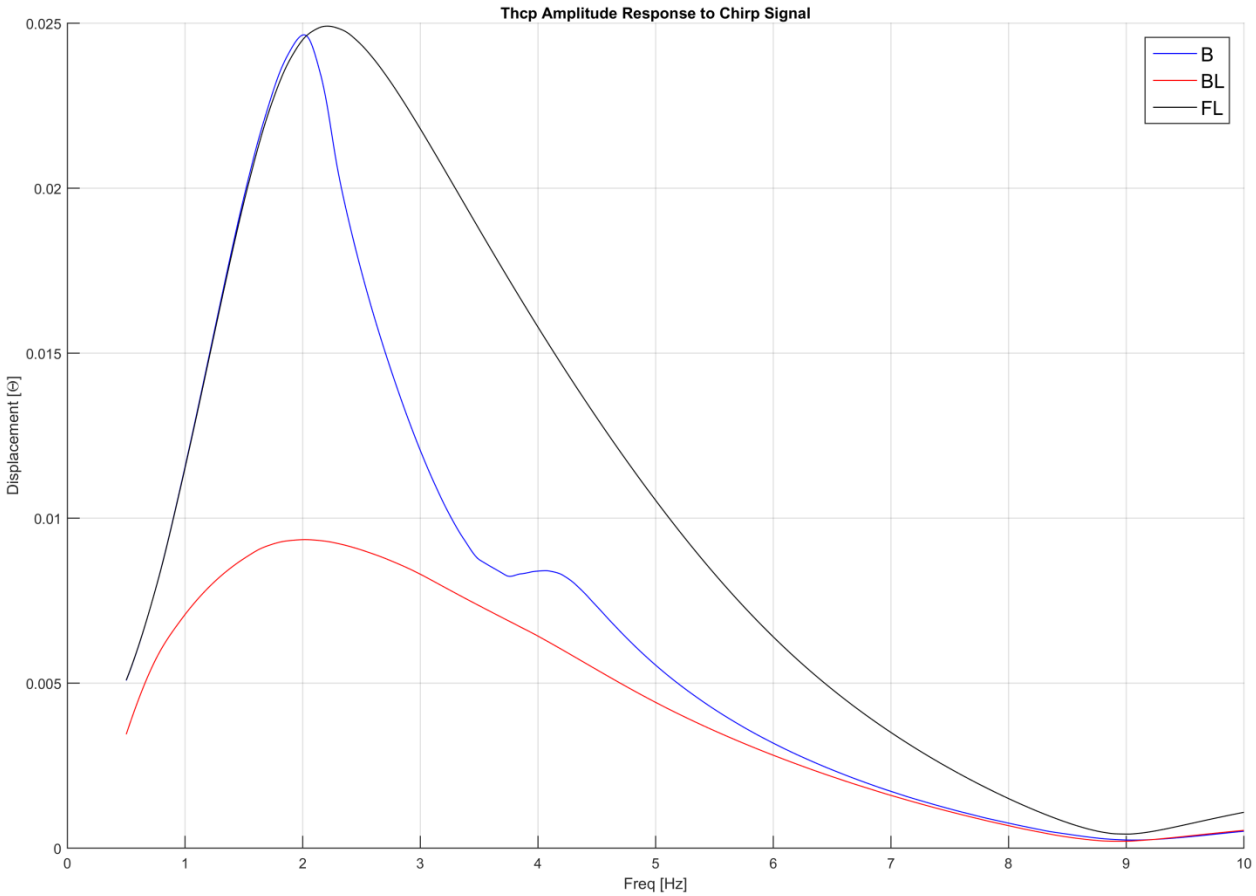

Figure 58 - Full Car Chassis Pitch Amplitude to Chirp Input

Figure 59 illustrates a reduction of contact patch force variation for both front and rear wheels (left and right inputs and thus response are identical). Interestingly, the force response of the linear model is over three times as large at certain frequencies. Part of this difference is due to the contribution of the large negative tire force (when the ground is ‘pulling’ the wheel down).

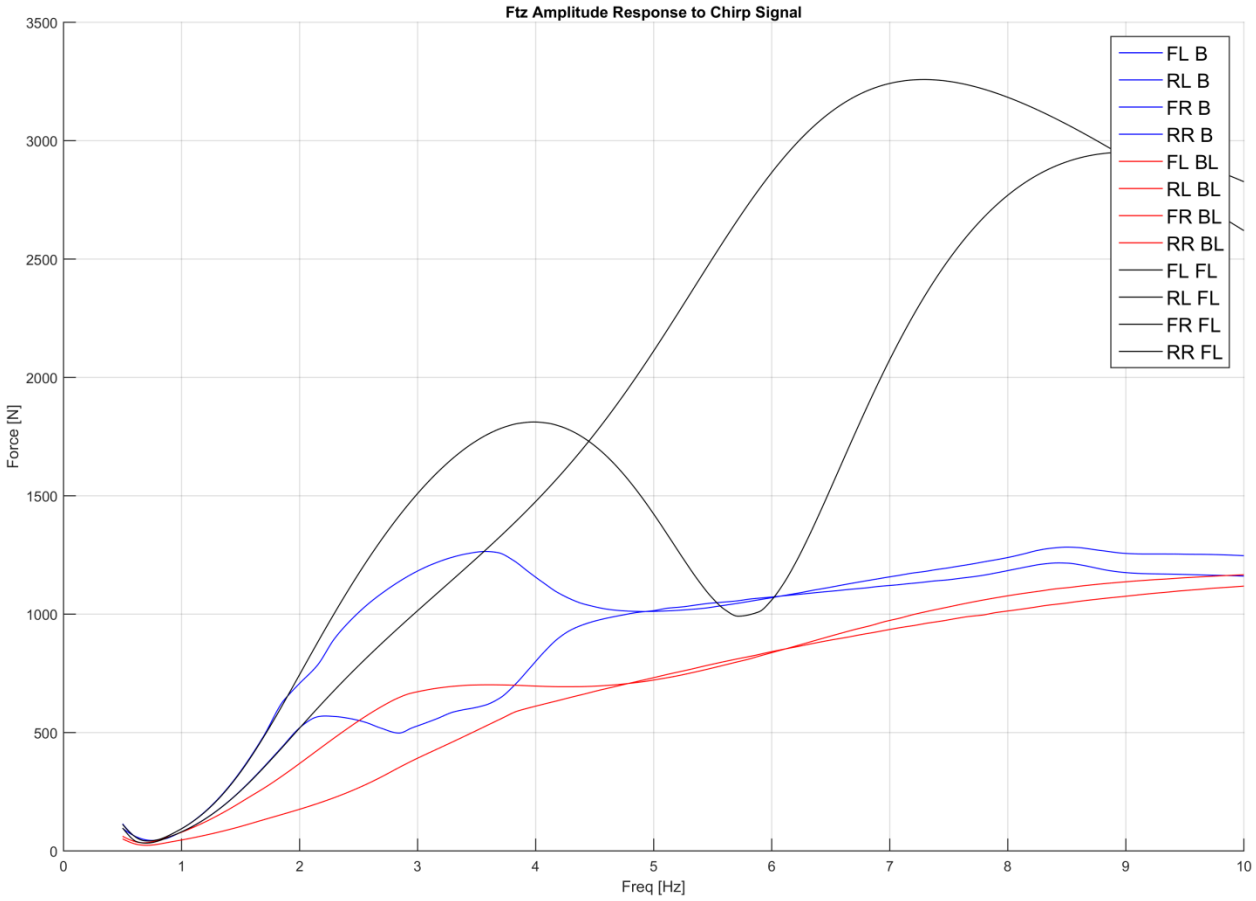

Figure 59 - Full Car Contact Patch Force Magnitude Variation to Chirp Input

Like the quarter car, peak force is requested from the actuators between 3 and 4Hz, the front wheels receiving a noticeably higher force as exhibited in Figure 60.

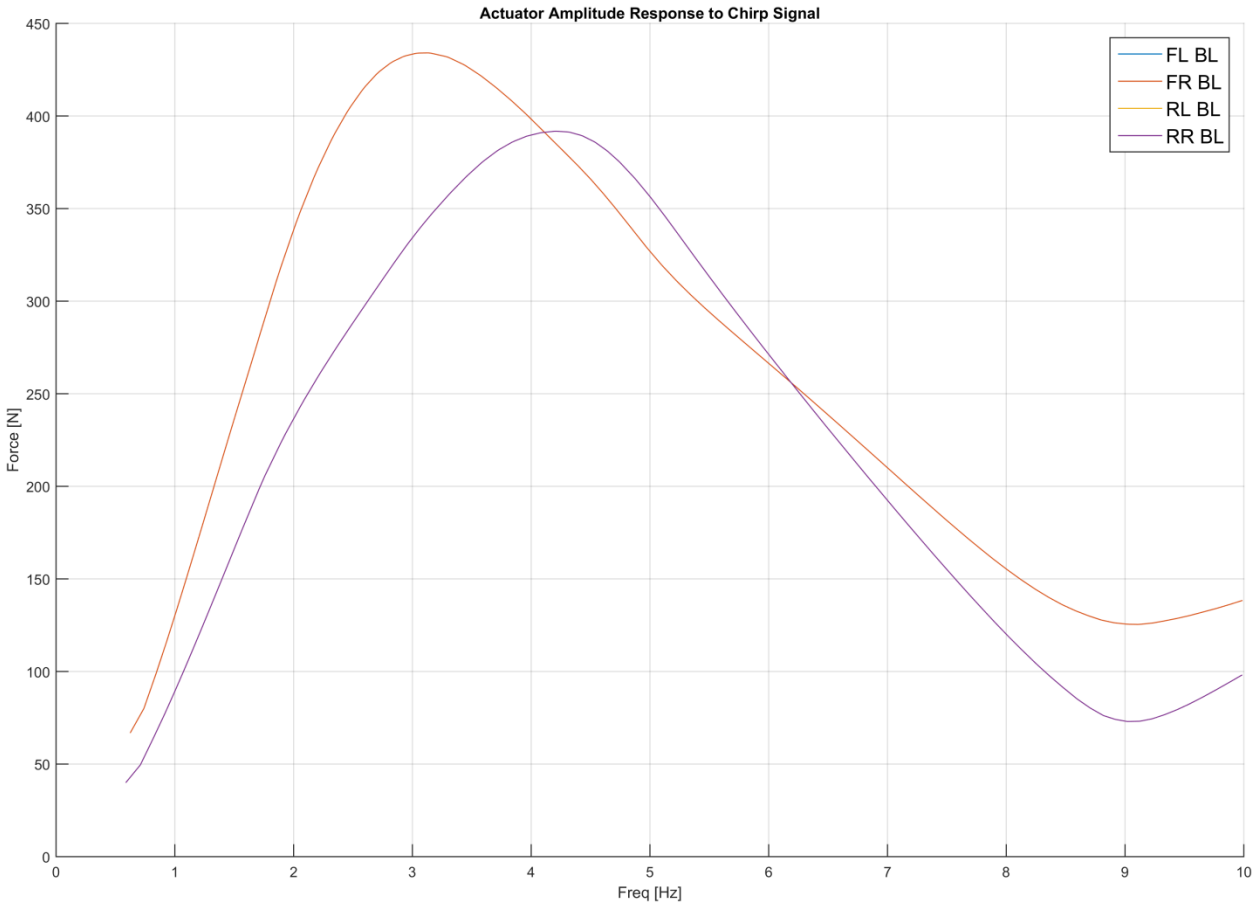

Figure 60 - Full Car Actuator Amplitude to Chirp Input

8. Results

While the plots in Chapter 7 provide good qualitative evidence that the controller is capable of effecting a desirable change in the vehicle's response, a more quantitative comparison can be found in Table 8.1 through Table 8.4. Detrimental contributions are highlighted in red.

8.1. Average Disturbance Magnitude Reduction

As described in Chapter 5.2.1, the primary quantification method was devised as follows. The Average Disturbance Magnitude Reduction is found by taking the average of the difference of the magnitudes (in absolute value) of the passive and the active response over the time duration of interest. This average value is then normalized by the maximum input magnitude of the disturbance. The resultant values for this method are given in Table 8.1 as percent reductions on a proportional basis (1.000 equates to 100% reduction). In this context, a positive number represents an improvement, while a negative number represents a detrimental impact.

Table 8.1 - Average Disturbance Magnitude Reduction

Input	**Quarter Car**	**Bicycle Model**	**Full Car**
StepUp	0.062	0.059	0.060
StepDown	0.117	0.109	0.101
Pothole	0.028	0.015	0.015
Sawtooth	0.018	0.015	0.017
2Hz Sin	0.078	0.339	0.331
10Hz Sin	-0.009	-0.064	-0.013

It is interesting to note that the behavior across the models is relatively consistent. The controller improved the ADMR for all but the 10Hz sin input. Some of the inputs were only slightly improved (the Pothole and Sawtooth) while other inputs such as the 2Hz sin were significantly enhanced. Fortunately, even though the response to 10Hz input with the controller is worse than that without, its detrimental impact appears relatively small in comparison with the improvements afforded to the other inputs.

8.2. Load Fluctuation Rate

As the only quantification method conceived outside of this project itself, the results of this test are an important validation. Detailed in 5.2.2, this method provides a scaled RMS difference between the tire motion and the ground. The values provided in Table 8.2 are the percent reduction of the calculated Load Fluctuation Rate between the passive Ballistic model and the LQR Ballistic model. Again, a positive number is indicative of a response improvement on a proportional basis.

Table 8.2 – Load Fluctuation Rate

Input	Quarter Car	Bicycle Model	Full Car
StepUp	0.352	0.370	0.375
StepDown	0.373	0.411	0.421
Pothole	0.189	0.195	0.211
Sawtooth	-0.040	-0.020	-0.007
2Hz Sin	0.228	0.638	0.615
10Hz Sin	-0.054	-0.064	-0.056

This method shows a greater quantitative improvement in general, than the ADRM method. It is important to note however, that the core of this method is based upon the *displacement* of the tire with respect to ground, which is not necessarily guaranteed to be proportional to the *force* between the tire and ground. Nonetheless, the controller appears to improve the response to all inputs except for the Sawtooth bump and the 10Hz sinusoid.

8.3. Contact Patch Force Standard Deviation

While this method is fundamentally similar to the Load Fluctuation Rate, it is a direct comparison of the standard deviation *of the force between the tire and the ground* directly. The values given in Table 8.3 represent the percent reduction of the Contact Patch Force Standard

Deviation between the passive and active Ballistic models. Again, positive values denote improvement on a proportional basis.

Table 8.3 – Contact Patch RMS Force

	Quarter Car	Bicycle Model	Full Car
StepUp	0.345	0.366	0.372
StepDown	0.316	0.321	0.325
Pothole	0.166	-0.124	-0.128
Sawtooth	0.078	0.065	0.072
2Hz Sin	0.228	0.586	0.568
10Hz Sin	-0.029	-0.048	-0.039

8.4. Time of Flight Reduction

The final quantification method presented in this thesis is probably the simplest to visualize and understand. It is nothing more than the increase or decrease of time that the tire spends in contact with the ground during an input disturbance. It is important to note that not all inputs cause the model response to become ballistic, thus this method is effectively undefined for some inputs. The values provided in Table 8.4 are the amount of *additional* time the tire spends in contact with the ground in the active model relative to the passive model, in seconds. While these times are a little nebulous, for reasons outlined in 5.1, an increase of tire contact time will always improve potential performance.

Table 8.4 – Time of Flight Reduction (seconds)

	Quarter Car	Bicycle Model	Full Car
StepUp	0.020	0.000	0.000
StepDown	0.011	0.023	0.024
Pothole	0.010	0.014	0.014
Sawtooth	-0.009	-0.014	-0.013

2Hz Sin	0.000	0.387	0.354
10Hz Sin	-0.045	-0.048	-0.048

Much like each of the previous methods, the Time of Flight method suggests improved active performance in all cases except for the Sawtooth and 10Hz sin inputs. Values of 0.000 denote models and input combinations that did not see ballistic motion.

9. Conclusions

The most interesting and probably most important conclusion is that for most cases, the linear controller appears capable of improving the system response in terms of the presented quantification methods by between 5 and 60% when compared to the response of the passive system.

Next, the parallel actuator augmentation (using a linear actuator as a third force element in parallel with the passive spring and damper as presented in Diagrams and Coordinate Systems) is able to provide useful control input to the system. While it is possible (and has been utilized), to use a single actuator in place of the spring and damper, *much* higher power usage is required since the entirety of the vehicle must be supported by the system at all times in addition to the control force required in response to inputs. This method might allow for more control, but at a large penalty. The parallel actuation method as proposed uses the existing passive elements for the steady state support and control of the car, while the actuators add to or subtract from that passively generated force as necessary. It was discovered by experimentation and trial and error that the decreasing the passive damping coefficient increased the effectiveness of the controller and used less power. If the passive damping coefficient was decreased too much however, (less than 25% of its original value) the system regained significant oscillatory characteristics. Thus, it appears with current control design and actuator size, the passive damper should not be removed completely. This effect was not evaluated exhaustively, and may be of interest for future exploration.

Furthermore, for a car of *similar size and weight as the modeled UWashington FSAE car*, an actuator capable of 500N is sufficiently large to provide measurable impact to the system. However, "sufficiently" is difficult to define precisely since the impact of such control systems in racecars and safety applications frequently consider even small improvements as advantageous. Any system or change that increases the performance even slightly is important when races are decided by hundredths of seconds, and lives are saved by millimeter misses. That said, an actuator of any size provides beneficial forces, but in general – the larger the actuator, the more authority it has to correct or stabilize the response of the system.

One additional product of this project is a tool that allows all of the *dynamic* suspension and linkage forces to be calculated, where as previously, only steady state forces could be estimated when sizing parts and fasteners and applying load cases to finite stress simulations.

This project also yields a set of standard bump or ground inputs for use in future parts of this project or new projects. After a significant amount of searching, it became apparent that there are very few publicly available test standards for the evaluation of bump performance. Most automotive companies seem to have their own closely guarded and proprietary methods. Semi-trucks and other large vehicles are routinely run over bumps during testing, but at a scale far too large for racecar use, and typically designed for other purposes such as imparting violent, repeated loads for cycle testing. Because of this, a number of reasonable inputs were created based on observation of track surfaces at team testing sites and competition courses. These inputs range from the classical step input, to a non-infinite impulse, pothole, and sinusoids of fixed and varying frequency.

Finally, there are limitations to the use of this model and controller. The model is currently in the vertical translational (Z axis), and roll and pitch rotational axes (A and B axes). For purposes of suspension motion analysis, this is sufficient, but if the model were to be extended into a larger simulation with X and Y motions, modification would be needed. In addition, the vast majority of the work on this model has been targeted at and modeled after small, lightweight formula SAE style vehicles. These vehicles are very high performance. The model may not necessarily extend gracefully to large automobiles and inputs.

10. Future Work

Because of the tremendous potential scope of this project, there are numerous areas that could be explored in future projects.

10.1. Optimal Controller Design

The most beneficial and immediate improvement to this project is a thorough exploration of the controller parameters to optimize the system response over all inputs. Because of time and scope constraints, only a limited set of controller weightings were explored. The perceived controller effectiveness despite this limitation is very promising. In the case of the full car model, there are 14 error weightings contained in just the diagonal of the Q matrix. While most of these were quickly explored in terms of zero vs non-zero weighting, nothing comprehensive or systematic was established. The most promising error weightings were found to be the velocity states, but there may be others. Explicitly, there are off diagonals of the Q matrix. There seem to be few if any resources on this topic but nonetheless it provides interesting possibilities for exploration. Hypothetically, a specific state could only trigger the controller in the co-existence of another. For instance, in other words, the controller could only try to correct errors in chassis pitch when there is *also* a chassis roll error. This could become an enormously complex optimization however, and it might be more time effective to implement a gain scheduling scheme as discussed later in this chapter.

10.1.1. Controller Selection

A further step involves increasing the controller scheme complexity to incorporate LQG control (since not all states are available on the physical car, and because any sensor installed on the car *will* be subject to noise).

Another improvement would be to implement a gain scheduling scheme, either of discrete LQR or LQG controllers. As indicated in Chapter 8, the proposed, simple controller appears to improve the system response for all inputs *except* the Sawtooth and high frequency (10Hz) sinusoids. Presumably there is a different set of Q and R weighting matrices that would better control those inputs. By detecting *when* such inputs are about to occur or are occurring, the scheduler could utilize the controller proven to be most effective with those inputs. In theory, multiple controller weightings could also extend the effectiveness of the controller by allowing it

to prioritize different state errors in different situations such as chassis stability in low speed corners vs bump absorption in high speed segments. Since the vehicle may undergo extreme ranges of inputs – from gentle ground undulations to violent holes and steps, in addition to driver inputs, there are compromises that must be made within a single controller that decrease its effectiveness to other inputs. Examination of driver input would allow certain events such as braking, shifting, or cornering can be detected in addition to the unexpected ground disturbances and bumps.

Care must be taken to prevent "confusing" the scheduler with mixed inputs. Scheduling should likely be implemented through Fuzzy Logic to prevent sudden controller transitions that could hypothetically cause their own disruptions on the system.

10.1.2. Parameters

Since a model is only as useful as the quality of its inputs, the various parameters used throughout the simulation must be closely validated relative to the final vehicle in which it will be installed. In particular, it would be advisable to not only to confirm published specs and parameters, but to test as many as possible, particularly the passive dampers. Passive dampers are well known to have a large degree of manufacturing variability. In order of priority, the parameters that should be verified are the chassis dampers, the spring rates, masses, and inertial properties.

10.1.3. Coefficients

Due to the nature of the LQR controller, its response to certain track conditions and car setups may need to be empirically tuned. On a very smooth track, more emphasis can be placed on attitude control (roll and pitch) while bumpy tracks may require prioritization of wheel or chassis motion. In addition, smoother tracks will use less actuator power over the course of an event and can thus be weighted more heavily to affect more control over relatively smaller disturbances while still meeting power requirements.

10.2. Actuator Design

In order for the controller to be effective, suitable actuators must be designed and built. The only commercially available linearly motors that meet the force, power, and dimensional constraints that could be found are made by LinMot, but are prohibitively expensive at approximately $2000

per actuator and $1000 per controller. Most commercial motors are designed for industrial automation and thus target absolute performance above size, power, and cost.

Some preliminary research and quick calculation indicate that it is not unrealistic to create small (approximately 25mm diameter), high force (>250 N), low voltage (24V) three phase motors. N52 Neodymium magnets are the clear choice for their magnetic flux density and relatively wide availability. The magnet stack should be housed in a tube that serves as the stator, surrounded by coils and commutated with three phase power circuitry driven by a microcontroller. Position should be measured via resolvers.

10.3. Physical Implementation

Once the mathematical control has been sufficiently optimized, they physical system should be designed, constructed, tested, and tuned. Based on the results of this project, it is clear that the proposed active system has real potential and should be validated on a vehicle. Once fitted, there will no doubt be some ‘tuning’ of the controller required to achieve the best possible performance.

The physical implementation of the actuators will be challenging. The racecar is tightly packaged and there is very little excess space, particularly that which is cool, dry, and shielded from flying road debris. Ideally the actuators are mounted to the existing bell cranks on an additional mounting point.

10.4. Other Considerations

One interesting possibility that came up toward the end of this project was the idea of a hybrid active/passive system. The primary motivation for this approach is due to a strict power budget. With unlimited power available, the most effective setup would be to forgo the passive spring and damper entirely, providing all control forces via control strategy and a powerful linear force actuator. This requires supporting the full vehicle weight at all times which requires a very large power draw, and has poor failure modes. However, when the actuator is used as a third element in parallel, it is at times combating the relatively large forces generated by the passive damper. If the passive damper were replaced by a magnetorheological damper, it could be ‘turned off’ during excessively high velocity events allowing the linear actuator to have a higher percentage

of overall force. In order to accommodate such a system, the control system would need to be expanded to control an additional four system inputs.

In addition, this project focused primarily on controlling the response of the vehicle due to inputs from below (the ground). However, these are not the only inputs – there are others due to aerodynamic downforce, lateral and longitudinal acceleration, and shifting. The model has been constructed with these inputs in mind, but not explored.

In a real world system, it is very likely to encounter multiple inputs at the same time. Some effort should be put into exploring simultaneous inputs of similar and dissimilar types (such as a pothole under one lateral half of the vehicle, and a Sawtooth bump on the other). There are also a number of mixed inputs (such as high lateral acceleration and bumps) that have been observed to cause near instabilities in the physical vehicle. These combinations should be evaluated in the virtual model.

Since the real car is likely to experience 'random' input, experimentation with random noise inputs may yield interesting results. Unfortunately, most random signal generation functions within Simulink are discrete and discontinuous – which are not appropriate for the reasons discussed in Mathematical Limitations. The communications toolbox has several functions which may be helpful in this case, but was not available during the course of this project. Thus, a proposed signal would consist of, a composite, weighted sinusoid. A selection of 10 frequencies from 1 to 10 Hz were summed together and weighted according to the desired focus (high frequency or low frequency) a sample of which is seen in Figure 61. This idea will require further future development, as the frequency and weighting factors are currently arbitrary.

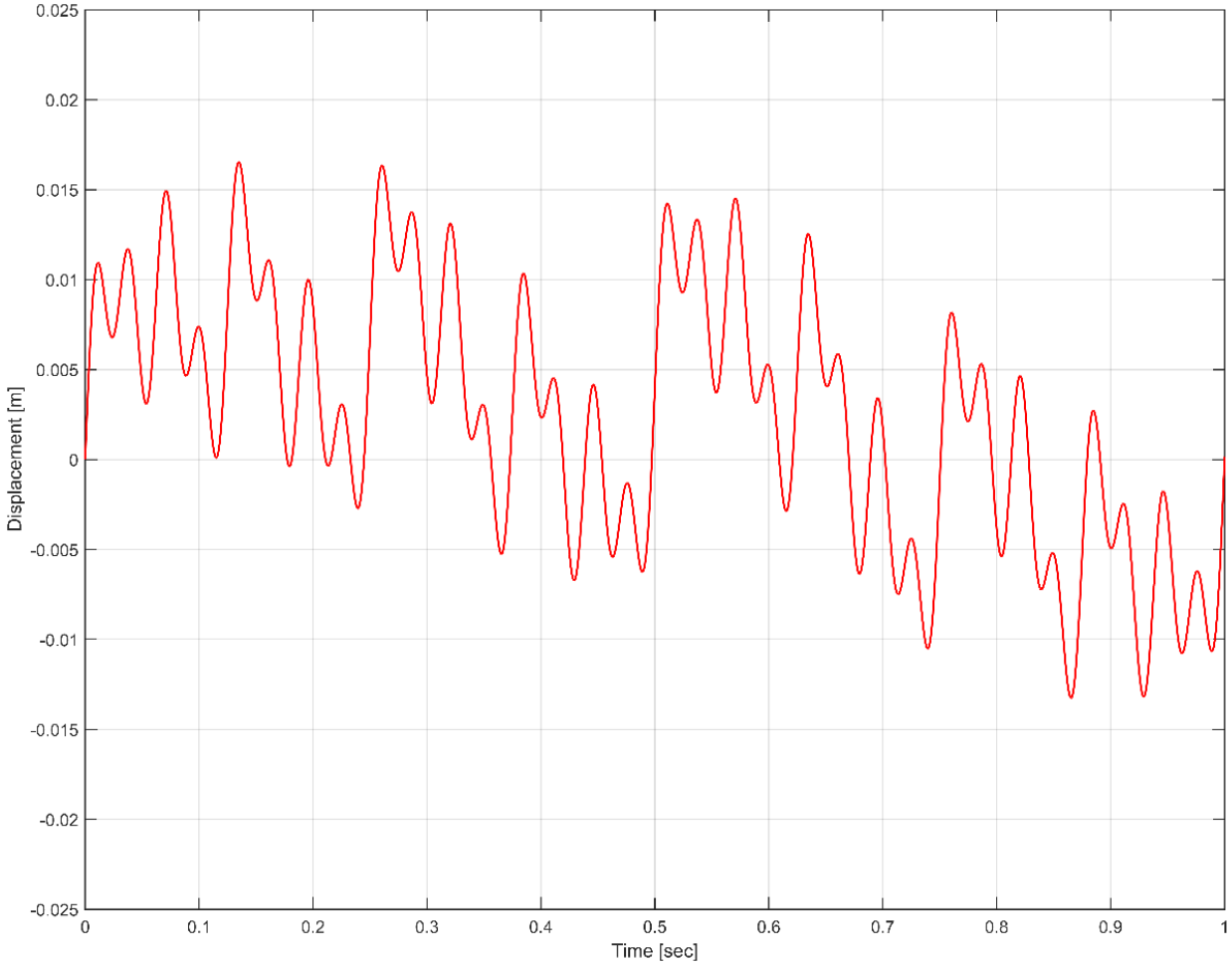

Figure 61 - Sudo Random Noise Input

Finally, because of the complexity of this model and its requirement for a significant amount of input data, it is best suited for looking at the combined vehicle response to various driver inputs, accelerations, and ground irregularities with and without active elements for *limited* sections of track, such as important corners and transition (braking into cornering, cornering into accelerating, etc.) zones. However, long term, it could be incorporated into the team's quasi-steady state CompSim simulator to get more accurate response to the full course simulations.

APPENDICIES

Appendix A – Dynamic Equation Derivations

For the linearized state space models, the equations of motion were all derived symbolically in MATLAB using Lagrangian techniques. It was found that this automated method was the most precise, preventing sign errors or variable mixing, and was relatively easy to script.

For the Simulink models, the block ‘equations’ were developed through inspection of the aforementioned Lagrangian derived equations for the initial linear system, and then through inspection of the non-linear aspects of the physical system. This method is in fact one of the advantages of Simulink – the relationship between complex systems and their models is readily visible and easy to debug as opposed to complex sets of simultaneous equations.

The specific details of the derivation are not within the scope of this project, but the general approach was to write the Kinetic and Potential equations by inspection of the system illustrations provided in Diagrams and Coordinate Systems. Next, the non-conservative parts of the system (tire and chassis dampers, and force actuators) were incorporated by applying the Rayleigh dissipation function. The resulting equations of motion were then generated through the mechanical application of the appropriate partial differentials. Finally, those equations of motion were factored into the A state matrix and B input matrices. The key equations and resultant matrices are provided in the next section.

Appendix B – Linear State Space Modeling

Resultant Equations:

Single Mass

Equation 1 – Single Mass Lagrange T – Kinetic Energy Relations

$$\frac{M_m \dot{Z_c}^2}{2}$$

Equation 2 – Single Mass Lagrange V – Potential Energy Relations

$$\frac{K_m \left(Z_c - Z_g\right)^2}{2}$$

Equation 3 - Single Mass Vertical Chassis Translation – Equation of Motion

$$F_{act} - F_{vd} M_m \ddot{Z_c} C_m \left(\dot{Z_c} - \dot{Z_g}\right) K_m \left(Z_c - Z_g\right)$$

Equation 4 - Single Mass A Matrix – State or System Matrix

$$\begin{pmatrix} 0 & 1 \\ -\frac{K_m}{M_m} & -\frac{C_m}{M_m} \end{pmatrix}$$

Equation 5 – Single Mass B Matrix – Input Matrix

$$\begin{pmatrix} 0 & 0 & 0 & 0 \\ \frac{K_m}{M_m} & \frac{C_m}{M_m} & -\frac{1}{M_m} & \frac{1}{M_m} \end{pmatrix}$$

Quarter Car

Equation 6 – Quarter Car Lagrange T – Kinetic Energy Relations

$$\frac{M_c \dot{Z_c}^2}{2} \frac{M_t \dot{Z_t}^2}{2}$$

Equation 7 – Quarter Car Lagrange V – Potential Energy Relations

$$\frac{K_c \left(Z_c - Z_t\right)^2}{2} \frac{K_t \left(Z_g - Z_t\right)^2}{2}$$

Equation 8 - Quarter Car Vertical Chassis Translation – Equation of Motion

$$M_c \ddot{Z}_c - F_{vd} - F_{act} C_c \left(\dot{Z}_c - \dot{Z}_t\right) K_c \left(Z_c - Z_t\right)$$

Equation 9 - Quarter Car Vertical Tire Translation – Equation of Motion

$$F_{act} M_t \ddot{Z}_t - C_c \left(\dot{Z}_c - \dot{Z}_t\right) - C_t \left(\dot{Z}_g - \dot{Z}_t\right) - K_c \left(Z_c - Z_t\right) - K_t \left(Z_g - Z_t\right)$$

Equation 10 - Quarter Car A Matrix – State or System Matrix

$$\begin{pmatrix} 0 & 1 & 0 & 0 \\ -\frac{K_c}{M_c} & -\frac{C_c}{M_c} & \frac{K_c}{M_c} & \frac{C_c}{M_c} \\ 0 & 0 & 0 & 1 \\ \frac{K_c}{M_t} & \frac{C_c}{M_t} & -\frac{K_c+K_t}{M_t} & -\frac{C_c+C_t}{M_t} \end{pmatrix}$$

Equation 11 – Quarter Car B Matrix – Input Matrix

$$\begin{pmatrix} 0 & 0 & 0 & 0 \\ 0 & 0 & \frac{1}{M_c} & \frac{1}{M_c} \\ 0 & 0 & 0 & 0 \\ \frac{K_t}{M_t} & \frac{C_t}{M_t} & -\frac{1}{M_t} & 0 \end{pmatrix}$$

Bicycle Model

Equation 12 – Bicycle Model Lagrange T – Kinetic Energy Relations

$$\frac{I_c \dot{\theta_{cp}}^2}{2} \frac{M_c \dot{Z_c}^2}{2} \frac{M_{tf} \dot{Z_{tf}}^2}{2} \frac{M_{tr} \dot{Z_{tr}}^2}{2}$$

Equation 13 – Bicycle Model Lagrange V – Potential Energy Relations

$$\frac{K_{cf}\left(Z_{tf} - Z_c A_a \theta_{cp}\right)^2}{2} \frac{K_{cr}\left(Z_c - Z_{tr} B_b \theta_{cp}\right)^2}{2} \frac{K_{tf}\left(Z_{gf} - Z_{tf}\right)^2}{2} \frac{K_{tr}\left(Z_{gr} - Z_{tr}\right)^2}{2}$$

Equation 14 - Bicycle Model Vertical Chassis Translation – Equation of Motion

$$K_{cf} Z_c - F_r - F_f K_{cr} Z_c - K_{cf} Z_{tf} - K_{cr} Z_{tr} M_c \ddot{Z}_c C_{cf} \dot{Z}_c C_{cr} \dot{Z}_c - C_{cf} \dot{Z}_{tf} - C_{cr} \dot{Z}_{tr} - A_a C_{cf} \dot{\theta_{cp}} B_b C_{cr} \dot{\theta_{cp}} - A_a K_{cf} \theta_{cp} B_b K_{cr} \theta_{cp}$$

Equation 15 - Bicycle Model Vertical Front Tire Translation – Equation of Motion

$$F_f - K_{cf} Z_c K_{cf} Z_{tf} - K_{tf} Z_{gf} K_{tf} Z_{tf} M_{tf} \ddot{Z_{tf}} - C_{cf} \dot{Z_c} C_{cf} \dot{Z_{tf}} - C_{tf} \dot{Z_{gf}} C_{tf} \dot{Z_{tf}} A_a C_{cf} \dot{\theta_{cp}} A_a K_{cf} \theta_{cp}$$

Equation 16 - Bicycle Model Vertical Rear Tire Translation – Equation of Motion

$$F_r - K_{cr} Z_c K_{cr} Z_{tr} - K_{tr} Z_{gr} K_{tr} Z_{tr} M_{tr} \ddot{Z_{tr}} - C_{cr} \dot{Z_c} C_{cr} \dot{Z_{tr}} - C_{tr} \dot{Z_{gr}} C_{tr} \dot{Z_{tr}} - B_b C_{cr} \dot{\theta_{cp}} - B_b K_{cr} \theta_{cp}$$

Equation 17 - Bicycle Model Chassis Pitch – Equation of Motion

$$A_a F_f - T_c - B_b F_r I_c \ddot{\theta_{cp}} A_a C_{cf} \left(\dot{Z_{tf}} - \dot{Z_c} A_a \dot{\theta_{cp}}\right) B_b C_{cr} \left(\dot{Z_c} - \dot{Z_{tr}} B_b \dot{\theta_{cp}}\right) A_a K_{cf} \left(Z_{tf} - Z_c A_a \theta_{cp}\right) B_b K_{cr} \left(Z_c - Z_{tr} B_b \theta_{cp}\right)$$

Equation 18 - Bicycle Model A Matrix – State or System Matrix

$$\begin{pmatrix} 0 & 1 & 0 & 0 & 0 & 0 & 0 & 0 \\ -\frac{K_{cf}+K_{cr}}{M_c} & -\frac{C_{cf}+C_{cr}}{M_c} & \frac{A_a K_{cf}-B_b K_{cr}}{M_c} & \frac{A_a C_{cf}-B_b C_{cr}}{M_c} & \frac{K_{cr}}{M_c} & \frac{C_{cr}}{M_c} & \frac{K_{cf}}{M_c} & \frac{C_{cf}}{M_c} \\ 0 & 0 & 0 & 1 & 0 & 0 & 0 & 0 \\ \frac{A_a K_{cf}-B_b K_{cr}}{I_c} & \frac{A_a C_{cf}-B_b C_{cr}}{I_c} & -\frac{K_{cf} {A_a}^2+K_{cr} {B_b}^2}{I_c} & -\frac{C_{cf} {A_a}^2+C_{cr} {B_b}^2}{I_c} & \frac{B_b K_{cr}}{I_c} & \frac{B_b C_{cr}}{I_c} & -\frac{A_a K_{cf}}{I_c} & -\frac{A_a C_{cf}}{I_c} \\ 0 & 0 & 0 & 0 & 0 & 1 & 0 & 0 \\ \frac{K_{cr}}{M_{tr}} & \frac{C_{cr}}{M_{tr}} & \frac{B_b K_{cr}}{M_{tr}} & \frac{B_b C_{cr}}{M_{tr}} & -\frac{K_{cr}+K_{tr}}{M_{tr}} & -\frac{C_{cr}+C_{tr}}{M_{tr}} & 0 & 0 \\ 0 & 0 & 0 & 0 & 0 & 0 & 0 & 1 \\ \frac{K_{cf}}{M_{tf}} & \frac{C_{cf}}{M_{tf}} & -\frac{A_a K_{cf}}{M_{tf}} & -\frac{A_a C_{cf}}{M_{tf}} & 0 & 0 & -\frac{K_{cf}+K_{tf}}{M_{tf}} & -\frac{C_{cf}+C_{tf}}{M_{tf}} \end{pmatrix}$$

Equation 19 – Bicycle Model B Matrix – Input Matrix

$$\begin{pmatrix} 0 & 0 & 0 & 0 & 0 & 0 & 0 \\ 0 & 0 & 0 & 0 & \frac{1}{M_c} & \frac{1}{M_c} & 0 \\ 0 & 0 & 0 & 0 & 0 & 0 & 0 \\ 0 & 0 & 0 & 0 & -\frac{A_a}{I_c} & \frac{B_b}{I_c} & \frac{1}{I_c} \\ 0 & 0 & 0 & 0 & 0 & 0 & 0 \\ \frac{K_{tr}}{M_{tr}} & \frac{C_{tr}}{M_{tr}} & 0 & 0 & 0 & -\frac{1}{M_{tr}} & 0 \\ 0 & 0 & 0 & 0 & 0 & 0 & 0 \\ 0 & 0 & \frac{K_{tf}}{M_{tf}} & \frac{C_{tf}}{M_{tf}} & -\frac{1}{M_{tf}} & 0 & 0 \end{pmatrix}$$

Full Car

Equation 20 – Full Car Lagrange T – Kinetic Energy Relations

$$\frac{\mathrm{I_{cp}} \dot{\theta_{cp}}^2}{2} + \frac{\mathrm{I_{cr}} \dot{\theta_{cr}}^2}{2} + \frac{\mathrm{M_c} \dot{X_c}^2}{2} + \frac{\mathrm{M_{tfl}} \dot{X_{tfl}}^2}{2} + \frac{\mathrm{M_{tfr}} \dot{X_{tfr}}^2}{2} + \frac{\mathrm{M_{trl}} \dot{X_{trl}}^2}{2} + \frac{\mathrm{M_{trr}} \dot{X_{trr}}^2}{2}$$

Equation 21 – Full Car Lagrange V – Potential Energy Relations

$$\frac{\mathrm{K_{farb}}\left(\mathrm{X_{tfl}}-\mathrm{X_{tfr}}\right)^2}{2} + \frac{\mathrm{K_{farb}}\left(\mathrm{X_{trl}}-\mathrm{X_{trr}}\right)^2}{2} + \frac{\mathrm{K_{tfl}}\left(\mathrm{X_{gfl}}-\mathrm{X_{tfl}}\right)^2}{2} + \frac{\mathrm{K_{tfr}}\left(\mathrm{X_{gfr}}-\mathrm{X_{tfr}}\right)^2}{2} + \frac{\mathrm{K_{trl}}\left(\mathrm{X_{grl}}-\mathrm{X_{trl}}\right)^2}{2} + \frac{\mathrm{K_{trr}}\left(\mathrm{X_{grr}}-\mathrm{X_{trr}}\right)^2}{2} +$$

$$\frac{K_{cfl}\left(X_c-X_{tfl}+\frac{\theta_{cr}W_b}{2}-A_a\theta_{cp}\right)^2}{2}+\frac{K_{cfr}\left(X_{tfr}-X_c+\frac{\theta_{cr}W_b}{2}+A_a\theta_{cp}\right)^2}{2}+\frac{K_{crl}\left(X_c-X_{trl}+\frac{\theta_{cr}W_b}{2}+B_b\theta_{cp}\right)^2}{2}+\frac{K_{crr}\left(X_c-X_{trr}-\frac{\theta_{cr}W_b}{2}+B_b\theta_{cp}\right)^2}{2}$$

Equation 22 - Full Car Vertical Chassis Translation – Equation of Motion

$$M_c\ddot{X}_c-F_{fr}-F_{rl}-F_{rr}-F_{fl}+C_{cfl}\left(\dot{X}_c-\dot{X}_{tfl}+\frac{\dot{\theta}_{cr}W_b}{2}-A_a\dot{\theta}_{cp}\right)-C_{cfr}\left(\dot{X}_{tfr}-\dot{X}_c+\frac{\dot{\theta}_{cr}W_b}{2}+A_a\dot{\theta}_{cp}\right)+C_{crl}\left(\dot{X}_c-\dot{X}_{trl}+\frac{\dot{\theta}_{cr}W_b}{2}+B_b\dot{\theta}_{cp}\right)+C_{crr}\left(\dot{X}_c-\dot{X}_{trr}-\frac{\dot{\theta}_{cr}W_b}{2}+B_b\dot{\theta}_{cp}\right)+$$

$$\frac{K_{cfl}\left(2X_c-2X_{tfl}+\theta_{cr}W_b-2A_a\theta_{cp}\right)}{2}-\frac{K_{cfr}\left(2X_{tfr}-2X_c+\theta_{cr}W_b+2A_a\theta_{cp}\right)}{2}+\frac{K_{crl}\left(2X_c-2X_{trl}+\theta_{cr}W_b+2B_b\theta_{cp}\right)}{2}+\frac{K_{crr}\left(2X_c-2X_{trr}-\theta_{cr}W_b+2B_b\theta_{cp}\right)}{2}$$

Equation 23 - Full Car Chassis Pitch – Equation of Motion

$$F_{fl}+F_{fr}-F_{rl}-F_{rr}-C_{cfl}\left(\dot{X}_c-\dot{X}_{tfl}+\frac{\dot{\theta}_{cr}W_b}{2}-A_a\dot{\theta}_{cp}\right)+C_{cfr}\left(\dot{X}_{tfr}-\dot{X}_c+\frac{\dot{\theta}_{cr}W_b}{2}+A_a\dot{\theta}_{cp}\right)+C_{crl}\left(\dot{X}_c-\dot{X}_{trl}+\frac{\dot{\theta}_{cr}W_b}{2}+B_b\dot{\theta}_{cp}\right)+C_{crr}\left(\dot{X}_c-\dot{X}_{trr}-\frac{\dot{\theta}_{cr}W_b}{2}+B_b\dot{\theta}_{cp}\right)+$$

$$\frac{4T_{cp}}{A_a}+I_{cp}\ddot{\theta}_{cp}-A_aK_{cfl}\left(X_c-X_{tfl}+\frac{\theta_{cr}W_b}{2}-A_a\theta_{cp}\right)+A_aK_{cfr}\left(X_{tfr}-X_c+\frac{\theta_{cr}W_b}{2}+A_a\theta_{cp}\right)+B_bK_{crl}\left(X_c-X_{trl}+\frac{\theta_{cr}W_b}{2}+B_b\theta_{cp}\right)+B_bK_{crr}\left(X_c-X_{trr}-\frac{\theta_{cr}W_b}{2}+B_b\theta_{cp}\right)$$

Equation 24 - Full Car Chassis Roll – Equation of Motion

$$F_{fr}-F_{fl}-F_{rl}+F_{rr}+C_{cfl}\left(\dot{X}_c-\dot{X}_{tfl}+\frac{\dot{\theta}_{cr}W_b}{2}-A_a\dot{\theta}_{cp}\right)+C_{cfr}\left(\dot{X}_{tfr}-\dot{X}_c+\frac{\dot{\theta}_{cr}W_b}{2}+A_a\dot{\theta}_{cp}\right)+C_{crl}\left(\dot{X}_c-\dot{X}_{trl}+\frac{\dot{\theta}_{cr}W_b}{2}+B_b\dot{\theta}_{cp}\right)-C_{crr}\left(\dot{X}_c-\dot{X}_{trr}-\frac{\dot{\theta}_{cr}W_b}{2}+B_b\dot{\theta}_{cp}\right)-$$

$$\frac{8T_{cr}}{W_b}+2I_{cr}\ddot{\theta}_{cr}+\frac{K_{cfl}W_b\left(X_c-X_{tfl}+\frac{\theta_{cr}W_b}{2}-A_a\theta_{cp}\right)}{2}+\frac{K_{cfr}W_b\left(X_{tfr}-X_c+\frac{\theta_{cr}W_b}{2}+A_a\theta_{cp}\right)}{2}+\frac{K_{crl}W_b\left(X_c-X_{trl}+\frac{\theta_{cr}W_b}{2}+B_b\theta_{cp}\right)}{2}-\frac{K_{crr}W_b\left(X_c-X_{trr}-\frac{\theta_{cr}W_b}{2}+B_b\theta_{cp}\right)}{2}$$

Equation 25 - Full Car FL Tire Vertical Translation – Equation of Motion

$$F_{fl}+M_{tfl}\ddot{X}_{tfl}-C_{tfl}\left(\dot{X}_{gfl}-\dot{X}_{tfl}\right)-C_{cfl}\left(\dot{X}_c-\dot{X}_{tfl}+\frac{\dot{\theta}_{cr}W_b}{2}-A_a\dot{\theta}_{cp}\right)+\frac{K_{farb}\left(2X_{tfl}-2X_{tfr}\right)}{2}-\frac{K_{tfl}\left(2X_{gfl}-2X_{tfl}\right)}{2}-\frac{K_{cfl}\left(2X_c-2X_{tfl}+\theta_{cr}W_b-2A_a\theta_{cp}\right)}{2}$$

Equation 26 - Full Car FR Tire Vertical Translation – Equation of Motion

$$F_{fr}+M_{tfr}\ddot{X}_{tfr}-C_{tfr}\left(\dot{X}_{gfr}-\dot{X}_{tfr}\right)+C_{cfr}\left(\dot{X}_{tfr}-\dot{X}_c+\frac{\dot{\theta}_{cr}W_b}{2}+A_a\dot{\theta}_{cp}\right)-\frac{K_{farb}\left(2X_{tfl}-2X_{tfr}\right)}{2}-\frac{K_{tfr}\left(2X_{gfr}-2X_{tfr}\right)}{2}+\frac{K_{cfr}\left(2X_{tfr}-2X_c+\theta_{cr}W_b+2A_a\theta_{cp}\right)}{2}$$

Equation 27 - Full Car RL Tire Vertical Translation – Equation of Motion

$$F_{rl}+M_{trl}\ddot{X}_{trl}-C_{trl}\left(\dot{X}_{grl}-\dot{X}_{trl}\right)-C_{crl}\left(\dot{X}_c-\dot{X}_{trl}+\frac{\dot{\theta}_{cr}W_b}{2}+B_b\dot{\theta}_{cp}\right)+\frac{K_{farb}\left(2X_{trl}-2X_{trr}\right)}{2}-\frac{K_{trl}\left(2X_{grl}-2X_{trl}\right)}{2}-\frac{K_{crl}\left(2X_c-2X_{trl}+\theta_{cr}W_b+2B_b\theta_{cp}\right)}{2}$$

Equation 28 - Full Car RR Tire Vertical Translation – Equation of Motion

$$F_{rr}+M_{trr}\ddot{X}_{trr}-C_{trr}\left(\dot{X}_{grr}-\dot{X}_{trr}\right)-C_{crr}\left(\dot{X}_c-\dot{X}_{trr}-\frac{\dot{\theta}_{cr}W_b}{2}+B_b\dot{\theta}_{cp}\right)-\frac{K_{farb}\left(2X_{trl}-2X_{trr}\right)}{2}-\frac{K_{trr}\left(2X_{grr}-2X_{trr}\right)}{2}-\frac{K_{crr}\left(2X_c-2X_{trr}-\theta_{cr}W_b+2B_b\theta_{cp}\right)}{2}$$

Equation 29 - Full Car A Matrix – State or System Matrix

$$\begin{pmatrix}
0 & 1 & 0 & 0 & 0 & 0 \\
-\frac{K_{cfl}+K_{cfr}+K_{crl}+K_{crr}}{M_c} & -\frac{C_{cfl}+C_{cfr}+C_{crl}+C_{crr}}{M_c} & \frac{K_{cfl}a+K_{cfr}a-K_{crl}b-K_{crr}b}{M_c} & \frac{C_{cfl}a+C_{cfr}a-C_{crl}b-C_{crr}b}{M_c} & -\frac{\frac{K_{cfl}w}{2}-\frac{K_{cfr}w}{2}+\frac{K_{crl}w}{2}-\frac{K_{crr}w}{2}}{M_c} & -\frac{\frac{C_{cfl}w}{2}-\frac{C_{cfr}w}{2}+\frac{C_{crl}w}{2}-\frac{C_{crr}w}{2}}{M_c} \\
0 & 0 & 0 & 1 & 0 & 0 \\
\frac{K_{cfl}a+K_{cfr}a-K_{crl}b-K_{crr}b}{I_{cp}} & \frac{C_{cfl}+C_{cfr}-C_{crl}-C_{crr}}{I_{cp}} & -\frac{K_{cfl}a^2+K_{cfr}a^2+K_{crl}b^2+K_{crr}b^2}{I_{cp}} & -\frac{C_{cfl}a+C_{cfr}a+C_{crl}b+C_{crr}b}{I_{cp}} & \frac{\frac{K_{cfl}aw}{2}-\frac{K_{cfr}aw}{2}-\frac{K_{crl}bw}{2}+\frac{K_{crr}bw}{2}}{I_{cp}} & \frac{\frac{C_{cfl}w}{2}-\frac{C_{cfr}w}{2}-\frac{C_{crl}w}{2}+\frac{C_{crr}w}{2}}{I_{cp}} \\
0 & 0 & 0 & 0 & 0 & 1 \\
-\frac{w\left(2K_{cfl}-2K_{cfr}+2K_{crl}-2K_{crr}\right)}{8I_{cr}} & -\frac{4C_{cfl}-4C_{cfr}+4C_{crl}-4C_{crr}}{8I_{cr}} & \frac{w\left(2K_{cfl}a-2K_{cfr}a-2K_{crl}b+2K_{crr}b\right)}{8I_{cr}} & \frac{4C_{cfl}a-4C_{cfr}a-4C_{crl}b+4C_{crr}b}{8I_{cr}} & -\frac{w^2\left(K_{cfl}+K_{cfr}+K_{crl}+K_{crr}\right)}{8I_{cr}} & -\frac{w\left(2C_{cfl}+2C_{cfr}+2C_{crl}+2C_{crr}\right)}{8I_{cr}} \\
0 & 0 & 0 & 0 & 0 & 0 \\
\frac{K_{crl}}{M_{trl}} & \frac{C_{crl}}{M_{trl}} & \frac{K_{crl}b}{M_{trl}} & \frac{C_{crl}b}{M_{trl}} & \frac{K_{crl}w}{2M_{trl}} & \frac{C_{crl}w}{2M_{trl}} \\
0 & 0 & 0 & 0 & 0 & 0 \\
\frac{K_{cfl}}{M_{tfl}} & \frac{C_{cfl}}{M_{tfl}} & -\frac{K_{cfl}a}{M_{tfl}} & -\frac{C_{cfl}a}{M_{tfl}} & \frac{K_{cfl}w}{2M_{tfl}} & \frac{C_{cfl}w}{2M_{tfl}} \\
0 & 0 & 0 & 0 & 0 & 0 \\
\frac{K_{crr}}{M_{trr}} & \frac{C_{crr}}{M_{trr}} & \frac{K_{crr}b}{M_{trr}} & \frac{C_{crr}b}{M_{trr}} & -\frac{K_{crr}w}{2M_{trr}} & -\frac{C_{crr}w}{2M_{trr}} \\
0 & 0 & 0 & 0 & 0 & 0 \\
\frac{K_{cfr}}{M_{tfr}} & \frac{C_{cfr}}{M_{tfr}} & -\frac{K_{cfr}a}{M_{tfr}} & -\frac{C_{cfr}a}{M_{tfr}} & -\frac{K_{cfr}w}{2M_{tfr}} & -\frac{C_{cfr}w}{2M_{tfr}}
\end{pmatrix}$$

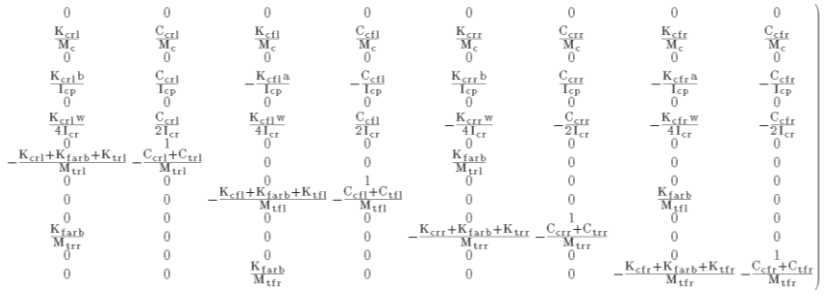

Equation 30 – Full Car B Matrix – Input Matrix

$$\begin{pmatrix} 0 & 0 & 0 & 0 & 0 & 0 & 0 & 0 & 0 & 0 & 0 & 0 & 0 & 0 \\ 0 & 0 & 0 & 0 & 0 & 0 & 0 & 0 & \frac{1}{M_c} & \frac{1}{M_c} & \frac{1}{M_c} & \frac{1}{M_c} & 0 & 0 \\ 0 & 0 & 0 & 0 & 0 & 0 & 0 & 0 & 0 & 0 & 0 & 0 & 0 & 0 \\ 0 & 0 & 0 & 0 & 0 & 0 & 0 & 0 & -\frac{1}{I_{cp}} & \frac{1}{I_{cp}} & -\frac{1}{I_{cp}} & \frac{1}{I_{cp}} & -\frac{4}{A_a I_{cp}} & 0 \\ 0 & 0 & 0 & 0 & 0 & 0 & 0 & 0 & 0 & 0 & 0 & 0 & 0 & 0 \\ 0 & 0 & 0 & 0 & 0 & 0 & 0 & 0 & \frac{1}{2I_{cr}} & \frac{1}{2I_{cr}} & -\frac{1}{2I_{cr}} & -\frac{1}{2I_{cr}} & 0 & \frac{4}{I_{cr}W_b} \\ 0 & 0 & 0 & 0 & 0 & 0 & 0 & 0 & 0 & 0 & 0 & 0 & 0 & 0 \\ \frac{K_{trl}}{M_{trl}} & \frac{C_{trl}}{M_{trl}} & 0 & 0 & 0 & 0 & 0 & 0 & 0 & -\frac{1}{M_{trl}} & 0 & 0 & 0 & 0 \\ 0 & 0 & 0 & 0 & 0 & 0 & 0 & 0 & 0 & 0 & 0 & 0 & 0 & 0 \\ 0 & 0 & 0 & 0 & \frac{K_{tfl}}{M_{tfl}} & \frac{C_{tfl}}{M_{tfl}} & 0 & 0 & -\frac{1}{M_{tfl}} & 0 & 0 & 0 & 0 & 0 \\ 0 & 0 & 0 & 0 & 0 & 0 & 0 & 0 & 0 & 0 & 0 & 0 & 0 & 0 \\ 0 & 0 & \frac{K_{trr}}{M_{trr}} & \frac{C_{trr}}{M_{trr}} & 0 & 0 & 0 & 0 & 0 & 0 & 0 & -\frac{1}{M_{trr}} & 0 & 0 \\ 0 & 0 & 0 & 0 & 0 & 0 & 0 & 0 & 0 & 0 & 0 & 0 & 0 & 0 \\ 0 & 0 & 0 & 0 & 0 & 0 & \frac{K_{tfr}}{M_{tfr}} & \frac{C_{tfr}}{M_{tfr}} & 0 & 0 & -\frac{1}{M_{tfr}} & 0 & 0 & 0 \end{pmatrix}$$

Full Car Linear Response to basic input:

In order to test the Lagrangian derived models, the models were subjected to two of the classical system dynamics inputs, the step and the impulse. These inputs were applied to all wheels simultaneously. It should be noted that both of the step and the impulse inputs were modified slightly to avoid causing an infinite input velocity, which would create infinite force in the tire damper, and cause solution complications. Then, a contrived input of a Sawtooth bump was applied first to the front wheels, and then the rear wheels after a time delay to simulate driving over a bump. This delay may be adjusted to simulate different traversal speeds.

The response to the step input shown in Figure 62 looks precisely as expected – very closely mirroring the simple quarter car model response seen in any elementary system dynamics textbook. The most important features to note is the symmetry of the response of the four tires

(identical masses, spring, and damping rates in this case), the lag of the chassis response in relation to the tire, and the slightly underdamped nature of the two masses.

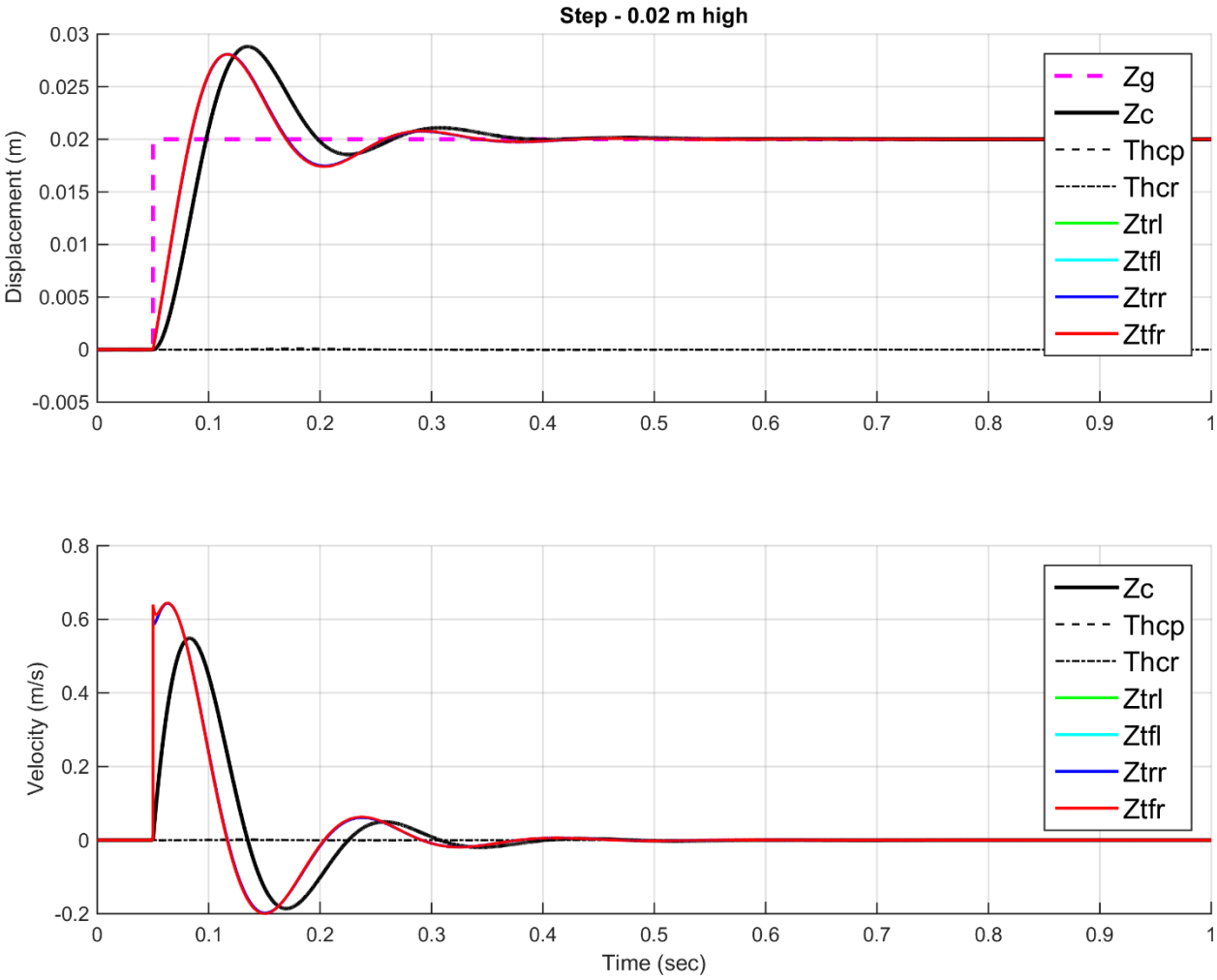

Figure 62 - Linear State Space Full Car Step Input Response

Another visualization of this response is provided by Figure 63. This plot shows the relationship between the velocity and the position of each system state. The initial equilibrium state exists at (0, 0). At the sharp edge of the step, the tire is accelerated rapidly, and the chassis demonstrates phase lag. Finally all states return to the new equilibrium point on top of the step.

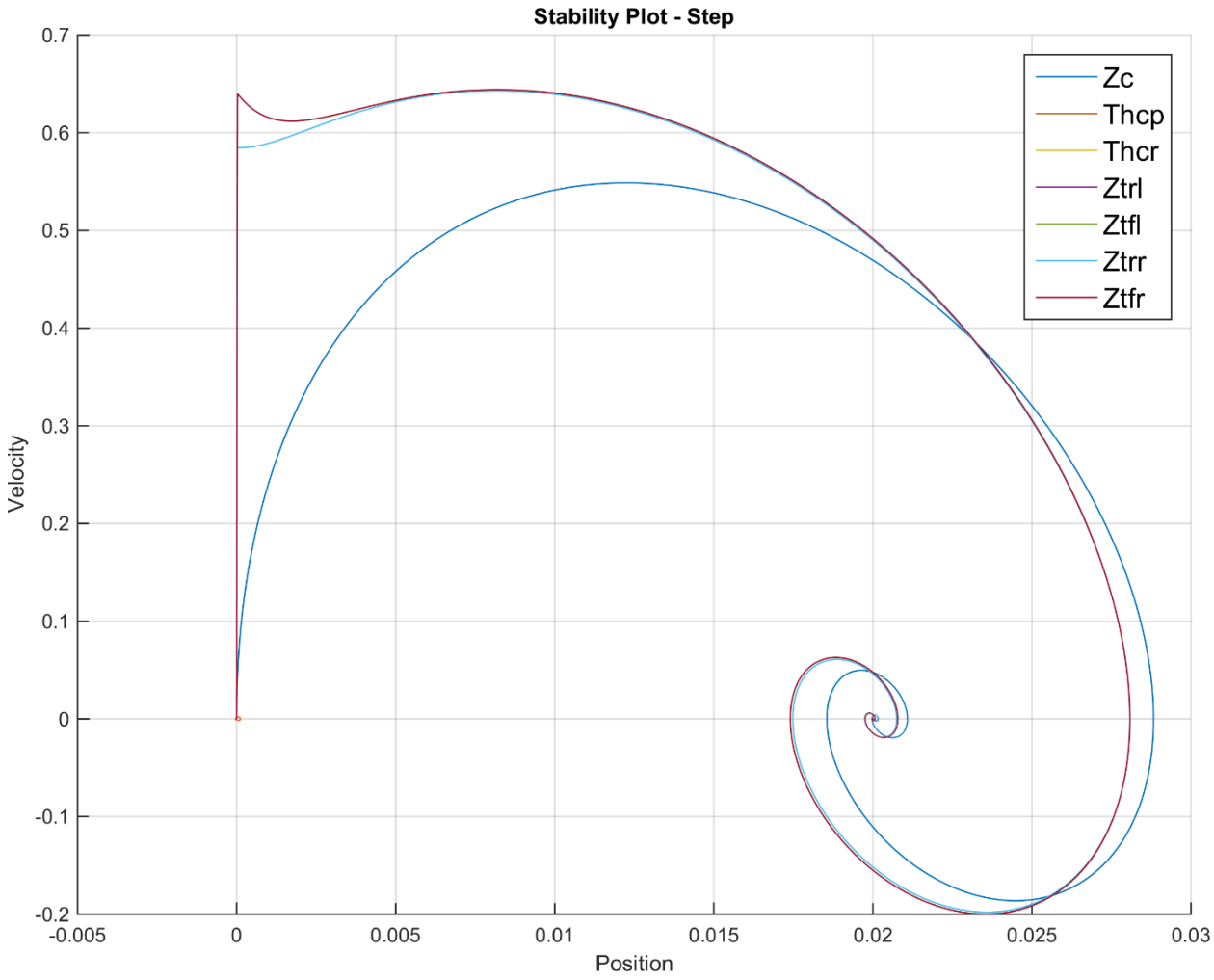

Figure 63 - Linear State Space Full Car Step Input Phase Plot

The impulse response is shown in Figure 64. Again, a typical impulse response is generated with the chassis lagging the tires, the tires displacing further than the chassis (high frequency content of the impulse is not transmitted into the chassis as well), and slightly underdamped behavior.

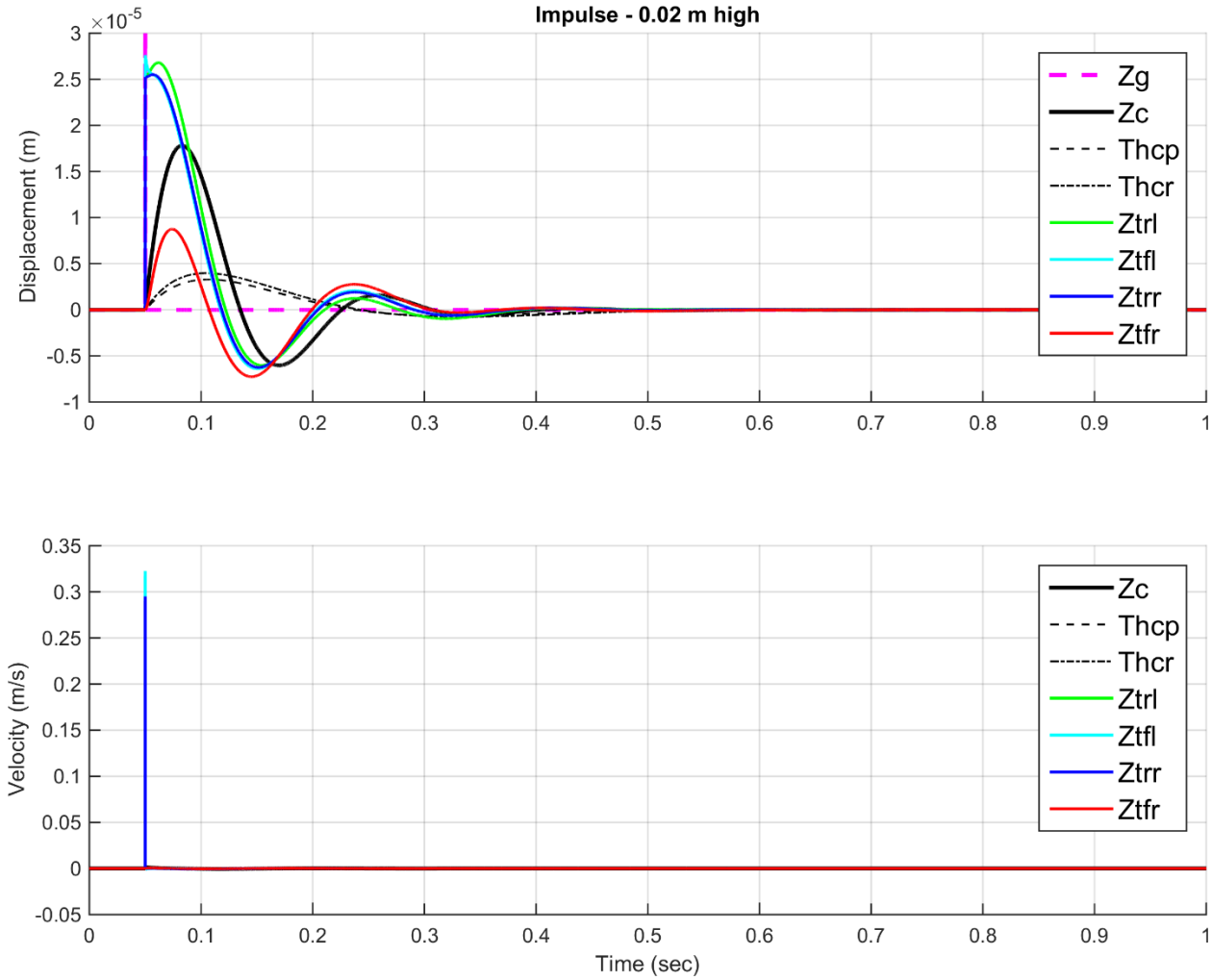

Figure 64 - Linear State Space Full Car Impulse Input Response

Because of the violence of the impulse input, the phase plot takes on a different and much sharper form as seen in Figure 65. Again, the phase lag of the chassis is clearly visible.

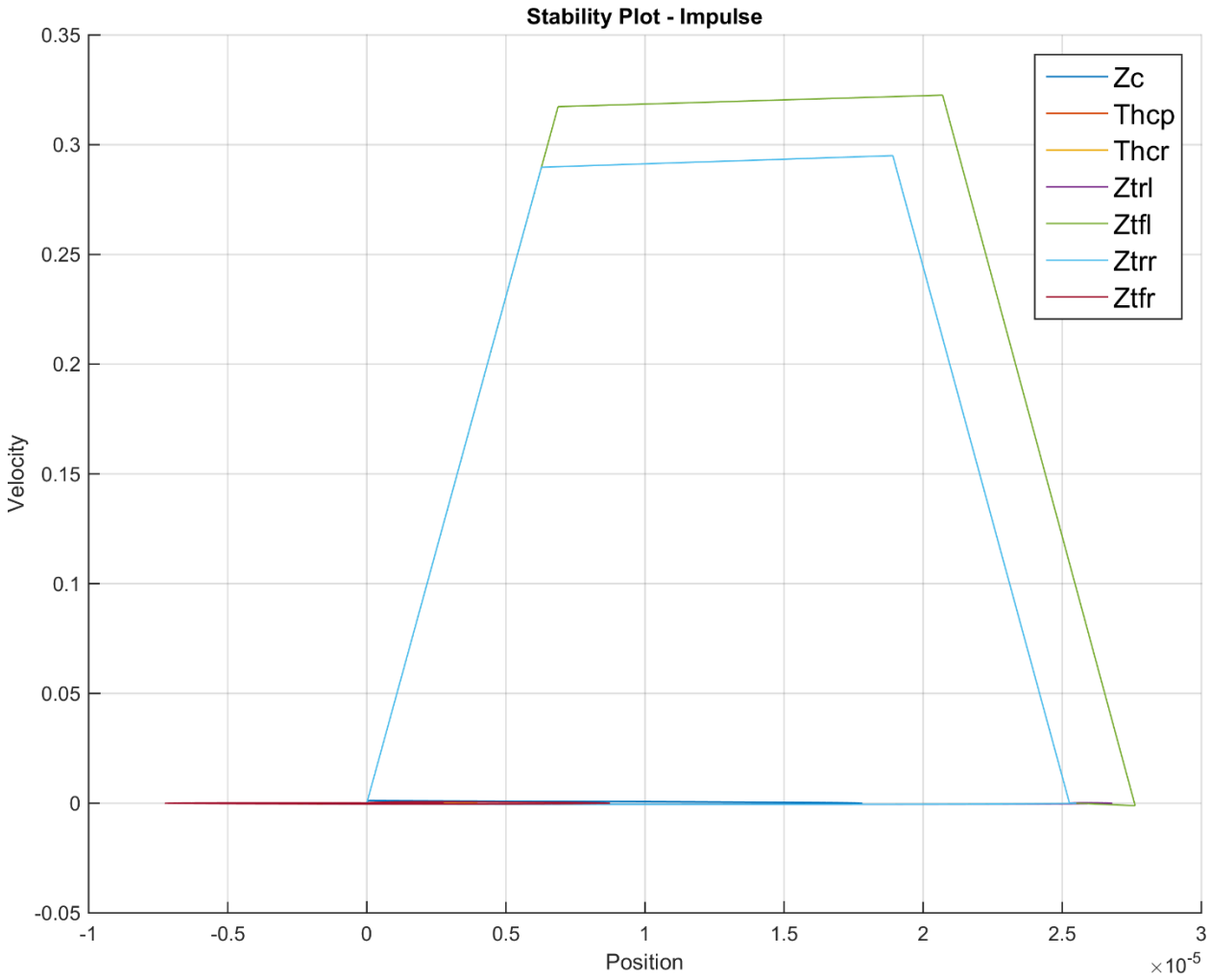

Figure 65 - Linear State Space Full Car Impulse Input Phase Plot

Finally, Figure 66 shows the response of driving over a relatively realistic bump. Many interesting and characteristic features can be extracted from this plot. First, the tires across each axle exhibit identical behavior as expected. Next, the tire spring and damper absorb over 75% of each bump before being transmitted into the chassis spring and damper, and then into the chassis. This behavior was found to be somewhat dependent upon the size of the bump, and also its frequency. Larger bumps use up more of the possible tire deflection, and lower frequencies tend to be less attenuated. Since the car is no longer being excited symmetrically, it can be seen first pitching back when the front tires contact the bump, then forward when the rear wheels make contact.

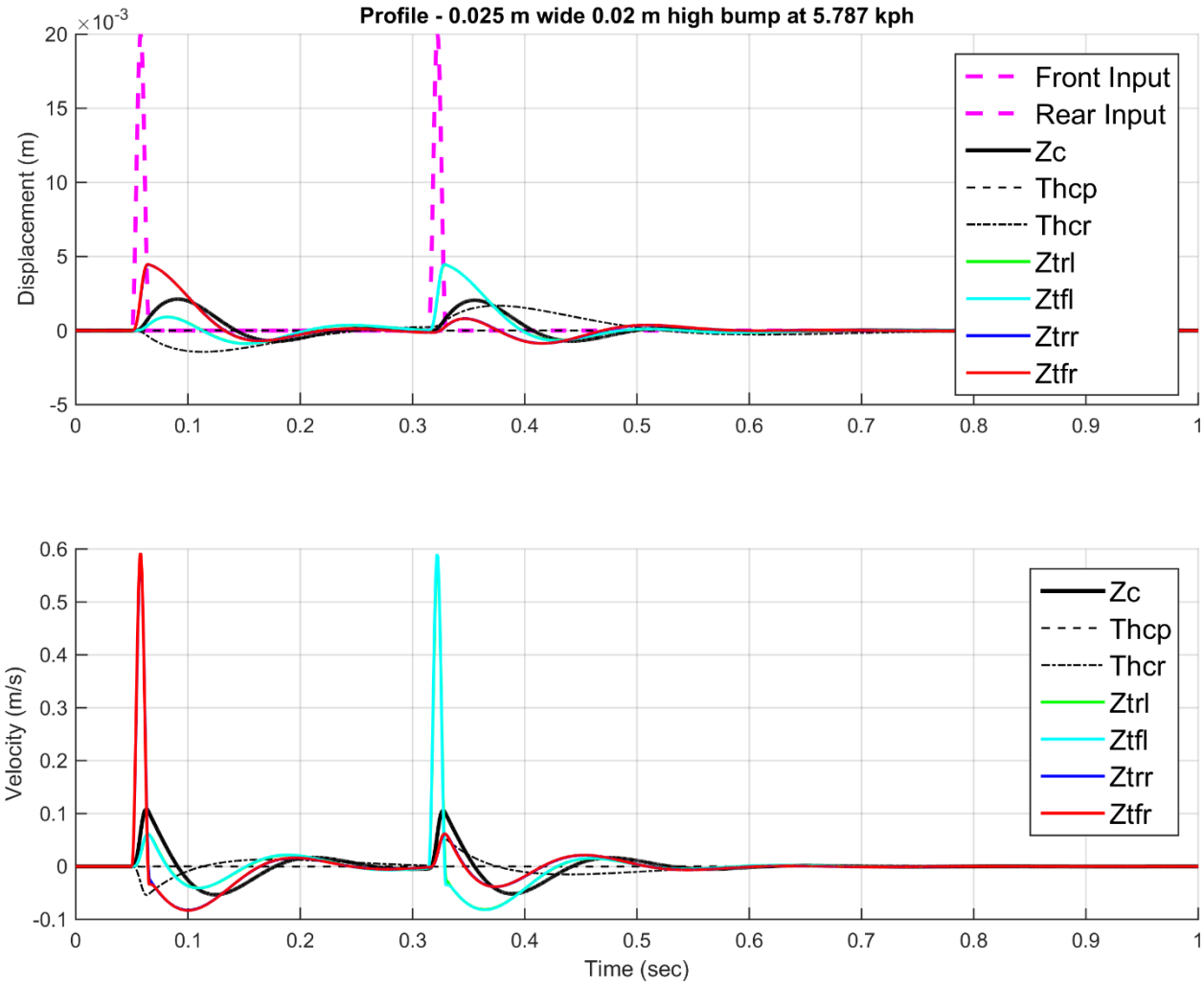

Figure 66 - Linear State Space Full Car Profile Input Response

Since the bump profile in this test case is relatively smooth compared to the step or impulse cases, the phase plot is significantly smoother. Yet again the expected chassis phase lag is seen, as well as the slightly underdamped response.

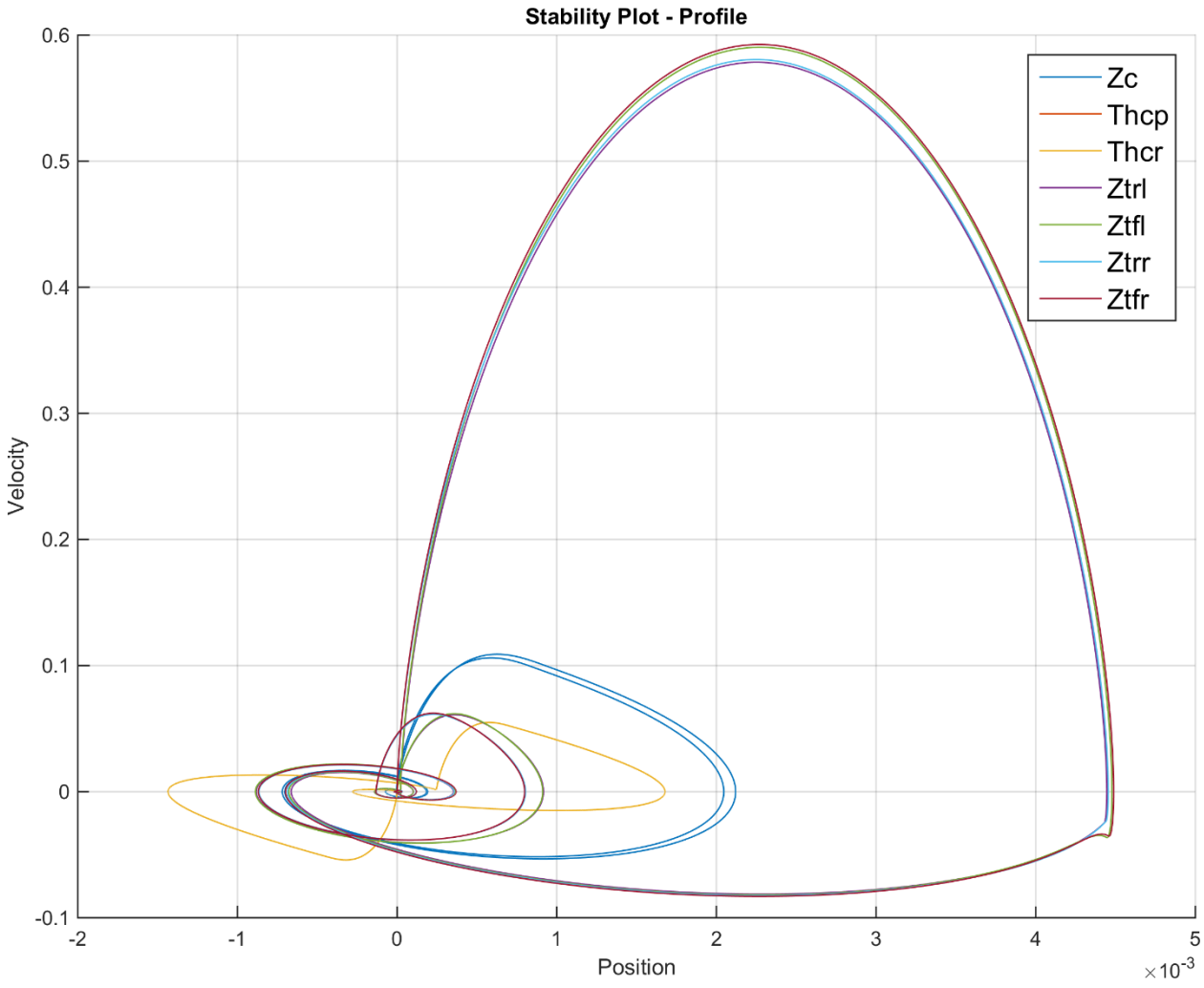

Figure 67 - Linear State Space Full Car Profile Input Phase Plot

Appendix C – Simulink Models

Models

The nature of the Simulink models make them difficult to represent in paper form, so the specific model files are provided as supplemental material. In general, the vehicle parameters and LQR controller design are performed within MATLAB scripts and then the Simulink models access the relevant variables directly from the workspace.

The left-hand portion of each model sets up and manipulates the inputs. As the model complexity increases, there are more options for applying inputs to only specific wheels, applying time delays, and mixing inputs. The right-hand side of each model performs the actual response computation. In order to compare different model setups (linear, ballistic, and LQR), all setups are run simultaneously as can be seen in the groups of Simulink blocks running vertically on the right. Data is collected by logging each signal of interest which is assigned to an output structure along with the time vector. In all models, the default ODE45 solver was found to converge sufficiently. The solver is allowed to use variable time steps, but the final output is discretized on as fixed dt basis. In order to simplify the models and to ensure consistence between types, frequently used blocks such as the non-linear damper, tire, and chassis were converted to unified libraries. Where possible, signals were bussed to allow for cleaner routing and easy expansion.

Single Mass

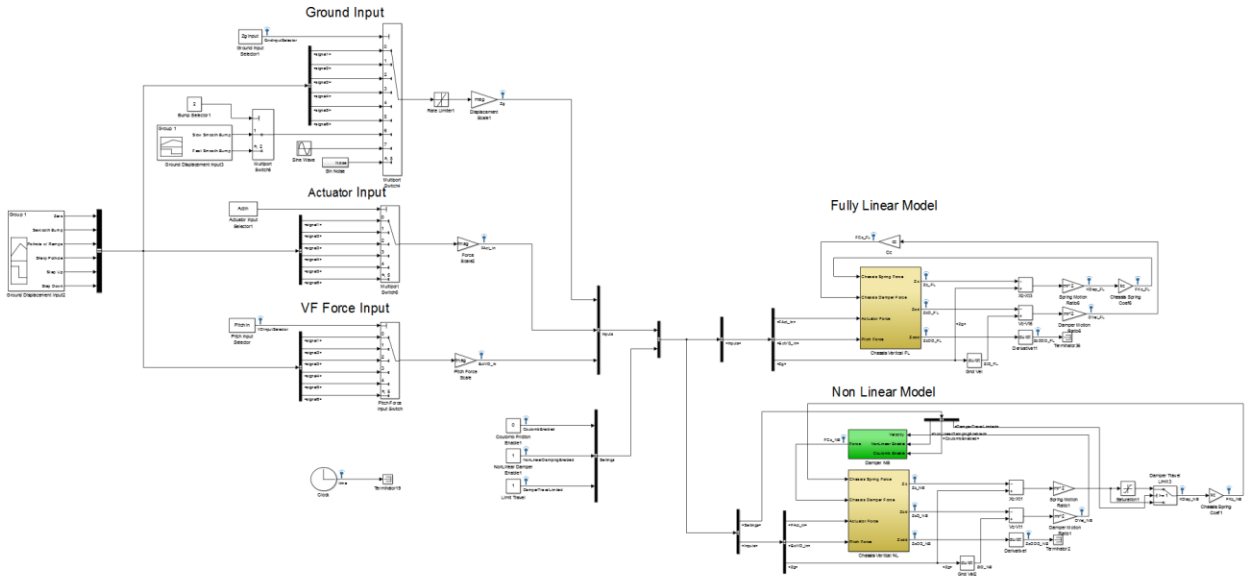

Figure 68 - Simulink Single Mass Linear and Non-Linear Models

Quarter Car

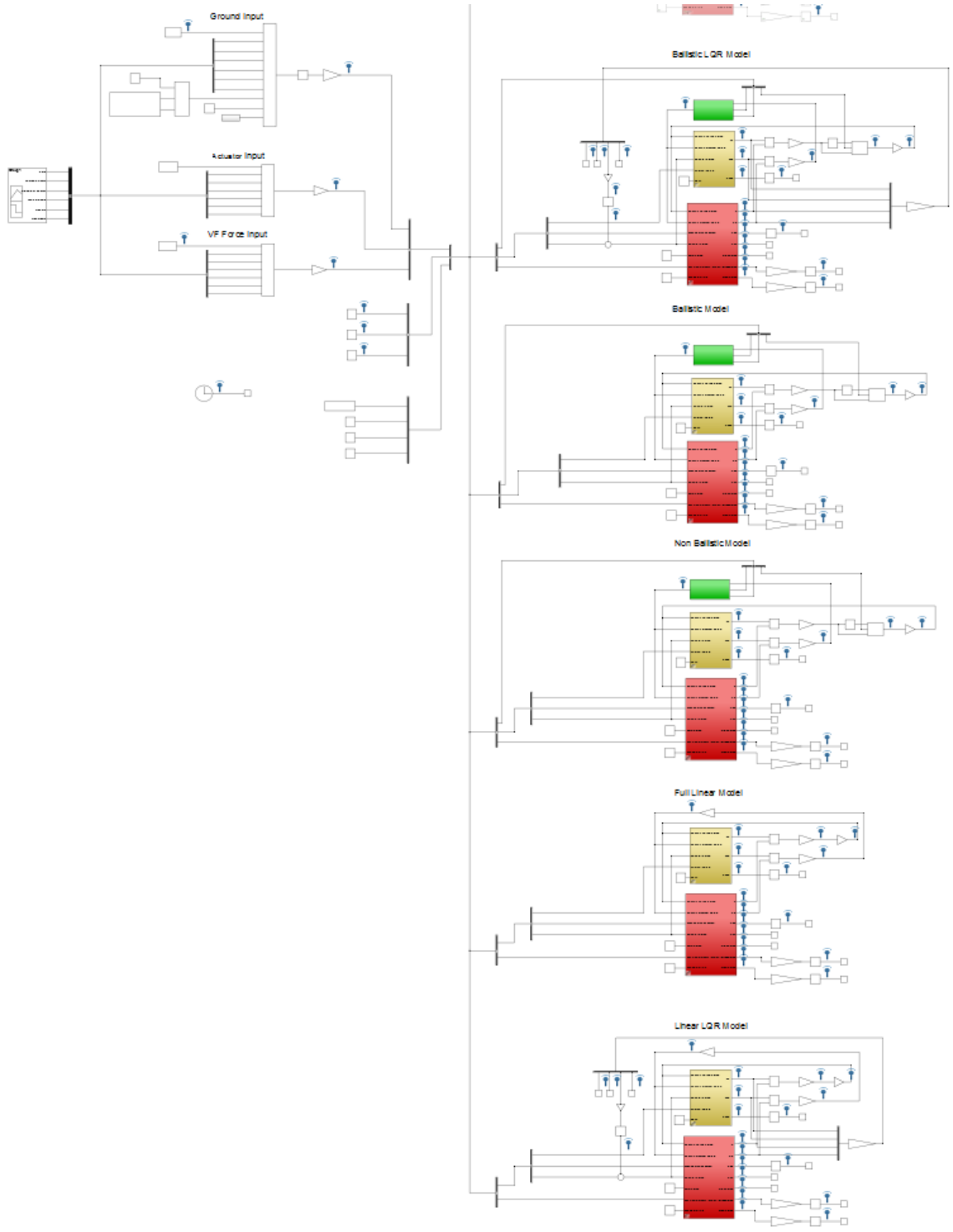

Figure 69 – Simulink Quarter Car Linear, Ballistic, and Ballistic with LQR Feedback Models

Bicycle Model

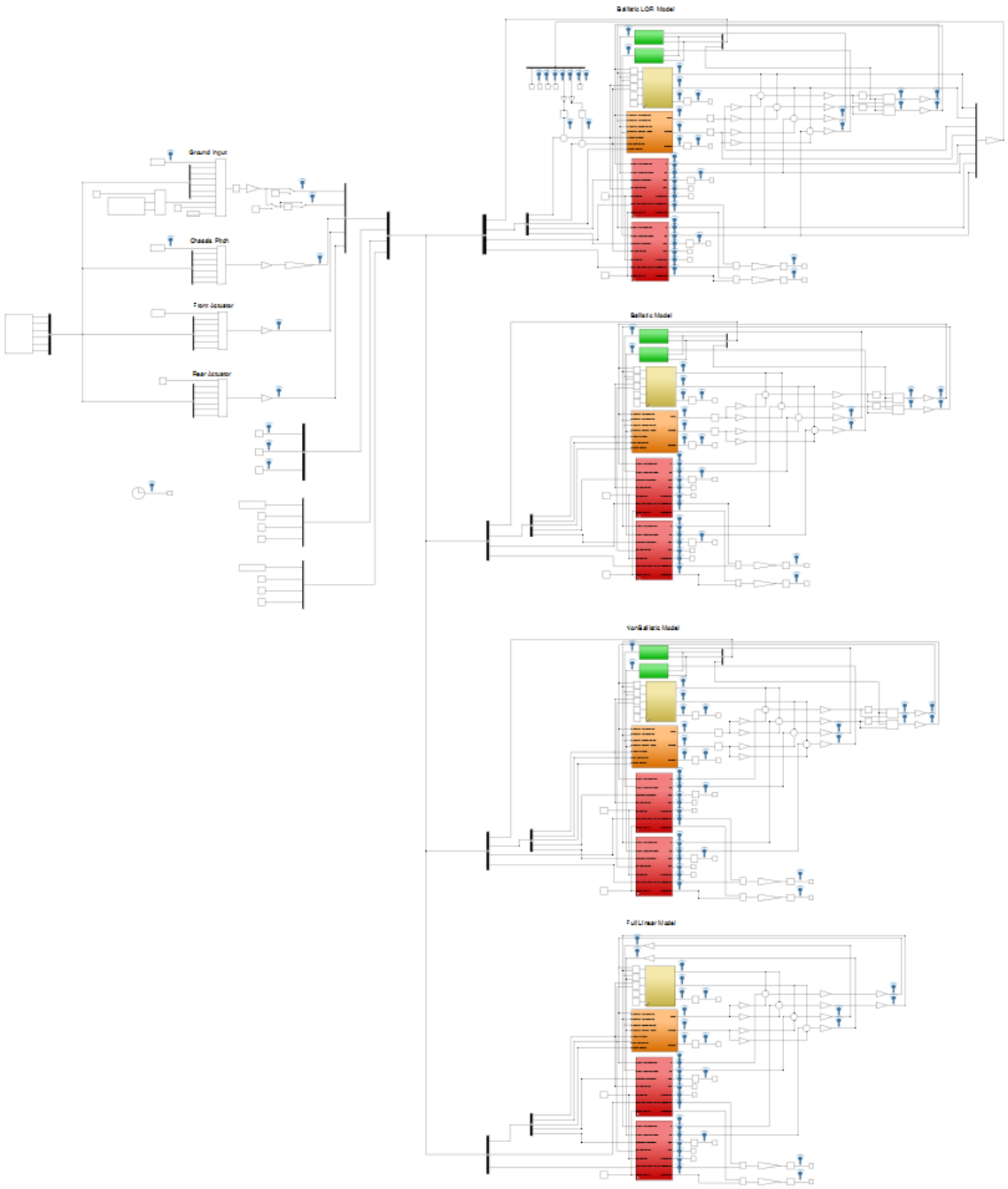

Figure 70 – Simulink Bicycle Linear, Ballistic, and Ballistic with LQR Feedback Models

Full Car

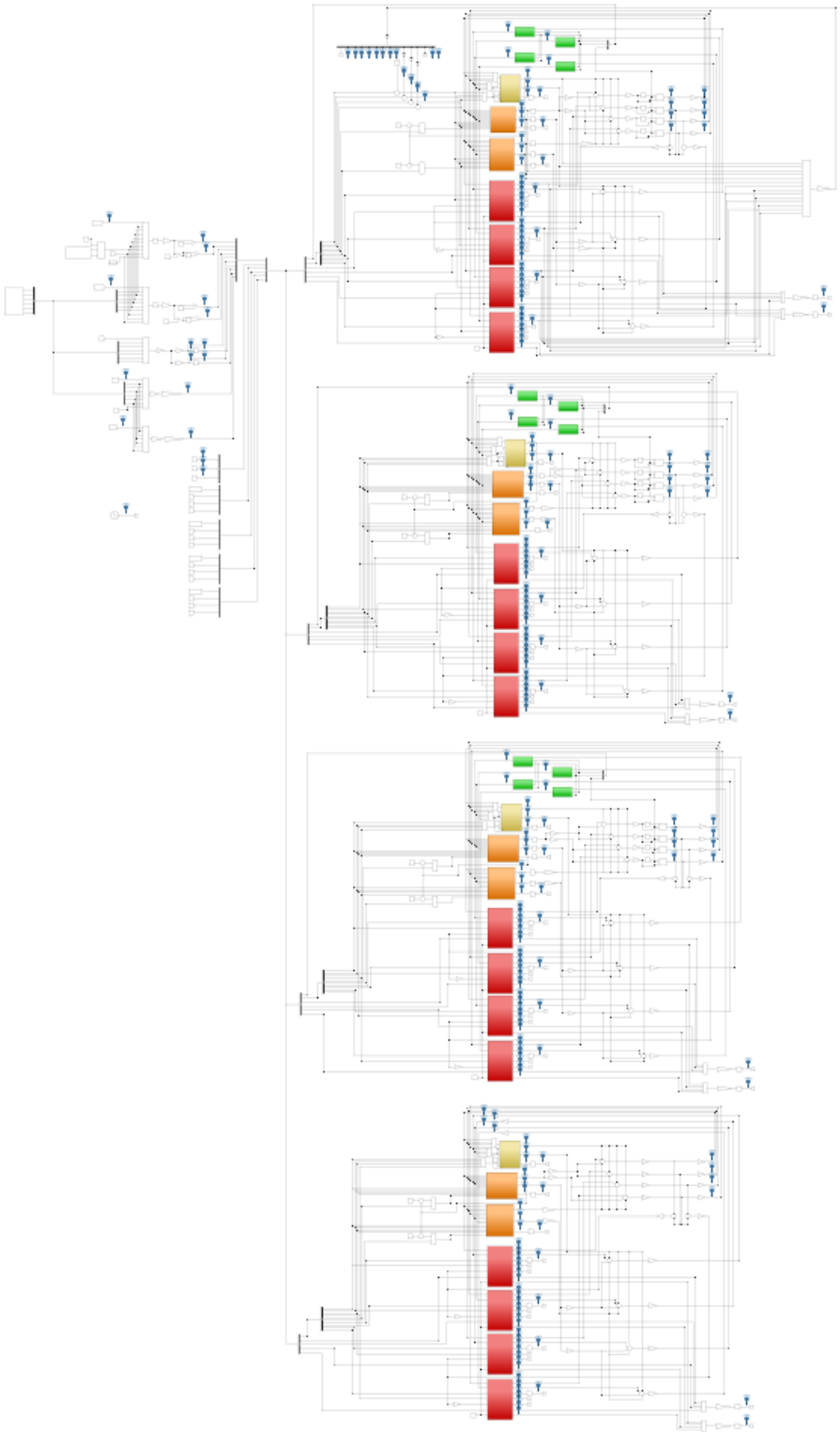

Figure 71 - Simulink Full Car Linear, Ballistic, and Ballistic with LQR Feedback Models

Blocks

Figure 72 shows the library block for the non-linear damper. From right to left, the linear damper follows the lower path, while the non-linear follows the upper. A provision for including viscus and/or Coulomb friction was included, but not utilized in this project.

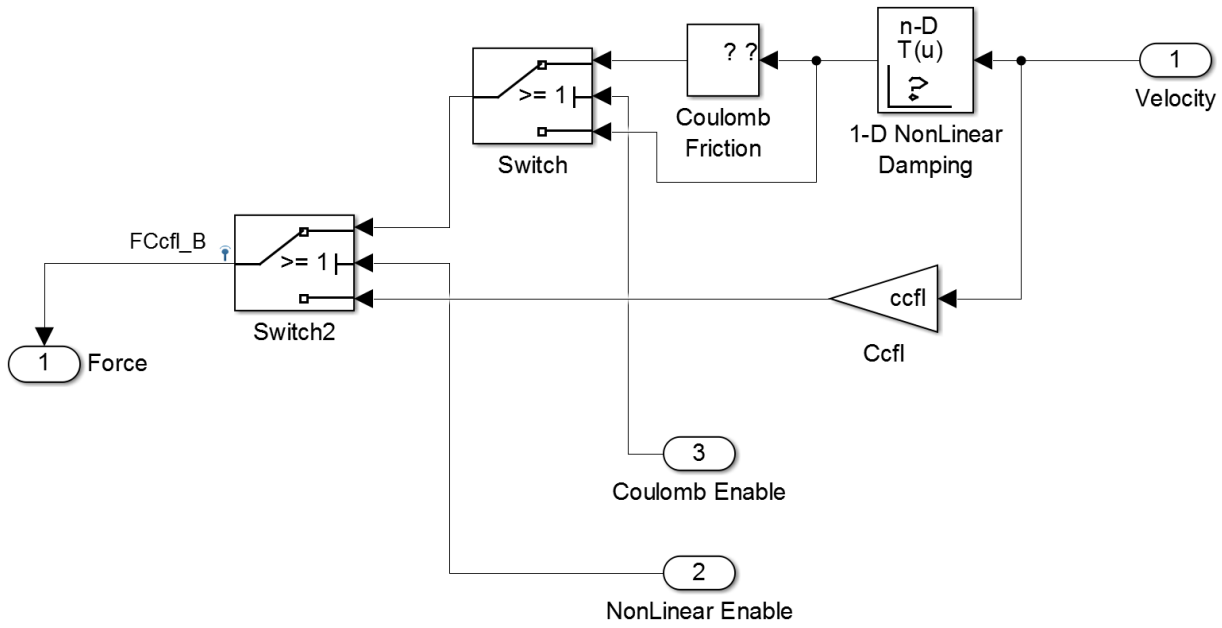

Figure 72 – Simulink Non-Linear Damper Subsystem Block

The vertical chassis motion blocks were also built into a library and are shown in Figure 73.

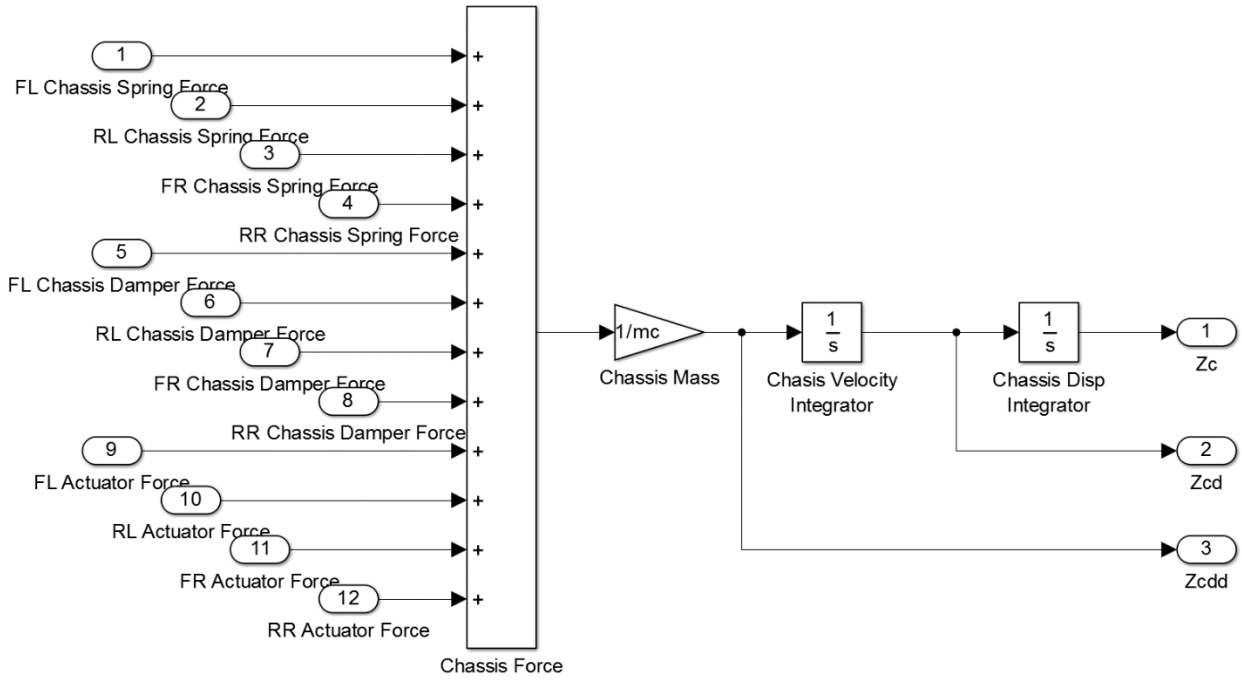

Figure 73 – Simulink Vertical Chassis Translation Subsystem

The chassis pitch and roll blocks are shown in Figure 74 and Figure 75 respectively.

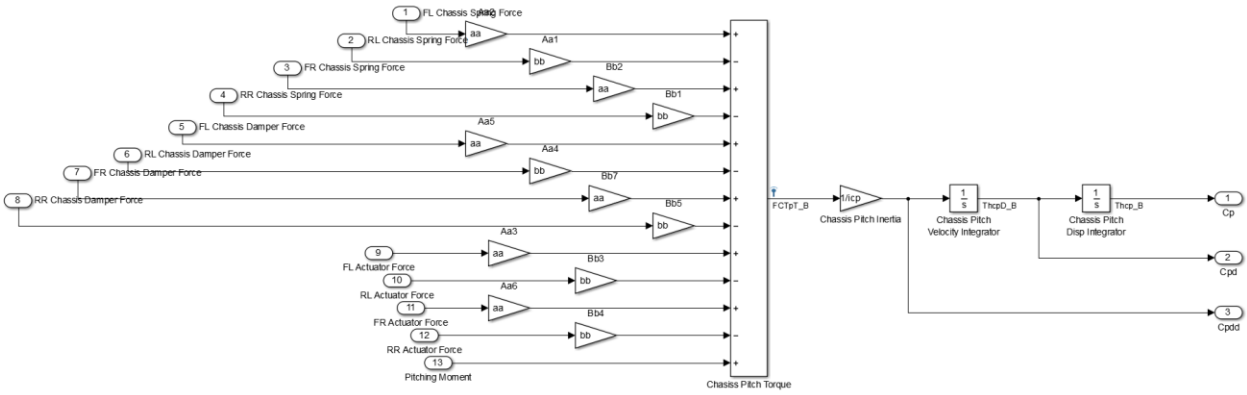

Figure 74 – Simulink Chassis Pitch Subsystem

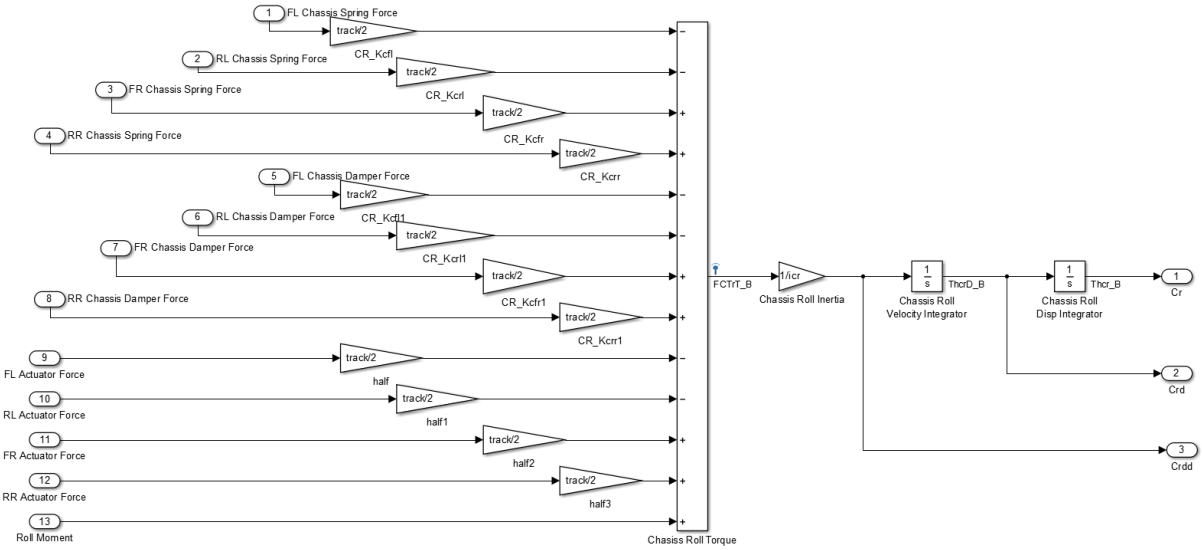

Figure 75 – Simulink Chassis Roll Subsystem

The most important block is the wheel subsystem as shown in Figure 76. The middle partition of the block is responsible for computation of the ballistic state. The tire is considered to have gone ballistic when the tire spring is fully uncompressed (which is calculated at the point where the relative displacement between the wheel spindle and ground is greater than the amount the tire is compressed when in equilibrium). Once the tire extends to this point, the displacement applied to the bottom of the tire is prevented from going negative. In this state, the only forces acting on the tire are the spring, damper, and actuator connected above it, and the force of gravity on the tire mass. Because the chosen point of linearization includes the effects of gravity, the force due to gravity is not included a second time.

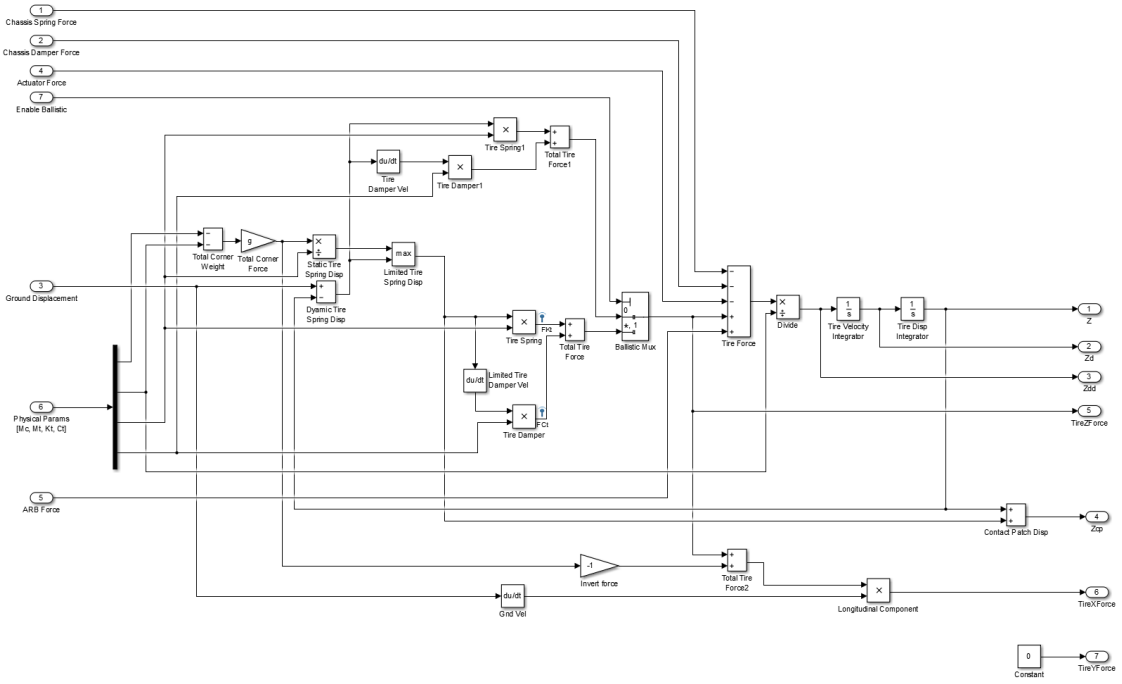

Figure 76 – Simulink Wheel Subsystem

Appendix D – MATLAB Code

All relevant MATLAB and Simulink code has been included in a separate .PDF format file.

Appendix E – Complete Bicycle Model Simulation Set

Because of the striking similarities between the bicycle and full car model response, the analysis of each plot will not be repeated here. It is by design that the bicycle and full car models are similar since the full car model is symmetric laterally, and excited with identical inputs relative to the bicycle model. Reference full car model plots found in chapter 6 for descriptions. Bicycle model figures are provided in this appendix for completeness. If inputs exciting the chassis roll mode had been explored within the scope of this project, the bicycle and full car responses would no longer be expected to match.

Ballistic vs Non Ballistic Comparison

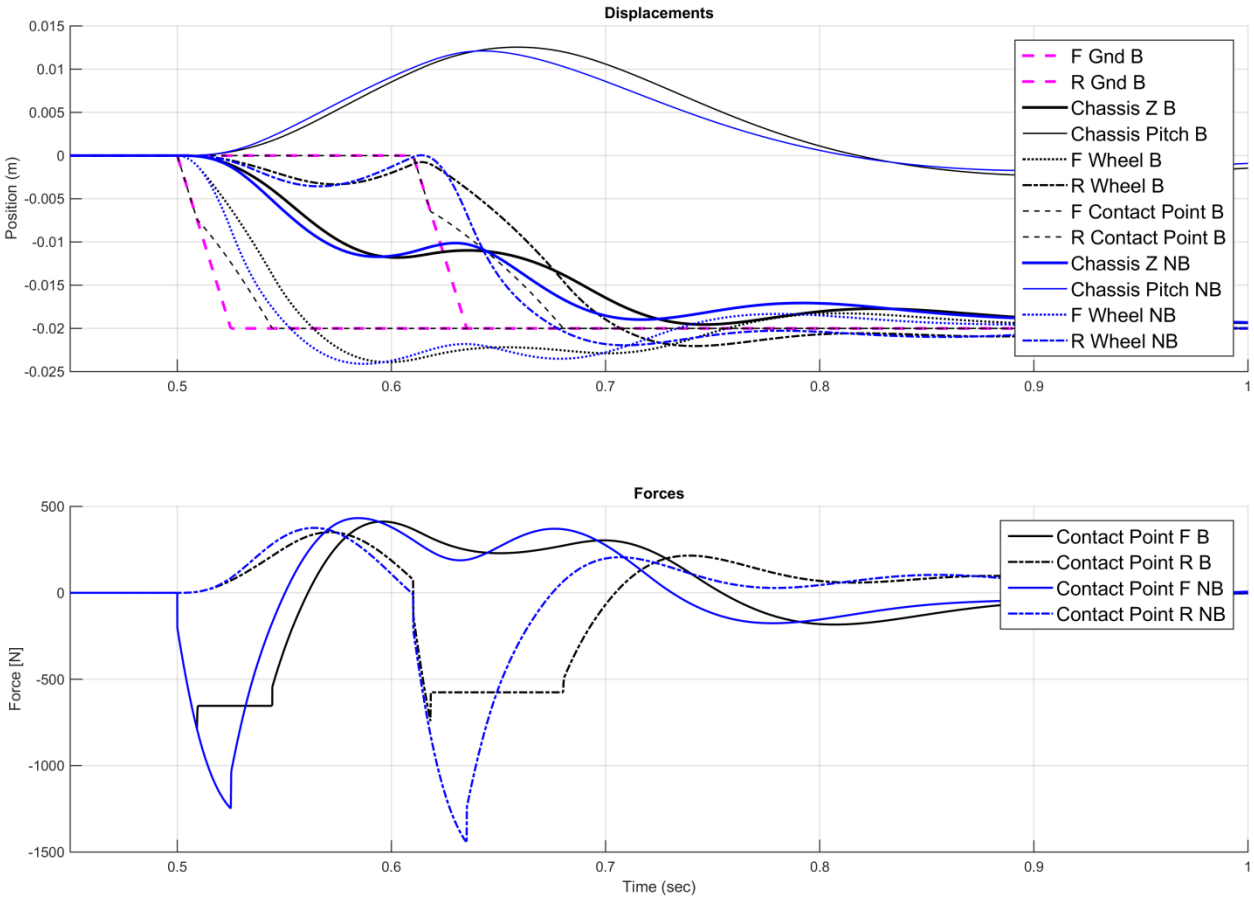

Figure 77 - Non-Linear Bicycle Model StepDown Response

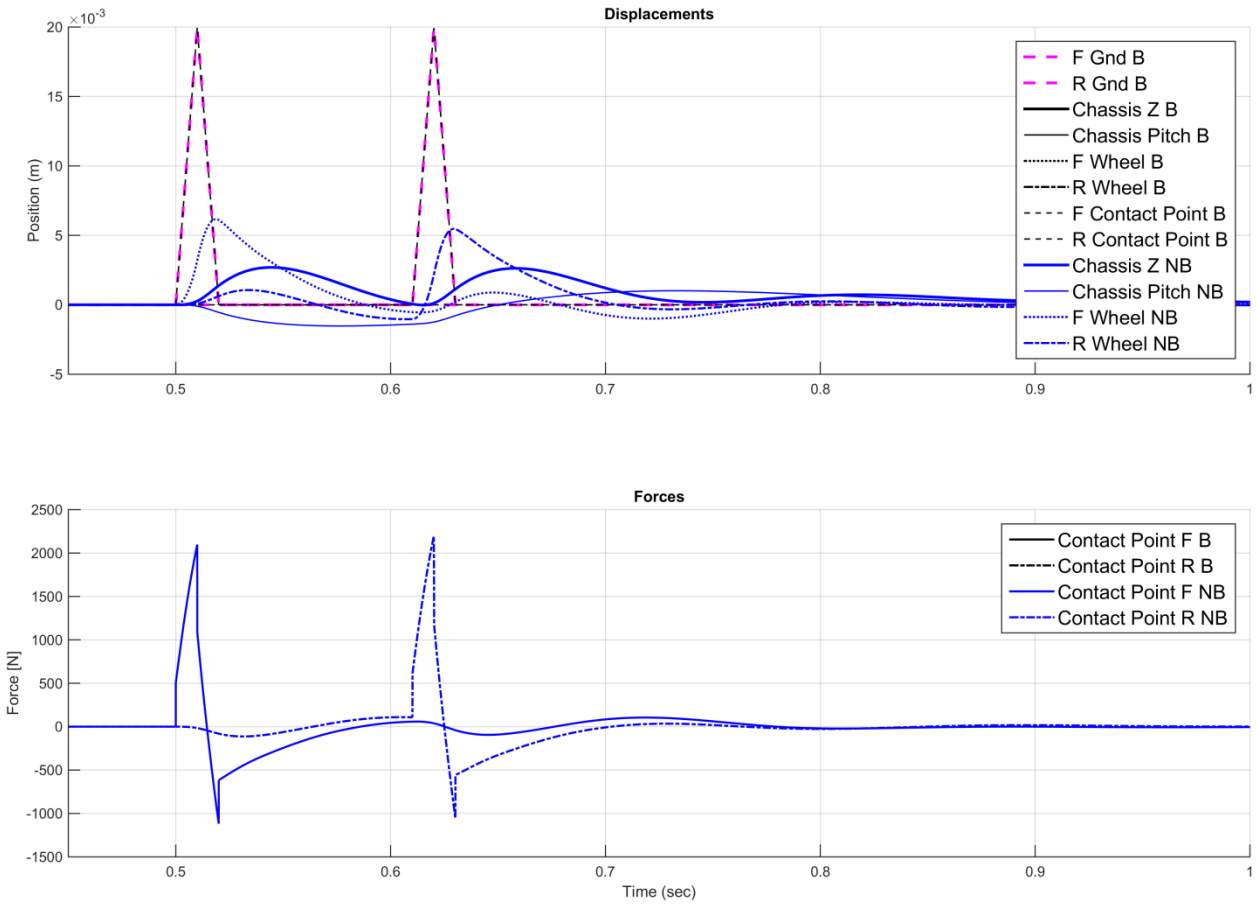

Figure 78 - Non-Linear Bicycle Model Sawtooth Response

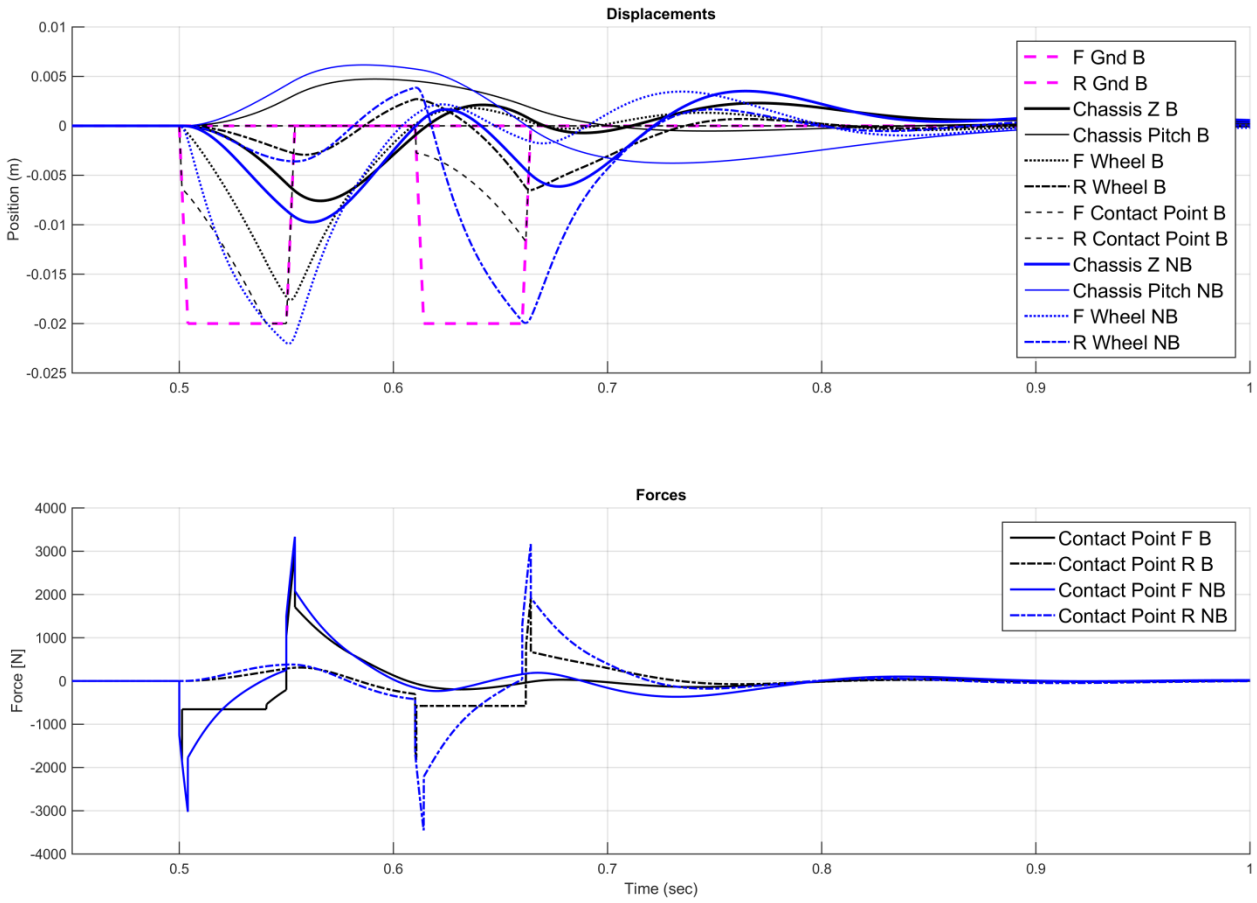

Figure 79 - Non-Linear Bicycle Model Pothole Response

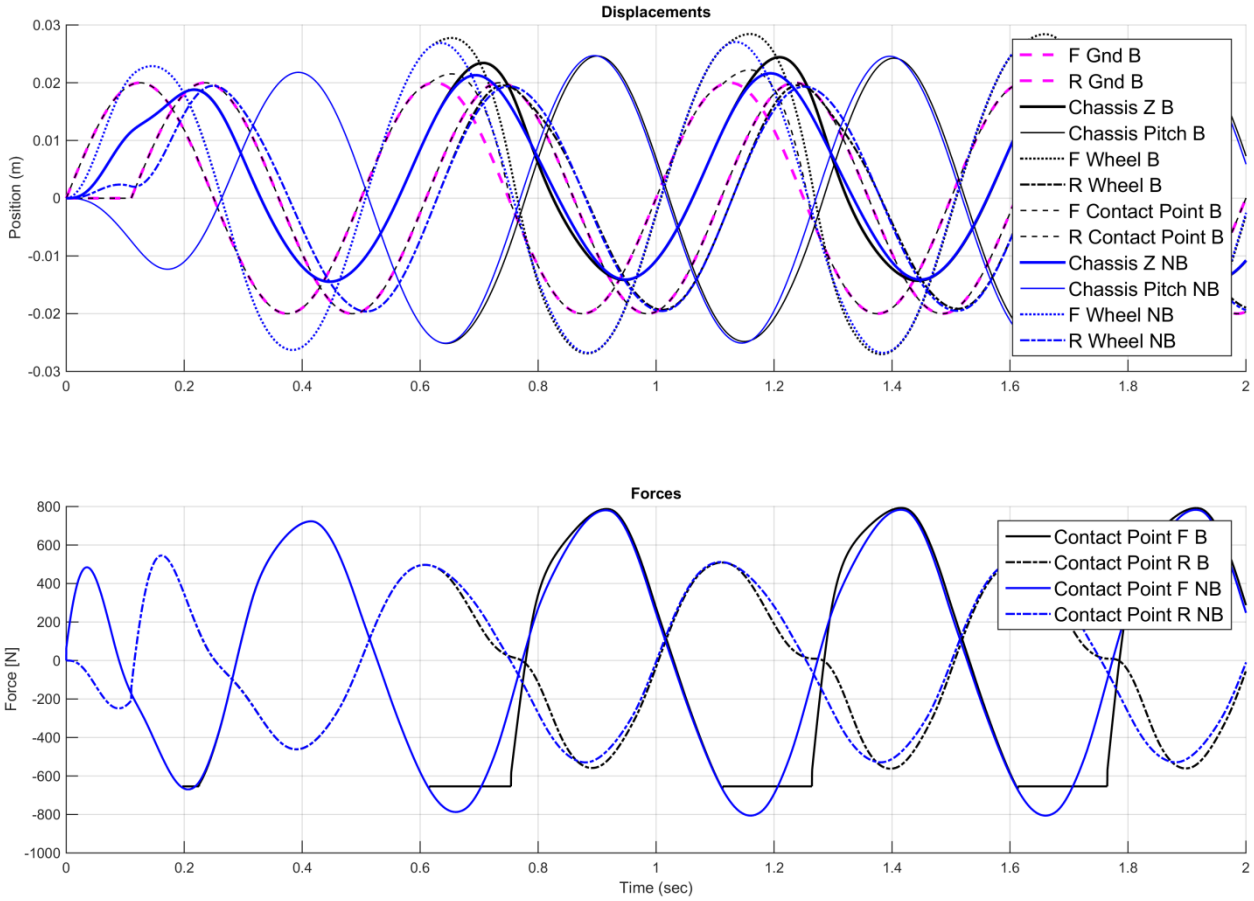

Figure 80 - Non-Linear Bicycle Model 2 Hz Sinusoid Response

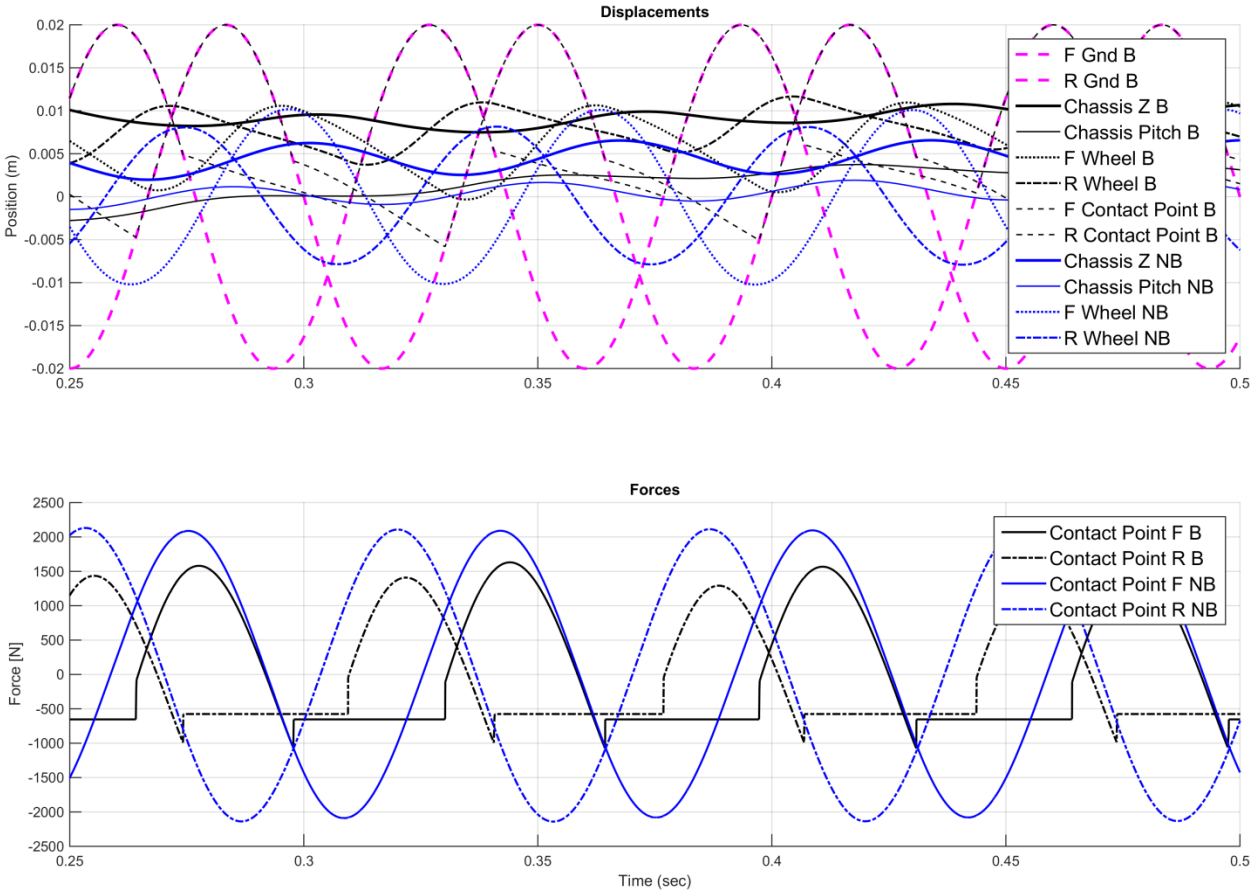

Figure 81 - Non-Linear Bicycle Model 10 Hz Sinusoid Response

Feedback Control Response

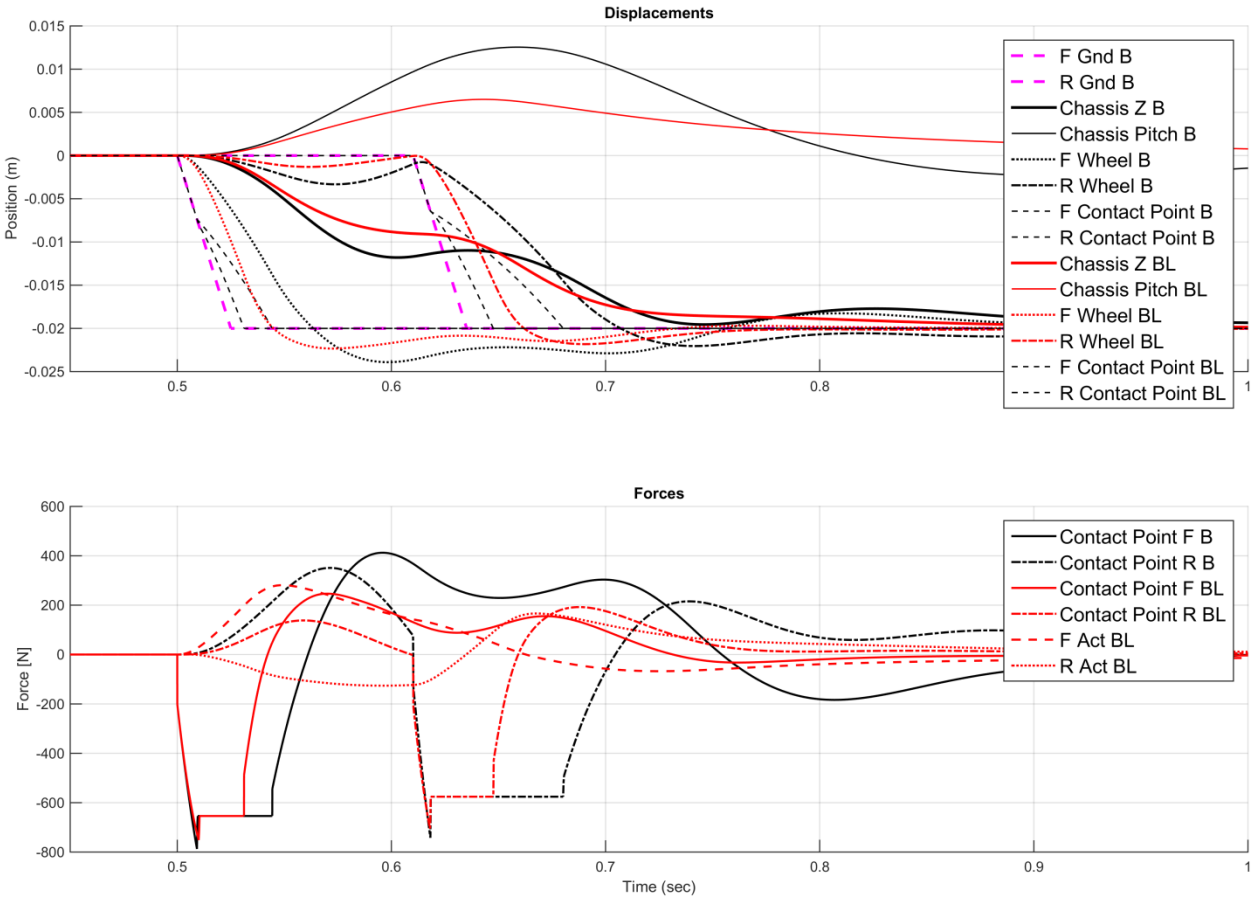

Figure 82 – Bicycle Model StepDown Response with LQR

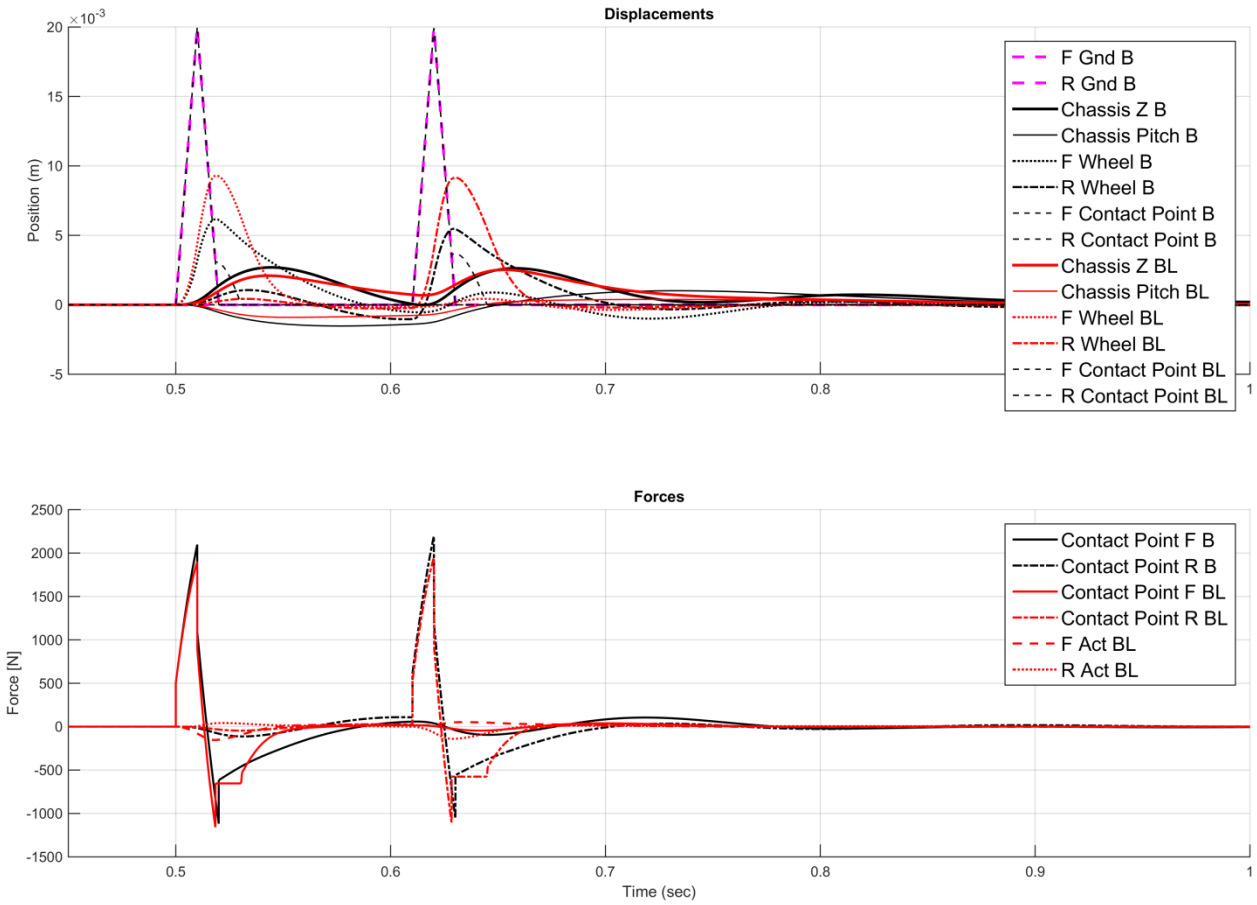

Figure 83 – Bicycle Model Sawtooth Response with LQR

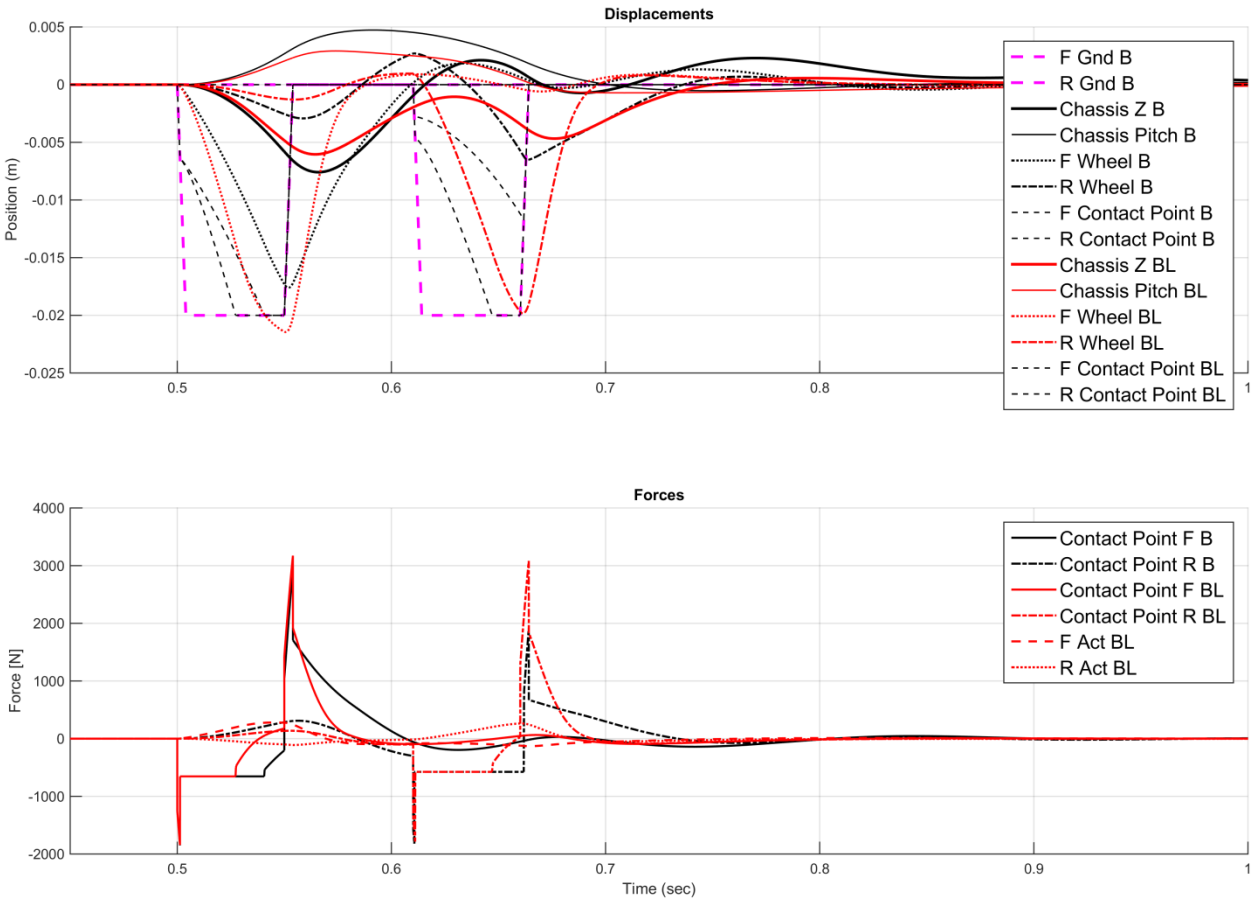

Figure 84 – Bicycle Model Pothole Response with LQR

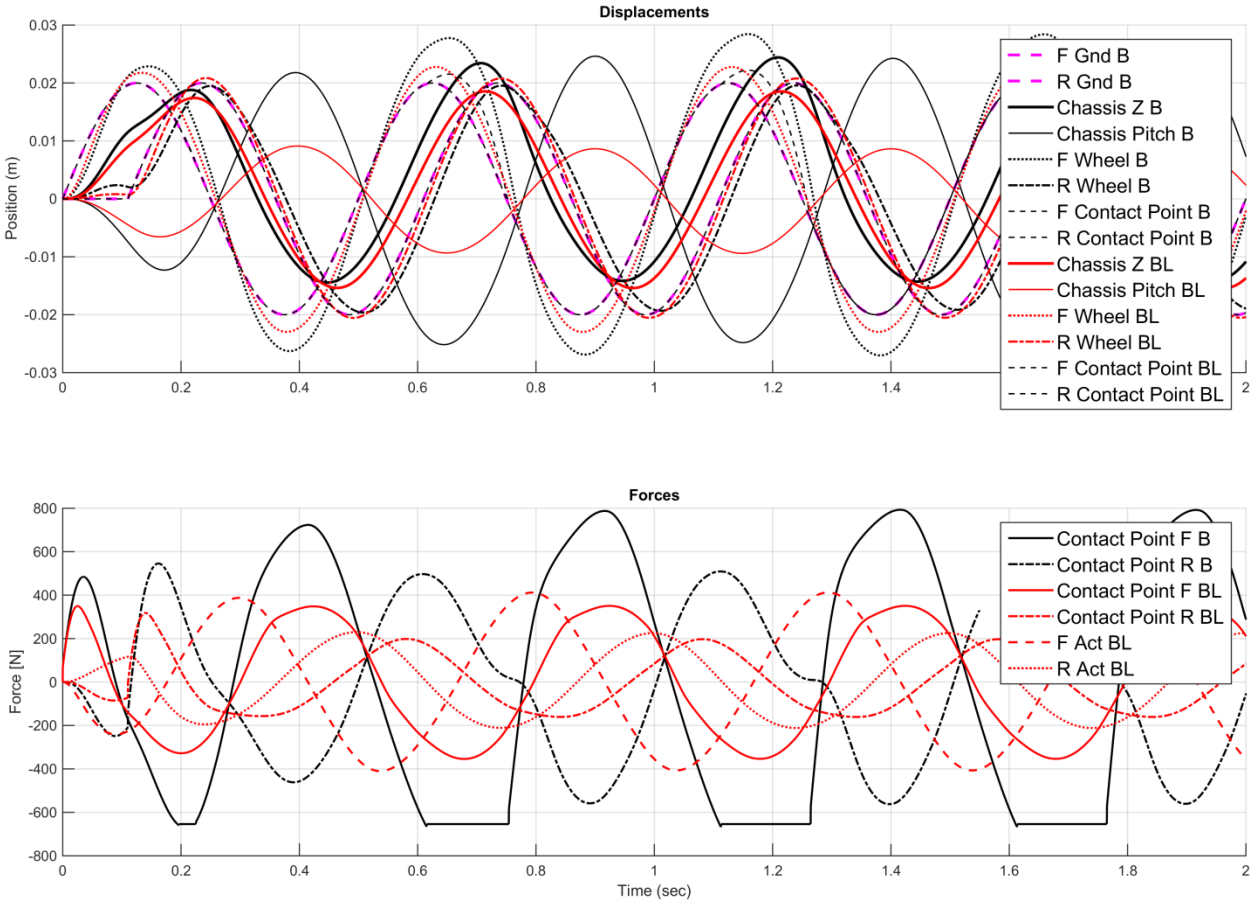

Figure 85 – Bicycle Model 2 Hz Sinusoid Response with LQR

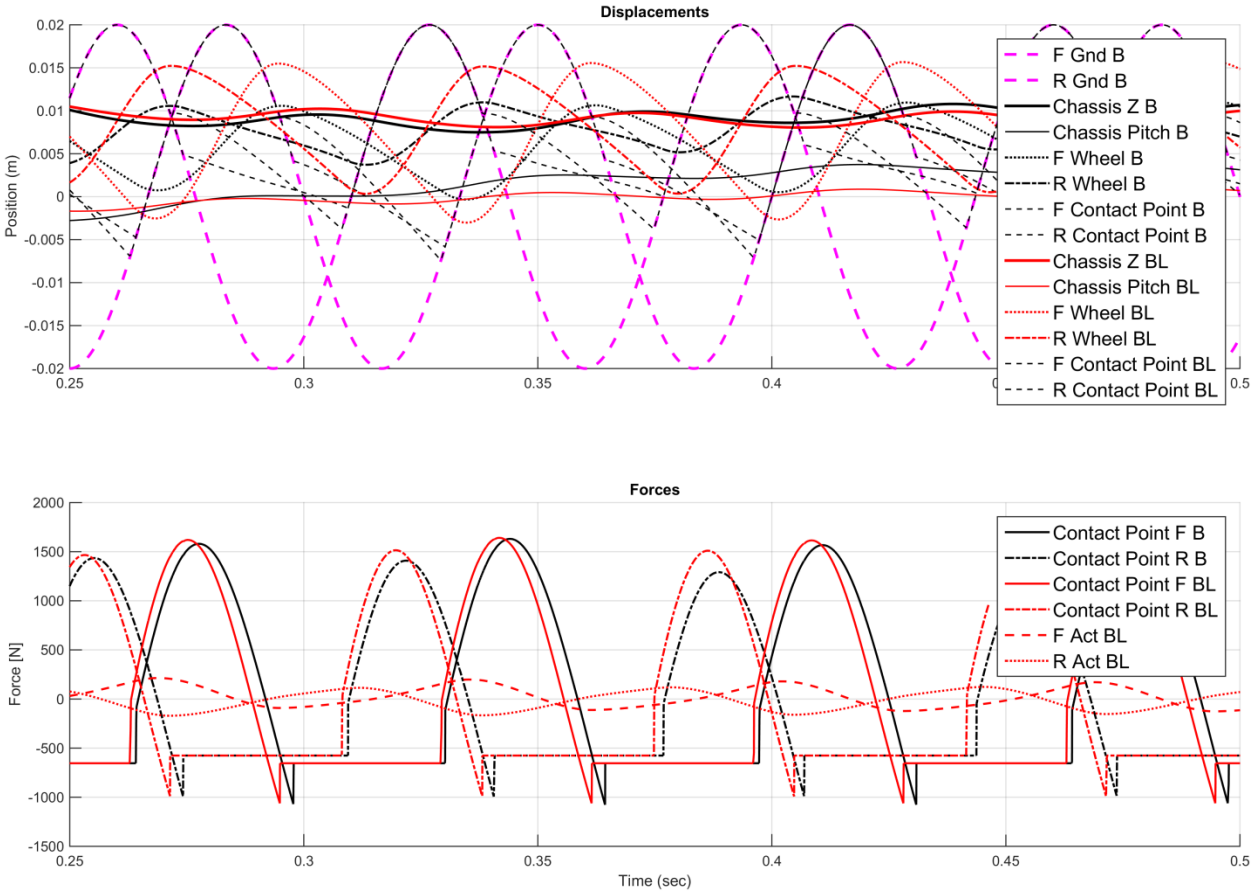

Figure 86 – Bicycle Model 10 Hz Sinusoid Response with LQR

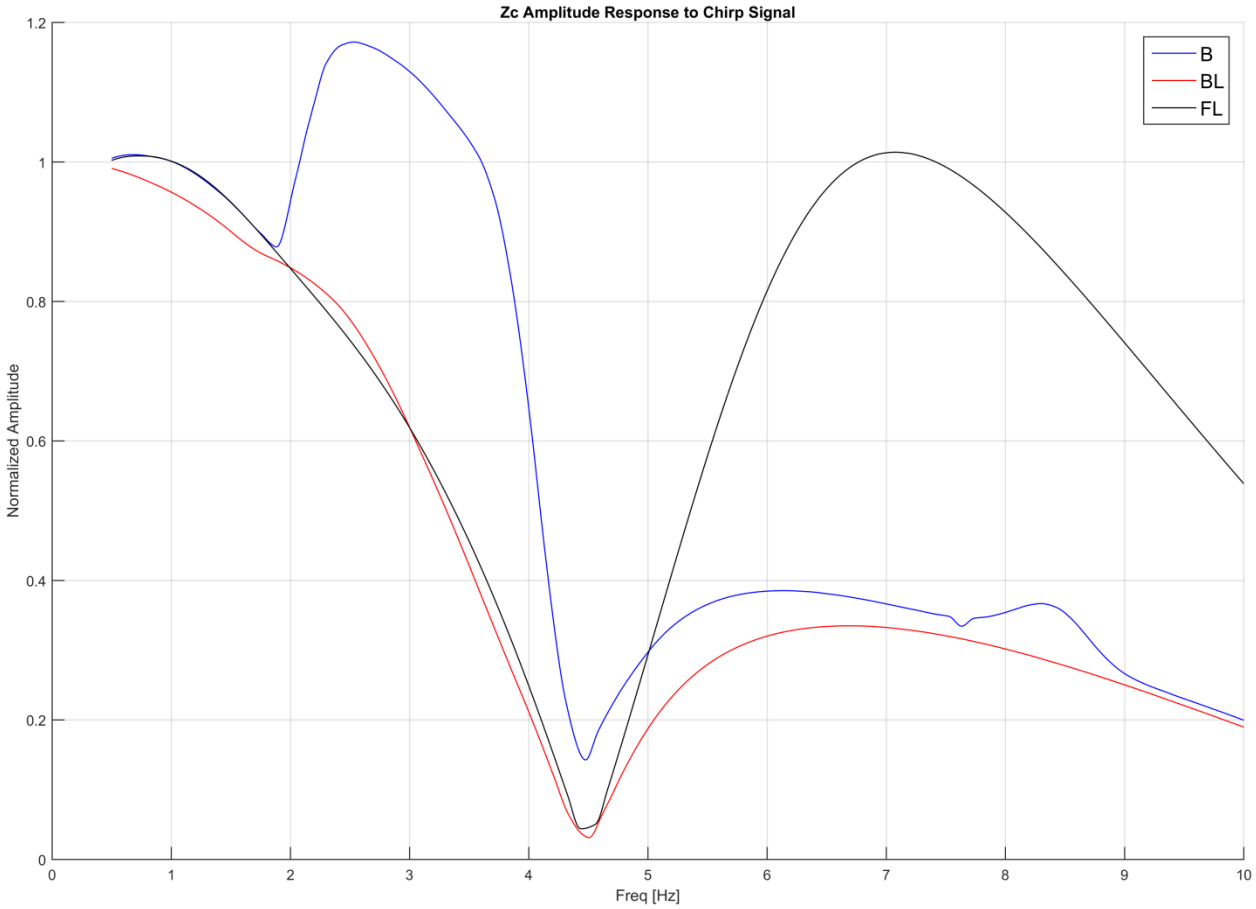

Figure 87 - Bicycle Model Zc Response Amplitude to Chirp Input

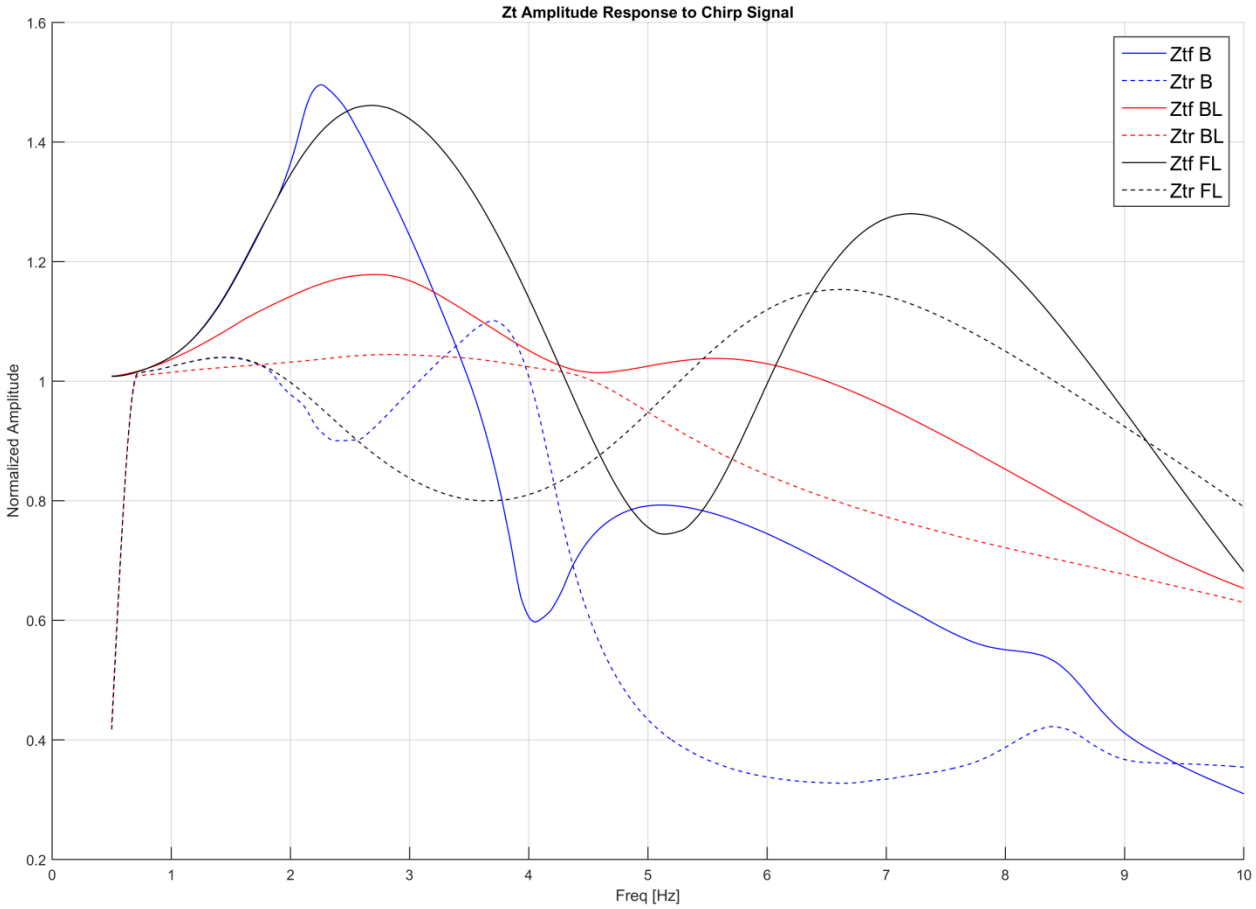

Figure 88 - Bicycle Model Zt Response to Chirp Input

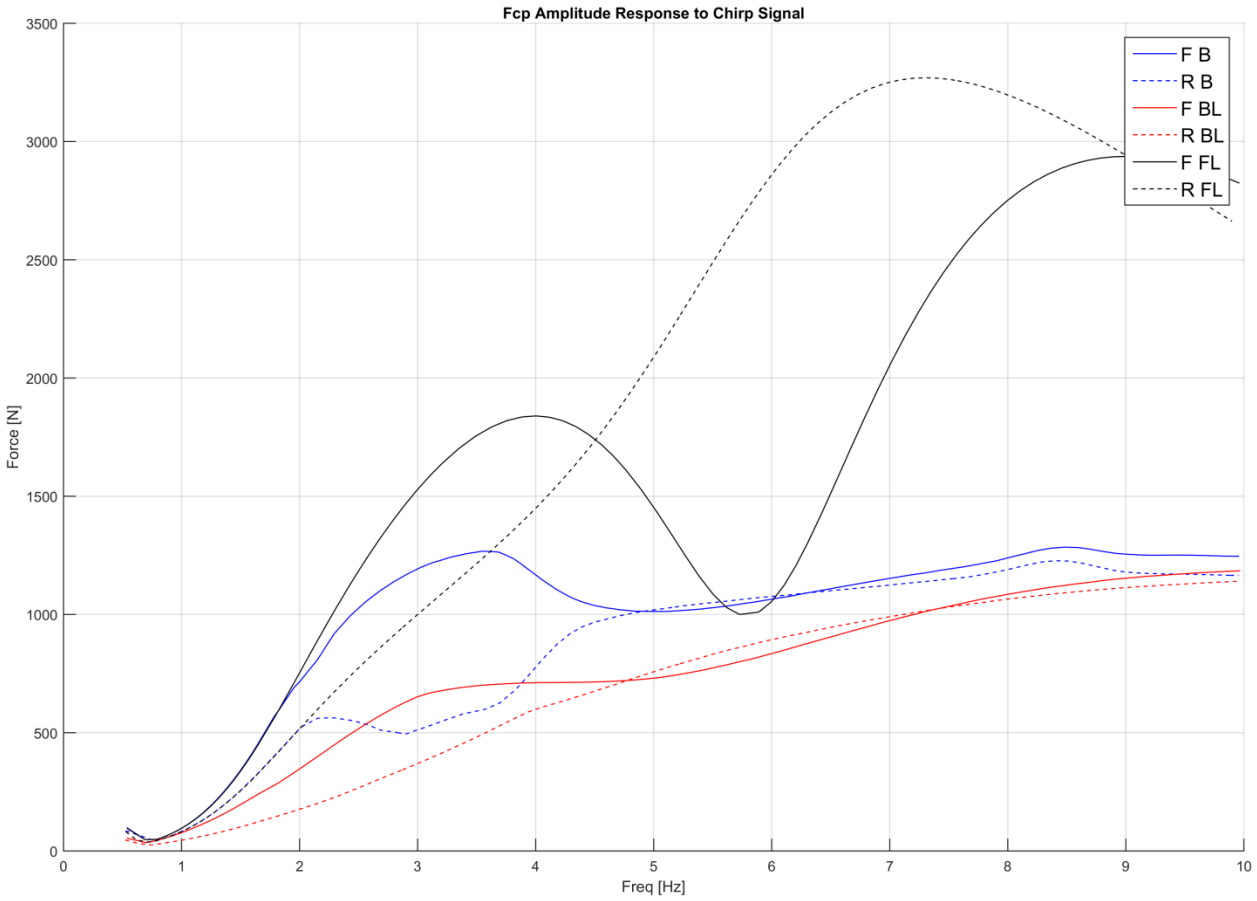

Figure 89 - Bicycle Model Contact Patch Force Response to Chirp Input

Appendix F – Comparison of Ballistic and Non-Ballistic Model

Based on the model response to range of inputs, it is apparent that only high frequency and large magnitude inputs are capable of exciting the Ballistic motion modes. If the input is sufficiently small or slow, the compliance of the rubber tire is generally capable of 'absorbing' the disturbance while the rest of the suspension system catches up. This frequency and amplitude threshold can be difficult to quantify, but an example is shown in Figure 90 where the RMS difference in response between a Ballistic and Non-Ballistic Quarter Car model is calculated over a range of sinusoidal input frequencies. While there is no definitive cutoff, it is clear that for this car, the two models are relatively similar between 0 Hz and ~7.5 Hz, but diverge quickly after that. It is interesting to note that the natural frequency between the chassis and tire in this model is approximately 6 Hz. I thus hypothesize that, as a rule of thumb, inputs of frequencies greater than the natural frequency between the chassis and tire require Ballistic representation. I also propose that 'sharp' inputs of magnitude greater than the static tire deflection also require Ballistic analysis. A grey area is reached when both parameters approach their critical states.

A practical example of the difference in response can be seen in Figure 27 at about 0.75 sec. Excited by a combination of frequency and magnitude, the road surface recedes from the tire which proceeds to fall in a parabolic trajectory until it contacts the ground again.

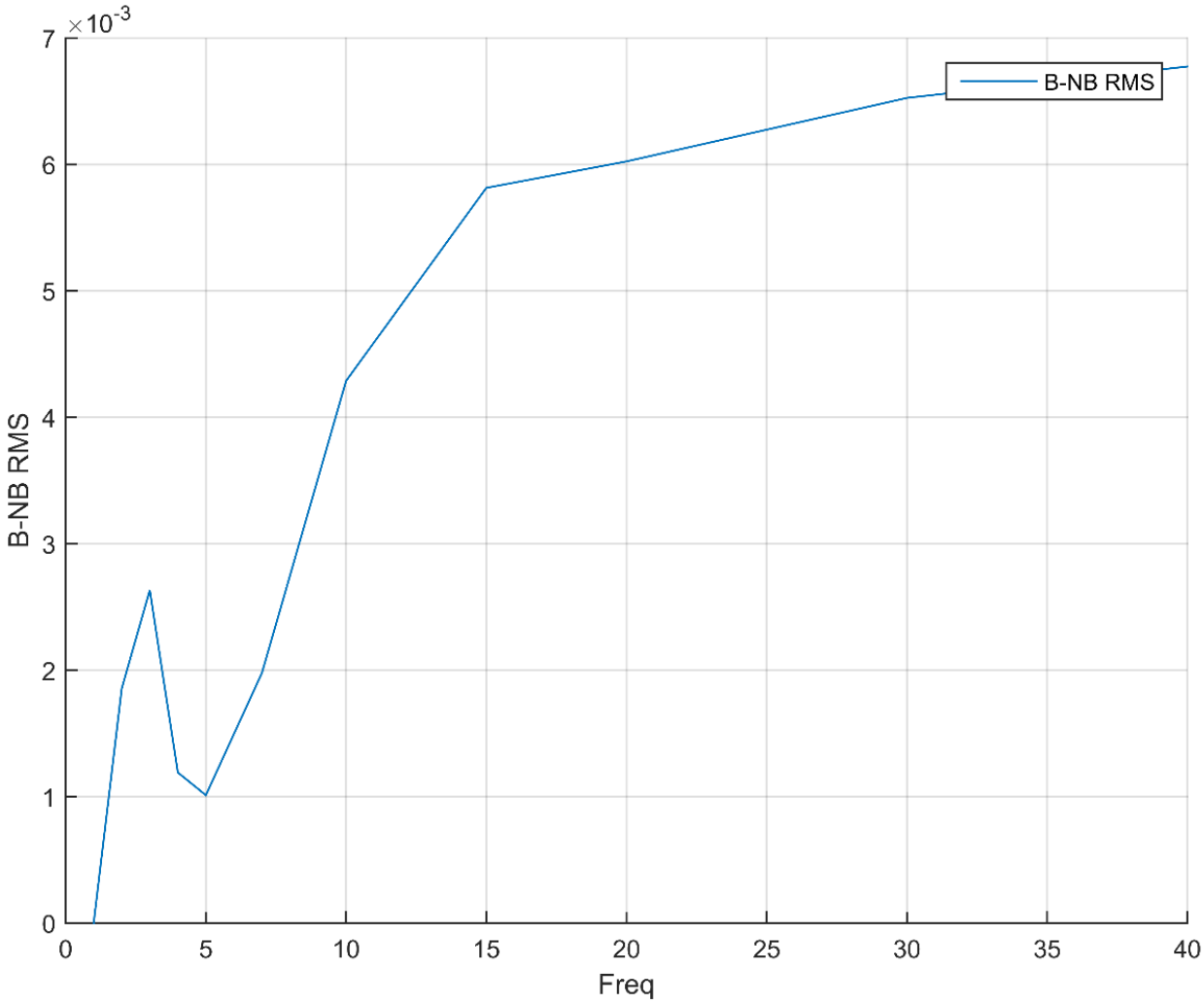

Figure 90 - RMS Difference Between Ballistic and Non-Ballistic Quarter Car Models

Appendix G – Bump Profile Development

StepUp

The StepUp input was created as the analog of the typical ‘Step’ input used when evaluating linear (particularly state space models). However, in this case, the step itself is not perfectly vertical, but has a defined slope. This eliminates the infinite velocity associated with a sharp step, which causes infinite force spikes when tire damping is included in the system.

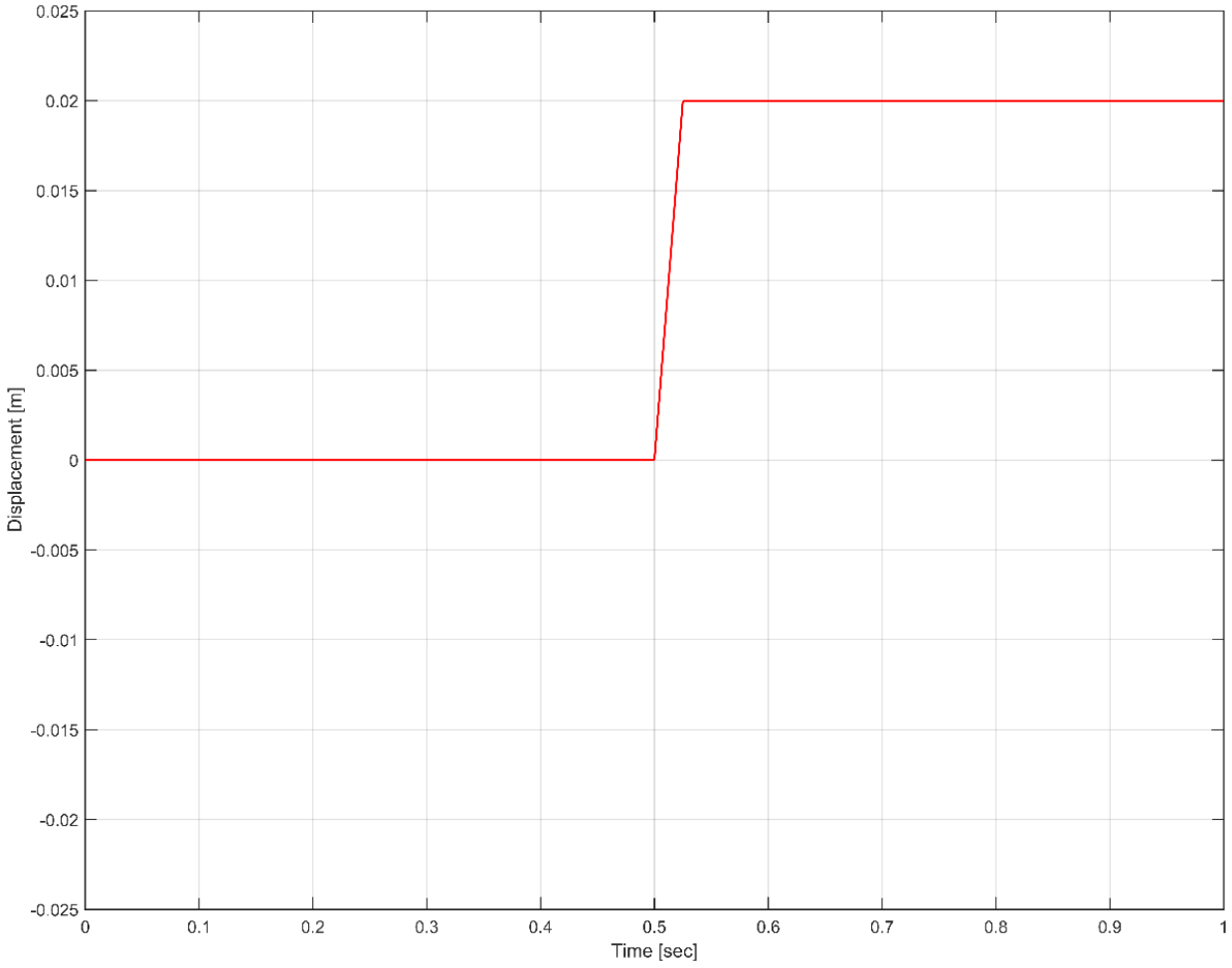

Figure 91 - StepUp Input

StepDown

Like the StepUp input, the StepDown eliminates the infinite velocity associated with a sharp step.

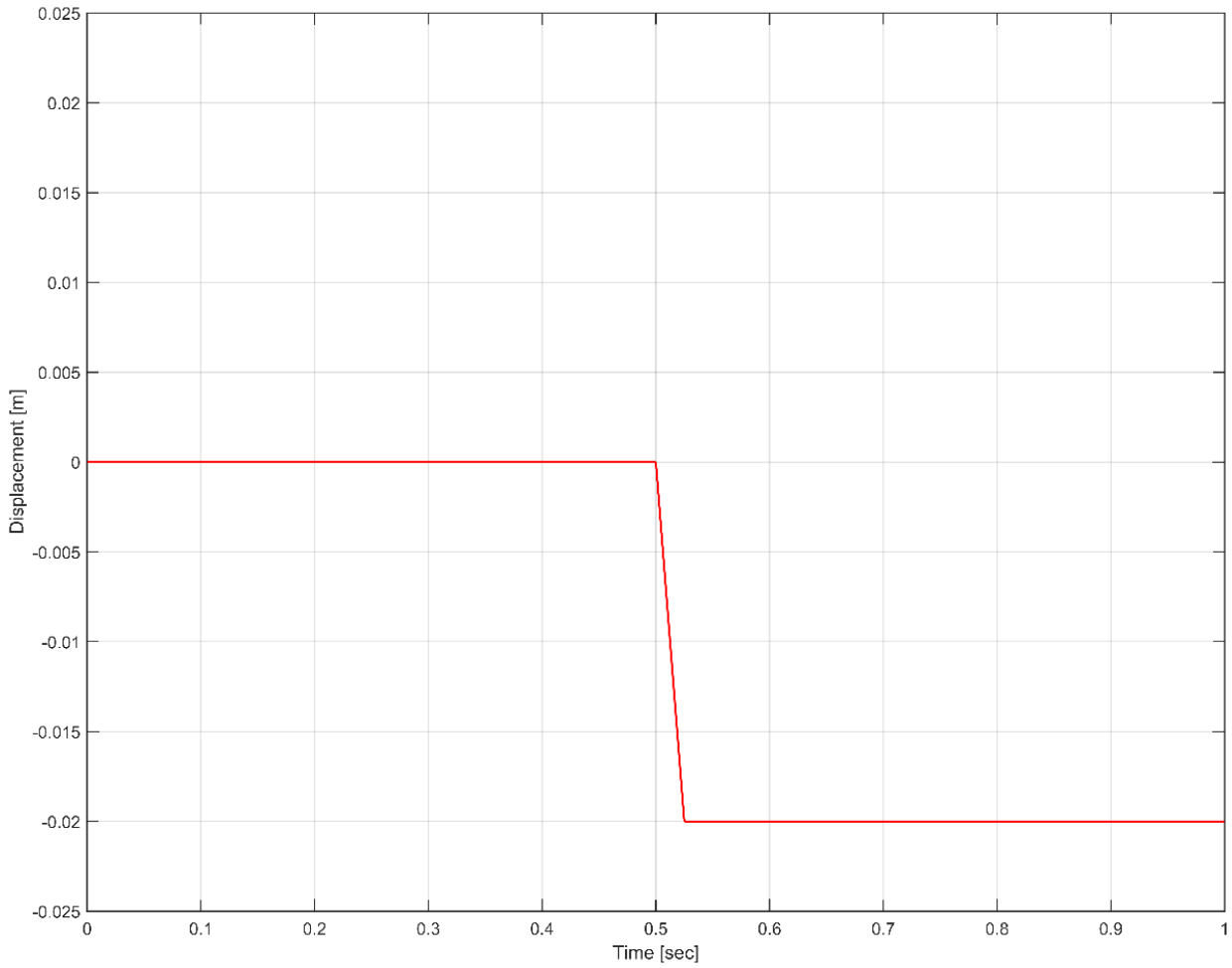

Figure 92 - StepDown Input

Sawtooth

The idea behind the ‘sharp’ Sawtooth is to create a roughly triangular profile that mimics the ‘Impulse’ input, but with defined derivatives.

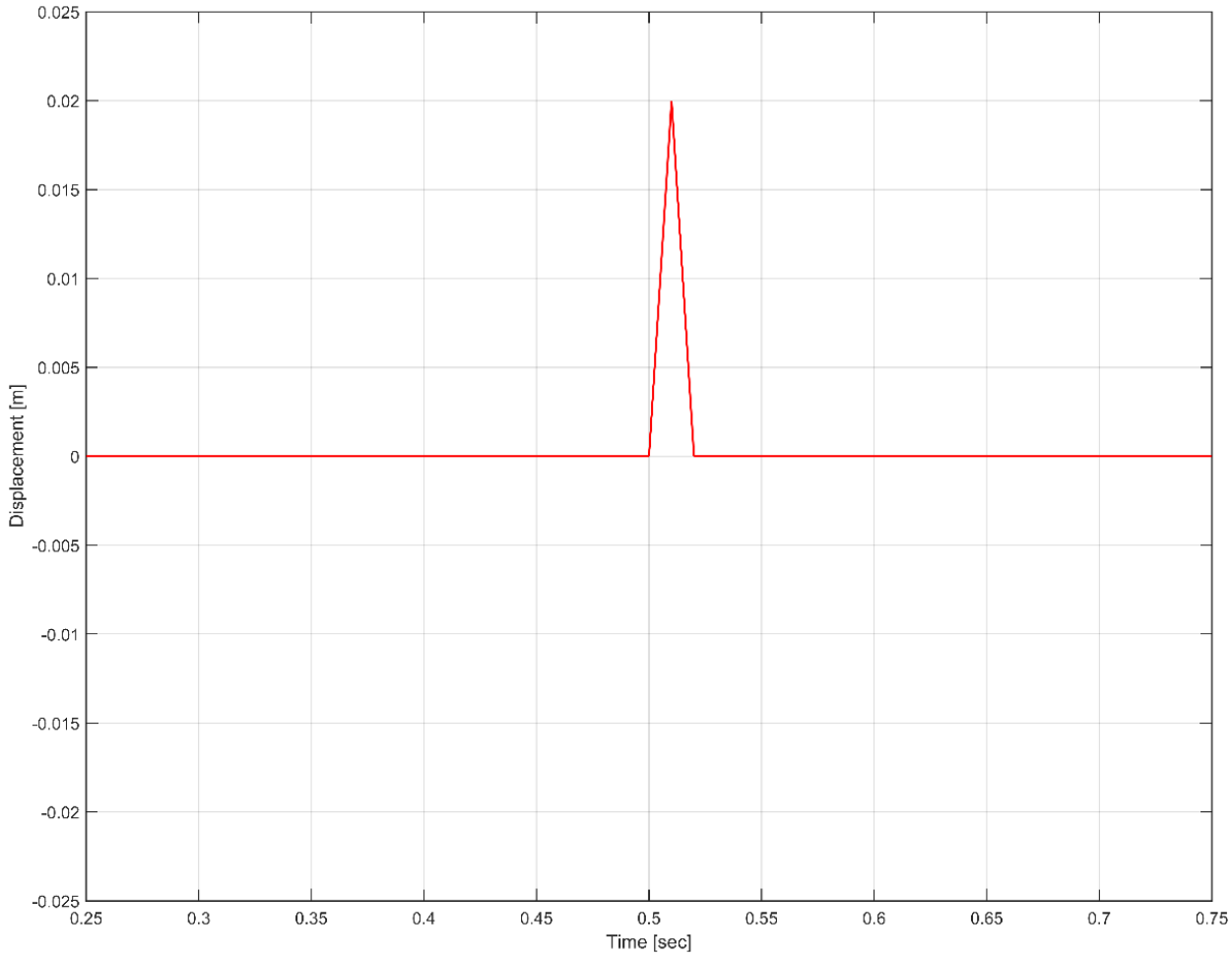

Figure 93 - Sawtooth Input

Pothole

The Pothole input is the first divergence from the classical system dynamics input set. This input was designed after its physical analog, a pothole or other gap in the roadway – a very common occurrence.

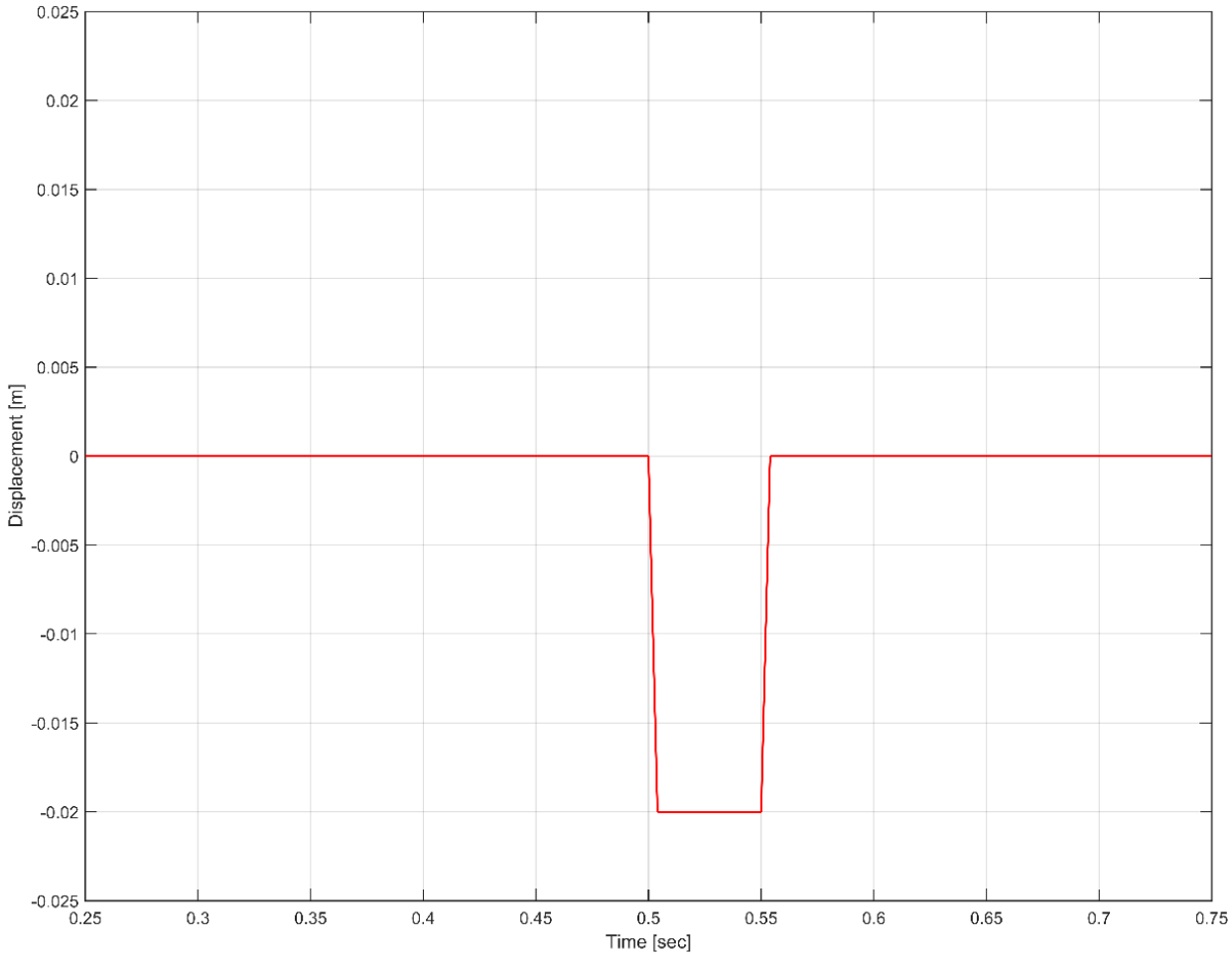

Figure 94 - Pothole Input

Sinusoid

The sinusoid inputs allow for approximation of the response of the car to varying frequencies, which is particularly important in trying to find instabilities and controller weaknesses.

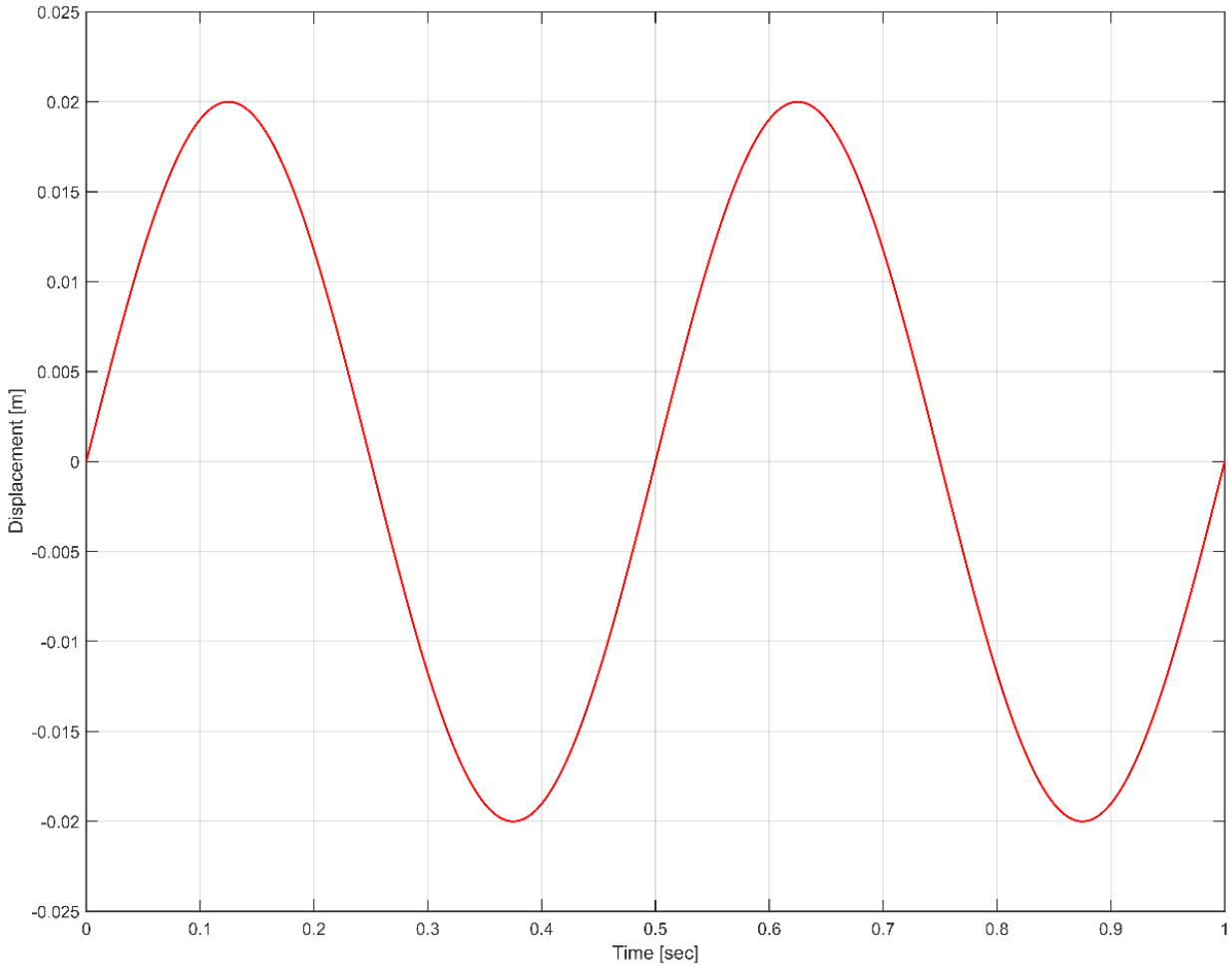

Figure 95 - Sinusoid Input

Chirp

The chirp input was created in order to simulate a frequency response of the system. The chirp signal is defined as a sin wave with a linear varying frequency. Frequency analysis of actual drive data indicated most vehicle input occurs under 5Hz. Thus, a range of 0.5 to 10Hz was chosen to represent a range of input that extends to twice the expected frequency. The frequency was varied between these two bounds over 60 seconds to prevent rapid variations of input frequency from having a large input on the response. The span was determined experimentally by varying the duration of the sweep, increasing the end time for each run until the response envelope remained constant. The frequency of the input and the input waveform can be seen in Figure 96.

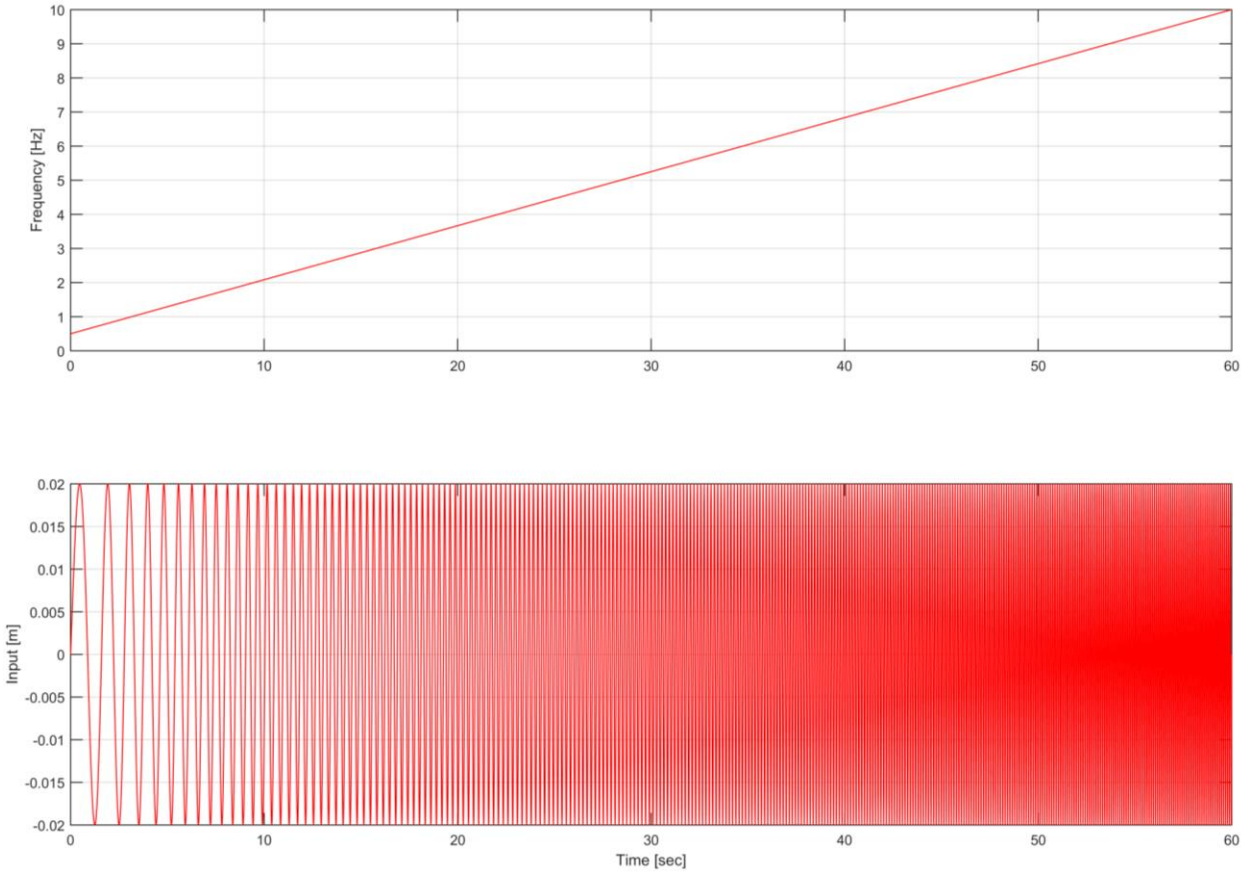

Figure 96 - Chip Input Frequency and Waveform

Appendix H – Additional Model Functions and Capabilities

It should be noted that several additional capabilities not explored in this thesis were implemented into the model for use in future explorations.

Some of these features are as follows:

1. Coulomb and Frictional Damping
    a. Will require measurement and parametrization of columbic and frictional coefficients
    b. Expected response impact is small for large disturbances
2. Longitudinal (X) DOF (preliminary)
3. Lateral (Y) DOF (preliminary)
    a. Should be incorporated along with a Pacejka tire model with tire and vehicle slip angle relations
    b. Could incorporate simplistic Driver In Loop steering feedback
4. Asymmetric (left/right) inputs and response in full car model
    a. Currently includes anti-roll bars
    b. Could include chassis torsional rigidity with minor modifications

BIBLIOGRAPHY

Barbosa, R. S. (2012). Vehicle Vibration Response Subjected to Longwave Measured Pavement Irregularity. *Journal of Mechanical Engineering and Automation*, 18.

Calspan Corporation. (n.d.). FSAE TTC Data. Buffalo, NY.

Dassault Systemes AB. (n.d.). Dymola. Sweeden.

Haney, P. (2004, 02 15). *Chapter 6: Tire Behavior*. Retrieved from Inside Racing Technology: http://insideracingtechnology.com/tirebkexerpt2.htm

Mechanical Simulation Corporation. (n.d.). CarSim. Ann Arbor, MI.

Mouzouris, A. (2012). *F1 Tires...Part 2*. Retrieved from The Technical World of Formula 1 Explained : http://technicalf1explained.blogspot.com/2012/10/f1-tirespart-2.html

MSC Software. (n.d.). Adams/Car. Newport Beach, California.

Öhlins USA. (2015). *TTX25 MkII.* Retrieved from Öhlins USA: http://www.ohlinsusa.com/files/files/2011_TTX25MkII_M.pdf

Optimum G. (n.d.). Denver, CO.

Pacejka, H. (2012). *Tire and Vehicle Dynamics* (3rd ed.). Oxford, UK: Elsevier Ltd.

Shahin, M. (1994). *Pavement Management for Airports, Roads and Parking Lots.* Norwell, MA: Kluwer Academic Publishers.

Smith, C. (1978). *Tune to Win.* Fallbrook, CA: Aero Publishers Inc.

Sugasawa, F. (n.d.). "Electronically Controlled Shock Absorber System Used as a Road Sensor wich Utilizes Supersonic Waves".

Tesis DYNAware. (n.d.). veDYNA. Munich, Germany.

The Mathworks, Inc. (n.d.). MATLAB and Simulink Release 2014b. Natick, Massachusetts, United States.

The Modelica Association. (n.d.). Modelica. Linköping, Sweeden.